The Generation of Tools to Interrogate Carbohydrate Metabolism During Cereal Germination

Michael Daniel Rugen

This thesis is submitted in fulfilment of the requirements of the degree of Doctor of Philosophy at the University of East Anglia

Department of Biological Chemistry

John Innes Centre

Norwich

September 2015

30/09/2015

I declare that the work contained in this thesis, submitted by me for the degree of Doctor of Philosophy, is to the best of my knowledge my own original work, except where due reference is made.

Signed

Michael D. Rugen

Abstract

Starch metabolism during barley germination is important to seedling establishment and has applications in malting and brewing. There remains a lack of understanding of how this process is controlled. It has previously been shown that the iminosugar 1-deoxynojirimycin (DNJ) retards grain starch loss during germination but also causes stunted root growth in the presence of exogenous glucose, possibly by interfering with glycoprotein processing.

To analyse the effects of other iminosugars on germination, a library of 391 *N*-substituted DNJ analogues were screened against Arabidopsis and a monocot alternative *Eragrostis tef*. The most potent compound identified, *N*-5-(adamantane-1-yl-ethoxy)pentyl-ido-DNJ (Ido-AEP-DNJ), inhibited root growth by 92% and 89% in Arabidopsis and tef, respectively, at 10 μM. Further analysis implicated glucosylceramide synthase as a target responsible for the effect caused by *Ido*-AEP-DNJ.

Effective small molecule inhibitors have previously been identified for the barley enzymes α-amylase, β-amylase and α-glucosidase. The debranching enzyme limit dextrinase (LD) is the sole enzyme responsible for the hydrolysis of α-1,6-linked dextrins during germination, to date, no potent inhibitors have been identified for LD. When assayed against LD (expressed in *Pichia pastoris*) the glycosylated variants of DNJ: G1M and G2M show inhibition of 80% and 90%, respectively, at 1 mM. Potential peptide inhibitors, based on the sequence of the proteinaceous LD inhibitor (LDI) were also analysed.

To enable further study, genes encoding LD and LDI were cloned and expressed as hexahistidine fusions in *E. coli*. Soluble LD was purified 75 fold by nickel affinity, β-cyclodextrin affinity and size-exclusion chromatography. LDI expressed in an insoluble form, but was solubilised and purified using β-mercaptoethanol, urea and nickel affinity chromatography. Polyclonal antibodies were raised against the recombinant proteins. Homozygous RNAi lines for knock-down of LD and LDI, alongside constructs to study subcellular localisation, were also generated to further probe the roles of these proteins *in planta*.

Acknowledgements

First of all I would like to thank Rob Field for giving me the opportunity to carry out this research under his supervision. His support, patience and willingness to discuss science have enabled both my scientific and personal development. I would also like to thank Alison Smith for all of her support, suggestions and ideas.

I would like to thank our collaborators. Malene Vester-Christensen, Marie Sofie Møller and Birte Svensson, from Technical University of Denmark, for sharing enzymes, unpublished data and for help with attempted protein crystallography; Anne Dell, Stuart Haslam and Aristotelis Antonopoulos from Imperial College London for glycoproteomics support; Hermen Overkleeft and his associates for provision of the iminosugar library.

A special mention should go to both Vasillios Andriotis and Martin Rejzek for all of their support in technical aspects and for imparting their knowledge of their respective fields.

Thanks to all of the people I have had the pleasure of working directly with. Amalia- for her help with chemical genetic screens. Mathieu- for his assistance in protein overexpression and chemical genetic screening, as well as being keen to learn from me. Dimitris and Crisitina- for synthesising iminosugars. Am- for her knowledge of isoamylase and of course her big smile. Ivone- for her collaboration on iminosugar inhibitors. Marilyn, Cristina and Brendan- for their support with particular biological techniques.

Thanks to Sergey, Irina, Giulia, Mati and Mike P for their chemistry support; Ellis ‘Spode’ O’Neill for showing me his “unique” science skills; the newcomers- Ben, Ed, Becky, Alex, Sue and Brydie for making the lab a fun place to work; Matt D, for his friendship, advice, and for the few times he did mass spec. Cheers to Steph for bequeathing his pipettes to me- without them none of this would have been possible!

I wish to thank all of the support staff at the JIC: the horticultural team; media kitchen team; librarians; stores and purchasing team; reception and security teams; Andrew Davis for photography; Gerhard Saalbach for metabolomics; Wendy Harwood, Mark Smedley and the BRACT team for help generating the transgenic barley lines.

I would like to thank all of the friends I have made during my PhD: Claire, Matt, John, Annis, Rob, Chris, Jo, Rach, Olu, Arti, Ruth, Lucy, Simon, Stuart, Doreen, Luca, Hadrien, Jenny and Edd for all of the good times we have had! Thanks to my friends from home and University: Nick, Claire, Steven, Leanne, Joe, Robyn, Dave, Claire, Rob, Alex and Buzz for being there if an escape from science was required.

Special thanks to Will for providing me with a distraction during my first year in Norwich and for his completely different view on scientific endeavours, discussed at length in many drinking establishments; and to Richard, my perpetual neighbour, for his unwavering friendship, lab shenanigans and biochemistry discussions.

Thanks to my parents: Jayne and John, the best teachers in the world! None of this would have been possible without their love and support. And to Matt for being a caring, funny and supportive brother.

Finally, thank you to Philippa for being so tolerant during the writing up process, for her love, support and the late night discussions on starch metabolism. She has been both an inspiration and a rock throughout this time.

Table of Contents

List of Figures

List of Tables

List of Abbreviations

ABA	Abscisic Acid
ACN	Acetonitrile
AGPase	ADP-glucose phosphorylase
Amp	Ampicillin
AMY	Alpha-Amylase
AUX	Auxin
BAM	Beta-Amylase
BCA	Bicinchoninic acid
BE	Branching Enzyme
bp	base pairs
BRs	Brassinosteroids
BSA	Bovine Seum Albumin
$CaCl_2$	Calcium Chloride
Cam	Chloramphenicol
Car	Carbenicillin
CBM	Carbohydrate binding module
cDNA	Complementary DNA
CESA	Cellulose Synthase
CH_2Cl_2	Dichloromethane
CK	Cytokinin
CM	Chloroform-Methanol
CSC	Cellulose Synthase Complex
CTI	Cereal Type Inhibitor
cTP	Chloroplast Transit Peptide
CV	Column Volume
DMSO	Dimethylsulfoxide
DNJ	1-Deoxynojirimycin
DNS	3,5-Dinitrosalicylic acid
dNTPs	deoxynucleotide triphosphates
dpi	days post imbibition
DTT	Dithiothreitol
EDTA	Ethylenediaminetetraacetic acid
ER	Endoplasmic Reticulum
EtOH	Ethanol
Fuc	Fucose
G-1-P	Glucose-1-phosphate
GA	Gibberellic Acid
Gal	Galactose
GC	Glucosylceramide
GCase	Glucocerebrosidase
GCS	Glucosylceramide Synthase
GFP	Green Fluorescent Protein
GH	Glycosyl hydrolase
Glc	Glucose
GlcNAc	*N*-Acetylglucosamine

GM	Genetically Modified
GW	Gateway
GWD	Glucan Water Dikinse
H_2O	Water
HCl	Hydrochloric Acid
HTS	High Throughput Screen
Hyg	Hygromycin
IAA	Iodoacetamide
IPTG	Isopropyl β-D-1-thiogalactopyranoside
ISA	Isoamylase
JA	Jasmonic Acid
Kan	Kanamycin
KCl	Potassium Chloride
kDa	Kilodaltons
LB	Lysogeny Broth
LD	Limit Dextrinase
LDI	Limit Dextrinase Inhibitor
Mal	Maltose
MeOH	Methanol
$MgCl_2$	Magnesium Chloride
MS	Murashige and Skoog medium
NaCl	Sodium Chloride
NaOAc	Sodium Acetate
NHS	*N*-hydroxysuccinimide
NJ	Nojirimycin
NMR	Nuclear Magnetic Resonance
PAMI	Peptide amylase inhibitor
PCD	Programmed Cell Death
PCR	Polymerase Chain Reaction
PGI	Phosphoglucoisomerase
PGM	Phosphoglucomutase
PHS	Pre-Harvest Sprouting
pNP	para-Nirtophenol
PWD	Phosphoglucan water dikiase
Rif	Rifampicin
RNA	Ribonucleic Acid
RNAi	RNA interference
rpm	revolutions per minute
RT	Room Temperature
RT-PCR	Reverse transcription-PCR
SA	Salicylic Acid
SBS	Surface Binding Site
SDS	Sodium dodecyl sulfate
SDS-PAGE	Sodium Dodecyl Sulfate Polyacrylamide Gel Electrophoresis
SOC	Super Optimal Broth with Catabolite Repression
SP	Signal Peptide
Spc	Spectinomycin

SS	Starch Synthase
TCEP	tris(2-carboxyethyl)phosphine
TG	Transglycosylation
Tris	Tris(hydroxymethyl)aminomethane
Trx	Thioredoxin
Ubi	Ubiquitin
WB	Western Blot
Xyl	Xylose
β-CD	Beta-cyclodextrin
β-ME	Beta-mercaptoethanol

Chapter 1- Introduction

1.1 The Importance of Carbohydrates

Carbohydrates are the most abundant organic structures found within biology, playing vital roles in the functioning of all organisms on Earth. They are essential to the processes central to plant metabolism: photosynthesis and respiration. Other important roles include those of a structural and protective nature, as seen in plant cellulose, bacterial peptidoglycan and insect chitin (Hancock, 1997, Merzendorfer and Zimoch, 2003, Gilbert, 2010). Alongside this, carbohydrates also act as ligands, often conjugated to proteins, lipids or small molecules, involved in signalling and cell adhesion (Varki, 1993, An et al., 2009).

Carbohydrate structures, both in solution and in the solid state, are still not fully understood. With major advances in genomics – the study of nucleic acids – and proteomics – the study of proteins – carbohydrates, the third biopolymer, have been left behind. This neglect derives from the amorphous nature of carbohydrates, their complicated regulation and the lack of specific genome based coding (Solís et al., 2015).

1.2 Carbohydrate Rich Cereals

A large proportion of the calories consumed by humans is in the form of starch, with the cereals (wheat, maize, rice and barley) constituting the largest part of human diet (Cordain, 1999). Starch is a major constituent of staple food products including bread, breakfast cereals and pasta (Delcour and Hoseney, 2010b). The physical properties of starch are of paramount importance to the food industry with the gelling of desserts, the thickening of sauces and the structure of baked goods all being linked to starch structure. Raw starch can also be chemically or enzymatically converted into sugar syrups for use as sweeteners. Starch is also an important industrial commodity, particularly in the paper making and bioethanol industries (Smith, 2008).

A cereal rich diet has both benefits and costs. It is proposed that starch rich foods were important factors in human evolution, as complex carbohydrates were able to fuel the metabolic demands of increasing brain size (Hardy et al., 2015). However starch rich diets are now associated with dietary imbalance, diabetes and autoimmune disease (Cordain, 1999). Modification strategies for the future have been suggested to improve cereals for diet and health (Blennow et al., 2013, Borrill et al., 2014, Lafiandra et al., 2014).

The focus of this thesis lies principally with Barley (*Hordeum vulgare*), the 4th major cereal grain (after maize, rice and wheat, respectively) when measured in terms of quantity produced (Faostat, 2014). It is a self-pollinating member of the grass family that has a diploid genome with 14 chromosomes (Zohary et al., 2012). The barley genome is relatively simple making this species a useful tool for research with a view to application to the more complex cereals such as wheat (tetraploid or hexaploid). Barley is important as an animal feed, with over half of the USA's barley crop being used as cattle feed (Givens et al., 2004). It has been proposed that whole grain barley could provide a healthier alternative to other cereals. The high β-glucan content of barley is associated with lower cholesterol and increased satiety when part of the human diet (Baik and Ullrich, 2008). Further to its food use, barley is frequently used as a source of enzymes and fermentable material for the brewing of beer and the creation of distilled beverages such as whisky.

1.3 Structures of Relevant α-Linked Carbohydrate Polysaccharides

The majority of carbohydrate polymers are composed of glucose (Klemm et al., 2005). The simplest way of classifying the major polysaccharides is by the glycosidic bond anomeric configuration, giving α-linked and β-linked. Differences in these configurations gives rise to drastically different structures (e.g. helical amylose and linear cellulose, respectively, Figure 1.1).

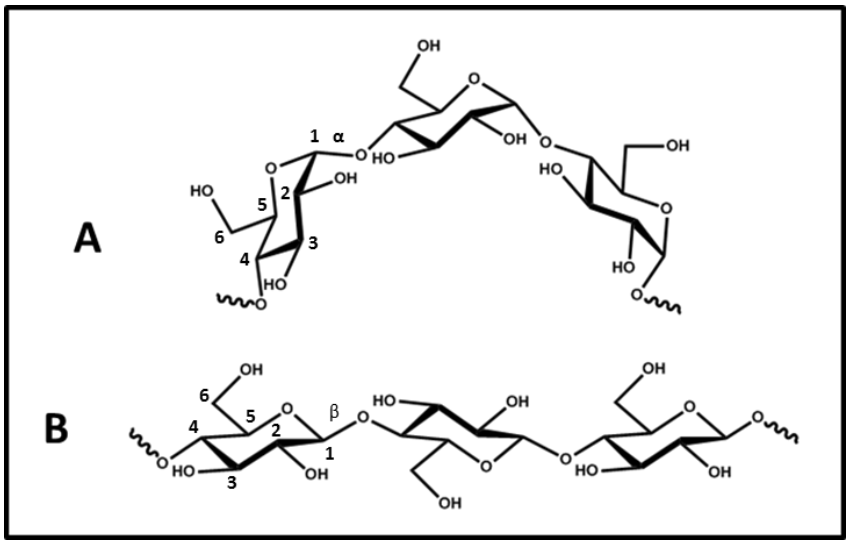

Figure 1.1 The difference in structure caused by change in anomeric configuration.
A. α-1,4 linked amylose and **B**. β-1,4 linked cellulose. Both polymers are composed of 1,4-linked glucose, the only difference driving their divergent properties and structure is their anomeric form.

The structure and function of the polysaccharides relevant to this work are outlined, namely- pullulan, starch and glycogen.

1.3.1 Pullulan

As it is soluble, easily purified and has a constant ratio of α-1,4 to α-1,6 glycosidic linkages, pullulan (Figure 1.2, A) is an ideal substrate for the assay of α-1,6 hydrolysing (debranching) enzymes (Mccleary, 1992). This linear polysaccharide of glucose is linked by both α-1,4 and α-1,6 glycosidic bonds. Maltotriose is produced upon treatment with the pullulan degrading enzyme pullulanase, which hydrolyses the α-1,6 linkages specifically, leading to the description of pullulan as an α-1,6 linked polymer of maltotriose subunits (Bender and Wallenfels, 1961). Maltotetraose subunits have been identified in pullulan, being a minor constituent with a frequency between 1 % and 7 %, depending on the fungal strain (*Aureobasidium pullulans*) used to produce it (Carolan et al., 1983). Acid hydrolysis of pullulan results in a number of saccharide species, including isomaltose, maltose, panose and isopanose (Figure 1.2, B-F) (Bender et al., 1959, Bouveng et al., 1963).

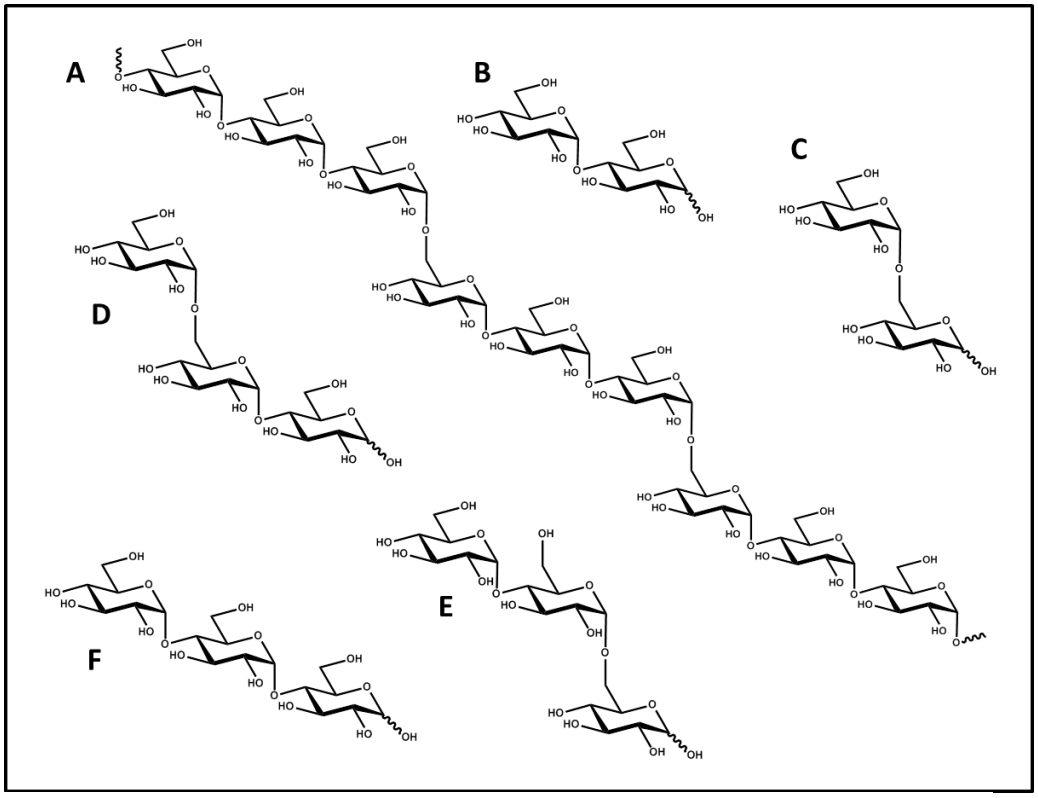

Figure 1.2 Structures associated with pullulan.
A. Pullulan. **B-F.** The degradation products produced by acid hydrolysis of pullulan: **B**. maltose. **C.** isomaltose. **D.** panose. **E.** isopanose. **F.** maltotriose.

Very few details on the enzymes involved in the biosynthesis of pullulan have been elucidated (Cheng et al., 2011) and it's physiological function remains uncertain. The accepted proposal is that pullulan serves as a protective layer, offering resistance to desiccation and allowing cells to adhere to environmental surfaces (Andrews et al., 1994).

1.3.2 Starch

Starch, a polymer of α-1,4 and α-1,6 linked glucose is the primary energy reserve in plants. It is synthesised as microscopic granules within many plant tissues: pollen, leaves, stems, roots, tubers, bulbs, rhizomes, fruits, flowers and seeds (Figure 1.3) (Preiss, 1996). Starch can be considered on three size levels: whole granule (μm), lamellae (9 nm) and molecular scale (0.1-1 nm) (Waigh et al., 2000).

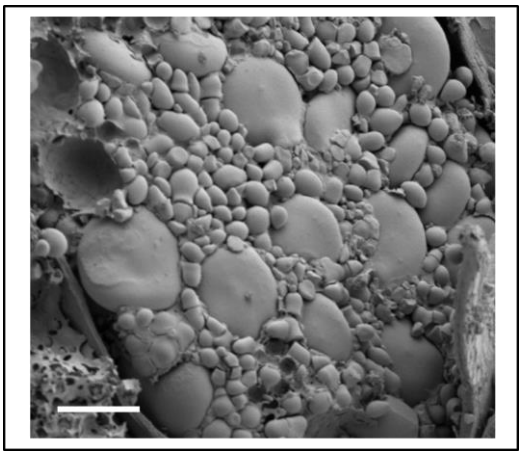

Figure 1.3 Electron micrograph of starch granules in the barley endosperm
Image from Vasilios Andriotis and Elaine Barclay. Large A type and small B type granules can be seen. Scale bar = 10 μm

Starch granules are roughly spherical, typically being 1 to 100 μm in diameter. Although starch granule size and shape varies depending on the plant of origin (Tester et al., 2004). Due to their compact nature, they are insoluble in water at ambient temperature (Halley and Avérous, 2014). The granular form of starch is responsible for many of its unique physical properties. When heated above 60 °C, starch granules are able to swell to form a gel in a process known as gelatinization (Tester and Morrison, 1990). This process has important implications within cooking and industrial food processing (Lund, 1984).

Starch granules are made up of two major α-glucan polymers, amylose and amylopectin, which constitute roughly 98-99 % of the dry weight (Vandamme et al., 2002). Cereal starches contain between 1-1.5 % lipid and usually <0.6 % protein and <0.4 % minerals. The ratios of the two polymers vary depending on plant species and variety (Vandamme et al., 2002). Barley has an

amylose content of around 30 % with the remaining 70 % being amylopectin (Gupta et al., 2010). Amylose and amylopectin have different structures and properties that are outlined in Figure 1.4 and Table 1.1 (Tester et al., 2004).

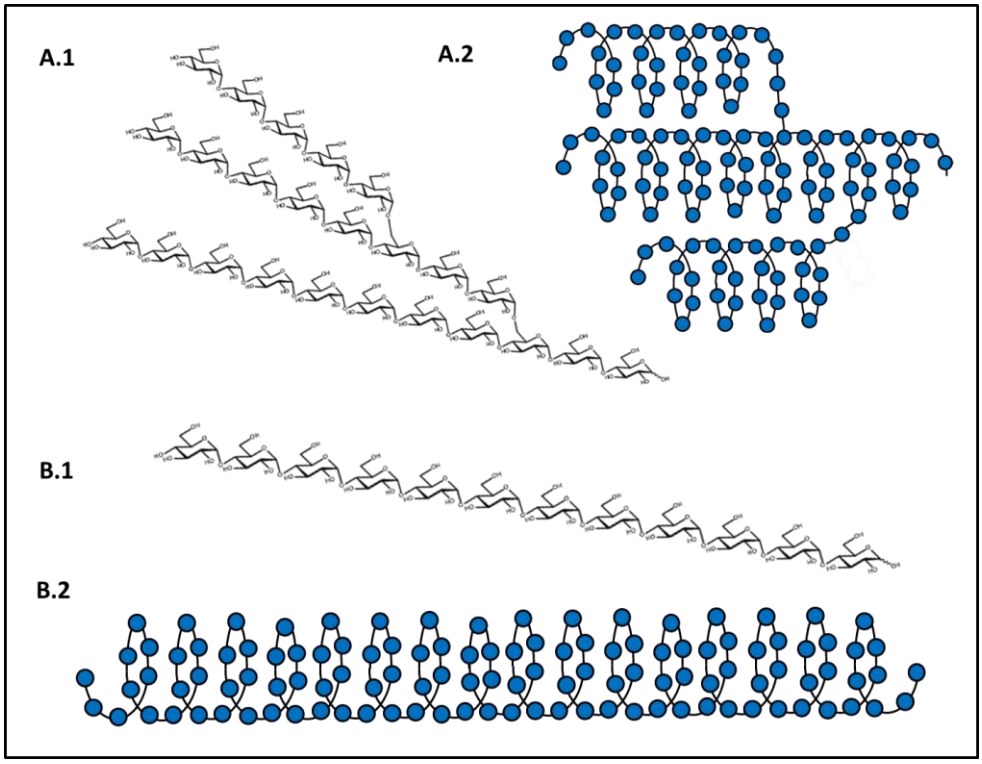

Figure 1.4 The structure of amylose and amylopectin.
Chemical structure of **A.1** amylopectin, **B.1** amylose. Cartoon representation of **A.2** amylopectin. **B.2** amylose. Glucose is represented by blue circles.

	Amylose	**Amylopectin**
Content in granules (%)	15-35	65-85
Molecular weight	1×10^6	1×10^7 - 1×10^9
Branching	Essentially linear α-1,4 linked	~5 % α-1,6 linkages
Average α-1,4 chain length (glc units)	200-700	12-25

Table 1.1 Structural features of amylose and amylopectin.
Generated using data from (Mua and Jackson, 1997, Fredriksson et al., 1998). Unit chain length and branching pattern depend on botanical origin (Tester et al., 2004).

The individual chains within amylopectin are classified depending on their chain length and position within the starch granule (Figure 1.5) (Hizukuri, 1985). Type A chains are unbranched and linked to B chains. B chains are branched and link to other B chains or the backbone (C chain) of the amylopectin molecule.

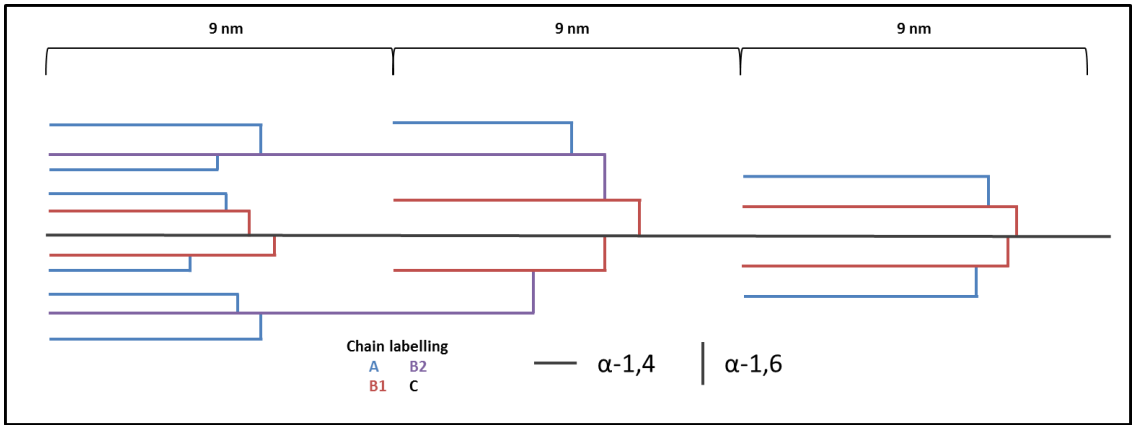

Figure 1.5 Branching patterns within amylopectin.
Figure adapted from (Hizukuri, 1986, Tester et al., 2004).

The growth ring appearance of starch (Figure 1.6), as seen under a light or electron microscope, is proposed to arise because of its semi-crystalline nature (Tester et al., 2004). These growth rings consist of semi-crystalline and amorphous rings (Pilling and Smith, 2003). The blocklet structure model proposes that the growth rings are made up of amylopectin lamellae organized into effectively round 20-50 nm 'blocklets', with the semi-crystalline rings being made up of large or "perfect" blocklets and the amorphous rings contain smaller or "defect" blocklets (Tang et al., 2006).

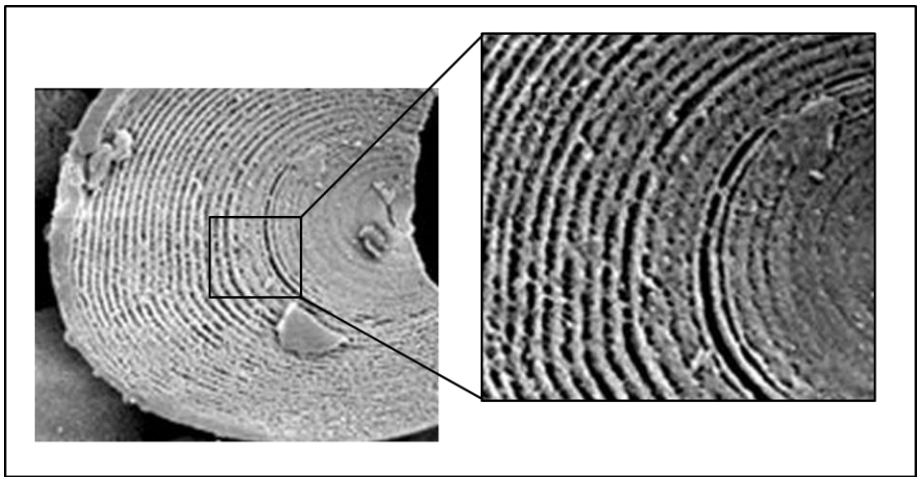

Figure 1.6 Growth rings in starch granule from potato.
Image adapted from (Pilling and Smith, 2003).

The semi-crystalline growth rings found in starch consist of alternating crystalline and amorphous lamellae with a repeat distance of 9 nm (Figure 1.8, C) (Jenkins et al., 1993). This pattern arises due to the existence of distinct branched (amorphous) and helical (crystalline) regions within amylopectin (Figure 1.8, C). The presence of helical structures within starch granules has been extensively studied using ^{13}C NMR spectroscopy which reveals the capacity to form double helical amylopectin, single helical amylopectin and spacer regions between helices and branches (Tester et al., 2004). Three polymorphic forms of crystalline amylopectin chave been observed by X-ray diffraction: A-type, B-type and C-type; a combination of A and B (Figure 1.7) (Hsien-Chih and Sarko, 1978, Imberty and Perez, 1988). The helical nature of the polymorphs is identical, only the packing differs. Further work to understand the composition and architecture of the blocklets and growth rings is required.

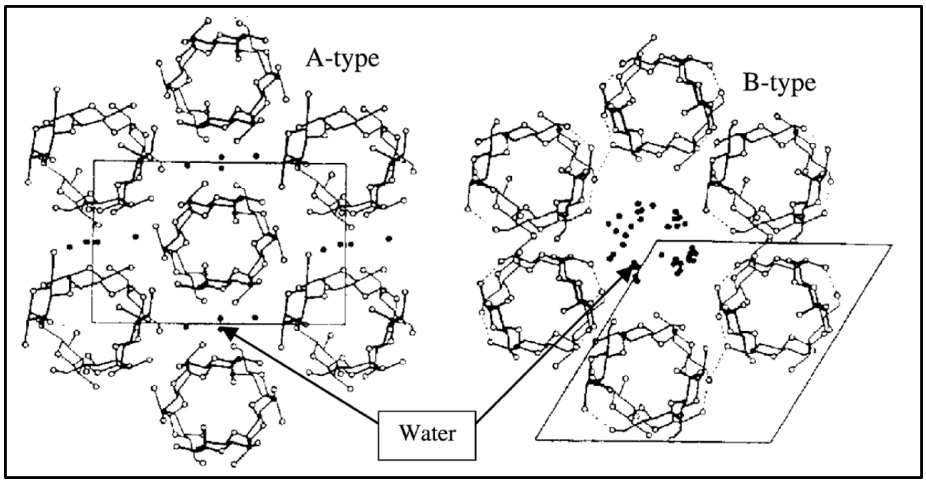

Figure 1.7 Helical packing of A and B polymorphs of amylopectin.
Figure from (Hsien-Chih and Sarko, 1978).

The current combination of knowledge proposes a model in which the semi-crystalline growth rings (140 nm) contain radiating clusters of amylopectin exterior chains interspaced with amorphous lamellae (Figure 1.8).

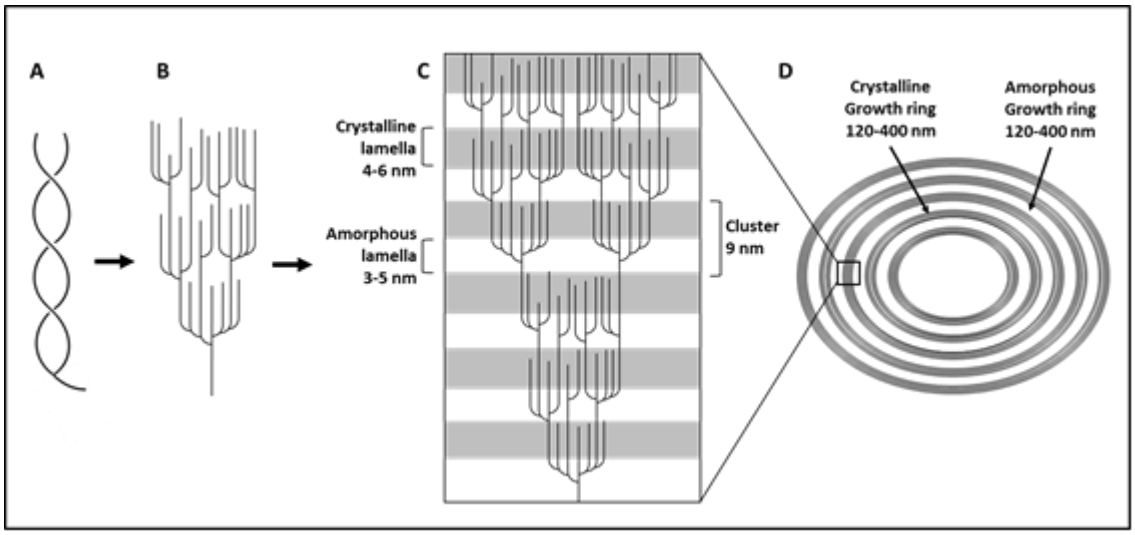

Figure 1.8 Growth ring model of the starch granule.
A. Amylopectin double helix **B.** Amylopectin molecule **C.** Section of semi-crystalline growth ring consisting of crystalline and amorphous lamella, with a 9 nm repeat. **D.** Starch granule cross section. Figure adapted from (Hamley, 2010).

1.3.3 Glycogen

Glycogen is a glucose polymer analogous to the amylopectin of starch. It is the secondary energy reserve within animal cells, the primary store being the fatty acids of the adipose tissue (Coelho et al., 2013). It is a polymer of α-1,4 linked glucose units with α-1,6 branch points occurring roughly every one in ten residues (Roach, 2002). Glycogen synthesis is initiated by glycogenin, an enzyme that auto-glucosylates using UDP-glucose to create a polymer at least 4 glucose units in length which primes synthesis (Figure 1.9) (Chaikuad et al., 2011). This primer is then extended by glycogen synthase. Glycogen branching enzyme generates branches by transferring a glucose polymer from a non-reducing end to create a branch point within the glucan chain (Akram et al., 2011).

Glycogen phosphorylase breaks down glycogen by the successive release of glucose in the form of glucose-1-phosphate (G-1-P) (Akram et al., 2011). This enzyme cannot cleave glucose within four residues of a branch point. Therefore glycogen debranching enzyme is required to remove branch points, this occurs in two steps (Liu et al., 1991). First, maltotriose is transferred from the branch to another chain leaving behind only one 1,6 linked glucose

residue. This residue is then hydrolysed therefore removing the branch point. The phosphorylation and activity of glycogen synthase and glycogen phosphorylase are tightly controlled *via* hormones (Jensen and Lai, 2009).

Starch and glycogen represent two physical states of the same type of storage polysaccharide. There are distinct similarities and differences between starch and glycogen as outlined in Table 1.2 (D'hulst and Merida, 2010).

	Starch	**Glycogen**
Monomer	α-glucose	α-glucose
Linkages	α-1,4 and α-1,6	α-1,4 and α-1,6
Solubility in water	Insoluble	Soluble
Size	0.1-100 um	40 nm
Primer of synthesis	Unknown	Glycogenin
Trimming of branches during synthesis	Yes	No
Branching	5-7 % total linkages with uneven distribution	<10 % total linkages with even distribution

Table 1.2 The similarities and differences between starch and glycogen.
Generated using data from (Smirnova et al., 2015).

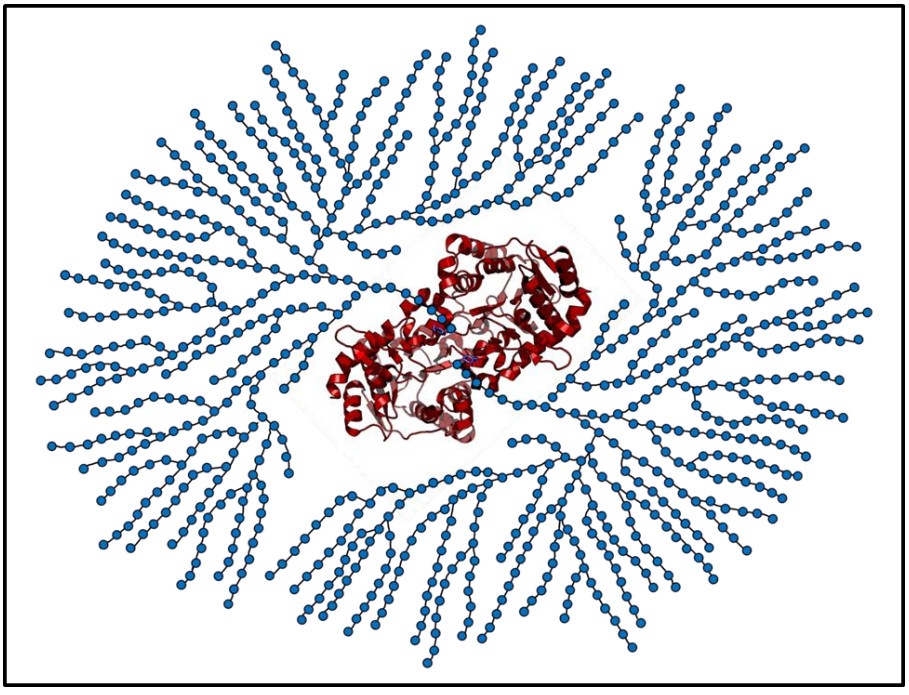

Figure 1.9 The structure of glycogen.
Dimeric glycogenin (red) is in the centre of the glycogen molecule. This is surrounded by α-1,4 and α-1,6 linked glucose residues (blue circles). Glycogenin auto glycosylates at Tyr195 to prime glycogen synthesis.

1.4 The Metabolism of Starch within Plants

The synthesis and degradation of starch is an area that has attracted substantial research efforts. Attention was first aimed at the characterization of enzymes directly involved, a large number of which have been identified in model and crop species (Grennan, 2006). Focus has now turned to understanding the nature and regulation of the processes (Kotting et al., 2010). There is increasing evidence for roles of redox regulation, protein phosphorylation, protein-protein interactions and allosteric regulation by metabolites in the control of starch metabolism (Kotting et al., 2010). Both the circadian clock (Graf et al., 2010) and trehalose-6-phosphate have also been implicated in whole plant signalling and orchestration of carbohydrate metabolism (Kolbe et al., 2005, Ponnu et al., 2011). To achieve manipulation of starch biochemistry a complete understanding of all processes involved in starch metabolism is required (Smith et al., 1997). Often a change in one gene can have unforeseen out comes due to the multiple pathways of synthesis and degradation, catalysed by a suite of enzymes that are able to compensate for each other (Smith et al., 2005, Streb et al., 2012).

1.4.1 Starch Metabolism in Different Plant Tissues

Starch biosynthesis occurs within three types of membrane bound organelle: chloroplasts, chloroamyloplasts and amyloplasts (Vandamme et al., 2002). Photosynthetic (source) tissues generate carbohydrate metabolic intermediates that are either utilised in transitory starch production or converted to sucrose and exported (Zeeman et al., 2004). Exported sucrose is either metabolised as an energy source or converted to reserve starch by tissues which are incapable of photosynthesis. Reserve starch biosynthesis occurs in storage (sink) organs such as tubers, roots and cotelydons of dicots or seeds (grains) of monocots.

Starch degradation is an important process that occurs in both the leaves (transitory starch) and within storage organs (reserve starch) (Figure 1.10). Leaf starch degradation is required to provide plants with sugar for growth during non-photosynthetic (night) periods (Graf et al., 2010). Reserve starch degradation, on the other hand, is required as a store of sugar for embryo development. Due to the different locations and temporal requirements the processes of transient and reserve starch biosynthesis and degradation have some distinct differences wich are outlined in the next sections (James et al., 2003, Lloyd and Kossmann, 2015).

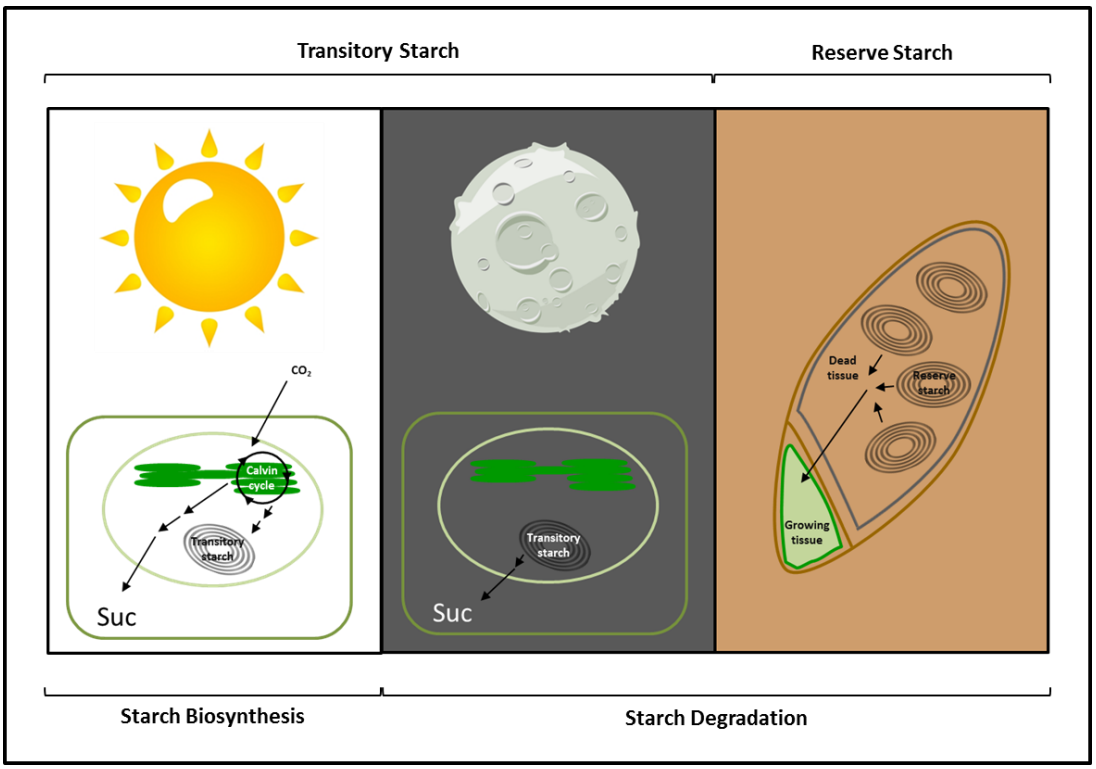

Figure 1.10 Transitory and reserve starch biosynthesis and degradation.
Transitory starch metabolism follows a diurnal cycle. During the light CO_2 is fixed by the Calvin-Benson cycle, the products are converted to transitory starch or sucrose. Sucrose is transported to other organs either to fuel respiration of starch synthesis. During periods of no light, transitory starch is catabolised to generate sucrose. Reserve starch acts as an energy store to fuel seedling growth.

1.4.2 Starch Synthesis

Three main enzymes are established in the synthesis of starch: ADP-glucose phosphorylase (AGPase), starch synthase (SS) and starch-branching enzyme (SBE) (Smith et al., 1997). A fourth enzyme family, debranching enzyme (DBE- ISA, LD) is also implicated in the regulation and control of branching during amylopectin synthesis (Figure 1.11) (Smith et al., 1997).

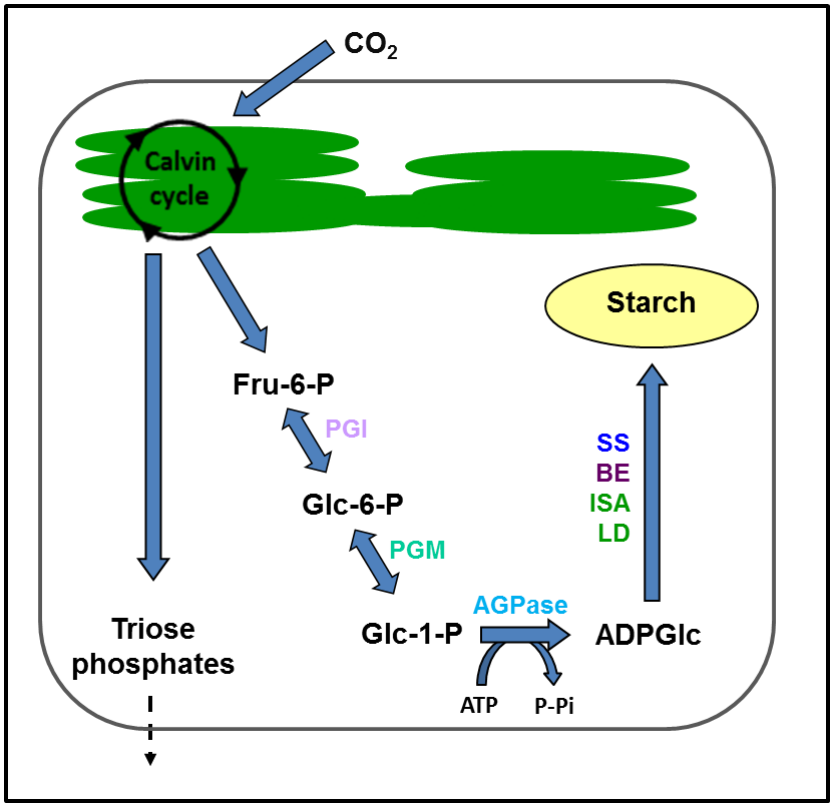

Figure 1.11 Proposed Pathway for Starch Synthesis.
During the day, starch is synthesised from substrates mainly derived from the Calvin-Benson cycle, some Glc-1-P may also come from the cyctosol. PGI, phosphoglucose isomerase. PGM, phosphoglucomutase. AGPase, ADP-glucose phosphorylase. SS, Starch synthase. BE, branching enzyme. ISA, isoamylase. LD, limit dextrinase. Adapted from (Stitt and Zeeman, 2012).

ADP-Glucose Phosphorylase

AGPase is the enzyme responsible for the synthesis of ADP-glucose: the glucosyl donor for starch synthesis. ADP-Glc is directly linked to the Calvin-Benson cycle by three catalytic steps catalysed by phosphoglucoisomerase (PGI), phosphoglucomutase (PGM) and AGPase. AGPase consists of large and small subunits that have different amino acid sequences (Smith-White and Preiss, 1992, Ventriglia et al., 2008). Differences between plant species exist in the number and expression patterns of encoding genes, with the genes encoding the different subunits also being differently regulated depending on organ (Smith et al., 1997).

Starch Synthases (SS)

There are five gene classes of SS: granule bound (GB) SS and SSI-IV. SSs are responsible for the repeated addition of α-1,4-linked glucose units to growing amylose and amylopectin chains (Smith et al., 1997). Multiple isoforms of SS have been identified yet not enough is currently known for the construction of a model that relates particular isoforms to specific aspects of amylopectin biosynthesis (Marshall et al., 1996, Martin and Smith, 1995). GBSS is proposed to be responsible for amylose synthesis (Denyer et al., 1995). Recently a protein involved in targeting GBSS to starch granules has been identified. Protein targeting to starch (PTST) is required for amylose synthesis. This protein has an N-terminal coiled coil and a C-terminal starch binding CBM48, involved in protein-protein and protein-carbohydrate interactions (Seung et al., 2015).

Starch Branching Enzymes (SBE)

Multiple isoforms of SBE, that catalyse the formation of starch α-1,6 branch points, are found within plant organs (Martin and Smith, 1995, Burton et al., 1995, Smith et al., 2005). Three categories of SBE exist (I, IIa and IIb): their differences are based on primary sequence data and substrate affinities (Burton et al., 1995). *In vitro*, isoform IIa preferentially branches amylopectin whereas isoform IIb has a preference for amylose (Guan and Preiss, 1993, Takeda et al., 1993). Mutations in loci corresponding to the IIa isoform results in an increase in average amylopectin chain length but starch granule structure is not dramatically affected (Bhattacharyya et al., 1990, Burton et al., 1995, Mizuno et al., 1993). RNA interference (RNAi) knock-down of all SBE generates amylose-only starch in barley, highlighting their importance in amylopectin biosynthesis (Carciofi et al., 2012).

Debranching Enzymes (DBE)

Two families of DBE exist in plants, isoamylase (ISA) type and limit dextrinase (LD) (pullulanase) type, defined by their inability and ability to hydrolyse pullulan respectively. Mutations at the *SUGARY1* locus of maize and rice affect the genes that encode DBE and lead to dramatic reductions in endosperm starch content alongside the production of water soluble, highly branched glucans, similar to glycogen (referred to as phytoglycogen) (Doehlert et al., 1993, Nakamura et al., 1996, Pan and Nelson, 1984). This gives rise to the suggestion that the native branching pattern is due to the concerted actions of both SBE and DBE (Smith et al., 1997). Limit dextrinase and isoamylase appear to have overlapping functions in starch synthesis. (Wu et al., 2002).

The three isoamylase isoforms, (ISA1-3) have been shown to have different catalytic properties. ISA1 and ISA2 were shown to be associated as a hetero- or homo- multimeric enzyme complex in Arabidopsis, potato and maize, whereas ISA3 is not associated with a complex (Lin et al., 2013, Myers et al., 2000). Data suggests that ISA1 and ISA2 act to debranch soluble glucans during starch synthesis, ISA3 has a different catalytic specificity indicating a different role in starch metabolism (Myers et al., 2000, Bustos et al., 2004, Delatte et al., 2006). ISA1 can function in starch metabolism in the maize endosperm and leaf without ISA2 but with reduced efficiency. Incorporation of ISA1 from maize into an Arabidopsis *ISA1/2* mutant confirmed that maize ISA1 is active alone whereas Arabidopsis ISA1 requires ISA2 to function (Facon et al., 2013). There is therefore some degree of functional conservation between monocot and dicot ISA (Streb and Zeeman, 2014).

A glucan trimming model that implicates SBE and DBE as the enzymes responsible for branching levels, and therefore amylopectin structure, has been proposed (Ball et al., 1996, Smith et al., 1997). It is suggested that soluble SS elongates very short chains at the granule periphery. These chains are initially insufficient in length to act as substrates for SBE and remain unbranched. When an appropriate length is reached, branches are introduced by SBE and elongated by SS. DBE is then able to remove the outer chains from these unorganised glucans, however it is unable to access branch points formed close to the organised double helical zone. Thus the action of DBE leaves a zone of short chains arising from branch points at the top of the double helical region, a further round of elongation can then occur.

Arabidopsis quadruple mutants lacking all four DBE proteins (ISA 1, 2 and 3 and LD) are devoid of starch granules and accumulate highly branched glucans, distinct from amylopectin and phytoglycogen (Wattebled et al., 2005, Streb et al., 2008). The branched glucan can be degraded by α- and β-amylases to produce maltose. Superficially these data support the hypothesis that starch DBEs are necessary for amylopectin synthesis. However, the additional loss of α-amylase (*AMY3*) partially reverts the phenotype of the quadruple DBE mutant, restoring starch granule biosynthesis (Streb et al., 2008). This leads to the proposal that DBEs function to promote amylopectin crystallisation during synthesis but may not be essential for starch granule synthesis.

1.4.3 Leaf Starch Degradation

Glucose (Glc) and maltose (Mal) are the major products produced by starch degradation within the chloroplast. Degradation occurs *via* a network of reactions (Figure 1.12) (Smith et al., 2005, Zeeman et al., 2007). Reserve starch degradation in living storage tissues proceeds in a similar way to transitory starch degradation.

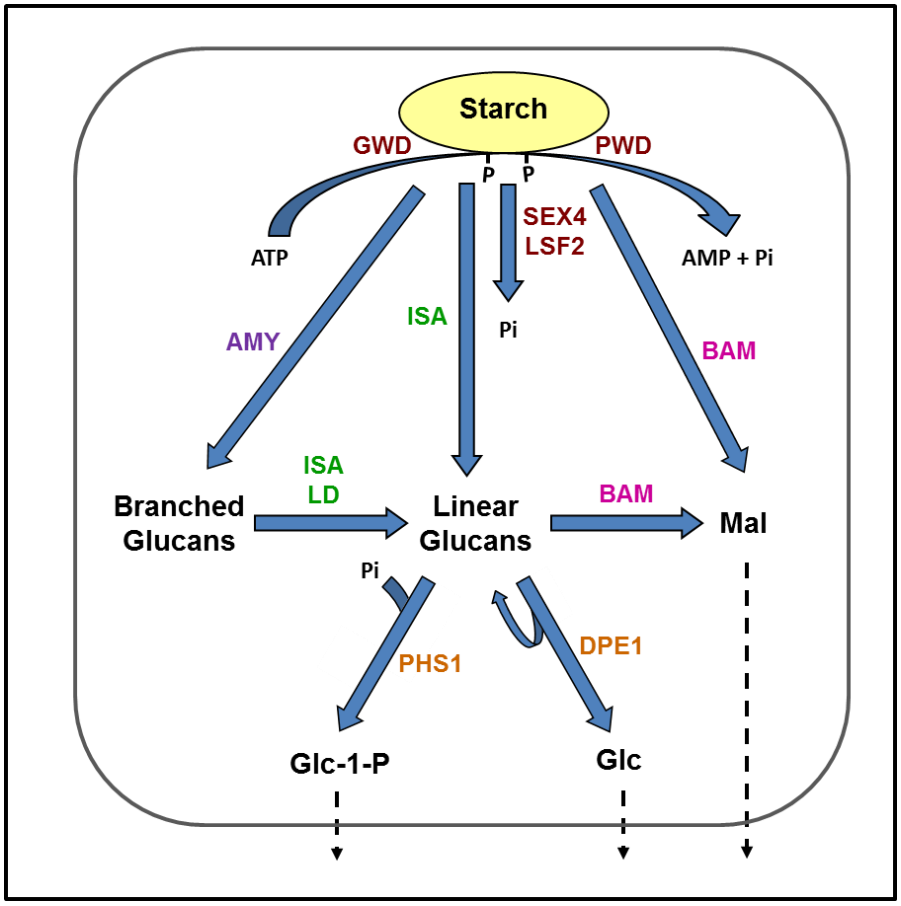

Figure 1.12 The proposed pathway for starch metabolism
Transitory starch degradation takes place in the plastid. The starch granule surface is disrupted by phosphorylation followed by simultaneous glucan hydrolysis and dephosphorylation. Glc, mal and Glc-1-P are exported to the cytosol. GWD, glucan water dikinase. PWD, phosphoglucan water dikinase. SEX4 and LSF2, phosphoglucan phosphatases. ISA, isoamylase. LD, limit dextrinase. AMY. α-amylase. BAM, β-amylase. PHS1, α-glucan phosphorylase. DPE1, dispropotionating enzyme.

Kinases and Phosphorylases

Starch breakdown is facilitated by kinases which initiate and control degradation. Glucan water dikinase (GWD) and phosphoglucan waker dikinase (PWD) phosphorylate glucosyl residues at the C6 and C3 respectively (Ritte et al., 2006). The phosphate groups disrupt the semi-crystalline surface of starch and hence affect the susceptibility of the granule surface to enzyme degradation by endo-acting hydrolases (Blennow et al., 2000, Blennow et al., 2002). Mutations that eliminate the *GWD* enzyme activity dramatically reduce the rate of starch

degradation (Mikkelsen et al., 2004). *In vitro* experiments show that in the presence of GWD (and ATP) enables hydrolytic enzymes to release more soluble glucans from starch (Edner et al., 2007). PWD is also required for normal starch breakdown in Arabidopsis though it relies on the prior action of GWD (Kotting et al., 2005, Baunsgaard et al., 2005).

Two phosphorylases play a role in balancing glucan levels during starch metabolism. The plastidial PHS1 converts linear glucans to glucose-1-phosphate (Malinova et al., 2014). Cytosolic PHS2 removes glucose from a complex cytosolic heteroglycan to release glucose-1-phosphate (Schopper et al., 2015).

Phosphatases

The removal of the phosphate groups present on glucans released from the surface of starch is performed by the phosphatases SEX4 (C3/C6 specific) (Hejazi et al., 2010) and LSF1 (C3 specific) (Silver et al., 2014). Phosphate removal is required because exo-acting enzymes are blocked by phosphate groups (Hizukuri et al., 1983). Mutation of *SEX4* in Arabidopsis decreases the rate of starch degradation and leads to accumulation of soluble phospho-oligosaccharides during the night (Zeeman et al., 1998, Niittyla et al., 2006, Kotting et al., 2009). *LSF1* mutants also produce a starch excess phenotype (Comparot-Moss et al., 2010).

β-Amylase

Exo-acting β-amylase catalyses the release of maltose from the reducing end of linear glucans. Four of the nine β-amylase proteins encoded by the Arabidopsis genome are predicted to be chloroplastic (Zeeman et al., 2010). Two β-amylases, *BAM1* and *BAM3*, are partially redundant, however the double mutant has a strong starch excess phenotype. *BAM2* mutants are indistinguishable from wild type (Fulton et al., 2008). BAM4 is non-catalytic but it is still required for normal starch synthesis (Fulton et al., 2008).

Debranching Enzymes (DBE)

Only two debranching proteins, ISA3 and LD, are thought to function in starch degradation (Zeeman et al., 2007, Wischmann et al., 1999). Both enzymes preferentially remove short glucan branches. The precise substrate preferences differ but there is overlap between the two enzymes (Hii et al., 2012). Mutants of Arabidopsis ISA3 have more leaf starch and a slower starch breakdown rate. When fused to GFP, ISA3 localises to granule like structures in chloroplasts, implying ISA3 acts at surface of starch granule (Delatte et al., 2006). When LD or α-amylase are mutated in addition to *ISA3* a starch excess phenotype is achieved (Figure 1.13).

However, removal of LD, α-amylase or both enzymes has no effect on starch degradation (Streb et al., 2012). This confirms that these enzymes are partially redundant and a severe phenotype is only produced when all steps are blocked (Streb et al., 2012).

Figure 1.13 The effect of mutation in α-amylase, isoamylase 3 and limit dextrinase on Arabidopsis growth.
Growth was proportional to starch excess phenotype. Image from (Streb et al., 2012).

α-Amylase

α-amylase is an endo-acting enzyme that cleaves in the middle of linear glucans. Arabidopsis mutants of α-amylase show that none of the isoforms are essential to starch degradation (Yu et al., 2005). *In vitro* analysis shows α-amylase is capable of releasing glucans from insoluble starch granules as well as soluble substrates (Seung et al., 2013). As discussed above, the absence of α-amylase can be compensated for by ISA3 (Streb et al., 2012).

Disproportionating Enzymes

β-Amylolytic degradation is expected to produce some maltotriose alongside maltose due to the inability of β-amylase to cleave chains shorter than four glucosyl residues in length (Lao et al., 1999). Disproportionating enzymes overcome this issue by catalysing the transfer of carbohydrate from soluble glucans and to other acceptor glucans. For insctance, DPE1 is active in the plastidial stroma and generates linear glucans from maltodextrins by transferring 1, 2 or 3 glucose residues (Kartal et al., 2011). Cytosolic DPE2 transfers 1 glucose unit from maltose to high molecular weight glucan and releases a single glucose residue (Dumez et al., 2006).

1.4.4 Grain Storage Starch Degradation

Starch degradation in the cereal endosperm takes place in non-living tissue; an acidic, apoplastic environment, devoid of compartmentalisation (Smith et al., 2005, Sreenivasulu and Wobus, 2013). Hydrolysis of starch is proposed to proceed *via* the concerted activities of four enzymes, α-amylase, β-amylase, LD and α-glucosidase, which result in the production of glucose and maltose for export to the growing embryo (Figure 1.14) (Smith et al., 2005, Aoki et al., 2006). The extent to which all four classes of enzyme are necessary for starch degradation in cereals is subject to considerable debate (Stanley et al., 2011). It is not clear whether additional enzymes are important for grain starch metabolism. Transcripts for other enzymes involved in starch synthesis and degradation are present during the grain filling period (Radchuk et al., 2009) and there is possibility that these may be carried over to germination.

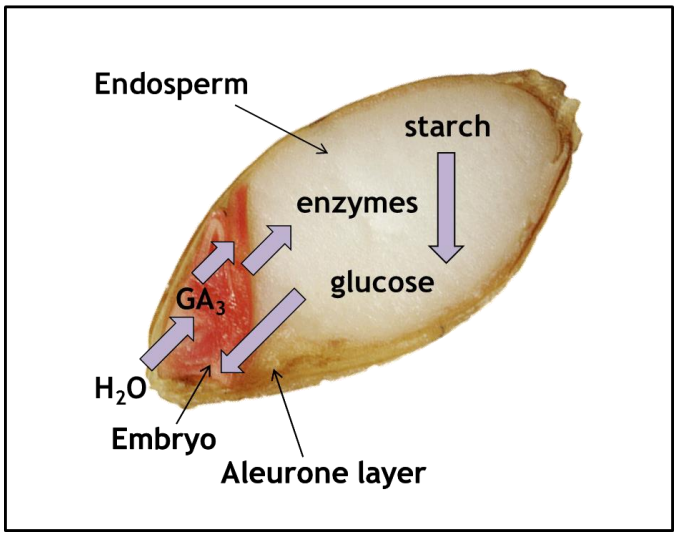

Figure 1.14 The steps involved in grain germination.
Germination is induced by the imbibition of water which acts to break grain dormancy and induces hormonal (gibberellic acid, GA and abscisic acid, ABA) changes within the grain (Lovegrove and Hooley, 2000). This results in the synthesis, release and activation of the starch degrading enzymes from the aleurone layer, a thin layer of cells surrounding the endosperm (Ritchie et al., 1999, Finnie et al., 2011). The maltose and glucose produced by hydrolysis of starch is utilised by the growing embryo.

α-Amylase

In germinating barley there are two classes of α-amylase, these are more closely related to the extraplastidial Arabidopsis AMY1 than chloroplastic AMY3. α-amylase is a GH13, endo-acting enzyme capable of directly attacking the starch granule and releasing linear glucans (Figure 1.15) (Nielsen et al., 2009). α-amylase has been extensively studied with regard to its gibberellic acid induced synthesis and release from the aleurone layer (Radchuk et al., 2009). α-amylase is not able to hydrolyse glucans within a close proximity to a branch point (Bak-Jensen et al., 2004).

β-Amylase

The importance of β-amylase in grain germination is not clear (Rejzek et al., 2011). β-amylase is an exo-acting enzyme that removes maltose from the non-reducing end of glucans (Figure 1.15). Rye and barley mutants with low β-amylase activities (Rorat et al., 1991, Kreis et al., 1987) and Tibetan β-amylase deficient barley (Kihara et al., 1999) all germinate normally suggesting β-amylase may not be required for successful germination. In barley, β-amylase is synthesised during grain development and is one of the major proteins present in mature grains, accounting for 1-2 % of total protein present in the endosperm (Hejgaard and Boisen, 1980, Evans et al., 1997), because of this fact β-amylase is often referred to as a storage protein.

Limit Dextrinase (LD)

LD is involved in both endosperm and leaf starch degradation alongside starch synthesis, as previously described. LD and its proteinaceous inhibitor (LDI) are further discussed in detail in chapter 5 (*in vitro* biochemistry and enzymology) and chapter 6 (*in planta* functions). LD is the only α-1,6-acting enzyme active during germination, hydrolysing the limit dextrins generated by α-amylase and β-amylase hydrolysis of starch (Macgregor et al., 1994). LDI is proposed to inhibit LD during germination (Macgregor et al., 2000), the *in vitro* interactions between the two proteins have been studied in detail (Møller et al., 2015), yet their roles in germination are unclear.

α-glucosidase

α-glucosidase has often been overlooked within the context of starch hydrolysis during brewing because of its heat lability. This fact has led to the belief that it is unimportant during the malting and mashing processes (Muslin et al., 2000, Bamforth, 2009). Evidence suggests that α-glucosidase can directly attack starch granules *in vitro* (Nakai et al., 2008, Sun and

Henson, 1991, Sissons et al., 1994). Multiple isoforms of α-glucosidase have been reported, with distinct specificities, in barley grain (Stark and Yin, 1987, Sun and Henson, 1990). Recent work using RNAi has shown that the α-glucosidase *HvAGL97* is involved in the conversion of maltose to glucose in the endosperm (Stanley et al., 2011). However this enzyme is not essential for starch degradation or normal seedling growth.

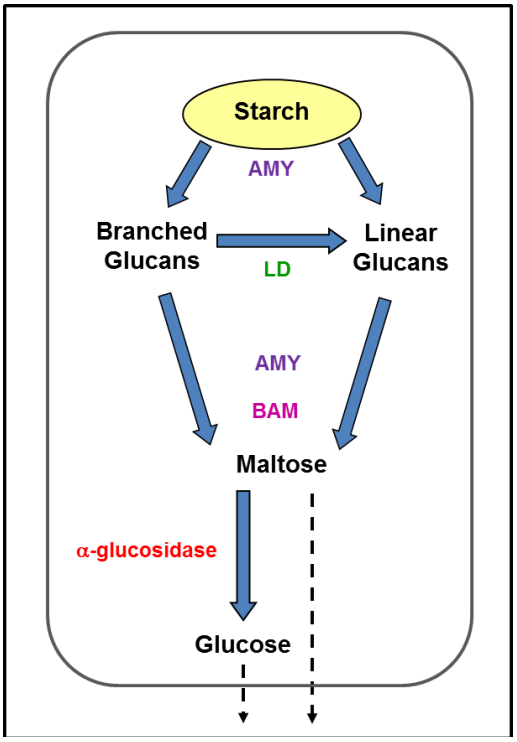

Figure 1.15 Proposed Pathway of Endosperm Starch Degradation.
α-Amylase attacks the starch granule and releases branched and linear glucans. Branched glucans are debranched by the action of LD. α-amylase and β-amylase act to hydrolyse linear glucans to produce maltose which is converted to glucose by α-glucosidase. Both glucose and maltose are taken up by the growing embryo.

1.5 The Brewing Process

1.5.1 Introduction

Malting is the controlled germination of cereal grain. The activities involved in grain germination constitute one of the three essential "enzyme reactor" stages of the brewing process, the other two being the mash tun and the yeast cell. All three of these systems are highly complex, consisting of a plethora of soluble and insoluble substrates with varying levels of enzymes, activators and inhibitors (Bamforth, 2009). Enzymatic activities, together with physical and chemical processes, such as the gelatinization of starch and the Maillard reaction, make this a complicated "melting pot" (Coghe et al., 2006).

1.5.2 Malting

Brewing (Figure 1.16) begins with malting, in which the germination process of grain is induced. Barley grains are steeped in water then are left to germinate (Gupta et al., 2010). Germination is then halted by kilning, a process in which grain is dried. (Macwilliam, 1972, Coghe et al., 2006, Palmer, 2006).

Figure 1.16 The brewing process.

1.5.3 Mashing

During mashing, milled malt is combined with water and heated. Starch is converted to glucose, maltose, maltotriose and other 1,4-linked glucans by the concerted action of the four enzymes: α-glucosidase, α-amylase, β-amylase and limit dextrinase (Figure 1.17) (Bamforth, 2009, Gupta et al., 2010,). Short, branched, limit dextrins are also formed, these cannot be metabolised by yeast but contribute to the mouthfeel and calorific value of beer (Tester and Qi, 2011, Ragot et al., 1989). Differences in 1,4 and 1,6 glucans contribute to the different qualities of different beer types (Petersen et al., 2012). Other sources of carbohydrate, termed adjuncts, can also be added to the malt to be converted to fermentable sugar.

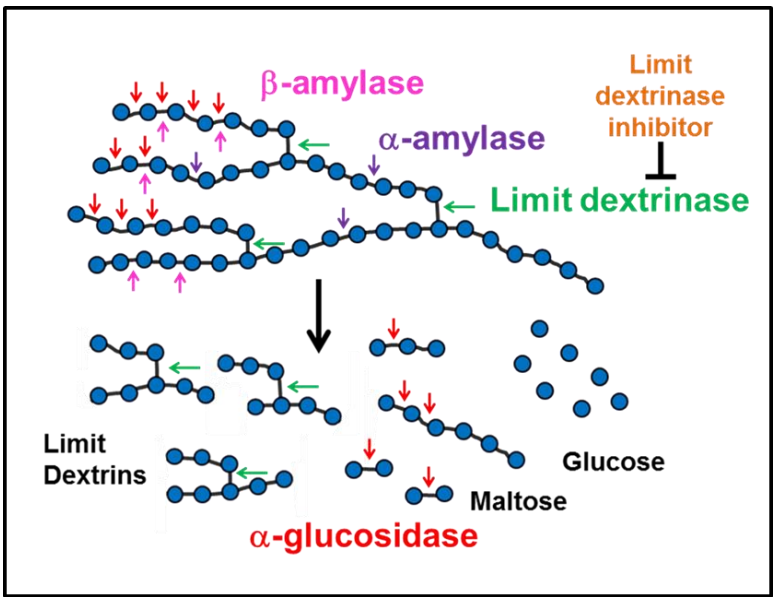

Figure 1.17 The enzymatic hydrolysis of starch during malting and mashing.
α-amylase cleaves in the middle of linear glucans. β-amylase releases maltose from the end of glucans. Limit dextrinase removes 1,6-branch points. Limit dextrinase activity is proposed to be inhibited by limit dextrinase inhibitor. α-glucosidase cleaves maltose to produce glucose.

Following mashing the sweet liquid (wort) is separated from the spent grain by filtration. The wort is boiled with hops to sterilise the liquid and add flavour (Natsume et al., 2015). The wort is then cooled and combined with yeast. The yeast (*Saccharomyces*) ferments the glucose, maltose and simple sugars to alcohol and carbon dioxide. The beer is finally filtered, bottled and aged. Distilled spirits are produced by a similar procedure, however there is no boiling step after mashing and the fermentation product is distilled (Delcour and Hoseney, 2010a).

1.6 Chemical Genetics

1.6.1 Introduction to Chemical Genetics

Due to the redundant nature of the enzymes involved in starch synthesis and degradation, genetic knockout can often produce unclear results. Chemical genetics offers a complementary approaches that can be utilised to gain a better understanding of starch metabolism. Recently chemical genetics has been utilised to dissect the enzymes involved in carbohydrate metabolism during barley germination (Stanley et al., 2011, Rejzek et al., 2011, Andriotis, 2015 unpublished). This literature is discussed in detail in later chapters.

Chemical genetics is defined as the systematic use of small molecules to elicit defined phenotypes in a biological system of interest (Stockwell, 2000). In contrast to traditional genetics, which disrupts a system at the nucleic acid level, chemical genetics affects a system at the protein level using small molecule (chemical) intervention (Spring, 2005). As with traditional genetics, both forward and reverse screens can be performed (Figure 1.18).

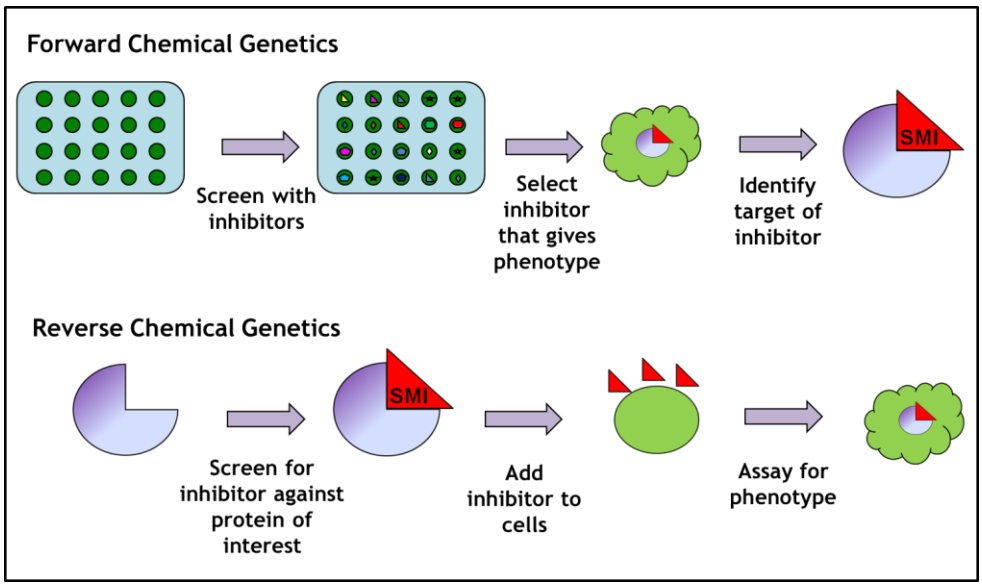

Figure 1.18 Forward and Reverse chemical genetics.
Within a forward screen a library of compounds is screened for a defined phenotype using the organism of interest (Stockwell, 2000). Following this, attempts are made to identify the target responsible for the change in phenotype, alongside the mode of action. Reverse chemical genetics involves screening a library of compounds against a purified protein of interest. Identified "hit" compounds are then tested on the biological system of interest to define the phenotype generated (Stockwell, 2000).

The use of small molecules has a number of advantages over molecular genetics (Spring, 2005). Small molecule inhibitor effects are reversible, titratable and conditional; they can be added at specific time points and in controlled concentrations, therefore allowing temporal and dose-response control (Stockwell, 2000). Further to this, they have a rapid effect, enabling study of immediate effects following addition of the compound compared with genetic manipulation in which a steady state is observed (Spring, 2005). As inhibitors typically work at a protein level a single compound can often affect several members of a multi-gene family thereby overcoming redundancy which would otherwise require time consuming and expensive multi-gene knockouts to study (O'Connor et al., 2011).

Small molecules can be used to study processes that would be affected beyond easy analysis by traditional genetic knock out, such as embryo development (Spring, 2005). As well as this, compounds can often be applied across species, overcoming issues such as large genomes, polyploidy and slow generation time which can often limit genetics, particularly in crop species (O'Connor et al., 2011). Perhaps the only disadvantage of chemical genetics is that currently it cannot be applied generally because of the requirement of a selective small molecule ligand for the protein of interest. To date, only a small fraction of known proteins have a suitable specific small molecule binder (O'Connor et al., 2011).

1.6.2 Requirements for Chemical Genetics

Three things are required for effective chemical genetics: a selective small molecule, biological target and a suitable biological screen or assay (Figure 1.19). This area has been the subject of numerous detailed reviews (Spring, 2005, Tóth and Van Der Hoorn, 2010, Toth and Van Der Hoorn, 2010, Fu, 2012).

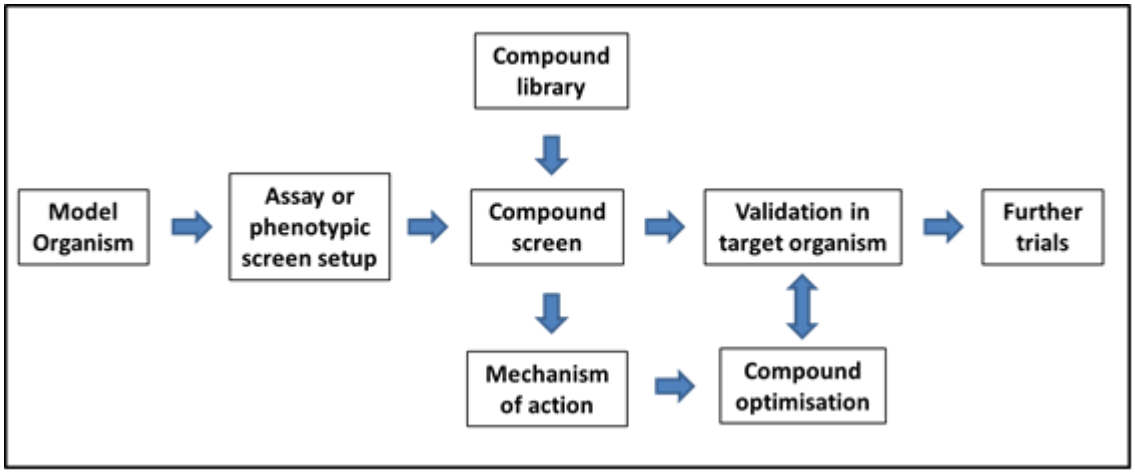

Figure 1.19 The pipeline of chemical genetics.
Adapted from (Fu, 2012)

1.6.3 Chemical Genetics in Plants

Chemical genetics are well established in eukaryotic systems (*Sacchatomyces cerevisiae, Caenorhabitis elegans, Drosphila melanogaster, Xenopus laevis* and *Danio rerio*) (reviewed (O'Connor et al., 2011, Stockwell, 2000, Gangadhar and Stockwell, 2007, Mayer, 2003)) and is emerging as a powerful complementary technique to classical biochemistry and genetic techniques within plant research.

Arabidopsis is the chosen plant for chemical genetics due to its ease of manipulation enabled by the small size of plants and seeds. These seeds can be utilised in microtitre plates (Zhao et al., 2007) and can be easily stored for long periods (Mccourt and Desveaux, 2010). It is further supported by being the first plant to have its genome sequenced (Arabidopsis-Genome-Initiative, 2000) making it a foundation for plant research (Bevan and Walsh, 2005). The genome, which is five times larger than that of yeast, is well annotated (TAIR-www.arabidopsis.org) and the plant is easily genetically manipulated, with extensive germplasm resources available. Comparison of human disease genes with the Arabidopsis genome reveals that 48 % (139/289) have homologues in Arabidopsis, making this plant a good

model for many human diseases (Arabidopsis-Genome-Initiative, 2000, Xu and Møller, 2011). Arabidopsis is also able to act as a model for other plants, although the evolutionary relationship between organisms and conservation of protein sequence, structure and function must be considered. Differences between plants, in particular, monocots and dicots can be extreme (Sreenivasulu and Wobus, 2013). Chemical genetic techniques have enabled recent advances within numerous areas of plant biology. This introduction will only focus on two aspects: cell wall biosynthesis and hormone signalling.

Inhibitors of Cellulose and Cell Wall Biosynthesis

The biosynthesis and deposition of cellulose within plant cell walls is not fully understood; being a complex process involving precise regulation, composition and arrangement of the proteins that catalyse it. Chemical genetics has played an important role in advancing the understanding of this process. (Debolt and Brabham, 2013). Cellulose synthase (CESA) proteins form a complex which is active at the plasma membrane where microfibrils are synthesised. There are 10 genes encoding CESA in Arabidopsis highlighting the likelihood of functional redundancy (Desprez et al., 2002). Three principle responses to chemical inhibition of cellulose biosynthesis have been documented utilising fluorescently tagged reporter proteins in combination with confocal microscopy (Brabham and Debolt, 2012), the compounds are outlined in Figure 1.20 and Table 1.3.

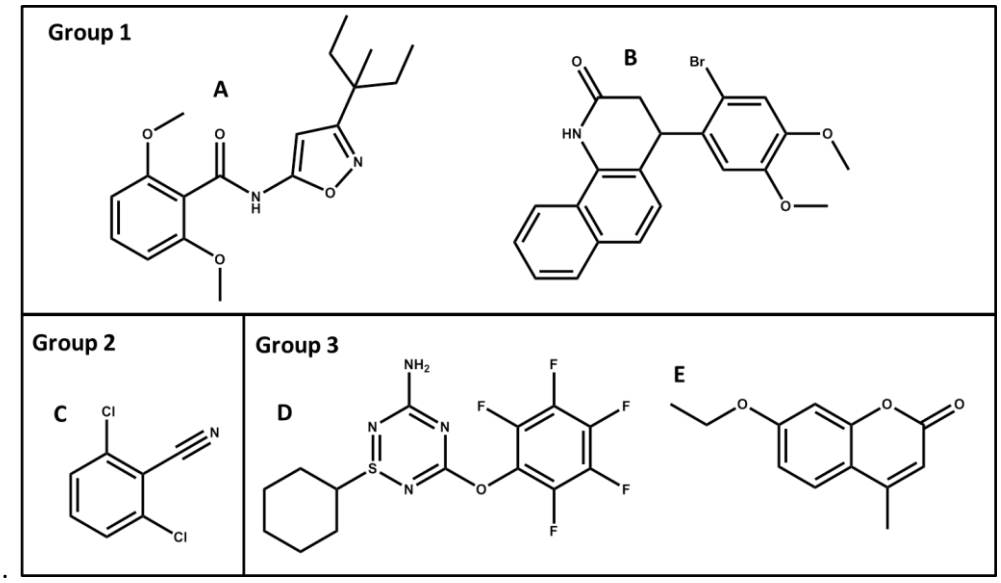

Figure 1.20 The structures of molecules able to interfere with cellulose biosynthesis.
A. Isoxaben**. B.** Quinoxyphen**. C.** DCB**. D.** Cobtorin**. E.** Morlin

Compound	Target	Use	Reference
Group 1. Deplete CESA from plasma membrane			
Isoxaben	Targets CESA3 & CESA6.	The observation that both compounds affect YFP-CESA6 localisation supports the notion that CESA 1, 3 and 6 interact to form functional cellulose synthase complex (CSC) required for cell wall biosynthesis. These inhibitors are useful for the study of non-CESA proteins associated with cellulose biosynthesis.	(Desprez et al., 2002, Robert et al., 2005).
Quinoxyphen	Targets CESA1.		(Gutierrez et al., 2009, Harris et al., 2012, Brabham and Debolt, 2012).
Group 2. Increase accumulation and cessation of CSC movement within the plasma membrane			
DCB	Targets MAP20, a microtubule associated protein.	Studies using this compound indicate MAPs could be necessary for primary and secondary cell wall development	(Delmer, 1987, Debolt et al., 2007, Rajangam et al., 2008).
Group 3. Disturb CESA and cortical microtubules			
Morlin	Causes disorganised CESA and hyper-bundled microtubules.	Molecular rail hypothesis suggests that microtubules act as a guidance mechanism for CSC; both morlin and cobtorin are useful tools to dissect the interplay between cellulose deposition and cortical microtubules.	(Giddings Jr and Staehelin, 1988, Debolt et al., 2007).
Cobtorin	Distorts the parallel alignment of microtubules and the behaviour of CESA.		(Yoneda et al., 2007, Yoneda et al., 2010).

Table 1.3 Molecules able to interfere with cellulose biosynthesis, identified by chemical genetics. Structures are given in Figure 1.20.

Inhibitors of Hormone Signalling

Plant hormones including auxins (AUX), cytokinins (CK), giberellins (GAs), abscisic acid (ABA), ethylene (ET), brassinosteriods (BRs), salicylic acid (SA) and jasmonates (JA) regulate multiple aspects of plant cell division, tissue patterning, gravitropism, root development, defence and adaptation (Wang and Irving, 2011). Recent development in genomics, genetics and molecular techniques have led to the discovery of a range of compounds capable of affecting most known hormone pathways, some of those with identified targets are outlined in Figure 1.21, Table 1.4 and Table 1.5 (Fonseca et al., 2014).

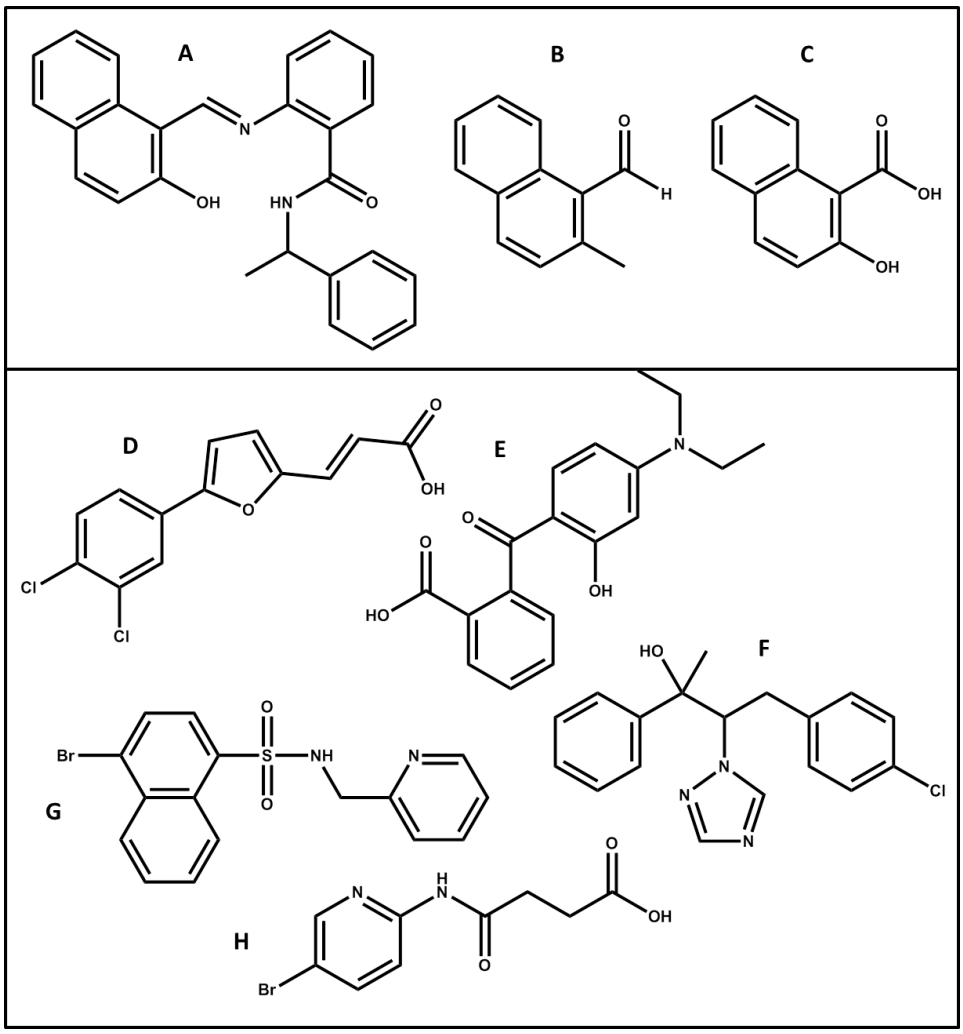

Figure 1.21 The structures of molecules involved in interfering with hormone signalling within plants. **A.** Sirtinol. **B.** HNC. **C.** HNA. **D.** Gravacin. **E.** BUM. **F.** Brassinazole. **G.** Pyrabactin. **H.** Bikinin.

Compound/ hormone affected	Screen	Notes	Use	Reference
Pyrabactin ABA	Arabidopsis seedling development.	Targets a sub set of novel ABA receptors (PYR/PYLs), which bind and inhibit type 2C protein phosphatases. Multiple genetic knockouts of the receptors showed no phenotype indicating genetic redundancy.	Affects ABA signalling. Quinabactin, a similar molecule also interacts with PYLs and is shown to regulate stomatal closure.	(Park et al., 2009, Okamoto et al., 2013).
Brassinazole BR	Arabidopsis screen for inhibitors causing dwarfism and altered leaf morphology.	Binds DWF4, a cytochrome p450 monooxygenase that catalyses the hydroxylation of BRs.	These compounds can complement the use of BR-deficient mutants to clarify the function of BRs in plants.	(Asami et al., 2000).
Bikinin BR	Phenotype based Arabidopsis screen.	Target was identified as glycogen synthase kinase 3 (GSK3)- BIN2 a key regulator in signalling pathways. Genome-wide transcript analyses demonstrate that bikinin simultaneously inhibits of seven GSK3s; a phenotype that could not be produced using genetics.		(De Rybel et al., 2009)

Table 1.4 Molecules able to interfere with hormone metabolism, identified by chemical genetics.

Compound/ hormone affected	Screen	Notes	Use	Reference
Sirtinol ABA	First identified in yeast screens.	Targets SIR1, an NAD-dependent deacetylase inhibitor causing stunted root growth phenotypes. More detailed studies revealed sirtinol is not an active compound but is a pro-drug that is taken up and activated to functional HNA and HNC by plant metabolic enzymes.	Affects ABA signalling.	(Grozinger et al., 2001, Dai et al., 2005)
Gravacin AUX	Identified using Arabidopsis in a 24-well plate based screen, involving a 90° reorientation of the plates during growth.	Inhibitor of root and shoot gravitropism, targets the p-glycoprotein-19, an auxin efflux transporter belonging to a family containing up to 129 genes.	Both gravacin and BUM leave PIN proteins unaffected making these compounds useful tools in auxin research.	(Surpin et al., 2005, Rojas-Pierce et al., 2007, Kim et al., 2010)
BUM AUX	Visual screen of Arabidopsis seedling development.	Inhibitor of ABCB (ATP binding cassette protein subfamily B) auxin efflux carriers.		(De Rybel et al., 2009)

Table 1.5 Molecules able to interfere with hormone metabolism, identified by chemical genetics

The Future of Chemical Genetics

New herbicides, pesticides and other agricultural chemical tools are required. Naturally occurring bioactive compounds have the potential to fulfil this requirement (Walsh, 2007, Dayan et al., 2012, Duke, 2012). Alleochemicals are found naturally in plants, only a few well studied examples exist: sorgoleone, a phytotoxic compound excreted by *Sorghum bicolor* roots (Figure 1.22, D) (Dayan et al., 2010), meta-tyrosine, a herbicidal root exudate from fescue grass (Figure 1.22, A) (Bertin et al., 2007), juglone, from black walnut *Juglans nigra* (Figure 1.22, C) (Hejl and Koster, 2004) which disrupts root plasma membrane H+ ATPase and strigolactones (SLs) from the parasitic plant *Striga asiatica* which induce host germination (Figure 1.22, B) (Gomez-Roldan et al., 2008, Umehara et al., 2008).

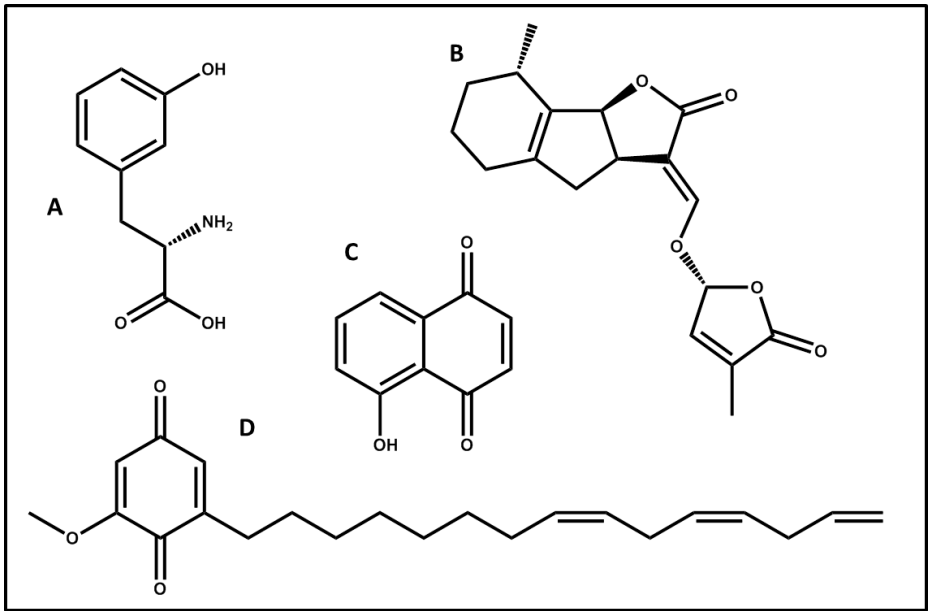

Figure 1.22 The structures of well studies alleochemicals.
A. Meta-tyrosine. **B.** Strigolactone. **C.** Juglone **D.** Sorgoleone.

Alongside natural products, combinatorial libraries have the potential to produce new agrochemicals. Analysis of the molecular properties of herbicides resulted in Tice's Rule-of-five (Tice, 2001), which follow the rules for drug design outlined by Lipinsky (Lipinski et al., 2001). In contrast, diversity oriented synthesis libraries represent new chemical space and have the potential for identification of novel biological modulators (Ibbeson et al., 2014).

1.7 Experimental Approach

Discovering the roles and importance of the enzymes directly and indirectly involved in starch degradation *in vivo* has been hampered by the lack of tools for analysis of these pathways. The existence of multiple genes and isoforms that correspond to different activities, expressed in different plant organs, makes genetic manipulation a non-trivial task.

However, a chemical genetic approach has been used within our group to dissect the pathway in question. These studies identified reversible and irreversible inhibitors for a number of starch active enzymes (Rejzek et al., 2011, Stanley et al., 2011) alongside providing evidence for the existence of previously unidentified enzymatic activities that are key to starch metabolism (Stanley et al., 2011).

This thesis will describe a similar chemical genetic approach which has been utilised to study barley limit dextrinase, the enzyme responsible for the hydrolysis of α-1,6-linked branch points found within glucans derived from starch. The aims of this work are fourfold:

- Identify novel iminosugar compounds which are able to interfere with germination and plant growth within dicots and monocots.

- Clone the genes encoding LD and the proteinaceous inhibitor, LDI, express protein in *E. coli* and purify the proteins to homogeneity.

- Carry out chemical genetic screens against LD protein in order to identify small molecule inhibitors.

- Establish LD and LDI RNAi transgenic barley lines and develop systems by which to analyse the roles of LD and LDI *in planta.*

1.8 References

Akram, M., Asif, H., Akhtar, N., Shah, P., Uzair, M., Shaheen, G. & Ahmad, K. 2011. Glycogen metabolism and glycogen storage diseases: A review. *Journal of Medicinal Plants Research,* 5, 4980-4983.

An, H. J., Kronewitter, S. R., De Leoz, M. L. & Lebrilla, C. B. 2009. Glycomics and disease markers. *Current Opinion in Chemical Biology,* 13, 601-7.

Andrews, J. H., Harris, R. F., Spear, R. N., Lau, G. W. & Nordheim, E. V. 1994. Morphogenesis and adhesion of *Aureobasidium pullulans*. *Canadian Journal of Microbiology,* 40, 6-17.

Aoki, N., Scofield, G. N., Wang, X.-D., Offler, C. E., Patrick, J. W. & Furbank, R. T. 2006. Pathway of sugar transport in germinating wheat seeds. *Plant Physiology,* 141, 1255-1263.

Arabidopsis-Genome-Initiative 2000. Analysis of the genome sequence of the flowering plant *Arabidopsis thaliana*. *Nature,* 408, 796-815.

Asami, T., Min, Y. K., Nagata, N., Yamagishi, K., Takatsuto, S., Fujioka, S., Murofushi, N., Yamaguchi, I. & Yoshida, S. 2000. Characterization of brassinazole, a triazole-type brassinosteroid biosynthesis inhibitor. *Plant Physiology,* 123, 93-100.

Baik, B.-K. & Ullrich, S. E. 2008. Barley for food: Characteristics, improvement, and renewed interest. *Journal of Cereal Science,* 48, 233-242.

Bak-Jensen, K. S., André, G., Gottschalk, T. E., Paës, G., Tran, V. & Svensson, B. 2004. Tyrosine 105 and threonine 212 at outermost substrate binding subsites –6 and +4 control substrate specificity, oligosaccharide cleavage patterns, and multiple binding modes of barley α-amylase 1. *Journal of Biological Chemistry,* 279, 10093-10102.

Ball, S., Guan, H.-P., James, M., Myers, A., Keeling, P., Mouille, G., Buléon, A., Colonna, P. & Preiss, J. 1996. From glycogen to amylopectin: A model for the biogenesis of the plant starch granule. *Cell,* 86, 349-352.

Bamforth, C. W. 2009. Current perspectives on the role of enzymes in brewing. *Journal of Cereal Science,* 50, 353-357.

Baunsgaard, L., Lütken, H., Mikkelsen, R., Glaring, M. A., Pham, T. T. & Blennow, A. 2005. A novel isoform of glucan, water dikinase phosphorylates pre-phosphorylated α-glucans and is involved in starch degradation in *Arabidopsis*. *The Plant Journal,* 41, 595-605.

Bender, H., Lehmann, J. & Wallenfels, K. 1959. Pullulan, ein extracelluläres glucan von pullularia pullulans. *Biochimica et biophysica acta,* 36, 309-316.

Bender, H. & Wallenfels, K. 1961. Untersuchungen an pullulan. 2. Spezifischer abbau durch ein bakterielles enzym. *Biochemische Zeitschrift,* 334, 79-&.

Bertin, C., Weston, L. A., Huang, T., Jander, G., Owens, T., Meinwald, J. & Schroeder, F. C. 2007. Grass roots chemistry: Meta-tyrosine, an herbicidal nonprotein amino acid. *Proceedings of the National Academy of Sciences of the United States of America,* 104, 16964-9.

Bevan, M. & Walsh, S. 2005. The *Arabidopsis* genome: A foundation for plant research. *Genome Research,* 15, 1632-1642.

Bhattacharyya, M. K., Smith, A. M., Ellis, T. N., Hedley, C. & Martin, C. 1990. The wrinkled-seed character of pea described by mendel is caused by a transposon-like insertion in a gene encoding starch-branching enzyme. *Cell,* 60, 115-122.

Blennow, A., Bay-Smidt, A. M., Olsen, C. E. & Møller, B. L. 2000. The distribution of covalently bound phosphate in the starch granule in relation to starch crystallinity. *International Journal of Biological Macromolecules,* 27, 211-218.

Blennow, A., Jensen, S. L., Shaik, S. S., Skryhan, K., Carciofi, M., Holm, P. B., Hebelstrup, K. H. & Tanackovic, V. 2013. Future cereal starch bioengineering: Cereal ancestors encounter gene technology and designer enzymes. *Cereal Chemistry Journal,* 90, 274-287.

Blennow, A., Nielsen, T. H., Baunsgaard, L., Mikkelsen, R. & Engelsen, S. B. 2002. Starch phosphorylation: A new front line in starch research. *Trends in Plant Science,* 7, 445-450.

Borrill, P., Connorton, J. M., Balk, J., Miller, A. J., Sanders, D. & Uauy, C. 2014. Biofortification of wheat grain with iron and zinc: Integrating novel genomic resources and knowledge from model crops. *Frontiers in Plant Science,* 5, 53.

Bouveng, H. O., Kiessling, H., Lindberg, B. & Mckay, J. 1963. Polysaccharides elaborated by *Pullularia pullulans*. *Acta Chemica Scandinavica,* 17, 797-800.

Brabham, C. & Debolt, S. 2012. Chemical genetics to examine cellulose biosynthesis. *Frontiers in Plant Science,* 3, 309.

Burton, R. A., Bewley, J. D., Smith, A. M., Bhattacharyya, M. K., Tatge, H., Ring, S., Bull, V., Hamilton, W. & Martin, C. 1995. Starch branching enzymes belonging to distinct enzyme families are differentially expressed during pea embryo development. *The Plant Journal,* 7, 3-15.

Bustos, R., Fahy, B., Hylton, C. M., Seale, R., Nebane, N. M., Edwards, A., Martin, C. & Smith, A. M. 2004. Starch granule initiation is controlled by a heteromultimeric isoamylase in potato tubers. *Proceedings of the National Academy of Sciences of the United States of America,* 101, 2215-20.

Carciofi, M., Blennow, A., Jensen, S., Shaik, S., Henriksen, A., Buléon, A., Holm, P. & Hebelstrup, K. 2012. Concerted suppression of all starch branching enzyme genes in barley produces amylose-only starch granules. *BMC Plant Biology,* 12, 1-16.

Carolan, G., Catley, B. J. & Mcdougal, F. J. 1983. The location of tetrasaccharide units in pullulan. *Carbohydrate Research,* 114, 237-243.

Chaikuad, A., Froese, D. S., Berridge, G., Von Delft, F., Oppermann, U. & Yue, W. W. 2011. Conformational plasticity of glycogenin and its maltosaccharide substrate during glycogen biogenesis. *Proceedings of the National Academy of Sciences of the United States of America,* 108, 21028-33.

Cheng, K.-C., Demirci, A. & Catchmark, J. 2011. Pullulan: Biosynthesis, production, and applications. *Applied Microbiology and Biotechnology,* 92, 29-44.

Coelho, M., Oliveira, T. & Fernandes, R. 2013. Biochemistry of adipose tissue: An endocrine organ. *Archives of Medical Science : AMS,* 9, 191-200.

Coghe, S., Gheeraert, B., Michiels, A. & Delvaux, F. R. 2006. Development of maillard reaction related characteristics during malt roasting. *Journal of the Institute of Brewing,* 112, 148-156.

Comparot-Moss, S., Kötting, O., Stettler, M., Edner, C., Graf, A., Weise, S. E., Streb, S., Lue, W.-L., Maclean, D., Mahlow, S., Ritte, G., Steup, M., Chen, J., Zeeman, S. C. & Smith, A. M. 2010. A putative phosphatase, lsf1, is required for normal starch turnover in *Arabidopsis* leaves. *Plant Physiology,* 152, 685-697.

Cordain, L. 1999. Cereal grains: Humanity's double-edged sword. *World Review of Nutrition and Dietetics,* 84, 19-73.

D'hulst, C. & Merida, A. 2010. The priming of storage glucan synthesis from bacteria to plants: Current knowledge and new developments. *New Phytologist,* 188, 13-21.

Dai, X., Hayashi, K., Nozaki, H., Cheng, Y. & Zhao, Y. 2005. Genetic and chemical analyses of the action mechanisms of sirtinol in *Arabidopsis*. *Proceedings of the National Academy of Sciences of the United States of America,* 102, 3129-34.

Dayan, F. E., Owens, D. K. & Duke, S. O. 2012. Rationale for a natural products approach to herbicide discovery. *Pest Management Science,* 68, 519-28.

Dayan, F. E., Rimando, A. M., Pan, Z., Baerson, S. R., Gimsing, A. L. & Duke, S. O. 2010. Sorgoleone. *Phytochemistry,* 71, 1032-9.

De Rybel, B., Audenaert, D., Vert, G., Rozhon, W., Mayerhofer, J., Peelman, F., Coutuer, S., Denayer, T., Jansen, L., Nguyen, L., Vanhoutte, I., Beemster, G. T., Vleminckx, K., Jonak, C., Chory, J., Inze, D., Russinova, E. & Beeckman, T. 2009. Chemical inhibition of a subset of *Arabidopsis thaliana* gsk3-like kinases activates brassinosteroid signaling. *Chemistry and Biology,* 16, 594-604.

Debolt, S. & Brabham, C. 2013. Chemical genetics to examine cellulose biosynthesis. *Frontiers in Plant Science,* 3.

Debolt, S., Gutierrez, R., Ehrhardt, D. W., Melo, C. V., Ross, L., Cutler, S. R., Somerville, C. & Bonetta, D. 2007. Morlin, an inhibitor of cortical microtubule dynamics and cellulose synthase movement. *Proceedings of the National Academy of Sciences of the United States of America,* 104, 5854-9.

Delatte, T., Umhang, M., Trevisan, M., Eicke, S., Thorneycroft, D., Smith, S. M. & Zeeman, S. C. 2006. Evidence for distinct mechanisms of starch granule breakdown in plants. *The Journal of Biological Chemistry,* 281, 12050-9.

Delcour, J. & Hoseney, R. C. 2010a. Chapter 11: Malting and brewing. *Principles of cereal science and technology.* AACC International, Inc.

Delcour, J. A. & Hoseney, R. C. 2010b. Chapter 2: Starch. *Principles of cereal science and technology.* AACC International, Inc.

Delmer, D. P. 1987. Cellulose biosynthesis. *Annual Review of Plant Physiology,* 38, 259-290.

Denyer, K., Hylton, C., Jenner, C. F. & Smith, A. 1995. Identification of multiple isoforms of soluble and granule-bound starch synthase in developing wheat endosperm. *Planta,* 196, 256-265.

Desprez, T., Vernhettes, S., Fagard, M., Refregier, G., Desnos, T., Aletti, E., Py, N., Pelletier, S. & Hofte, H. 2002. Resistance against herbicide isoxaben and cellulose deficiency caused by distinct mutations in same cellulose synthase isoform cesa6. *Plant Physiology,* 128, 482-90.

Doehlert, D. C., Kuo, T. M., Juvik, J. A., Beers, E. P. & Duke, S. H. 1993. Characteristics of carbohydrate metabolism in sweet corn (sugary-1) endosperms. *Journal of the American Society for Horticultural Science,* 118, 661-666.

Duke, S. O. 2012. Why have no new herbicide modes of action appeared in recent years? *Pest Management Science,* 68, 505-12.

Dumez, S., Wattebled, F., Dauvillee, D., Delvalle, D., Planchot, V., Ball, S. G. & D'hulst, C. 2006. Mutants of *Arabidopsis* lacking starch branching enzyme ii substitute plastidial starch synthesis by cytoplasmic maltose accumulation. *Plant Cell,* 18, 2694-709.

Edner, C., Li, J., Albrecht, T., Mahlow, S., Hejazi, M., Hussain, H., Kaplan, F., Guy, C., Smith, S. M., Steup, M. & Ritte, G. 2007. Glucan, water dikinase activity stimulates breakdown of starch granules by plastidial beta-amylases. *Plant Physiology,* 145, 17-28.

Evans, D. E., Macleod, L. C., Eglinton, J. K., Gibson, C. E., Zhang, X., Wallace, W., Skerritt, J. H. & Lance, R. C. M. 1997. Measurement ofbeta-amylase in malting barley (hordeum vulgarel.). I. Development of a quantitative elisa forbeta-amylase. *Journal of Cereal Science,* 26, 229-239.

Facon, M., Lin, Q., Azzaz, A. M., Hennen-Bierwagen, T. A., Myers, A. M., Putaux, J. L., Roussel, X., D'hulst, C. & Wattebled, F. 2013. Distinct functional properties of isoamylase-type starch debranching enzymes in monocot and dicot leaves. *Plant Physiology,* 163, 1363-75.

Faostat. 2014. *Food and agriculture organization of the united nations statistics division* [Online]. Available: http://faostat3.fao.org/home/E.

Finnie, C., Andersen, B., Shahpiri, A. & Svensson, B. 2011. Proteomes of the barley aleurone layer: A model system for plant signalling and protein secretion. *Proteomics,* 11, 1595-605.

Fonseca, S., Rosado, A., Vaughan-Hirsch, J., Bishopp, A. & Chini, A. 2014. Molecular locks and keys: The role of small molecules in phytohormone research. *Frontiers in Plant Science,* 5, 709.

Fredriksson, H., Silverio, J., Andersson, R., Eliasson, A. C. & Åman, P. 1998. The influence of amylose and amylopectin characteristics on gelatinization and retrogradation properties of different starches. *Carbohydrate Polymers,* 35, 119-134.

Fu, H., Ed. 2012. *Chemical genomics*, Cambridge University Press.

Fulton, D. C., Stettler, M., Mettler, T., Vaughan, C. K., Li, J., Francisco, P., Gil, M., Reinhold, H., Eicke, S., Messerli, G., Dorken, G., Halliday, K., Smith, A. M., Smith, S. M. & Zeeman, S. C. 2008. Beta-amylase 4, a noncatalytic protein required for starch breakdown, acts upstream of three active beta-amylases in *Arabidopsis* chloroplasts. *Plant Cell,* 20, 1040-58.

Gangadhar, N. M. & Stockwell, B. R. 2007. Chemical genetic approaches to probing cell death. *Current Opinions in Chemical Biology,* 11, 83-7.

Giddings Jr, T. H. & Staehelin, L. A. 1988. Spatial relationship between microtubules and plasma-membrane rosettes during the deposition of primary wall microfibrils in *Closterium* sp. *Planta,* 173, 22-30.

Gilbert, H. J. 2010. The biochemistry and structural biology of plant cell wall deconstruction. *Plant Physiology,* 153, 444-455.

Givens, D. I., Davies, T. W. & Laverick, R. M. 2004. Effect of variety, nitrogen fertiliser and various agronomic factors on the nutritive value of husked and naked oats grain. *Animal Feed Science and Technology,* 113, 169-181.

Gomez-Roldan, V., Fermas, S., Brewer, P. B., Puech-Pages, V., Dun, E. A., Pillot, J.-P., Letisse, F., Matusova, R., Danoun, S., Portais, J.-C., Bouwmeester, H., Becard, G., Beveridge, C. A., Rameau, C. & Rochange, S. F. 2008. Strigolactone inhibition of shoot branching. *Nature,* 455, 189-194.

Graf, A., Schlereth, A., Stitt, M. & Smith, A. M. 2010. Circadian control of carbohydrate availability for growth in *Arabidopsis* plants at night. *Proceedings of the National Academy of Sciences of the United States of America*, 107, 9458-9463.

Grennan, A. K. 2006. Regulation of starch metabolism in *Arabidopsis* leaves. *Plant Physiology,* 142, 1343-1345.

Grozinger, C. M., Chao, E. D., Blackwell, H. E., Moazed, D. & Schreiber, S. L. 2001. Identification of a class of small molecule inhibitors of the sirtuin family of NAD-dependent deacetylases by phenotypic screening. *Journal of Biological Chemistry,* 276, 38837-43.

Guan, H. P. & Preiss, J. 1993. Differentiation of the properties of the branching isozymes from maize (*Zea mays*). *Plant Physiology,* 102, 1269-1273.

Gupta, M., Abu-G., N. & Gallaghar, E. 2010. Barley for brewing: Characteristic changes during malting, brewing and applications of its by-products. *Comprehensive Reviews in Food Science and Food Safety,* 9, 318-328.

Gutierrez, R., Lindeboom, J. J., Paredez, A. R., Emons, A. M. & Ehrhardt, D. W. 2009. *Arabidopsis* cortical microtubules position cellulose synthase delivery to the plasma membrane and interact with cellulose synthase trafficking compartments. *Nature Cell Biology,* 11, 797-806.

Halley, P. & Avérous, L. 2014. *Starch polymers: From genetic engineering to green applications*, Newnes.

Hamley, I. W. 2010. Liquid crystal phase formation by biopolymers. *Soft Matter,* 6, 1863-1871.

Hancock, I. C. 1997. Bacterial cell surface carbohydrates: Structure and assembly. *Biochemical Society Transactions,* 25, 183-7.

Hardy, K., Brand-Miller, J., Brown, K. D., Thomas, M. G. & Copeland, L. 2015. The importance of dietary carbohydrate in human evolution. *The Quarterly Review of Biology,* 90, 251-268.

Harris, D. M., Corbin, K., Wang, T., Gutierrez, R., Bertolo, A. L., Petti, C., Smilgies, D.-M., Estevez, J. M., Bonetta, D., Urbanowicz, B. R., Ehrhardt, D. W., Somerville, C. R., Rose, J. K. C., Hong, M. & Debolt, S. 2012. Cellulose microfibril crystallinity is reduced by mutating C-terminal transmembrane region residues cesa1a903v and cesa3t942i of cellulose synthase. *Proceedings of the National Academy of Sciences of the United States of America,* 109, 4098-4103.

Hejazi, M., Fettke, J., Kotting, O., Zeeman, S. C. & Steup, M. 2010. The laforin-like dual-specificity phosphatase sex4 from *Arabidopsis* hydrolyzes both C6- and C3-phosphate esters introduced by starch-related dikinases and thereby affects phase transition of alpha-glucans. *Plant Physiology,* 152, 711-22.

Hejgaard, J. & Boisen, S. 1980. High-lysine proteins in hiproly barley breeding: Identification, nutritional significance and new screening methods. *Hereditas,* 93, 311-320.

Hejl, A. M. & Koster, K. L. 2004. Juglone disrupts root plasma membrane H+-ATPase activity and impairs water uptake, root respiration, and growth in soybean (*Glycine max*) and corn (*Zea mays*). *Journal of Chemical Ecology,* 30, 453-471.

Hii, S. L., Tan, J. S., Ling, T. C. & Ariff, A. B. 2012. Pullulanase: Role in starch hydrolysis and potential industrial applications. *Enzyme Research,* 2012.

Hizukuri, S. 1985. Relationship between the distribution of the chain length of amylopectin and the crystalline structure of starch granules. *Carbohydrate Research,* 141, 295-306.

Hizukuri, S. 1986. Polymodal distribution of the chain lengths of amylopectins, and its significance. *Carbohydrate Research,* 147, 342-347.

Hizukuri, S., Shirasaka, K. & Juliano, B. O. 1983. Phosphorus and amylose branching in rice starch granules. *Starch - Stärke,* 35, 348-350.

Hsien-Chih, H. W. & Sarko, A. 1978. The double-helical molecular structure of crystalline A-amylose. *Carbohydrate Research,* 61, 27-40.

Ibbeson, B. M., Laraia, L., Alza, E., O' Connor, C. J., Tan, Y. S., Davies, H. M. L., Mckenzie, G., Venkitaraman, A. R. & Spring, D. R. 2014. Diversity-oriented synthesis as a tool for identifying new modulators of mitosis. *Nature Communications,* 5.

Imberty, A. & Perez, S. 1988. A revisit to the three-dimensional structure of B-type starch. *Biopolymers,* 27, 1205-1221.

James, M. G., Denyer, K. & Myers, A. M. 2003. Starch synthesis in the cereal endosperm. *Current Opinion in Plant Biology,* 6, 215-222.

Jenkins, P. J., Cameron, R. E. & Donald, A. M. 1993. A universal feature in the structure of starch granules from different botanical sources. *Starch - Stärke,* 45, 417-420.

Jensen, J. & Lai, Y. C. 2009. Regulation of muscle glycogen synthase phosphorylation and kinetic properties by insulin, exercise, adrenaline and role in insulin resistance. *Archives of Physiology and Biochemistry,* 115, 13-21.

Kartal, Ö., Mahlow, S., Skupin, A. & Ebenhöh, O. 2011. Carbohydrate-active enzymes exemplify entropic principles in metabolism. *Molecular Systems Biology,* 7, 542.

Kihara, M., Kaneko, T., Ito, K., Aida, Y. & Takeda, K. 1999. Geographical variation of β-amylase thermostability among varieties of barley (*Hordeum vulgare*) and β-amylase deficiency. *Plant Breeding,* 118, 453-455.

Kim, J. Y., Henrichs, S., Bailly, A., Vincenzetti, V., Sovero, V., Mancuso, S., Pollmann, S., Kim, D., Geisler, M. & Nam, H. G. 2010. Identification of an abcb/p-glycoprotein-specific inhibitor of auxin transport by chemical genomics. *Journal of Biological Chemistry,* 285, 23309-17.

Klemm, D., Heublein, B., Fink, H.-P. & Bohn, A. 2005. Cellulose: Fascinating biopolymer and sustainable raw material. *Angewandte Chemie International Edition,* 44, 3358-3393.

Kolbe, A., Tiessen, A., Schluepmann, H., Paul, M., Ulrich, S. & Geigenberger, P. 2005. Trehalose 6-phosphate regulates starch synthesis via posttranslational redox activation of ADP-glucose pyrophosphorylase. *Proceedings of the National Academy of Sciences of the United States of America,* 102, 11118-11123.

Kotting, O., Kossmann, J., Zeeman, S. C. & Lloyd, J. R. 2010. Regulation of starch metabolism: The age of enlightenment? *Current Opinions in Plant Biology,* 13, 321-9.

Kotting, O., Pusch, K., Tiessen, A., Geigenberger, P., Steup, M. & Ritte, G. 2005. Identification of a novel enzyme required for starch metabolism in *Arabidopsis* leaves. The phosphoglucan, water dikinase. *Plant Physiology,* 137, 242-52.

Kotting, O., Santelia, D., Edner, C., Eicke, S., Marthaler, T., Gentry, M. S., Comparot-Moss, S., Chen, J., Smith, A. M., Steup, M., Ritte, G. & Zeeman, S. C. 2009. Starch-excess 4 is a laforin-like phosphoglucan phosphatase required for starch degradation in *Arabidopsis thaliana*. *Plant Cell,* 21, 334-46.

Kreis, M., Williamson, M., Buxton, B., Pywell, J., Hejgaard, J. & Svendsen, I. 1987. Primary structure and differential expression of beta-amylase in normal and mutant barleys. *European Journal of Biochemistry,* 169, 517-25.

Lafiandra, D., Riccardi, G. & Shewry, P. R. 2014. Improving cereal grain carbohydrates for diet and health. *Journal of Cereal Science,* 59, 312-326.

Lao, N. T., Schoneveld, O., Mould, R. M., Hibberd, J. M., Gray, J. C. & Kavanagh, T. A. 1999. An *Arabidopsis* gene encoding a chloroplast-targeted β-amylase. *The Plant Journal,* 20, 519-527.

Lin, Q., Facon, M., Putaux, J. L., Dinges, J. R., Wattebled, F., D'hulst, C., Hennen-Bierwagen, T. A. & Myers, A. M. 2013. Function of isoamylase-type starch debranching enzymes isa1 and isa2 in the *Zea mays* leaf. *New Phytologist,* 200, 1009-21.

Lipinski, C. A., Lombardo, F., Dominy, B. W. & Feeney, P. J. 2001. Experimental and computational approaches to estimate solubility and permeability in drug discovery and development settings. *Advanced Drug Delivery Review,* 46, 3-26.

Liu, W., Madsen, N. B., Braun, C. & Withers, S. G. 1991. Reassessment of the catalytic mechanism of glycogen debranching enzyme. *Biochemistry,* 30, 1419-1424.

Lloyd, J. R. & Kossmann, J. 2015. Transitory and storage starch metabolism: Two sides of the same coin? *Current Opinion in Biotechnology,* 32, 143-148.

Lovegrove, A. & Hooley, R. 2000. Gibberellin and abscisic acid signalling in aleurone. *Trends in Plant Science,* 5, 102-10.

Lund, D. 1984. Influence of time, temperature, moisture, ingredients, and processing conditions on starch gelatinization. *Critical Reviews in Food Science and Nutrition,* 20, 249-73.

Macgregor, A. W., Macri, L. J., Schroeder, S. W. & Bazin, S. L. 1994. Purification and characterisation of limit dextrinase inhibitors from barley. *Journal of Cereal Science,* 20, 33-41.

Macgregor, E. A., Bazin, S. L., Ens, E. W., Lahnstein, J., Macri, L. J., Shirley, N. J. & Macgregor, A. W. 2000. Structural models of limit dextrinase inhibitors from barley. *Journal of Cereal Science,* 31, 79-90.

Macwilliam, I. C. 1972. Effect of kilning on malt starch and on the dextrin content of resulting worts and beers. *Journal of the Institute of Brewing,* 78, 76-81.

Malinova, I., Mahlow, S., Alseekh, S., Orawetz, T., Fernie, A. R., Baumann, O., Steup, M. & Fettke, J. 2014. Double knockout mutants of *Arabidopsis* grown under normal conditions reveal that the plastidial phosphorylase isozyme participates in transitory starch metabolism. *Plant Physiology,* 164, 907-21.

Marshall, J., Sidebottom, C., Debet, M., Martin, C., Smith, A. M. & Edwards, A. 1996. Identification of the major starch synthase in the soluble fraction of potato tubers. *The Plant Cell,* 8, 1121-1135.

Martin, C. & Smith, A. M. 1995. Starch biosynthesis. *The Plant Cell,* 7, 971-985.

Mayer, T. U. 2003. Chemical genetics: Tailoring tools for cell biology. *Trends in Cell Biology,* 13, 270-7.

Mccleary, B. V. 1992. Measurement of the content of limit-dextrinase in cereal flours. *Carbohydrate Research,* 227, 257-268.

Mccourt, P. & Desveaux, D. 2010. Plant chemical genetics. *New Phytologist,* 185, 15-26.

Merzendorfer, H. & Zimoch, L. 2003. Chitin metabolism in insects: Structure, function and regulation of chitin synthases and chitinases. *Journal of Experimental Biology,* 206, 4393-4412.

Mikkelsen, R., Baunsgaard, L. & Blennow, A. 2004. Functional characterization of alpha-glucan,water dikinase, the starch phosphorylating enzyme. *Biochemistry Journal,* 377, 525-32.

Mizuno, K., Kawasaki, T., Shimada, H., Satoh, H., Kobayashi, E., Okumura, S., Arai, Y. & Baba, T. 1993. Alteration of the structural properties of starch components by the lack of an isoform of starch branching enzyme in rice seeds. *Journal of Biological Chemistry,* 268, 19084-19091.

Møller, M. S., Vester-Christensen, M. B., Jensen, J. M., Abou Hachem, M., Henriksen, A. & Svensson, B. 2015. Crystal structure of barley limit dextrinase:Limit dextrinase inhibitor (LD:LDI) complex reveals insights into mechanism and diversity of cereal-type inhibitors. *Journal of Biological Chemistry*, 290, 12614–12629.

Mua, J. P. & Jackson, D. S. 1997. Relationships between functional attributes and molecular structures of amylose and amylopectin fractions from corn starch. *Journal of Agricultural and Food Chemistry,* 45, 3848-3854.

Muslin, E. H., Kanikula, A. M., Clark, S. E. & Henson, C. A. 2000. Overexpression, purification, and characterization of a barley α-glucosidase secreted by pichia pastoris. *Protein Expression and Purification,* 18, 20-26.

Myers, A. M., Morell, M. K., James, M. G. & Ball, S. G. 2000. Recent progress toward understanding biosynthesis of the amylopectin crystal. *Plant Physiology,* 122, 989-998.

Nakai, H., Tanizawa, S., Ito, T., Kamiya, K., Kim, Y.-M., Yamamoto, T., Matsubara, K., Sakai, M., Sato, H., Imbe, T. O., Okuyama, M., Mori, H., Chiba, S., Sano, Y. & Kimura, A. 2008. Rice α-glucosidase isozymes and isoforms showing different starch granules-binding and -degrading ability. *Biocatalysis and Biotransformation,* 26, 104-110.

Nakamura, Y., Umemoto, T., Ogata, N., Kuboki, Y., Yano, M. & Sasaki, T. 1996. Starch debranching enzyme (R-enzyme or pullulanase) from developing rice endosperm: Purification, cDNA and chromosomal localization of the gene. *Planta,* 199, 209-218.

Natsume, S., Takagi, H., Shiraishi, A., Murata, J., Toyonaga, H., Patzak, J., Takagi, M., Yaegashi, H., Uemura, A., Mitsuoka, C., Yoshida, K., Krofta, K., Satake, H., Terauchi, R. & Ono, E. 2015. The draft genome of hop (*Humulus lupulus*), an essence for brewing. *Plant Cell Physiology,* 56, 428-41.

Nielsen, M. M., Bozonnet, S., Seo, E. S., Motyan, J. A., Andersen, J. M., Dilokpimol, A., Abou Hachem, M., Gyemant, G., Naested, H., Kandra, L., Sigurskjold, B. W. & Svensson, B. 2009. Two secondary carbohydrate binding sites on the surface of barley alpha-amylase 1 have distinct functions and display synergy in hydrolysis of starch granules. *Biochemistry,* 48, 7686-97.

Niittyla, T., Comparot-Moss, S., Lue, W. L., Messerli, G., Trevisan, M., Seymour, M. D., Gatehouse, J. A., Villadsen, D., Smith, S. M., Chen, J., Zeeman, S. C. & Smith, A. M. 2006. Similar protein phosphatases control starch metabolism in plants and glycogen metabolism in mammals. *Journal of Biological Chemistry,* 281, 11815-8.

O'Connor, C. J., Laraia, L. & Spring, D. R. 2011. Chemical genetics. *Chemical Society Reviews,* 40, 4332-45.

Okamoto, M., Peterson, F. C., Defries, A., Park, S. Y., Endo, A., Nambara, E., Volkman, B. F. & Cutler, S. R. 2013. Activation of dimeric ABA receptors elicits guard cell closure, aba-regulated gene expression, and drought tolerance. *Proceedings of the National Academy of Sciences of the United States of America,* 110, 12132-7.

Palmer, G. H. 2006. *Barley and malt. Handbook of brewing,* CRC Press, Taylor & Francis Group.

Pan, D. & Nelson, O. E. 1984. A debranching enzyme deficiency in endosperms of the sugary-1 mutants of maize. *Plant physiology,* 74, 324-328.

Park, S. Y., Fung, P., Nishimura, N., Jensen, D. R., Fujii, H., Zhao, Y., Lumba, S., Santiago, J., Rodrigues, A., Chow, T. F., Alfred, S. E., Bonetta, D., Finkelstein, R., Provart, N. J., Desveaux, D., Rodriguez, P. L., Mccourt, P., Zhu, J. K., Schroeder, J. I., Volkman, B. F. & Cutler, S. R. 2009. Abscisic acid inhibits type 2c protein phosphatases via the pyr/pyl family of start proteins. *Science,* 324, 1068-71.

Petersen, B. O., Meier, S. & Duus, J. O. 2012. Nmr assignment of structural motifs in intact beta-limit dextrin and its alpha-amylase degradation products *in situ*. *Carbohydrate Research,* 359, 76-80.

Pilling, E. & Smith, A. M. 2003. Growth ring formation in the starch granules of potato tubers. *Plant Physiology,* 132, 365-371.

Ponnu, J., Wahl, V. & Schmid, M. 2011. Trehalose-6-phosphate: Connecting plant metabolism and development. *Frontiers in plant science,* 2, 70.

Preiss, J. 1996. Starch synthesis in sinks and sources. *Photoassimilate distribution in plants and crops*, 63-96. CRC Press.

Radchuk, V. V., Borisjuk, L., Sreenivasulu, N., Merx, K., Mock, H.-P., Rolletschek, H., Wobus, U. & Weschke, W. 2009. Spatiotemporal profiling of starch biosynthesis and degradation in the developing barley grain. *Plant Physiology,* 150, 190-204.

Ragot, F., Guinard, J. X., Shoemaker, C. F. & Lewis, M. J. 1989. The contribution of dextrins to beer sensory properties part i. Mouthfeel. *Journal of the Institute of Brewing,* 95, 427-430.

Rajangam, A. S., Kumar, M., Aspeborg, H., Guerriero, G., Arvestad, L., Pansri, P., Brown, C. J.-L., Hober, S., Blomqvist, K., Divne, C., Ezcurra, I., Mellerowicz, E., Sundberg, B., Bulone, V. & Teeri, T. T. 2008. Map20, a microtubule-associated protein in the secondary cell walls of hybrid aspen, is a target of the cellulose synthesis inhibitor 2,6-dichlorobenzonitrile. *Plant Physiology,* 148, 1283-1294.

Rejzek, M., Stevenson, C. E., Southard, A. M., Stanley, D., Denyer, K., Smith, A. M., Naldrett, M. J., Lawson, D. M. & Field, R. A. 2011. Chemical genetics and cereal starch metabolism: Structural basis of the non-covalent and covalent inhibition of barley beta-amylase. *Molecular Biosystems,* 7, 718-30.

Ritchie, S., Mccubbin, A., Ambrose, G., Kao, T.-H. & Gilroy, S. 1999. The sensitivity of barley aleurone tissue to gibberellin is heterogeneous and may be spatially determined. *Plant Physiology,* 120, 361-370.

Ritte, G., Heydenreich, M., Mahlow, S., Haebel, S., Kotting, O. & Steup, M. 2006. Phosphorylation of c6- and C3-positions of glucosyl residues in starch is catalysed by distinct dikinases. *FEBS Letters,* 580, 4872-6.

Roach, P. J. 2002. Glycogen and its metabolism. *Current molecular medicine,* 2, 101-120.

Robert, S., Bichet, A., Grandjean, O., Kierzkowski, D., Satiat-Jeunemaître, B., Pelletier, S., Hauser, M.-T., Höfte, H. & Vernhettes, S. 2005. An *Arabidopsis* endo-1,4-β-D-glucanase involved in cellulose synthesis undergoes regulated intracellular cycling. *The Plant Cell,* 17, 3378-3389.

Rojas-Pierce, M., Titapiwatanakun, B., Sohn, E. J., Fang, F., Larive, C. K., Blakeslee, J., Cheng, Y., Cutler, S. R., Peer, W. A., Murphy, A. S. & Raikhel, N. V. 2007. *Arabidopsis* p-glycoprotein19 participates in the inhibition of gravitropism by gravacin. *Chemistry and Biology,* 14, 1366-76.

Rorat, T., Sadowski, J., Grellet, F., Daussant, J. & Delseny, M. 1991. Characterization of cdna clones for rye endosperm β-amylase and analysis of β-amylase deficiency in rye mutant lines. *Theoretical and Applied Genetics,* 83, 257-263.

Schopper, S., Mühlenbock, P., Sörensson, C., Hellborg, L., Lenman, M., Widell, S., Fettke, J. & Andreasson, E. 2015. *Arabidopsis* cytosolic alpha-glycan phosphorylase, phs2, is important during carbohydrate imbalanced conditions. *Plant Biology,* 17, 74-80.

Seung, D., Soyk, S., Coiro, M., Maier, B. A., Eicke, S. & Zeeman, S. C. 2015. Protein targeting to starch is required for localising granule-bound starch synthase to starch granules and for normal amylose synthesis in *Arabidopsis*. *PLoS Biology,* 13, e1002080.

Seung, D., Thalmann, M., Sparla, F., Abou Hachem, M., Lee, S. K., Issakidis-Bourguet, E., Svensson, B., Zeeman, S. C. & Santelia, D. 2013. *Arabidopsis thaliana* amy3 is a unique redox-regulated chloroplastic alpha-amylase. *Journal of Biological Chemistry,* 288, 33620-33.

Silver, D. M., Kötting, O. & Moorhead, G. B. G. 2014. Phosphoglucan phosphatase function sheds light on starch degradation. *Trends in Plant Science,* 19, 471-478.

Sissons, M. J., Lance, R. C. M. & Wallace, W. 1994. Bound and free forms of barley limit dextrinase. *Cereal Chemistry*.

Smirnova, J., Fernie, A. R. & Steup, M. 2015. Starch degradation. *In:* Nakamura, Y. (ed.) *Starch Metabolism and Structure.* Springer Japan.

Smith-White, B. J. & Preiss, J. 1992. Comparison of proteins of adp-glucose pyrophosphorylase from diverse sources. *Journal of molecular evolution,* 34, 449-464.

Smith, A. M. 2008. Prospects for increasing starch and sucrose yields for bioethanol production. *The Plant Journal,* 54, 546-58.

Smith, A. M., Denyer, K. & Martin, C. 1997. The synthesis of the starch granule. *Annual Review of Plant Physiology and Plant Molecular Biology,* 48, 67-87.

Smith, A. M., Zeeman, S. C. & Smith, S. M. 2005. Starch degradation. *Annual Review of Plant Biology,* 56, 73-98.

Solís, D., Bovin, N. V., Davis, A. P., Jiménez-Barbero, J., Romero, A., Roy, R., Smetana Jr, K. & Gabius, H.-J. 2015. A guide into glycosciences: How chemistry, biochemistry and biology cooperate to crack the sugar code. *Biochimica et Biophysica Acta (BBA) - General Subjects,* 1850, 186-235.

Spring, D. R. 2005. Chemical genetics to chemical genomics: Small molecules offer big insights. *Chemical Society Reviews,* 34, 472.

Sreenivasulu, N. & Wobus, U. 2013. Seed-development programs: A systems biology-based comparison between dicots and monocots. *Annual Review of Plant Biology,* 64, 189-217.

Stanley, D., Rejzek, M., Naested, H., Smedley, M., Otero, S., Fahy, B., Thorpe, F., Nash, R. J., Harwood, W., Svensson, B., Denyer, K., Field, R. A. & Smith, A. M. 2011. The role of alpha-glucosidase in germinating barley grains. *Plant Physiology,* 155, 932-43.

Stark, J. & Yin, X. 1987. Evidence for the presence of maltase and α-glucosidase isoenzymes in barley. *Journal of the Institute of Brewing,* 93, 108-112.

Stitt, M. & Zeeman, S. C. 2012. Starch turnover: Pathways, regulation and role in growth. *Current Opinion in Plant Biology,* 15, 282-92.

Stockwell, B. R. 2000. Chemical genetics: Ligand-based discovery of gene function. *Nature Reviews Genetics,* 1, 116-25.

Streb, S., Delatte, T., Umhang, M., Eicke, S., Schorderet, M., Reinhardt, D. & Zeeman, S. C. 2008. Starch granule biosynthesis in *Arabidopsis* is abolished by removal of all debranching enzymes but restored by the subsequent removal of an endoamylase. *Plant Cell,* 20, 3448-66.

Streb, S., Eicke, S. & Zeeman, S. C. 2012. The simultaneous abolition of three starch hydrolases blocks transient starch breakdown in *Arabidopsis*. *Journal of Biological Chemistry,* 287, 41745-56.

Streb, S. & Zeeman, S. C. 2014. Replacement of the endogenous starch debranching enzymes isa1 and isa2 of *Arabidopsis* with the rice orthologs reveals a degree of functional conservation during starch synthesis. *PLoS ONE,* 9, e92174.

Sun, Z. & Henson, C. A. 1990. Degradation of native starch granules by barley alpha-glucosidases. *Plant Physiology,* 94, 320-7.

Sun, Z. & Henson, C. A. 1991. A quantitative assessment of the importance of barley seed α-amylase, β-amylase, debranching enzyme, and α-glucosidase in starch degradation. *Archives of Biochemistry and Biophysics,* 284, 298-305.

Surpin, M., Rojas-Pierce, M., Carter, C., Hicks, G. R., Vasquez, J. & Raikhel, N. V. 2005. The power of chemical genomics to study the link between endomembrane system components and the gravitropic response. *Proceedings of the National Academy of Sciences of the United States of America,* 102, 4902-4907.

Takeda, Y., Guan, H.-P. & Preiss, J. 1993. Branching of amylose by the branching isoenzymes of maize endosperm. *Carbohydrate Research,* 240, 253-263.

Tang, H., Mitsunaga, T. & Kawamura, Y. 2006. Molecular arrangement in blocklets and starch granule architecture. *Carbohydrate Polymers,* 63, 555-560.

Tester, R. F., Karkalas, J. & Qi, X. 2004. Starch—composition, fine structure and architecture. *Journal of Cereal Science,* 39, 151-165.

Tester, R. F. & Morrison, W. R. 1990. Swelling and gelatinization of cereal starches. I. Effects of amylopectin, amylose, and lipids. *Cereal Chemistry,* 67, 551-557.

Tester, R. F. & Qi, X. 2011. B-limit dextrin – properties and applications. *Food Hydrocolloids,* 25, 1899-1903.

Tice, C. M. 2001. Selecting the right compounds for screening: Does Lipinski's rule of 5 for pharmaceuticals apply to agrochemicals? *Pest Management Science,* 57, 3-16.

Toth, R. & Van Der Hoorn, R. A. 2010. Emerging principles in plant chemical genetics. *Trends in Plant Science,* 15, 81-8.

Umehara, M., Hanada, A., Yoshida, S., Akiyama, K., Arite, T., Takeda-Kamiya, N., Magome, H., Kamiya, Y., Shirasu, K., Yoneyama, K., Kyozuka, J. & Yamaguchi, S. 2008. Inhibition of shoot branching by new terpenoid plant hormones. *Nature,* 455, 195-200.

Vandamme, E., De Baets, S. & Steinbüchel, A. 2002. *6: Polysaccharides ii: Polysaccharides from eukaryotes*, Weinheim: Wiley-VCH.

Varki, A. 1993. Biological roles of oligosaccharides: All of the theories are correct. *Glycobiology,* 3, 97-130.

Ventriglia, T., Kuhn, M. L., Ruiz, M. T., Ribeiro-Pedro, M., Valverde, F., Ballicora, M. A., Preiss, J. & Romero, J. M. 2008. Two *Arabidopsis* ADP-glucose pyrophosphorylase large subunits (apl1 and apl2) are catalytic. *Plant Physiology,* 148, 65-76.

Waigh, T. A., Kato, K. L., Donald, A. M., Gidley, M. J., Clarke, C. J. & Riekel, C. 2000. Side-chain liquid-crystalline model for starch. *Starch - Stärke,* 52, 450-460.

Walsh, T. A. 2007. The emerging field of chemical genetics: Potential applications for pesticide discovery. *Pest Management Science,* 63, 1165-71.

Wang, Y. H. & Irving, H. R. 2011. Developing a model of plant hormone interactions. *Plant Signaling & Behavior,* 6, 494-500.

Wattebled, F., Dong, Y., Dumez, S., Delvalle, D., Planchot, V., Berbezy, P., Vyas, D., Colonna, P., Chatterjee, M., Ball, S. & D'hulst, C. 2005. Mutants of arabidopsis lacking a chloroplastic isoamylase accumulate phytoglycogen and an abnormal form of amylopectin. *Plant Physiologyogy,* 138, 184-95.

Wischmann, B., Nielsen, T. H. & Møller, B. L. 1999. In vitro biosynthesis of phosphorylated starch in intact potato amyloplasts. *Plant physiology,* 119, 455-462.

Wu, C., Colleoni, C., Myers, A. M. & James, M. G. 2002. Enzymatic properties and regulation of zpu1, the maize pullulanase-type starch debranching enzyme. *Archives of Biochemistry and Biophysics,* 406, 21-32.

Xu, X. M. & Møller, S. G. 2011. The value of arabidopsis research in understanding human disease states. *Current Opinion in Biotechnology,* 22, 300-7.

Yoneda, A., Higaki, T., Kutsuna, N., Kondo, Y., Osada, H., Hasezawa, S. & Matsui, M. 2007. Chemical genetic screening identifies a novel inhibitor of parallel alignment of cortical microtubules and cellulose microfibrils. *Plant and Cell Physiology,* 48, 1393-1403.

Yoneda, A., Ito, T., Higaki, T., Kutsuna, N., Saito, T., Ishimizu, T., Osada, H., Hasezawa, S., Matsui, M. & Demura, T. 2010. Cobtorin target analysis reveals that pectin functions in the deposition of cellulose microfibrils in parallel with cortical microtubules. *The Plant Journal,* 64, 657-667.

Yu, T.-S., Zeeman, S. C., Thorneycroft, D., Fulton, D. C., Dunstan, H., Lue, W.-L., Hegemann, B., Tung, S.-Y., Umemoto, T., Chapple, A., Tsai, D.-L., Wang, S.-M., Smith, A. M., Chen, J. & Smith, S. M. 2005. A-amylase is not required for breakdown of transitory starch in *Arabidopsis* leaves. *Journal of Biological Chemistry,* 280, 9773-9779.

Zeeman, S. C., Delatte, T., Messerli, G., Umhang, M., Stettler, M., Mettler, T., Streb, S., Reinhold, H. & Kötting, O. 2007. Starch breakdown: Recent discoveries suggest distinct pathways and novel mechanisms. *Functional Plant Biology,* 34, 465.

Zeeman, S. C., Kossmann, J. & Smith, A. M. 2010. Starch: Its metabolism, evolution, and biotechnological modification in plants. *Annual Review of Plant Biology,* 61, 209-34.

Zeeman, S. C., Northrop, F., Smith, A. M. & Rees, T. 1998. A starch-accumulating mutant of *Arabidopsis thaliana* deficient in a chloroplastic starch-hydrolysing enzyme. *The Plant Journal,* 15, 357-65.

Zeeman, S. C., Smith, S. M. & Smith, A. M. 2004. The breakdown of starch in leaves. *New Phytologist,* 163, 247-261.

Zhao, Y., Chow, T. F., Puckrin, R. S., Alfred, S. E., Korir, A. K., Larive, C. K. & Cutler, S. R. 2007. Chemical genetic interrogation of natural variation uncovers a molecule that is glycoactivated. *Nature Chemical Biology,* 3, 716-21.

Zohary, D., Hopf, M. & Weiss, E. 2012. *Domestication of plants in the old world: The origin and spread of domesticated plants in southwest asia, europe, and the mediterranean basin*, Oxford University Press on Demand.

Chapter 2- Materials and Methods

2.1 Materials

2.1.1 Chemical Reagents

Reagents specific to particular techniques have the supplier given in the methods text. All other reagents were purchased from Sigma.

2.1.2 Plasmids

Vectors used for cloning are outlined in Table 2.1. Gateway compatible vectors were propagated in *E. coli ccd*B Survival 2 T1R cells, other vectors were propagated in *E. coli* TOP10.

Name	**Antibiotic Resistance**	**Use**	**Vector Size (bp)**
pCR8/GW/TOPO	Spc^R	Entry vector for Gateway cloning.	2817
pDEST17	Amp^R/ Car^R	Gateway compatible destination vector for *E. coli* protein expression with N-terminal His_6 tag.	6354
pETG-10A	Amp^R/ Car^R	Gateway compatible destination vector for *E. coli* protein expression with N-terminal His_6 tag.	7103
pDEST42	Amp^R/ Car^R	Gateway compatible destination vector for *E. coli* protein expression with C-terminal His_6 tag.	7440
pOPIN27b	Kan^R	In-Fusion compatible vector for *E. coli* protein expression with N-terminal bacterial PelB secretion sequence and His_6 tag.	5360

Table 2.1 Plasmid vectors used within this study.

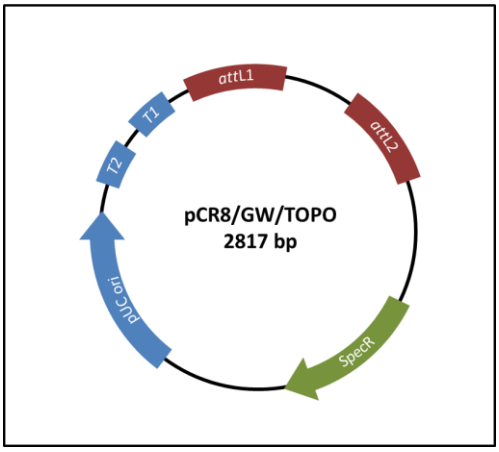

Figure 2.1 Plasmid map pCR8/GW/TOPO Gateway entry vector.

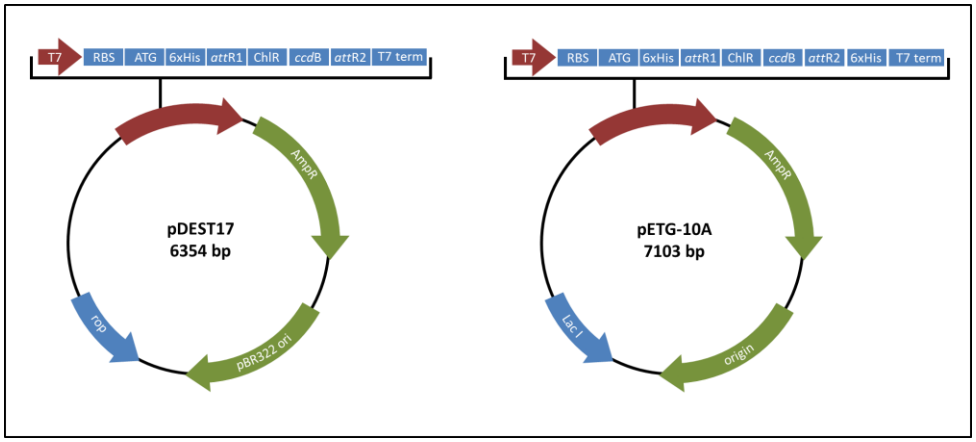

Figure 2.2 Plasmid map pDEST17 and pETG-10A Gateway destination vectors.

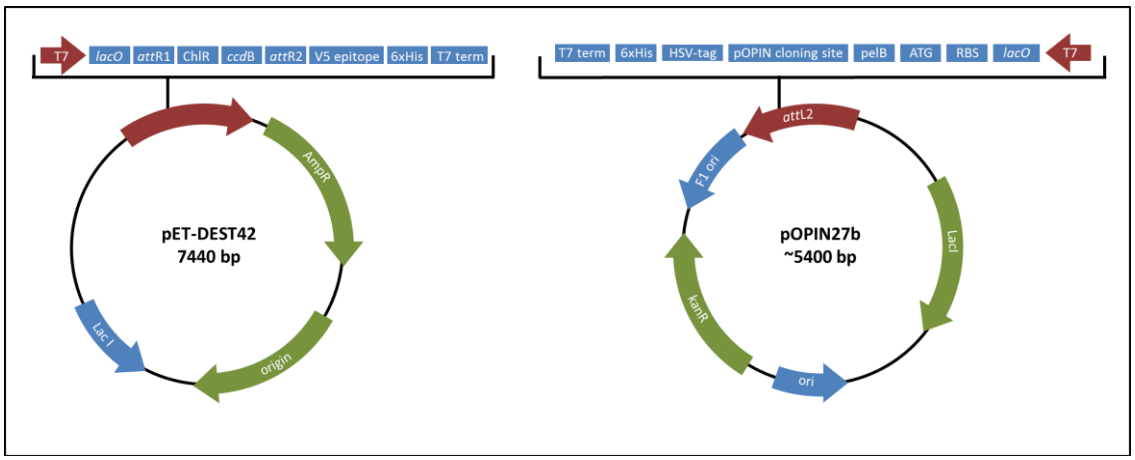

Figure 2.3 pETDEST42 Gateway destination and pOPIN27b In-Fusion vectors.

2.1.3 Bacterial Strains

A number of bacterial strains were used for cloning and protein overexpression, these are outlined in Table 2.2. Bacterial strains were stored as 25 % glycerol stocks. Stocks were prepared by combining 750 µL from a 5 mL overnight culture and 750 µL of sterile 50 % glycerol.

Supplier and Strain	Resistance	Use and Features
Invitrogen One Shot TOP10	Str^R	Cloning. Efficient transformation and plasmid propagation.
Invitrogen One Shot *ccd*B Survival 2 T1R	Str^R	Cloning. Propagation of Gateway plasmids containing the *ccd*B gene.
Agilent BL21 Codon Plus	Cam^R	Protein expression. Contains tRNAs for rare codons AGG/AGA (arginine), AUA (isoleucine) and CUA (leucine).
Novagen Rosetta 2 (DE3)	Cam^R	Protein expression. Contains tRNAs for rare codons - as above, plus CGG (arginine), CCC (proline), and GGA (glycine).
Novagen Rosetta 2 (DE3) pLysS	Cam^R	Protein expression. As above, plus supresses basal expression, *via* T7 lysozyme, prior to induction.
Novagen Rosetta-gami (DE3) pLysS	Cam^R	Protein expression. As above, plus enhanced disulfide bond formation.
Genlantis SoluBL21	None	Protein expression. Enhanced protein solubility.
NEB SHuffle	Str^R, Spc^R	Protein expression. Engineered to form proteins containing disulfide bonds in the cytoplasm.

Table 2.2. *E. coli* strains used within this study.

2.1.4 Primers

All primers were purchased from MWG Eurofins (Ebersberg, Germany) at HPSF purity. Primers were diluted with nuclease free H_2O to a stock concentration of 100 µM. Primers are outlined in Table 2.3.

ID	Name	Sequence (5'-3')	Use	Tm°C	CG %	nt
MR1	GAPDH F	CCACCGGTGTCTTCACTG	Housekeeping gene	63	61	18
MR2	GAPDH R	GCCTTAGCATCAAAAGATG	Housekeeping gene	58	42	19
MR3	LD F	ATGCCAATGCCGATGCGAACGA	LD Full length cloning	77	54	22
MR4	LD R	TCAACACCGAGGTTCGACAAAGAC	LD Full length cloning	70	50	24
MR5	LDI F	ATGGCATCCGACCATCGTC	LDI Full length cloning	68	57	19
MR6	LDI R	TCATCCATCTGCCAGTAGCAC	LDI Full length cloning	65	52	21
MR9	LD NoSto R	ACACCGAGGTTCGACAAAGAC	LD No stop cloning	65	52	21
MR10	LDI NoSto R	TCCATCTGCCAGTAGCAC	LDI No stop cloning	60	55	18
MR12	LD NoSec F	ATGGCGGTCGGGGAGA	LD No sec signal cloning	68	68	16
MR13	LDI NoSec F	ATGACCCTGGAGAGCGTCAAG	LDI No sec signal cloning	68	57	21
MR23	LD Probe F	GTGCATTTGCATATCAGG	LD Probe	58	44	18
MR24	LD Probe R	TAAGGCTTTGAAGAGCAGA	LD Probe	58	42	19
MR25	LD KpnI F	GATCGGTACCATGGCGGTCGGGGAGACCGG	LD Fragment cloning	86	70	30
MR26	LD XbaI F	CAGGCCCTCAATCGCATAGG	LD Fragment cloning	69	60	20
MR27	LD BglI F	GGGAATACCCTTCTTCCACGC	LD Fragment cloning	67	57	21
MR28	LD NotI R	GCTGGCGGCCGCTCAACACCGAGGTTCGACAA	LD Fragment cloning	88	6	32
MR29	LD XbaI R	GAGCTGATACCGCAGGGGCC	LD Fragment cloning	72	70	20
MR30	LD BglI R	CCAGAGTTATATGAATCTCGG	LD Fragment cloning	58	42	21
MR 35	LDI Sec Sto R	TCAGGCGGCGGCGAC	Stop Codon LDI Sec	72	80	15
MR 36	LDI Sec NoSto R L	GGCGGCGGCGACGGCGAGGACCGAGAGCAAGA	LDI sec signal cloning	92	75	32
MR 37	LDI Sec NoSto R S	GGCGGCGGCGACGGCGA	LDI sec signal cloning	82	88	17
MR38	GFP Fusion F	ACACGCTGAACTTGTGG	GFP fusion cloning	58	52	17
MR39	GFP Fusion R	CCACAAGTTCAGCGTGT	GFP fusion cloning	58	52	17
MR40	LD Gene Art F	ACTATAGGGCGAATTGTAGAAG	LD Sequencing	58	40	22
MR41	LD Gene Art R	GGAAAGCGGGCAGTGATAGAAG	LD Sequencing	68	54	22
MR42	GW1	GTTGCAACAAATTGATGAGCAATGC	Gateway Sequencing	70	40	25
MR43	GW2	GTTGCAACAAATTGATGAGCAATTA	Gateway Sequencing	65	32	25
MR44	M13 F	GTAAAACGACGGCCAGT	Gateway Sequencing	59	52	17
MR45	M13 R	CAGGAAACAGCTATGAC	Gateway Sequencing	51	47	17
MR46	LD Sec R	GGGCGTCCTCCGCCG	LD Secretion cloning	72	86	15
MR53	pOPINLDI Full F	AAGTTCTGTTTCAGGGCCCGATGGCATCCGACCATCGTCGCTT	LDI pOPIN cloning	89	55	43
MR54	pOPINLDI NoSec F	AAGTTCTGTTTCAGGGCCCGATGACCCTGGAGAGCGTCAA	LDI pOPIN cloning	86	55	40
MR55	pOPINLDI NoSt R	ATGGTCTAGAAAGCTTTATCCATCTGCCAGTAGCACCAA	LDI pOPIN cloning	77	43	39
MR47	Hyg F	ACTCACCGCGACGTCTGTCG	PCR of transgenic lines	71	65	20
MR48	Hyg R	GCGCGTCTGCTGCTCCATA	PCR of transgenic lines	70	63	19
MR49	UbiPro F	ATGCTCACCCTGTTGTTTGG	PCR of transgenic lines	65	50	20
MR50	IV2intron R	CATCGTTGTATGCCACTGGA	PCR of transgenic lines	65	50	20
MR51	IV2intron F	CCAAAATTTGTTGATGTGCAG	PCR of transgenic lines	63	38	21
MR52	NosTerm R	TGTTTGAACGATCCTGCTTG	PCR of transgenic lines	64	45	20
MR56	Hv GCS F	ATGAGGCGCAAAATGGCA	GCS cloning	68	50	18
MR57	Hv GCS R	TCAGACATCATACTTCTTCG	GCS cloning	55	40	20

Table 2.3. Primers used within this study.

2.1.5 Antibiotics

Antibiotics were used to select for positive transformants following transformation, as well as being used in culture medium, these are outlined in Table 2.4.

Antibiotic	Abbreviation	Stock Concentration	Final Concentration
Ampicillin	Amp	100 mg/mL in H_2O	100 µg/mL
Carbenicillin	Car	100 mg/mL in H_2O	100 µg/mL
Kanamycin	Kan	50 mg/mL in H_2O	50 µg/mL
Rifampicin	Rif	50 mg/mL in MeOH	50 µg/mL
Spectinomycin	Spt	50 mg/mL in H_2O	50 µg/mL
Chloramphenicol	Cam	34 mg/mL in EtOH	34 µg/mL

Table 2.4. Antibiotic stocks used within this study.

2.1.6 Media

The composition of bacterial and plant culture media is outlined in Table 2.5.

Abbreviation	Medium Name	Composition
LB	Lysogeny Broth	1 % (w/v) tryptone, 0.5 % (w/v) yeast extract, 171 mM NaCl, pH 7.0.
LB-Agar	Lysogeny Broth Agar	As above, with 1.5 % (w/v) agar added.
SOC	Super Optimal broth with catabolite repression	0.5 % (w/v) yeast extract, 2 % (w/v) tryptone, 10 mM NaCl, 2.5 mM KCl, 10 mM $MgCl_2$, 10 mM $MgSO_4$ pH 7.5, following sterilisation by autoclave, add glucose to final concentration of 20 mM.
½MS	Half strength Murashige and Skoog medium	Micro and macro nutrients including vitamins at half standard concentration.
½MS-Agar	Half strength Murashige and Skoog medium agar	As above, with 1 % (w/v) agar added.
Agar	Agar	1 % (w/v) agar in H_2O.

Table 2.5. Bacterial and plant culture media used within this study.

2.2 Molecular Biology

2.2.1 General

All nucleic acid concentrations were determined using a Nanodrop (Thermo) set to Nucleic Acid mode. PCRs were performed using a G-Storm thermocycler (Gene Technologies), specific cycling conditions are given in the necessary sections. Successful cloning was confirmed by colony PCR, restriction digest and sequencing (Eurofins MWG). The buffer components of kits are given by their abbreviated names, for more details see manufacturer's instructions.

2.2.2 Preparation of RNA using QIAGEN RNeasy Kit

A QIAGEN RNeasy Kit was used for the preparation of RNA. All surfaces and equipment were cleaned using 70 % EtOH then RNase Away (Sigma). Up to 100 mg of plant tissue sample was homogenised in a mortar and pestle by grinding under liquid nitrogen. Sample was transferred to a pre-chilled Eppendorf and resuspended in 450 µL RLT buffer. This was then centrifuged, 14,000 rpm, 1 min, and the supernatant transferred to a QIAshredder column. The flow through from this column was combined with half a volume of EtOH then added to an RNeasy spin column and centrifuged. The flow through was discarded and 700 µL RW1 buffer added to the column. The column was again centrifuged and the flow through discarded. Column was then washed by centrifugation two times with 500 µL RPE buffer. Finally RNA was eluted with 30 µL H_2O. RNA samples were flash frozen in liquid nitrogen and stored at -80 °C.

2.2.3 Preparation of RNA using Phenol-Chloroform

A second method of RNA purification was also used based on phenol-chloroform extraction. Homogenised plant tissue samples were prepared as for RNA using a QIAGEN RNeasy Kit. Following homogenisation, sample was transferred to a 2 mL Eppendorf to which 600 µL RE buffer (0.1 M Tris pH 8.0, 5 mM EDTA, 0.1 M NaCl, 0.5 % SDS, 1 % β-ME) was added. This was mixed thoroughly and incubated at 60 °C for 30 s to thaw samples. 200 µL of Plant RNA Isolation Aid (Life Technologies) was added to this and mixed. Sample was centrifuged at 14,000 rpm for 10 min and the supernantant transferred to a 1.5 ml Eppendorf. 300 µL of acidic phenol:chloroform (pH 4.3) (Sigma-Aldrich) was then added and mixed thoroughly for 10 min. Sample was centrifuged, 14,000 rpm for 5 min then the upper aqueous phase was transferred to a fresh Eppendorf containing 240 µL isopropanol and 30 µL sodium acetate (3 M, pH 5.2) and mixed thoroughly. Nucleic acids were precipitated at -80 °C for 15 min followed by centrifugation at 14,000 rpm for 30 min. The supernantant was discarded and the pellet washed with 600 µL 70 % EtOH followed by centrifugation at 14,000 rpm for 5 min. Supernatant was discarded and RNA pellets allowed to dry in a fume hood at RT for 30-60 min.

RNA was dissolved in 100 µL H_2O. Samples were flash frozen in liquid nitrogen and stored at -80 °C.

2.2.4 Synthesis of cDNA from RNA Template

cDNA was generated from the RNA prepared from plant tissues. RNA for use in cDNA synthesis was first treated with DNase I (Sigma-Aldrich). 8 µL of RNA (50-100 ng/µL) was combined with 1 µL 10x reaction buffer and 1 µL DNase I (1 U/ µL). The reaction was incubated at room temperature for 15 min then terminated by the addition of 1 µL Stop solution (50 mM EDTA) and heating to 70 °C for 10 min. First strand cDNA synthesis was carried out using Superscript II Reverse Transcriptase (Invitrogen). 10 µL of DNase treated RNA sample was combined with 1 µL of $Oligo(dT)_{15}$ primers (Promega) (500 µg/µL) and 1 µL dNTP mix (10 mM each). This mixture was heated to 65 °C for 5 min then chilled on ice. 4 µL of 5x buffer and 2 µL DTT (0.1 M) were then added and incubated at 42 °C for 2 min. Finally, 2 µL Superscript II RT was added to the mix and incubated at 42 °C for 50 min then 70 °C for 15 min. cDNA was stored at -20 °C.

2.2.5 Standard Polymerase Chain Reaction

For routine analytical PCR *Taq* DNA polymerase (NEB) was used. Reactions were set up as shown in Table 2.6.

Component	**1x**
10x *Taq* Buffer	5 µL
dNTP mix (10 mM each)	1 µL
Primer F (10 µM)	1 µL
Primer R (10 µM)	1 µL
Template DNA	100 ng
DMSO	1.5 µL
Taq Polymerase	0.25 µL
H_2O	to 50 µL

Table 2.6. Standard PCR setup.

The thermal cycler program consisted of initial denaturation at 95 °C for 30 s. Followed by 30 cycles of denaturation at 95 °C for 20 s, annealing at a temperature suitable for the primers used for 30 s and elongation at 68 °C for 2 min. Final extension was at 68 °C for 5 min. For a colony PCR, template DNA was replaced by a colony sample taken by touching the colony with a sterile toothpick then adding it to an individual reaction mix.

2.2.6 High-Fidelity Polymerase Chain Reaction

Phusion polymerase (NEB) was used for applications which required a high-fidelity polymerase, such as amplifying genes of interest for cloning. Reactions were set up as shown in Table 2.7.

Component	1x
5x Phusion Buffer	10 µL
dNTP mix (10 mM each)	1 µL
Primer F (10 µM)	2.5 µL
Primer R (10 µM)	2.5 µL
Template DNA	100 ng
DMSO	1.5 µL
Phusion Polymerase	0.5 µL
H_2O	to 50 µL

Table 2.7 High-fidelity PCR setup.

Thermal cycler program: denaturation at 98 °C for 30 s. Followed by 35 cycles of denaturation at 98 °C for 10 s, annealing at a temperature suitable for the primers used for 30 s and elongation at 72 °C for 90 s. Final extension was at 72 °C for 10 min.

2.2.7 GC-Rich Polymerase Chain Reaction

The Roche GC-Rich PCR System was used to amplify GC rich genes. Reactions were set up as shown in Table 2.8.

Component	1x
Primer F (2 µM)	5 µL
Primer R (2 µM)	5 µL
dNTP mix (10 mM each)	1 µL
Template DNA	50 ng
5x GC-Rich Buffer	10 µL
GC-Rich Enzyme Mix	1 µL
H_2O	to 50 µL

Table 2.8 GC Rich PCR setup.

Thermal cycler program: initial denaturation at 95 °C for 3 min. Followed by 35 cycles of denaturation at 95 °C for 30 s, annealing at annealing at a temperature suitable for the primers used for 30 s and elongation at 68 °C for 2 min. Final extension was at 68 °C for 10 min.

2.2.8 Reverse Transcription- Polymerase Chain Reaction

RT-PCR was performed using QIAGEN OneStep RT-PCR kit. Components were thawed on ice and a reaction mix was prepared according to Table 2.9.

Component	1x
5x RT-PCR Buffer	10 µL
dNTP mix (10 mM each)	2 µL
Primer F (6 µM)	5 µL
Primer R (6 µM)	5 µL
Enzyme Mix	2 µL
5x Q Solution	10 µL
Template RNA	2 µg
H_2O	to 50 µL

Table 2.9. RT-PCR Setup.

Thermal cycler program: reverse transcription at 50 °C for 30 min, then PCR activation at 95 °C for 15 min. Followed by 35 cycles of denaturation at 94 °C for 30 s, annealing at a temperature suitable for the primers used for 40 s and elongation at 72 °C for 2 min. Final elongation was at 72 °C for 10 min.

2.2.9 Isolation of Plasmid DNA from *E. coli*

Isolation of plasmid DNA from *E. coli* was performed using a QIAGEN Miniprep kit. The kit utilises alkaline lysis of cells followed by purification of DNA by adsorption to silica. *E. coli* was grown in 5 mL LB cultures supplemented with suitable antibiotic(s) overnight at 37 °C. Cells were harvested by centrifugation at 4,000 rpm for 10 min and the supernatant discarded. The cell pellet was resuspended in 250 µL of buffer P1, lysed with 250 µL buffer P2 followed by inversion to mix, and then neutralised by addition of 350 µL buffer N3. Cell debris was precipitated by centrifugation at 14,000 rpm for 10 min. The supernatant was added to a QIAprep spin column and centrifuged for 1 min at 14,000 rpm. The column was washed with 500 µL of buffer PB and centrifuged again. The column was washed with 750 µL of buffer PE and centrifuged again. DNA was eluted with 35 µL H_2O. Plasmid DNA was stored at -20 °C.

2.2.10 Preparation of Competent *E. coli* Cells

Chemically competent *E. coli* cells were produced from a starter culture (5 mL) grown for 16 h at 37 °C with shaking. This was then sub-cultured 1:100 into 50 mL fresh LB medium and allowed to grow at 37 °C, with shaking, until an OD_{600} reading of 0.4-0.5. Cells from this culture were then harvested by centrifugation at 4,000 rpm and 4 °C for 10 min. Cells were washed by resuspension in 50 mL ice cold 0.1 M $MgCl_2$, pelleted again by centrifugation and washed once more in 0.1 M $CaCl_2$. The final pellet, following washes, was resuspended in 2.5 ml 0.1 M $CaCl_2$, 20 % glycerol, divided into aliquots, frozen in liquid nitrogen and stored at -80 °C

2.2.11 Transformation of *E. coli* Cells

Competent cells were allowed to thaw on ice. 1-2 µL of plasmid DNA (approx. 100 ng DNA) was then added to cells and incubated on ice for 30 min. Cells were then heat shocked at 42 °C for 30 s and returned immediately to ice. 250 µL SOC media was then added to cells, followed by incubation at 37 °C for 1 hour with shaking. For plating out, 50 µL was spread onto LB agar plates containing suitable antibiotic(s). After this the culture was pelleted by centrifugation, the supernatant decanted and the pellet resuspended in residual media and plated out. Plates were incubated overnight at 37 °C. Antibiotic concentrations used are given in Table 2.4.

2.2.12 Agarose Gel Electrophoresis

Agarose gels were produced using 1 % w/v acrylamide dissolved by heating (microwave) in TBE buffer (89 mM Tris-HCl, 89 mM Boric acid, 2 mM EDTA). SYBR Safe DNA gel stain (Invitrogen) was added at a 1:10,000 dilution once the gel had cooled but was still liquid. 2 µL of 6x loading buffer (NEB) was combined with 10 µL of DNA/RNA sample. Samples were loaded into the gel and ran at 100 V until the dye front reached the bottom of the gel. TBE buffer was used as the running buffer. Gels were visualised and imaged using a GeneGenius bioimaging system (Syngene).

2.2.13 DNA Sequencing

DNA was sequenced using the chain termination method including dideoxynucleotide triphosphates (ddNTPs). Sequencing reactions were performed using a BigDye Terminator v3.1 Cycle Sequencing kit (ThermoFisher) with the setup shown in Table 2.10.

Component	1x (µL)
Plasmid DNA	1
Primer (10 µM)	1
Big Dye Buffer (5x)	2
H_2O	5
BigDye 3.1	1
Total	10

Table 2.10. DNA Sequencing reaction setup.

The sequencing reaction included 25 cycles of 96 °C for 10 min, 50 °C for 10 min and 60 °C for 4 min. Products of the reactions were analysed by Eurofins MWG. Sequencing data was analysed using BioEdit Biological sequence alignment editor (Tom Hall, Ibis Biosciences).

2.2.14 Restriction Digest

Restriction digests were performed with enzymes and reagents from either Invitrogen or NEB. Conditions were dependent on the DNA and restriction enzymes used. Manufacturer's instructions were followed. The general reaction setup is shown in Table 2.11. For double digests compatible buffers were used.

Component	1x
DNA	< 1 µg
10x Buffer	2 µL
Restriction Enzyme(s)	1 µL (each)
H_2O	to 20 µL

Table 2.11. Restriction digest setup.

Digests were incubated at 37 °C overnight. Reactions were scaled up as necessary for downstream purposes. Products from digests were used immediately or stored at -20 °C.

2.2.15 Gel Purification of DNA

Gel purification was carried out using a QIAGEN QIAquick Gel Extraction kit. DNA was separated on an agarose gel. Bands were visualised using a Dark Reader Transilluminator (Clare Chemical Research) and excised using a clean razor blade. Gel samples were transferred to a 1.5 mL Eppendorf and combined with 3 volumes buffer QG and incubated at 50 °C for 10 min. One volume of isopropanol was added to melted samples. Samples were loaded into a spin column and centrifuged (14,000 rpm, 1 min), the flow through was discarded. The column was then washed by centrifugation at 14,000 rpm for 1 min with 500 µL buffer QG then 750 µL buffer PE. DNA was eluted using 35 µL H_2O. DNA was used immediately after purification or stored at -20 °C.

2.2.16 PCR Product Clean-up

QIAGEN QIAquick PCR Purification kit was used for PCR product clean-up. 5 volumes of buffer PB was added to the PCR reaction mixture, this was then added to a spin column and centrifuged at 14,000 rpm for 1 min. Supernatant was discarded and the column washed by centrifugation at 14,000 rpm for 1 min with 750 µL PE buffer. DNA was eluted with 35 µL H_2O. DNA was used immediately after purification or stored at -20 °C.

2.2.17 TOPO Cloning

TOPO cloning utilises DNA topoisomerase I technology. A linearised DNA vector with topoisomerase covalently attached to at the 5' and 3' ends is used. Free 5' and 3' ends of a purified PCR product attack the bond between topoisomerase and vector forming covalent attachment and a circularised vector containing the PCR product (Figure 2.4).

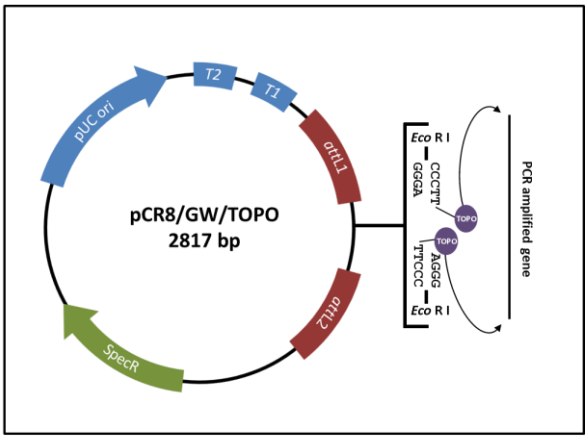

Figure 2.4 TOPO cloning reaction.

TOPO cloning requires 3' A- overhangs, these were added using *Taq* (NEB), as proof reading enzymes (Phusion, NEB) removes overhangs, producing blunt-end PCR fragments. Addition of poly(A) to PCR products from Phusion amplifications was performed according to Table 2.12.

Component	1x (µL)
Gel Purified PCR Product	35
dNTP mix (10 mM each)	0.4
10x Buffer	4
Taq Polymerase	0.2
H_2O	0.4

Table 2.12. Poly(A) addition reaction setup.

The reaction was incubated at 72 °C for 10 min then placed on ice. The product of the poly(A) extension was purified following the PCR Product Clean-up protocol. Cloning of PCR fragments into pCR8/GW/TOPO was then performed according to Table 2.13.

Component	1x (µL)
Clean PCR Product	3
Salt Solution	1
H_2O	1.5
pCR8/GW/TOPO	0.5

Table 2.13. TOPO cloning reaction setup.

The reaction was incubated at RT for 10 min then placed onto ice. The reaction product was transformed into chemically competent *E. coli.*

2.2.18 Gateway Cloning LR Recombination Reaction

The gene cloned into the pCR8 entry plasmid is flanked by attL sites, the Gateway cassette in the destination vector is flanked by attR sites. The clonase enzyme exchanges these sequences. For the LR reaction a Gateway LR Clonase II (ThermoFisher) enzyme mix was used. 100 ng of entry plasmid DNA was combined with 150 ng destination vector and TE buffer (10 mM Tris, 1mM EDTA, pH 8.0) in a final volume of 8 µL. To this mix, 2 µL LR Clonase enzyme mix was added. The reaction was incubated at 25 °C for 1 h then terminated by addition of 1 µL Proteinase K solution and incubation at 37 °C for 10 min. Reaction product was used directly in an *E. coli* transformation.

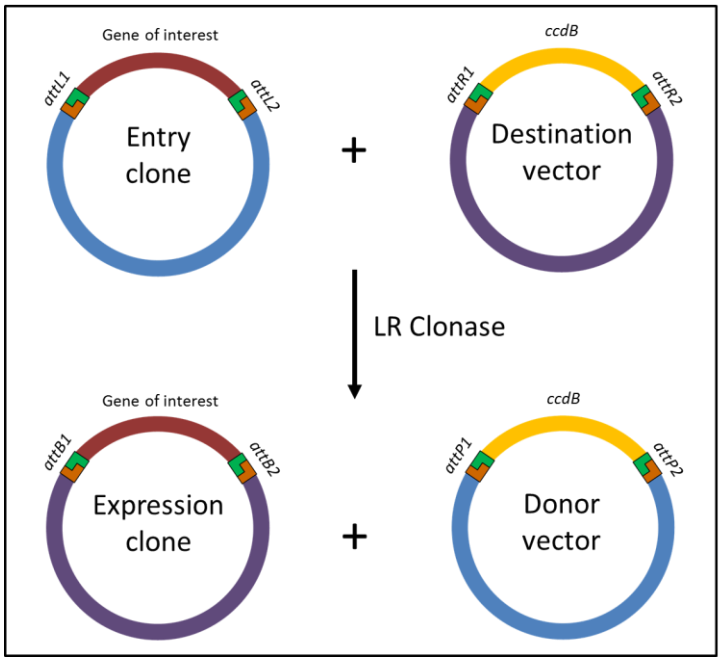

Figure 2.5 Gateway reaction.
att sites enable recombination catalysed by LR clonase. The *ccd*B cassette encodes a DNA gyrase inhibitor that aids selection of positive recombinants.

2.2.19 In-Fusion Cloning

In-Fusion cloning utilises the addition of flanking regions to the gene of interest by PCR and linearization of the destination vector, these two DNA fragments are combined by a proprietary enzyme. A PCR product from a gel purification and linearised vector from a cleaned up restriction digest were combined with reaction mix (Table 2.14) and incubated at 50 °C for 15 min. The product of this reaction was used directly in an *E. coli* transformation.

Component	**1x**
PCR Product	50 ng
Linearised Vector	100 ng
5x In-Fusion HD Enzyme Mix	2 µL
H_2O	to 10 µL

Table 2.14. In-Fusion cloning setup.

2.3 Protein Expression and Purification

2.3.1 Protein Quantification

Protein Quantification was performed by Bradford assay using Bradford Ultra (Expedeon). Standards of BSA ranging from 2 mg/ml to 0.2 µg/mL were utilised depending on the protein sample being analysed. The assay was performed in 96 well plates. For high range samples (0.1 mg/mL to 1.5 mg/mL) 10 µL of sample was combined with 150 µL of Bradford Ultra. For low range samples (1 µg/mL to 25 µg/mL) 100 µL of sample was combined with 100 µL of Bradford Ultra. Samples were mixed thoroughly. Assays were performed in either duplicate or triplicate. Absorbance of samples was measured at 595nm. A standard curve was produced and used to determine the sample concentration.

A Direct Detect IR Spectrophotometer (EMD Millipore) was also used to quantify protein samples by measuring in the amide region between 1600-1690 cm^{-1}. 2 µL of sample was loaded onto the supplied card and analysed following manufacturer's instructions.

2.3.2 Protein Concentration and Buffer Exchange

Protein samples were concentrated using Amicon Ultra Centrifugal Filters, 15 mL or 50 mL size units (EMD Millipore). Sample cut-offs of 10 kDa, 30 kDa or 50 kDa were used depending on the size of the protein being concentrated. Centrifugation was performed at 4,000 rpm.

Buffer exchange and desalting was performed using NAP-5 or NAP-10 columns (Illustra, GE). For NAP-5: the column was equilibrated with 10 mL buffer, 0.5 mL sample applied and eluted with 1 mL of appropriate buffer. For NAP-10: the column was equilibrated with 15 mL buffer, 1 mL sample applied and eluted with 1.5 mL of appropriate buffer.

2.3.3 Protein Dialysis

Dialysis of proteins was performed against 5 L of appropriate buffer. SnakeSkin dialysis tubing, Mw cutoff: 3.5 kDa (Life Technologies) was prepared by pre-soaking in appropriate buffer. Protein sample was added to the tubing and incubated in pre-cooled buffer at 4 °C overnight with constant stirring.

2.3.4 Protein Analysis by Sodium Dodecyl Sulphate Polyacrylamide Gel Electrophoresis (SDS-PAGE)

Protein samples were analysed by SDS-PAGE, which separates proteins according to mass, to determine their size and purity. Precision Plus Protein Prestained Standards (BioRad) were used. 10 %, 12 %, 15 % or 4-12 % RunBlue pre-cast gels (Expedeon) were used with RunBlue Tris-Tricine run buffer (Expedeon). Gels were also prepared using the Laemmli method (Laemmli, 1970). SDS-PAGE samples were prepared by combining 20 µL of sample with 5 µL of 5x SDS sample loading buffer (250 mM Tris-HCl pH 6.8, 5 % β-ME, 0.02 % bromophenol blue, 10 % SDS, 30 % glycerol). Samples were heated to 70 °C, briefly centrifuged and loaded into the gel. Protein gels were stained using InstantBlue (Expedeon). Gels were run at 180 V (Expedeon gel tank) Gels were imaged using a GeneGenius bioimaging system (Syngene).

2.3.5 Native Polyacrylamide Gel Electrophoresis and Zymography

For native gel electrophoresis, 7.5 % gels were made according to Laemmli (Laemmli, 1970), however SDS was omitted from the gel and SDS and β-ME were omitted from sample loading buffer. Samples were not heated. Gels were run at 4 °C and 100 V.

For red pullulan zymography, gels were run as for native PAGE, 10 mg/mL red pullulan (Megazyme) was added to the gel before it set. Gels were incubated in incubation buffer (10 mM NaOAc, 0.5 M NaCl, 1 mM DTT, 1 mM $CaCl_2$, 1 mM $MgCl_2$, pH 5.5) at 37 °C until zones of clearing could be seen. Gels were imaged using a GeneGenius bioimaging system (Syngene).

2.3.6 Western Blot Analysis of Proteins

Western blot analysis was used to determine the presence of specific proteins. Equal loading was achieved either by quantifying the amount of protein in the sample loaded or by using samples which had been treated identically. SDS-PAGE was performed on protein samples as described previously. Following this, proteins were transferred to a nitrocellulose membrane (Sigma) by electrophoresis in transfer buffer (25 mM Tris-HCl, 250 mM glycine, 10 % MeOH). Blots were run at 4 °C for 80 min at 95 mA or 16 h at 35 mA. Following blotting the membrane was removed from the cassette, washed once with TBS buffer (50 mM Tris, 150 mM NaCl, pH 7.6) and blocked with blocking buffer (5 % Marvel milk powder in TBS) for 1 hour at RT or 16 h at 4 °C. Following blocking the membrane was washed three times with TBST (TBS with 0.05 % Tween 20) and once with TBS. Primary antibody was added (1:4,000 dilution in TBS, 1 % Marvel milk powder) and incubated for 1 h at RT. Membrane was then washed three times with TBST and once with TBS. Secondary antibody was added (1:5,000 dilution in TBS, 1 %

Marvel milk powder) and incubated for 1 h at RT. Membrane was washed three times with TBST and once with TBS. Imaging the blot involved using ECL western blotting substrate (Promega), 0.5 mL of component A and 0.5 mL of component B were combined in a petri dish, into this the membrane was placed and incubated at room temperature for 1 min. The blot was dried with paper towel to remove excess substrate. Chemiluminescence was then imaged using the ImageQuant LAS 500 (GE). Blots were stained for protein with ponceau stain and imaged with a GeneGenius bioimaging system (Syngene). For detection of His_6 QIAexpress anti-His mouse antibody (QIAGEN) was used as the primary antibody and goat anti-mouse IgG-HRP (Santa Cruz Biotechnology) was used as the secondary. For detecting primary antibodies produced in rabbit, goat anti-rabbit IgG-HRP (Santa Cruz Biotechnology) was used as the secondary antibody.

2.3.7 Preparation of Protein Gel Slices for Mass Spectrometry Analysis

Mass Spectrometry was used to identify proteins present in SDS-PAGE bands. Bands were excised from gels using a clean, sterile scalpel and transferred to a low bind Eppendorf. Gel slices were destained with three washes in 30 % EtOH at 65 °C for 15 min. Then washed with 50 mM TEAB (Sigma)/50 % ACN for 15 min (all further wash steps were 15 min unless stated). Followed by incubation with 10 mM DTT at 55 °C for 30 min. DTT was decanted and IAA (30 mM iodoacetamide in 50 mM TEAB) was add and incubated for 30 min at RT, with protection from light. IAA was removed and the gel washed with TEAB/50 % ACN, then washed with 50 mM TEAB. Buffer was removed and the gel sliced into small pieces on a petri dish and transferred to a low bind Eppendorf. Sliced gel was washed with 50 mM TEAB/50 % ACN. Finally gel was washed with ACN, this was then decanted and residual solvent evaporated. Protein sample was then digested with trypsin and the product of digestion was analysed by MS.

2.3.8 Cell Culture and Protein Expression in *E. coli*

Starter cultures were prepared by picking a colony or adding 20 µL of a glycerol stock to 5 mL LB plus antibiotic. The culture was incubated at 37 °C with shaking for 16 h. Cells were subcultured by a 1:100 dilution in LB and allowed to grow until reaching OD_{600} of 0.6. The culture was then induced with IPTG (to a final concentration of 1 mM, 0.5 mM or 0.2 mM-dependent on the expression conditions being tested). Induced cultures were grown for 16 h. The temperature used for growth varied with experiment (18 °C, 20 °C, 22 °C, 28 °C or 37 °C). Cells were harvested by centrifugation at 4,000 rpm for 10 min and either used immediately or stored at -20 °C.

2.3.9 *E. coli* Cell Lysis

A cell pellet was resuspended in a maximum of 50 mL lysis buffer (50 mM Tris-HCl pH 7.5, 0.5 mM NaCl, 20 mM imidazole, protease inhibitor cocktail (Sigma) 1/100 v/v, 2 mg DNase, 2 mM DTT). The suspension was passed through a Cell Disruptor (Constant Systems) in one shot mode at a pressure of 25 kpsi. Samples were run through the disruptor 3 times to ensure complete lysis. Following lysis the lysate was centrifuged at 21,000 rpm for 15 min at 4 °C to produce a soluble supernatant and an insoluble pellet.

2.3.10 Preparation of Inclusion Bodies and β-Mercaptoethanol Soluble Protein from *E. coli*

Inclusion bodies were purified from the insoluble pellet produced after cell lysis and centrifugation. The pellet from 4 L of culture was resuspended in 100 mL urea buffer (50 mM Tris-HCl pH 8.0, 6 M urea) then centrifuged at 21,000 rpm for 10 min at 4 °C. This wash step was repeated twice more, each time the supernatant was removed and kept for further analysis. The urea acts to solubilise and unfold proteins by interacting with hydrogen bonds that would otherwise hold the protein in shape. The unfolded proteins were centrifuged to separate out the highly insoluble proteins that contain mixed inter- and intra-molecular disulfides. Urea is not able to fully denature and solubilise disulfide linked proteins therefore they remain present in the insoluble material.

The pellet was then resuspended in 50 mL β-ME buffer (50 mM Tris-HCl pH 8.0, 6 M urea, 140 mM β-ME) and β-ME soluble proteins were solubilised by vortexing. The β-ME breaks the disulfide bonds that form between cysteine residues, reducing them back to free thiol groups therefore enabling solubilisation. The solution was then centrifuged at 21,000 rpm for 10 min at 4 °C. The supernatant was saved as the β-ME soluble fraction. Other reducing agents (DTT, TECP) were tested in this process but produced lower yields of solubilised protein.

2.3.11 Preparation of Periplasmic Fraction from *E. coli*

Osmotic shock was used for purification of proteins that have been targeted to the periplasmic space. A pellet from a 100 mL bacterial culture was resuspended in 25 mL ice cold sucrose buffer (25 mM Tris pH7.5, 1 mM EDTA, 20 % sucrose) and incubated on ice with stirring for 10 min. The sample was then centrifuged at 4,000 rpm, 4 °C for 10 min. Supernatant was removed and the pellet resuspended in 10 mL ice cold 5 mM $MgCl_2$. This was then incubated on ice with stirring for 10 min. The sample was then centrifuged at 4,000 rpm, 4 °C for 10 min. The supernatant was the cold osmotic shock fluid and contained periplasmic proteins.

2.3.12 General Protein Chromatography Systems

For protein purification an ÅKTA FPLC chromatography system (GE) was used. The system was maintained at 10 °C to prevent protein degradation during purification. The system lines were stored in 20 % EtOH when not in use. Prior to use, pumps were washed and lines cleaned with 1 ml/min H_2O for 10 min. The column was connected to the system and washed with 1 ml/min H_2O until traces of EtOH were removed, the column was then disconnected. Pumps were washed with buffer(s) and the lines cleaned with 1 ml/min buffer for 10 min. The column was then reattached and equilibrated with buffer. Following use the pumps, lines and columns were washed with 1 ml/min H_2O for at least 1 CV. Pumps, lines and columns were finally washed with 1 ml/min 20 % EtOH for at least 1 CV. Columns were stored at 4 °C in 20 % EtOH.

2.3.13 Nickel Affinity Chromatography

Crude soluble extract or solubilised protein was first filtered through a 0.45 µm syringe filter to remove any aggregates that may block the system. The protein sample was loaded into a super loop (GE) loading column. Either a 1 mL or 5 mL His-Trap chelating column (GE) was used. The column was attached to the ÅKTA system and equilibrated with buffer A (50 mM Tris-HCl pH 7.5, 0.5 mM NaCl, 20 mM imidazole). The extract was then loaded onto the column. The flow through was retained for analysis. The column was washed with 10-25 CV of buffer A to remove non-specifically bound proteins. Wash samples were retained. Bound protein was eluted with buffer B (50 mM Tris-HCl pH 7.5, 0.5 mM NaCl, 500 mM Imidazole) in one step. The elution fractions were retained. A gradient elution was tested but was shown to make little difference during these purifications. Fractions were analysed by SDS-PAGE, fractions containing protein of interest were combined and concentrated.

2.3.14 Synthesis of 6-deoxy-6-amino-β-cyclodextrin

To enable coupling to a resin (NHS activated Sepharose, Sigma), β-CD was derivitised to produce 6-deoxy-6-amino-β-cyclodextrin. Derivitisation and coupling of β-cyclodextrin was performed according to (Chung et al., 2009). 10 g of dry β-cyclodextrin was transferred to a flask containing 10 ml fresh pyridine. A solution of carbonyldiimidazole (1.4 g) was dissolved in 10 mL fresh pyridine and added to the reaction mixture dropwise over 5 min, with gentle stirring. The activation reaction was allowed to proceed at room temperature for 2 h. Following this the activated cyclodextrin solution was added dropwise to a flask containing 1,3-diaminopropane (3.6 mL) with stirring. The reaction proceeded for 1 h at room temperature, after which, the cyclodextrin mixture was precipitated by adding the reaction solution dropwise to a flask containing 1 L CH_2Cl_2 with vigorous stirring. A flaky white

precipitate was isolated *via* suction through a fritted funnel. The precipitate was re-dissolved in toluene and dried by rotary evaporation three times to remove any residual toluene. The cyclodextrin product was analysed by MALDI-ToF MS (Appendix) and used without any further purification.

2.3.15 Generation of β-CD Sepharose Resin

Excess (2 g) activated β-CD (6-deoxy-6-amino-β-cyclodextrin) was dissolved in 10 mL 0.2 M $NaHCO_3$, 0.5 mM NaCl, pH 8.3 to form the coupling solution. 20 mL of NHS-activated Sepharose 4 fast flow (GE) was suspended in H_2O to form a slurry. This was added to a fritted column attached to a vacuum line and washed with 10 volumes of cold 1 mM HCl. The resin was transferred to a 50 mL tube, the coupling solution was added and incubated for 4 h at RT. Coupling solution was removed using a fritted column and vacuum line. The resin was transferred to a 50 mL tube and blocking of non-reacted NHS groups was performed by the addition of 20 mL 0.1 M Tris-HCl pH 8.5 for 2 h. Resin was transferred to a fritted column and washed with 3 x 25 mL 0.1 M Tris-HCl and 3 x 25 mL 0.1 M NaOAc pH 5.0. Resin was stored in 20 % EtOH.

2.3.16 β-Cyclodextrin Affinity Chromatography

β-CD affinity chromatography was carried out using 25 mL of β-CD-Sepharose loaded into an XK 26/20 column (GE). The preparation of β-CD-Sepharose is outlined in below. Protein sample was exchanged into buffer A (10 mM NaOAc, 0.5 M NaCl, 5 mM $CaCl_2$, pH 5.5) and loaded into a 2 mL loading loop. The column was attached to the ÅKTA system and equilibrated with Buffer A. The protein was loaded onto the column and the flow through retained for analysis. The column was washed with 4 CV of buffer A to remove non-specifically bound proteins, wash samples were retained for analysis. Bound protein was eluted with buffer B (10 mM NaOAc, 0.5 M NaCl, 5 mM $CaCl_2$, 7 mM β-CD, pH 5.5) in one step, elution fractions were retained. Fractions were analysed by SDS-PAGE, fractions containing protein of interest were combined and concentrated. The column was cleaned with buffer A, then water and stored in 20 % EtOH.

2.3.17 Anion Exchange Chromatography

Anion exchange chromatography was performed using a MonoQ 4.6/100 PE column (GE). The column was equilibrated with buffer A (50 mM Tris-HCl pH 7.5). Prior to loading, the protein sample was exchanged into buffer A. The sample was loaded onto the column using a 1 mL loading loop. Following injection onto the column, unbound proteins were eluted by washing with 10 CV buffer A. Flow through and wash fractions were retained for analysis. Bound proteins were eluted with either a linear or stepwise elution using buffer B (25 mM Tris pH7.5

1 M NaCl). Fractions were analysed by SDS-PAGE. For cleaning, the column was reversed and washed with 1 CV of each of the following: 2 M NaCl, 2 M NaOH, 2 M NaCl, 1 M HCl, 75 % AcOH, 2 M NaCl, in between each wash step the column was washed with 5 mL H_2O. Column was stored in 20 % EtOH.

2.3.18 Size-Exclusion Chromatography

Size exclusion chromatography was carried out on a 16/60 Superdex S200 column (GE), which is capable of protein fractionation between 10-1500 kDa. The column was equilibrated with 2 CV of buffer (50 mM Tris pH 7.5). The protein sample was exchanged into compatible buffer and loaded onto the column using a 2 mL loading loop. Isocratic elution was carried out over 2 CV. Fractions containing protein were collected and analysed by SDS-PAGE. Fractions containing protein of interest were combined and concentrated. Column was cleaned with 1 CV of 0.2 M NaOH at 1 ml/min.

2.3.19 Protein Refolding by Dilution

Protein refolding was performed on 100 mL β-ME soluble supernatant. This was first dialysed over night against 1.5 L of 50 mM Tris-HCl pH 8.0, 1 M guanidine hydrochloride, to remove a large proportion of the β-ME. The dialysed sample was combined with 100 mL 6M guanidine hydrochloride and incubated at room temp 30 min. DTT was added to 4 µM and incubated for 1 h. Cystine was then added to 14 mM and incubated for 10 min. The mixture was added dropwise to 1 L of 50 mM Tris HCl pH 8.0, 5.5 mM cysteine and incubated for 1 h. The product was concentrated by nickel affinity chromatography.

2.3.20 On-Column Protein Refolding

The β-ME soluble fraction from a protein solubilisation procedure was loaded into a super loop (GE) loading column. A 1 mL His-Trap chelating column (GE) was used. The procedure for nickel affinity chromatography was followed. Eluted fractions containing protein of interest were combined and concentrated.

2.3.21 Protein Refolding Using Quick Fold

QuickFold is a commercially available kit that can be used for screening different protein refolding conditions. The screen includes 15 different buffers which vary in their composition two basic buffers are used- MES pH 6.0 or Tris pH 8.5 with varying levels of DTT, reduced/oxidised glutathione, guanidine hydrochloride, Triton X-100, PEG, arginine, sucrose, and different NaCl concentrations. 50 µL of 1 mg/mL solubilised protein was slowly added to

each of the 950 µL refolding buffer and incubated at 22 °C for 2 h. Samples were then centrifuged to pellet insoluble material and analysed by SDS-PAGE.

2.3.22 Antibody Generation

Samples of recombinant LD (1.6 mg) and LDI (2 mg) were submitted to Eurogentec for antibody generation in rabbit (3 month programme). Each immunisation consisted of 1/8th of total submitted protein sample. Initial immunisation occurred at day 0 with boosters at 14, 28 and 56 days. Blood samples were taken at 0 days (pre-immune), 38 days (small bleed), 66 days (large bleed) and 87 days (final bleed), from which sera was produced. Isolated sera were stored at -20 °C.

2.3.23 Standard Enzyme Linked Immunosorbent Assay (ELISA)

Absorbance readings were performed using a FLUOstar Omega (BMG labtech) plate reader in absorbance mode at wavelength 405 nm. Each sample was run in either duplicate or triplicate, with the average result and standard error used for data analysis. Controls of no antigen, no primary antibody and no secondary antibody were included in each experiment and found to be within the expected range for each experiment.

A Corstar high binding polystyrene 96 well plate (Corning) was coated with 100 ng of antigen (in 100 µL) per well and incubated for 16 h at RT. The plate was washed three times with PBST (PBS with 0.1 % Tween 20). The plate was then blocked with 5 % w/v Marvel milk powder in PBST (200 µL per well) and incubated at room temperature for 1 h. During this incubation time serial dilutions of individual animal sera (1 in 100, 1 in 300, 1 in 900, 1 in 2700, 1 in 8100, 1 in 24,300 1 in 72,900, 1 in 218,700) were prepared in PBST. The plate was washed three times with PBST. 100 µL of serum dilution was added to each well and incubated at 37 °C for 1 h. The plate was washed three times with PBST. Secondary antibody, goat anti-rabbit IgG-HRP (Santa Cruz Biotechnology) at a 1:5,000 dilution in PBST was loaded (100 µL per well) and incubated at 37 °C for 1 h. The plate was washed three times with PBST. 100 µL ABTS peroxidase substrate (5 mg in sodium citrate with 0.02 % H_2O_2) was added to each well and incubated at room temperature for 30 min. Absorbance measurements were read at 405 nm.

2.4 Enzyme Assays

2.4.1 Bicinchoninic Acid Reducing End Assay of LD

BCA assay was performed using a modified protocol from (Doner and Irwin, 1992). Hydrolysis of pullulan (Sigma) by LD (recombinant) or *Kp* pullulanase (Megazyme, Specific activity: 34 U/mg at 40 °C, pH 5.0, 1% pullulan) was measured by the release of reducing ends. The concentration of reducing ends was measured by the reduction of Cu^{2+} to Cu^{+} which subsequently complexes with bicinchoninic acid creating a coloured complex that absorbs at 540nm. Enzyme was diluted to final concentrations (dependent on assay setup) in reaction buffer (20 mM NaOA pH 5.5). Inhibitors were added to a final concentration between 0.001 mM to 1mM (dependent on the assay setup). The inhibitor was incubated with LD at 30 °C for 30 min. Pullulan substrate was then added to a final concentration of 0.1 mg/ml. The reaction was allowed to proceed at 30 °C for 30 min. The reaction was terminated by the addition of 40 mM sodium carbonate, 5 mM disodium 2,2'-bicinchoninate, 5 mM copper (II) sulfate and 12 mM L-serine. This was then incubated at 80 °C for 30 min then at 4 °C for 15 min. Absorbance readings were performed at 540 nm using a FLUOstar Omega (BMG labtech) plate reader. Controls containing inactivated (boiled) enzyme were used to determine background readings. All assays were performed in triplicate.

2.4.2 Limit Dextrizyme and Red Pullulan Assays

Limit Dextrizyme and red pullulan assays were performed according to manufacturer's instructions (Megazyme). For Limit Dextrizyme assay 500 µL of protein extract in NaOAc pH 5.5, 25 mm DTT was equilibrated at 40 °C for 5 min. To this a Limit-Dextrizyme tablet was added. The hydrolysis was allowed to proceed for 10 min at RT. The reaction was terminated by the addition of 5 mL 1 % Tris followed by vortexing. Samples were clarified by filtration through filter paper and absorbance readings were performed at 590 nm. Controls containing no enzyme were included in the assays.

For red pullulan assay 1 mL of protein extract in NaOAc pH 5.5, 25 mm DTT was equilibrated at 40 °C for 5 min. To this 0.5 mL red pullulan solution (0.5 g in 25 mL of 0.5 M KCl) was added. The hydrolysis was allowed to proceed for 10 min at 40 °C. The reaction was terminated by the addition of 2.5 mL 95 % V/V EtOH followed by vortexing. Samples were allowed to equilibrate for 10 min then were centrifuged at 4000 rmp for 10 min. Supernatants were decanted and absorbance readings were performed at 510 nm. Controls containing no enzyme were included in the assays. Miniaturisation of both assays was attempted using $1/10^{th}$ of recommended reagents but yielded poor reproducibility.

2.4.3 Fluorimetric and Colorimetric Assay of LD using Hexafluor and Hexachrom

Assays using hexachrom (4,6-*O*-benzylidene-2-chloro-4-nitrophenyl-β-6^3-α-D-maltotriosyl-maltotriose) and hexafluor (4,6-*O*-benzylidene-4-methylumbelliferyl-β-6^3-α-D-maltotriosyl-maltotriose) were performed according to manufacturer's instructions (Megazyme). An assay mix consisting of substrate, either 12.4 mM hexachrom or 6.2 mM hexafluor in 1 mL DMSO (final assay concentration 4 mM or 2 mM, respectively), 50 µL α-glucosidase (1500 U/mL), 50 µL β-glucosidase (400 U/mL) and 2 mL H_2O was prepared. The 40 µL mix was pre-incubated at 40°C for 5 min. 40 µL limit-dextrinase containing protein extract (in NaOAc pH 5.5, 25 mm DTT) was also pre-incubated at 40°C for 5 min. Both pre incubated samples were combined and incubated at 40°C for 30 min. At the end of the 30 min incubation period, 100 µL 0.1 mM Tris pH 9.0 was added. The absorbance of the solutions and the reaction blank were measured at 400 nm using a FLUOstar Omega (BMG labtech) plate reader. Assays were performed in triplicate.

Preliminary assays were performed to ensure the correct assay setup. No inhibitor and boiled enzyme controls were included to account for background reading produced by the presence of protein and some compounds. These background data were subtracted from the assay results.

2.4.4 Glucosylceramide Synthase Assay

Assay was based on those reported in (Ichikawa et al., 1996, Niino et al., 2013), this utilises a synthetic fluorescent substrate- C6-NBD-Ceramide (ThermoFisher). Mung bean microsomes (a kind gift from Irina Ivanova) were created following (Abas and Luschnig, 2010). Substrate liposomes were prepared by combining 50 µg C6-NBD-Cer and 500 µg lecithin in 100 µl EtOH. Solvent was then evaporated. Mixture was resuspended in 1 ml water by sonication in sonication bath 10 min. 30 uL of microsomes, 10 µL of liposomes, and 1mM UDP-Glc were combined to a 50 µL final volume in buffer (100 mM MOPS KOH, pH7.2). Reactions were incubated at 30 °C with samples taken at 0, 4, 8, 16 hour time points.

After incubation lipids were extracted with $CHCl_3$/CH_3OH 2:1 (vol/vol) and evaporated to dryness. Then the lipid extract (lower phase) was redissolved in 10 µL $CHCl_3$/CH_3OH 2:1 (vol/vol). A TLC run using a silica plate in $CHCl_3$/CH_3OH/H_2O 65:25:4 (vol/vol). Lipid migration was visualised by UV illumination.

LC-MS was attempted using a Luna NH_2 Luna 3 µm NH_2 100 Å, LC Column 150 x 2 mm column (Phenomenex) coupled to a Thermo-Finnigan MS instrument equipped with a Deca XP ion trap. 10 µL of sample injected. A linear gradient of 90 % H_2O: 10 % Acetonitrile to 10 % H_2O: (0 % Acetonitrile was performed 5 min to separate sample components. A UV detector was used to detect absorbance, masses corresponding to peaks in absorbance were analysed.

2.5 Computational Methods

2.5.1 Peptide Molecular Modelling

Peptide secondary structure was analysed using PEP-Fold online software (Thevenet et al., 2012).

2.5.2 Molecular graphics

The PyMOL Molecular Graphics System (Version 1.7.4 Schrödinger, LLC.) and SPDB-viewer (Guex and Peitsch, 1997) were used to generate protein and peptide 3-D images.

2.5.3 Subcellular localisation prediction

SignalP-4.1, Protein Prowler and ChloroP-1.1 were used to predict the subcellular location of porteins from their primary sequences. SignalP-4.1 is a eukaryotic secretory protein predictor (Petersen et al., 2011) this server predicts the presence and location of signal peptide cleavage sites in amino acid sequences. Prowler determines the localisation of the protein among the following categories: secretory pathway, mitochondrion, chloroplast or other (nucleus, cytoplasmic) (Bodén and Hawkins, 2005). ChloroP predicts the presence of a chloroplast transit peptide and the location of potential cleavage sites (Emanuelsson et al., 1999).

2.5.4 Image Processing

Image processing was performed using Fiji (Schindelin et al., 2012).

2.5.5 Sequence Alignment

Sequence alignment was performed using BioEdit (Hall, 1999).

2.6 Plant methods

2.6.1 Barley Growth

Barley (var. Tipple) was surface sterilised by immersion in 4 % bleach (Parazone) solution. Traces of bleach were removed by repeated washing (ten times or more) with H_2O. Ten grains were plated out on two layers of filter paper pre-soaked with 2 mL H_2O in a petri dish. The petri dish was wrapped in foil to protect form the light and transferred to a dark Hybaid incubator (Thermo) at 17 °C. For inhibitor screens 2 mL H_2O was replaced with the compound dissolved in 2 mL H_2O.

For leaf material, germinated grains were moved into a sterile culture vessel containing ½MS agar and grown in light conditions at RT until reaching a suitable size. Sterile conditions were maintained during growth. Plant samples were harvested using a sterile scalpel and frozen in liquid nitrogen.

2.6.2 Arabidopsis and Tef Growth

Arabidopsis and tef were sterilised in an open Eppendorf for 4 h inside a desiccator jar with 50 mL of bleach acidified with 0.3 mL concentrated HCl. The desiccator jar was kept in a fume hood.

2 mL of 1 % Agar, ½ MS medium was added to the base of 20 mm wells (Sterilin, UK) of 25-well sterile plastic plates. ½MSAgar media was mixed with 2 µL of aqueous solution of inhibitor (in the case of water insoluble compound in DMSO solution). DMSO concentrations less than 0.1 % are shown to have no effect on seed germination (Erdman and Hsieh, 1969).

12 Arabidopsis seeds (var. Col-0) or 8 tef grains (var. Trotter) were placed in a straight line across each well. This was performed using a sterile toothpick. Plates were covered with a lid and sealed with micropore tape. Plates were stratified for 2 d at 4 °C then and incubated vertically. Arabidopsis was incubated at 22 °C in a controlled environment room (16 h light : 8 h dark, 22 °C, 250 µmol photosynthetically active radiation m^{-2} s^{-1}) for 10 d. Tef was incubated in a dark Hybaid incubator (Thermo) at 17 °C for 3 d.

2.6.3 Root and Shoot Length Analysis

Barley

Root and coleoptile length was measured by hand using a ruler. The length of the longest root was measured from the point where it emerges from the grain to the tip. Coleoptile length was measured from the point it meets the embryo to the root tip.

Arabidopsis and Tef

Roots were imaged by photography of the plate, then root length was manually measured using ImageJ (FIJI) software.

2.6.4 Grain weight measurement

Grain measurements were performed using a MARVIN grain analyser (GTA Sensorik GmbH) set to barley mode.

2.6.5 Barley grain dissection

Plant samples were dissected using a sterile scalpel and tweezers, then frozen in liquid nitrogen.

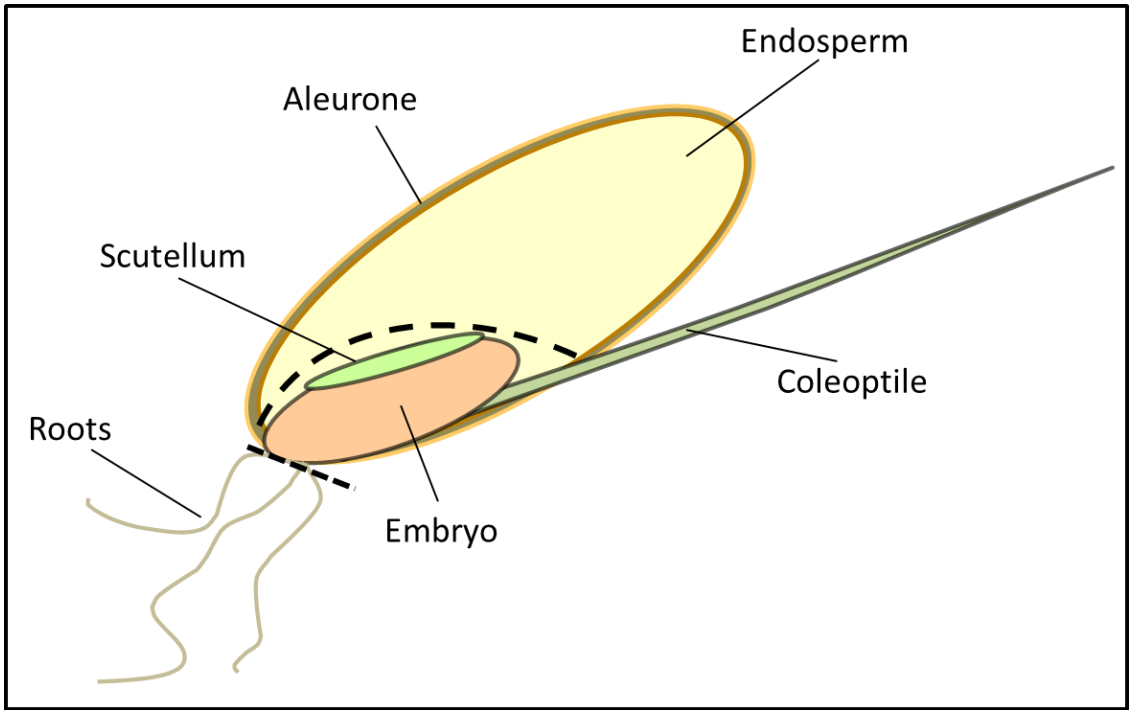

Figure 2.6 Barley grain sections used in dissection
Dashed lines represent points where cuts are made to separate roots, endosperm and embryo samples. Created using information from (Palmer, 2006).

2.6.6 Protein extraction

Protein extracts were prepared using 500 µL extraction buffer (100 mM MOPS-KOH pH7.2, 1 mM EDTA, 1 mM DTT, 10 % v/v ethylene glycol, protease inhibitor cocktail 10 µL/mL) per grain. Samples were homogenised by grinding in a mortar and pestle under liquid nitrogen. Samples were passed through a layer of muslin to remove solid material. Samples were incubated on ice for 15 min then centrifuged 4,000 rpm for 10 min at 4 °C. Supernatant was decanted and used as crude protein extract. To extract LDI samples were incubated overnight at 4 °C.

2.6.7 Preparation of barley protein extracts for glycoprotein MS analysis

To enable analysis of protein samples by MS a modified extraction process was utilised. Barley grains were germinated as previously described, for 5 days in either H_2O or 500 µM DNJ. 20 grains were harvested for each growth condition. Germinated barley grains were dissected into three parts:

- "Endosperm"- the grain including the endosperm, the aleurone and the pericarp
- "Root"- the roots, cut away from the rest of the growing embryo
- "Shoot"- the coleoptile and embryo including the scutellum

All dissected samples were homogenised by grinding in a mortar and pestle under liquid nitrogen. 3 mL MS extraction buffer (25 mM Tris-HCl pH7.4, 150 mM NaCl, 5 mM EDTA, protease inhibitor cocktail 10 µL/mL. 1 % CHAPS) was used. Samples were passed through a layer of muslin to remove solid material. Then crude extracts were incubated on ice for 15 min then centrifuged 4,000 rpm for 10 min at 4 °C. Supernatant was decanted and used as crude protein extract.

Protein samples were processed by treatment with different Peptide-*N*-Glycosidases (PNG-A and -F) and analysed by MALDI-TOF mass spectrometry.

2.7 Protein Localisation in *N. benthamiana*

2.7.1 Generation of Plasmid Constructs

pCR8 LD and LDI no stop vectors were used in Gateway LR reactions with pK7FWG2.0 (Figure 2.7) to generate plant expression C-terminal GFP fusion constructs.

2.7.2 Transformation of Agrobacterium

Agrobacterium tumifaciens LBA4404 cells were transformed with plasmid DNA by electroporation for 1 second at 2.5 kV. Cells were added to 200 µl SOC media and recovered for 2 h at 28 °C. Cells were plated on LB plates containing Spc and Rif and incubated at 28 °C for 3 d.

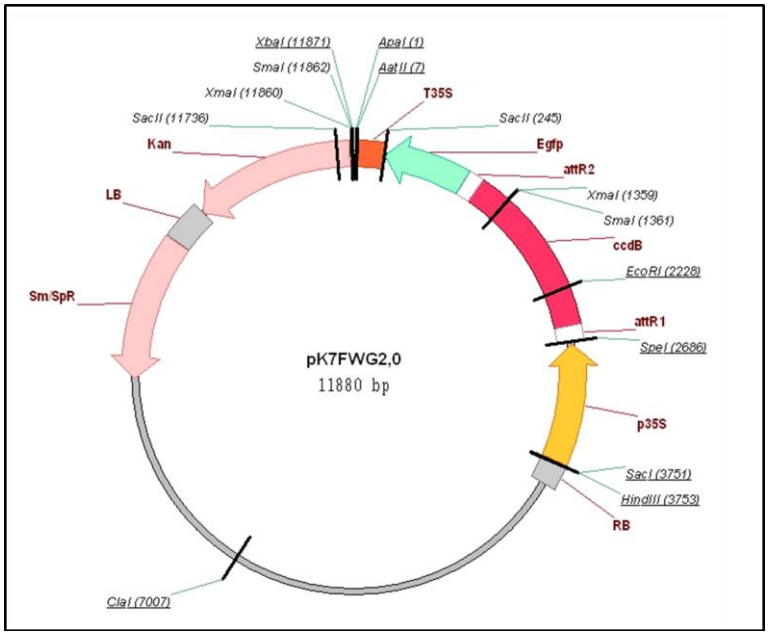

Figure 2.7 pK7FWG2.0 C-terminal GFP plant expression vector.

2.7.3 Protein Expression in *N. benthamiana*

Agrobacterium colonies were picked into 100 mL LB (spc and rif) and incubated at 28 °C for 3 d. The cells were pelleted by centrifugation at 4,000 rpm, 10 min, 4 °C.
Then resuspended in an appropriate volume of MMA buffer (10 mM MES pH 5.6, 1 mM $MgCl_2$, 10 µM acetosyringone) to give an OD_{600} of 0.4.

Cultures were used to infiltrate leaves of two plants (3 weeks old). Leaves were nicked using a sterile needle and infiltrated by forcing the solution into the extracellular space (Figure 2.8, A).

Plants were grown in a glasshouse maintained at 25 °C with supplemental lighting to provide 16 hours of daylight (Figure 2.8, B). The leaves were harvested 3 days post infiltration.

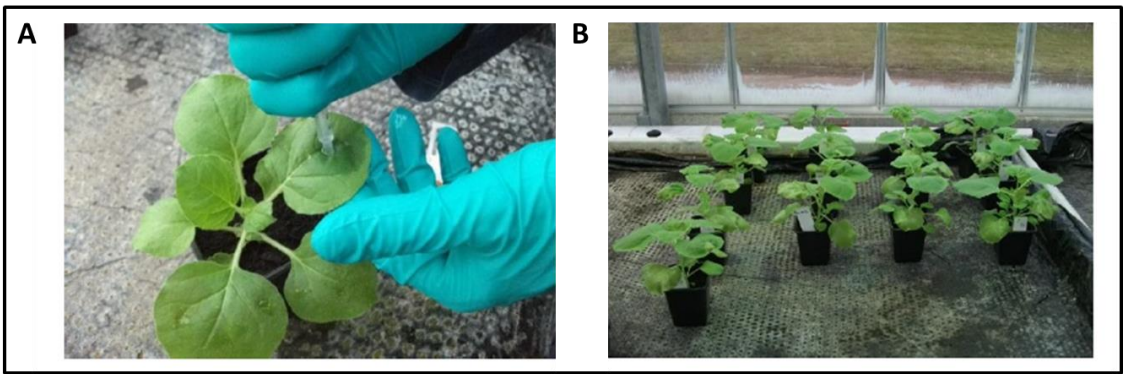

Figure 2.8 A. The infiltration process. B. Infiltrated plants in the glasshouse.
Image from Matthew Donaldson.

2.7.4 Confocal Microscopy of *N. benthamiana*

Leaves expressing the protein of interest were cut into 1 cm discs, mounted on a microscope slide and visualised using a Leica SP5 confocal microscope (Leica Microsystems) with a HCX PL APO CS 63.0x1.20 water immersion objective. For visualisation of GFP, samples were excited at 488 nm and the emission detected at 500-580 nm, laser power between 40-60 %.

2.8 Transgenic Plant Generation

2.8.1 Generation of Agrobacterium vectors for plant transformation

Performed following (Smedley and Harwood, 2015). Fragments of the sequences for LD (301 bp) or LDI (243 bp) were PCR amplified from genomic DNA purified from barley cultivar Golden Promise using primers: LD F aaagcgaaacattgcaaacc, LD R aaagatcttcggttgcttcg, LDI F ctgcgcatcctcatggac, LDI R actccgcttcattaccttgg. PCR products were cloned into pCR8/GW/TOPO using TOPO cloning. A Gateway LR reaction was used to transfer sequences from entry vector into pBRACT207 destination vector (Figure 2.9). pBRACT204 (Figure 2.10), a GUS overexpression construct was used to generate control plants. Correct sequences were confirmed by sequencing.

Agrobacterium strain AGL1 was transformed with pBRACT vectors, cells recovered at room temperature for 24 h, with shaking. A large culture was grown for 2-3 days, then used to transform immature plant embryos.

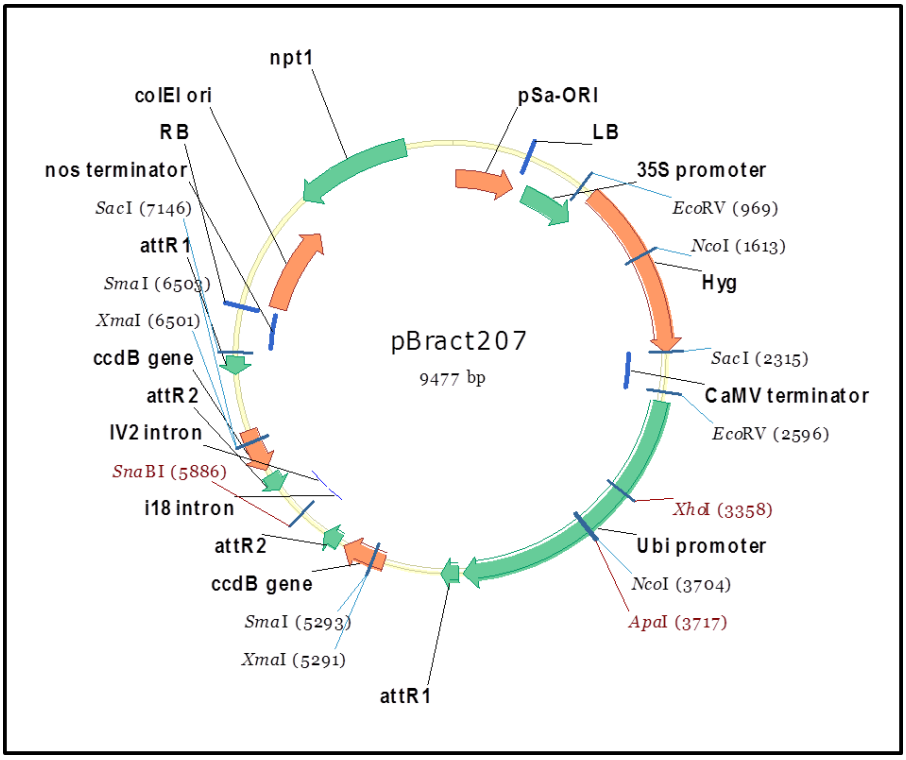

Figure 2.9 pBRACT207 vector used for RNAi.

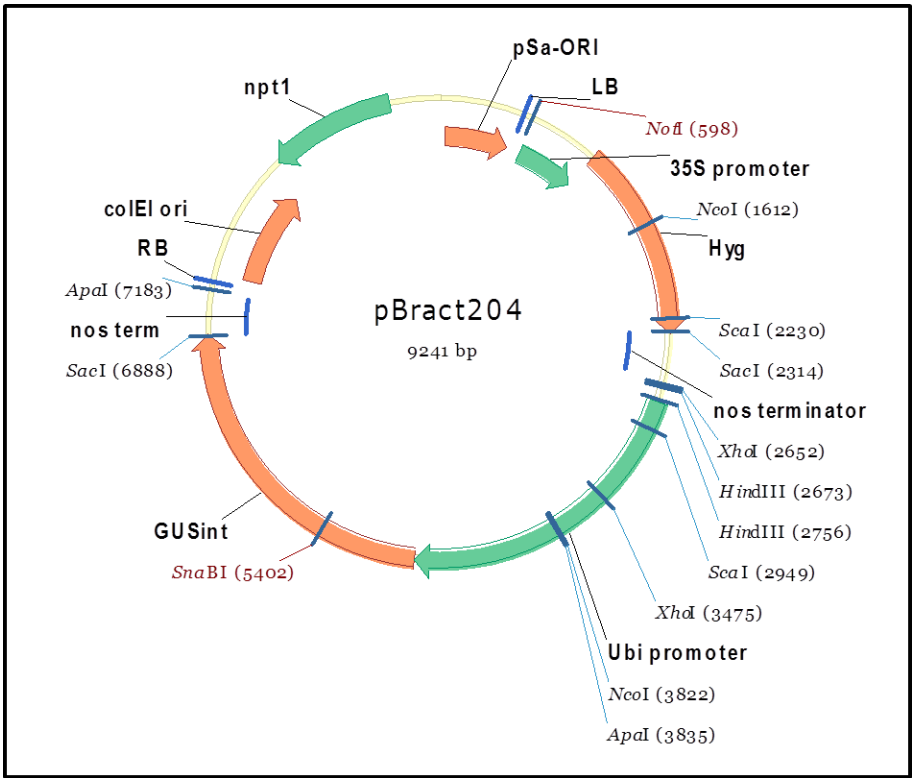

Figure 2.10 pBRACT204 vector used as control plasmid.

2.8.2 Transformation of Barley Plants

Plant transformation was carried out at the Biotechnology Resources for Arable Crop Transformation facility (BRACT, John Innes Centre). Transformation of plants was performed according to (Harwood et al., 2009), in which details of growth media and precise methods are given. In brief, immature embryos of barley Golden Promise were collected at a size of 1.5-2 mm in diameter. A small drop of agrobacterium was added to immature embryos and excess agrobacterium was removed. Embryos were placed scutellum side down on plates containing callus induction medium and co-cultivated for 3 d at 23 °C in the dark. Material was transferred to plates containing hygromycin as the selective agent and timentin to remove agrobacterium from cultures. Embryos were cultured at 23 °C in the dark for 2 weeks then transferred to fresh plates and grown for a further two weeks. Embryos were transferred to fresh plates a third time and grown for six weeks. Embryo derived callus was transferred into transition medium (containing hygromycin and timentin) and grown for 2 weeks at 23 °C with low light. At this point transformed lines produced small shoots and green areas.

Plants were regenerated, embryo derived material was transferred to regeneration medium (containing hygromycin and timentin) and grown until shoots were 2-3 cm long. Plantlets were transferred to glass culture tubes and grown until strong roots formed. Plats were then transferred to soil and covered with propagators to keep humidity levels high and establish growth in soil.

2.8.3 Plant growth conditions

Plants were grown in barley growth mix, consisting of 2:2:1 mix of Levington M3 compost: Perlite: Grit. The mix also included slow release fertiliser, Osmoote, added following manufacturers recommendations. Seedlings were sown in 5 cm pots and potted on into 13 cm pots roughly 30 days later, using the same growth mix. Plants were grown in a controlled environment room set to 15 °C day and 12 °C night temperatures, 80 % relative humidity, light levels 500 µmol/m^2/s^1.

2.8.4 Copy number analysis

Young leaf samples were taken to provide DNA samples. DNA preparation and copy number analysis was performed by iDna Genetics (Norwich BioIncubator, UK) using g-count genotyping technology. This utilises quantitative real-time PCR using primers for the hygromycin resistance cassette present in the pBRACT T-DNA insertion sequence.

2.9 References

Abas, L. & Luschnig, C. 2010. Maximum yields of microsomal-type membranes from small amounts of plant material without requiring ultracentrifugation. *Analytical Biochemistry,* 401, 217-27.

Bodén, M. & Hawkins, J. 2005. Prediction of subcellular localization using sequence-biased recurrent networks. *Bioinformatics,* 21, 2279-2286.

Chung, J. A., Wollack, J. W., Hovlid, M. L., Okesli, A., Chen, Y., Mueller, J. D., Distefano, M. D. & Taton, T. A. 2009. Purification of prenylated proteins by affinity chromatography on cyclodextrin-modified agarose. *Analytical Biochemistry,* 386, 1-8.

Doner, L. W. & Irwin, P. L. 1992. Assay of reducing end-groups in oligosaccharide homologues with 2,2'-bicinchoninate. *Analytical Biochemistry,* 202, 50-533.

Emanuelsson, O., Nielsen, H. & Von Heijne, G. 1999. Chlorop, a neural network-based method for predicting chloroplast transit peptides and their cleavage sites. *Protein Science,* 8, 978-984.

Erdman, H. E. & Hsieh, J. J. S. 1969. Dimethylsulfoxide (DMSO) effects on four economically important crops. *Agronomy Journal,* 61, 528-530.

Guex, N. & Peitsch, M. C. 1997. Swiss-model and the swiss-pdbviewer: An environment for comparative protein modeling. *Electrophoresis,* 18, 2714-2723.

Hall, T. A. Bioedit: A user-friendly biological sequence alignment editor and analysis program for windows 95/98/nt. Nucleic acids symposium series, 1999. 95-98.

Harwood, W. A., Bartlett, J. G., Alves, S. C., Perry, M., Smedley, M. A., Leyland, N. & Snape, J. W. 2009. Barley transformation using agrobacterium-mediated techniques. *Methods in Molecular Biology,* 478, 137-47.

Ichikawa, S., Sakiyama, H., Suzuki, G., Hidari, K. I. & Hirabayashi, Y. 1996. Expression cloning of a cDNA for human ceramide glucosyltransferase that catalyzes the first glycosylation step of glycosphingolipid synthesis. *Proceedings of the National Academy of Sciences of the United States of America,* 93, 4638-4643.

Laemmli, U. K. 1970. Cleavage of structural proteins during the assembly of the head of bacteriophage T4. *Nature,* 227, 680-685.

Niino, S., Nakamura, Y., Hirabayashi, Y., Nagano-Ito, M. & Ichikawa, S. 2013. A small molecule inhibitor of bcl-2, ha14-1, also inhibits ceramide glucosyltransferase. *Biochemical and Biophysical Research Communications,* 433, 170-1744.

Palmer, G. H. 2006. *Barley and malt. Handbook of brewing,* Boca Raton, Florida: , CRC Press, Taylor & Francis Group.

Petersen, T. N., Brunak, S., Von Heijne, G. & Nielsen, H. 2011. Signalp 4.0: Discriminating signal peptides from transmembrane regions. *Nature Methods,* 8, 785-786.

Schindelin, J., Arganda-Carreras, I., Frise, E., Kaynig, V., Longair, M., Pietzsch, T., Preibisch, S., Rueden, C., Saalfeld, S. & Schmid, B. 2012. Fiji: An open-source platform for biological-image analysis. *Nature Methods,* 9, 676-682.

Smedley, M. A. & Harwood, W. A. 2015. Gateway®-compatible plant transformation vectors. *Methods in Molecular Biology,* 1223, 3-16.

Thevenet, P., Shen, Y., Maupetit, J., Guyon, F., Derreumaux, P. & Tuffery, P. 2012. Pep-fold: An updated de novo structure prediction server for both linear and disulfide bonded cyclic peptides. *Nucleic Acids Research,* 40, W288-93.

Chapter 3- Chemical Genetics *in Planta* Identifies Novel Iminosugar Inhibitors of Root Growth

3.1.1 Iminosugars as Small Molecule Inhibitors of Carbohydrate Active Enzymes

Iminosugars are sugar-like molecules in which the endocyclic oxygen is replaced by a basic nitrogen atom. These molecules have a varied structure and represent the largest class of carbohydrate mimics (Compain and Martin, 2007). Mankind's exploitation of iminosugars began with the use of plant extracts as herbal remedies, these were only later revealed to contain high levels of iminosugars. One particular example is the white mulberry, *Morus alba*, one of the natural sources of deoxynojirimycin (DNJ) (Figure 3.1, B) (Asano et al., 1994b). The scientific interest in iminosugars began with early work on chemical synthesis of sugar derivatives containing heteroatoms (Jones and Turner, 1962, Paulsen and Todt, 1968). Shortly after this the first synthetic strategy for DNJ was outlined alongside the isolation of nojirimycin (NJ) (Figure 3.1, A) from *Streptomyces* (Paulsen, 1966, Ishida et al., 1967a, Ishida et al., 1967b). Interest soon turned to the use of iminosugars in medical applications following the discovery that DNJ inhibits α-glucosidase activity (Asano et al., 1994a). Advances in chemical synthesis and purification techniques have led to the modification of original scaffolds, enabling the generation of many iminosugar analogues and glycoconjugates (Gloster and Vocadlo, 2012).

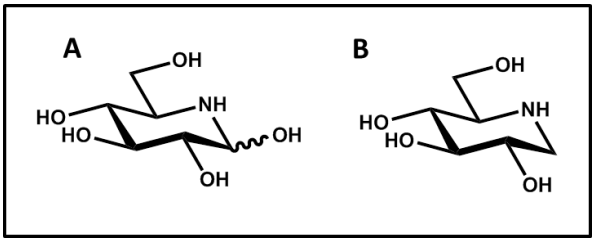

Figure 3.1 The structures of A. Nojirimycin and B. DNJ.

The presence of nitrogen within the ring gives some iminosugars a positive charge under physiological pH; the imino group is protonated forming a structure that mimics the oxocarbeneim ion transition state seen within glycosyl hydrolase enzymes (Figure 3.2, A) (Borges De Melo et al., 2006). Other iminosugars are mimics of a transition state shape (Figure 3.2, B). There are also compounds that mimic both shape and charge. Further affinity and specificity can be driven by extension of a molecule, for example, hydrophobic aromatic or alkyl groups can be used to extend binding to cover an enzymes sub-sites (Gloster and Vocadlo, 2012).

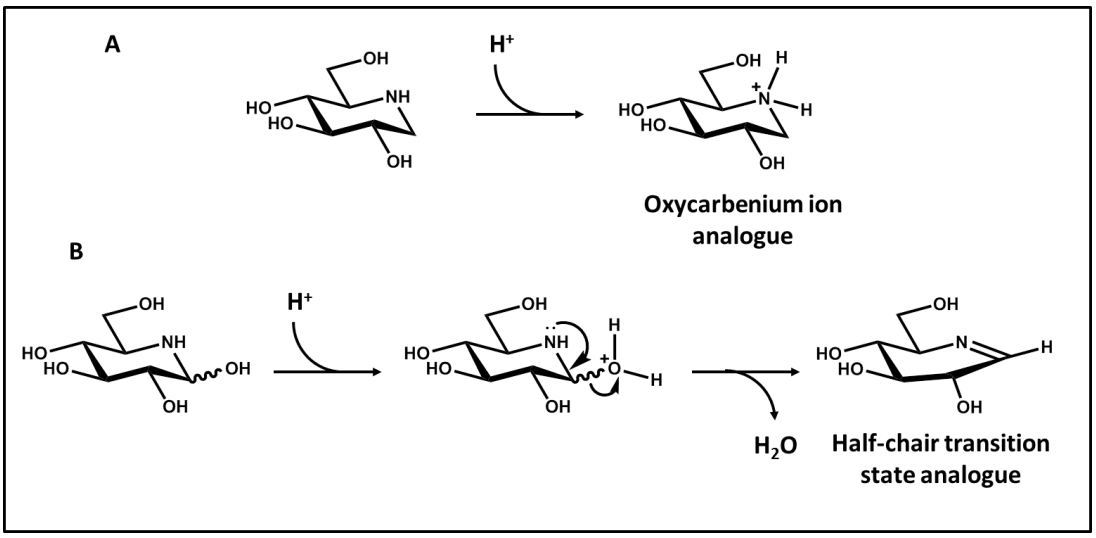

Figure 3.2 Mechanisms of glycosyl hydrolase inhibition by iminosugars.
A. Transition state charge mimic. DNJ is protonated to form a minic of the oxocarbonium transition state formed by glycosyl hydrolases. **B.** Transition state shape mimic. Nojirimycin forms a half-chair transition state mimic. Adapted from (Borges De Melo et al., 2006, Gloster and Vocadlo, 2012).

A wide range of other, non-iminosugar, α- and β- glucosidase inhibitors exist, these include carbasugars, pseudoaminosugars and thiosugars (Borges De Melo et al., 2006). Many covalent inhibitors for glycosidases have also been developed (Rempel and Withers, 2008). These molecules work by covalently trapping a substrate mimic within an enzymes active site (Figure 3.3). Compounds that function in this way are of particular use as molecular probes for labelling of glucosidases *in vivo*, enabling activity based protein profiling (Chandrasekar et al., 2014, Kallemeijn et al., 2012). This is a powerful method to identify functional targets within complex proteomes.

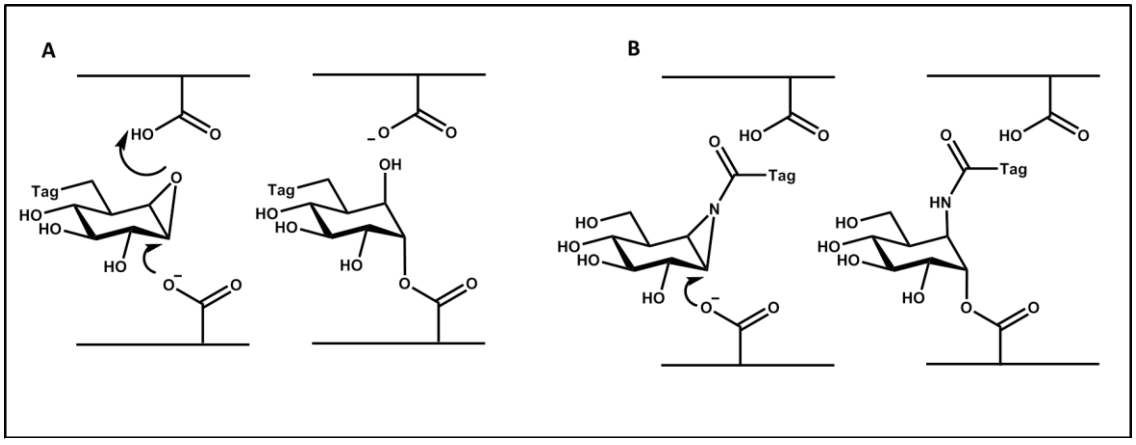

Figure 3.3 Mechanism of covalent glycosyl hydrolase inhibitor probes.
A. Cyclophellitol-epoxide type. **B.** Cyclophellitol-aziridine type. Adapted from (Kallemeijn et al., 2012).

There are now many examples of iminosugars that have either been synthetically developed or identified and purified from numerous different plant sources (Kumar et al., 2012). Due to their ability to alter carbohydrate metabolism, iminosugars have shown potential as therapeutics for conditions such as cystic fibrosis, psoriasis, cancers, viral diseases, diabetes as well as genetic disorders in metabolism (Nash et al., 2011). Various iminosugar derivatives are currently in clinical trials (Nash et al., 2011). A select few iminosugars are approved drugs, these are outlined in Table 3.1 and Figure 3.4.

Brand name	Name	Chemical name	Use	Reference
Glyset	Miglitol	*N*-hydroxyethyl-DNJ	Treatment of type II diabetes.	(Nash et al., 2011)
Zavesca	Miglustat	*N*-Butyl-DNJ	Treatment for Gaucher's disease (sphingolipid metabolism).	(Nash et al., 2011)
Galafold	Migalastat	Deoxygalactonojirimycin	Treatment of Fabry disease (sphingolipid metabolism).	(Winchester, 2009)

Table 3.1 Current iminosugars marketed as drugs.

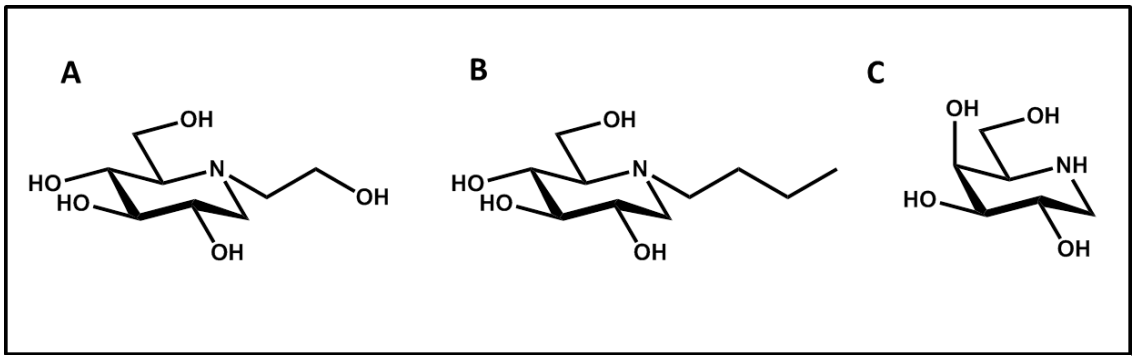

Figure 3.4 The structures of iminosugars marketed as drugs.
Structures of **A.** Miglitol- *N*-hydroxyethyl-DNJ. **B.** Miglustat- *N*-Butyl-DNJ and **C.** Migalastat-deoxygalactonojirimycin.

3.1.2 The Effect of Iminosugars on Glycoprotein Processing

N-linked glycoprotein processing occurs during the synthesis of membrane and secreted proteins (Peyrieras et al., 1983, Lerouge et al., 1998). The process begins with the cotranslational transfer of a $Glc_3Man_9GlcNAc_2$ precursor from a dolicol carrier onto an asparagine residue of a protein containing the correct glycosylation sequence (Asn-X-Ser/Thr, where X is any of the canonical amino acids except proline) (Elbein, 1991, Medzihradszky, 2008). Initial trimming begins in the endoplasmic reticulum (ER) with the removal of the outermost α-1,2 linked glucose unit by Glucosidase I. Glucosidase II then removes the two remaining α-1,3 linked glucose residues. The glycoprotein is then transported to the Golgi where it undergoes a number of hydrolytic trimming steps and is further processed by the addition of other carbohydrates (Figure 3.5).

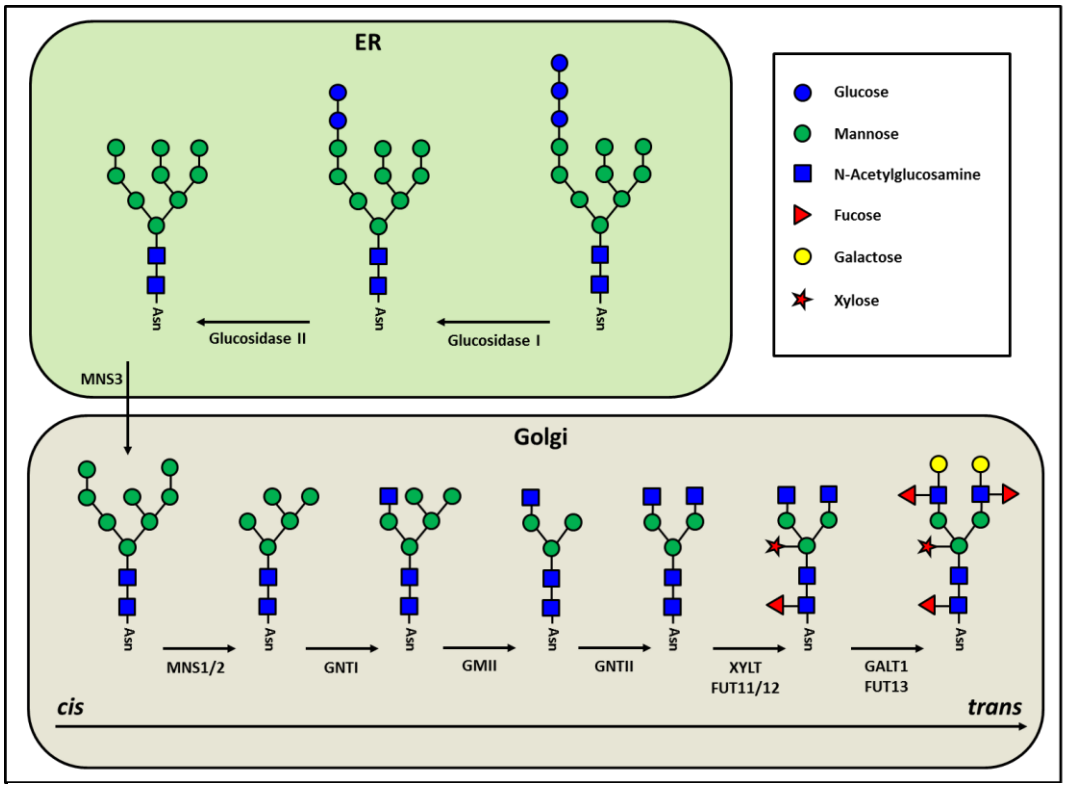

Figure 3.5 Proposed routes to the formation of complex *N*-linked glycans in plants.
A preassembled oligosaccharide ($Glc_3Man_9GlcNAc_2$) is transferred *en bloc* to the asparagine of a suitable protein. The first reactions occur in the endoplasmic reticulum (ER) and involve trimming of glucose residues *via* the actions of α-glucosidase I and II, alongside removal of mannose by α-mannosidase 3 (MNS3). The glycoprotein is transferred to the Golgi and further trimmed by α-mannosidase I (two largely redundant forms found in Arabidopsis) (MNS1/2). Complex glycan formation is initiated by addition of GlcNAc by β-1,2-*N*-acetylglucosaminyltransferase I (GNTI). The glycan is then further trimmed (carbohydrate removal) and processed (carbohydrate addition) by Golgi α-mannosidase II (GMII), β-1,2-*N*-acetylglucosaminyltransferase II (GNTII), β-1,3-xylosyltransfrase (XYLT), core α-1,3-fucosyltransferases (two largely redundant forms found in Arabidopsis) (FUT11/12), Lewis-type β-1,3-galactosyltransferase (GALT1) and α-1,4-fucosyltransferase (FUT13) to produce a range of complex glycans. Adapted from (Strasser, 2014).

Numerous iminosugars have been shown to be capable of inhibiting steps in glycoprotein trimming and processing. *N*-methyl-DNJ is able to inhibit both human α-glucosidase I and II (Figure 3.6, A) (Peyrieras et al., 1983). 1,4-dideoxy-1,4-iminoarabinitol (DAB), a potent inhibitor of yeast α-glucosidase, has also been identified as having activity against ER α-glucosidase II, Golgi α-mannosidase I and II, and human digestive α-glucosidase (Asano et al., 1994a).

Castanospermine (Figure 3.6, C) is isolated from the Australian legume *Castospermum australae*. When added to mammalian cell culture it prevents glycoprotein precessing, causing a build-up of $Glc_3Man_9GlcNAc_2$ meaning the actions of glucosidase I and II were blocked, thus preventing further trimming (Sasak et al., 1985, Palamarczyk and Elbein, 1985). Castanospermine is also a potent inhibitor of lysosomal α-glucosidase and disrupts lysosomal glycogen degradation (Saul et al., 1985, Molyneux et al., 1986).

α-homonojirimycin (α-HNJ) (Figure 3.6, D), alongside a glucosylated derivative (Glc-HNJ) were originally generated as potential diabetes treatments (Liu, 1987, Rhinehart et al., 1987). α-HNJ was evaluated for inhibition of *N*-linked oligosaccharide processing of viral glycoproteins influenza virus infected kidney cells. A build up in high mannose type viral glycoproteins proteins was produced, the predominant structure being $Glc_3Man_9GlcNAc_2$, again representing inhibition of glucosidase I and II (Zeng et al., 1997). Viral envelope glycoproteins are essential for viron assembly and infectivity, DNJ, *N*-Bu-DNJ and castanospermine all show some antiviral effects *in vitro* (Taylor et al., 1991, Fischer et al., 1995). However issues arise with achieving a sufficiently high concentration, *in vivo*, to elicit an effect without generating side effects, such as diarrhea (Cook et al., 1995). Many other antiviral applications of iminosugars are being investigated (Mehta et al., 1998, Jacob et al., 2007, Qu et al., 2011, Chang et al., 2013)

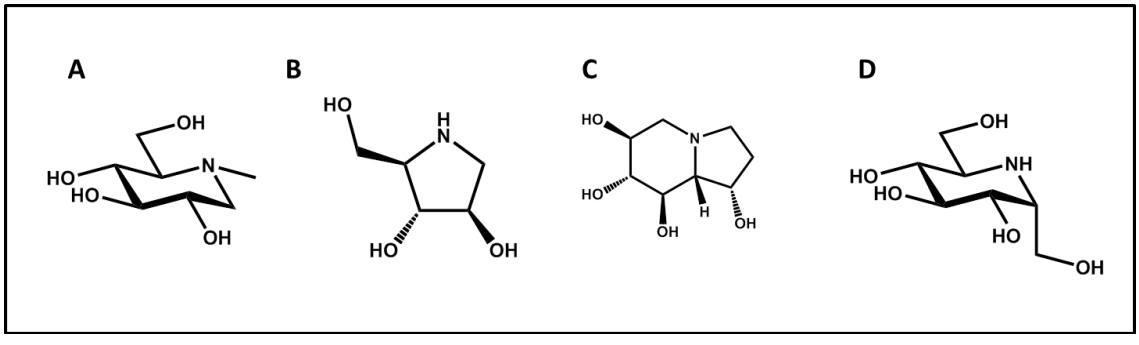

Figure 3.6 Structures of iminosugars which interfere with glycoprotein processing.
A. Methyl-DNJ. **B.** DAB. **C.** Castospermine. **D.** α-HNJ.

3.1.3 Iminosugar Inhibitors of Lysosomal Storage Disorders

A range of human genetic diseases are associated with disorders in lysosomal glycosphingolipid (GSL) metabolism. Lysosomes are membrane bound cytoplasmic organelles that are the major degradative compartment in eukaryotic cells (Kornfeld and Mellman, 1989). Disorders occur when mutation of one of the GSL glycosyl hydrolases blocks metabolism, these mutations affect protein folding and lead to build up of mutant proteins in ER or targets the protein for ER-associated degradation. This, in turn, causes a build-up of metabolites which cause symptoms such as osteoporosis and hepatomegaly (enlarged liver) (Bychkova and Ptitsyn, 1995). Examples of these diseases include Gaucher's disease, Sandhoft disease, Tay-Sachs disease and Fabry disease.

There are a number of possible treatment strategies for lysosomal storage disorders. Enzyme replacement therapy offers one potential solution, however this is only useful for treatment of a disease absent of neuropathy as enzymes are unable to cross the blood-brain barrier (Brady, 2006). This technique is also expensive. Pharmacological chaperone therapy offers another alternative. Intracellular activity of mutant enzymes can be restored by the addition of a competitive inhibitor that act as a folding chaperone to stabilise native folding in ER, thus allowing maturation and trafficking to lysosome (Fan, 2003, Cohen and Kelly, 2003). Gaucher's disease is caused by mutations in the gene encoding glucosylceramidase (GCase) (Figure 3.7), resulting in glucosylceramide (GC) accumulation (Brady et al., 1966). *N*-Bu-DNJ acts as a chemical chaperone for GCase, however it also inhibits glucosylceramide (GC) synthesis by inhibiting the action of glucosylceramide synthase (GCS).

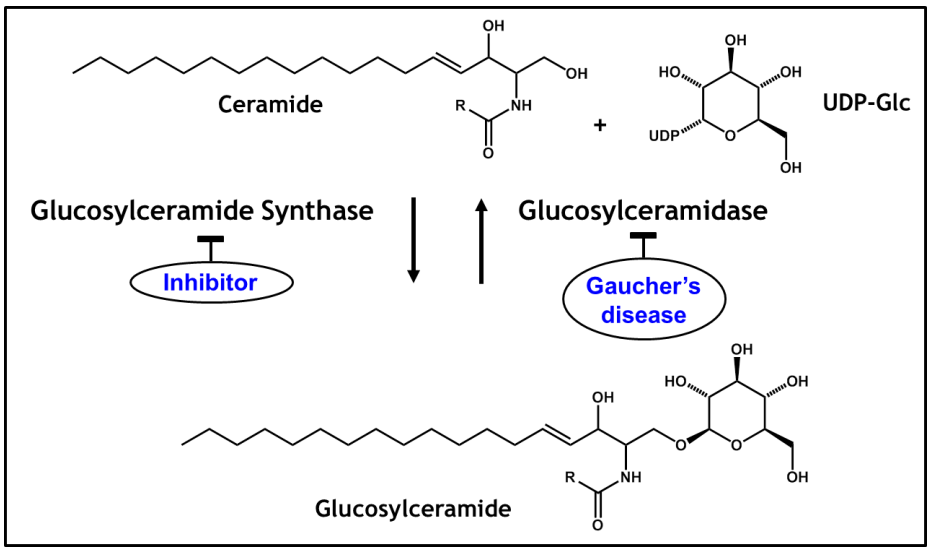

Figure 3.7 The reactions catalysed by glucosylceramide synthase and glucosylceramidase.

The direct inhibition of GCS led to the development of a third treatment strategy, termed substrate reduction therapy (Aerts et al., 2006, Platt et al., 2001, Mceachern et al., 2007)**.** *N*-Bu-DNJ lowers GC levels that can then be dealt with in mildly affected Gaucher's sufferers (Platt et al., 1994a, Cox et al., 2000). GCS has become an established target for treatment of Gaucher's disease. There are two archetypal GCS inhibitors: PDMP (Vunnam and Radin, 1980) and *N*-Bu-DNJ (Platt et al., 1994a) (Figure 3.8). Most reported inhibitors are based on these scaffolds. Reduction in GCS activity has been proposed to be beneficial to numerous disorders in lysosomal GSL metabolism by restricting flux through the pathway (Platt et al., 2001, Aerts et al., 2003, Aerts et al., 2006).

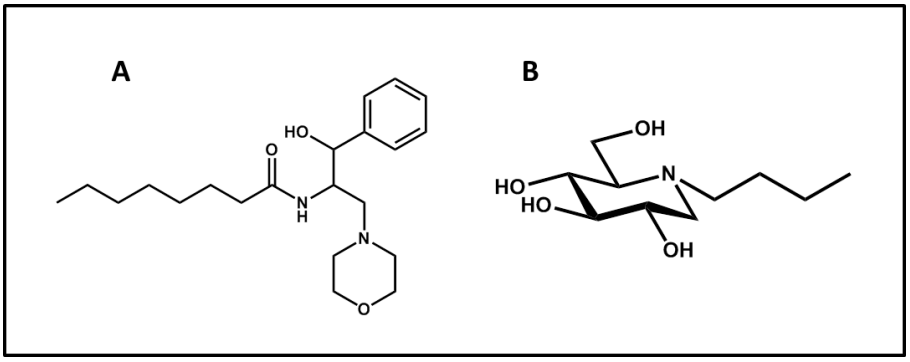

Figure 3.8 The structures of the two archetypal glucosylceramide synthase inhibitors.
A. PDMP. **B.** *N*-Bu-DNJ.

Specificity of iminosugar drugs is important, inhibition of glucosidase I and II can affect glycoprotein processing (Fan, 2003). Further to this there are two forms of GCase: lysosomal (GBA1) and non-lysosomal (GBA2). Whilst GBA1 is responsible for Guacher's disease, the precise function of GBA2 remains unclear (Korschen et al., 2013). DNJ derivatives with longer chains appended to the imino group enhance GCS inhibitory activity (Yu et al., 2006) (Overkleeft et al., 1998, Wennekes et al., 2007). In particular, *N*-5-(adamantane-1-yl-methoxy)pentyl-DNJ (AMP-DNJ) (Figure 3.9) has been developed as a very potent inhibitor of GCS, however this was accompanied by increased potency against GCase. (Overkleeft et al., 1998).

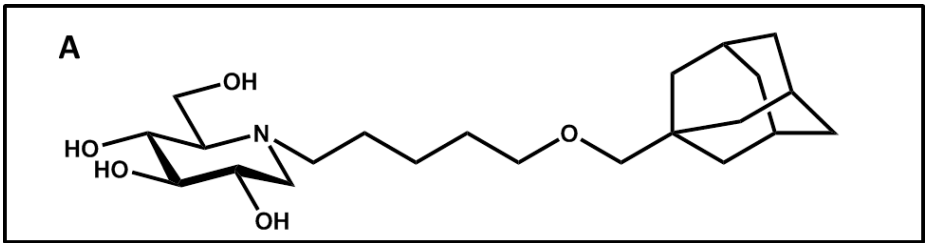

Figure 3.9 The structure potent glucosylceramide synthase inhibitor AMP-DNJ.

In mouse models AMP-DNJ is also associated with markedly lower circulating glucose levels, an improvement in sensitivity to insulin and shows inhibitory activity towards digestive glucosidases (Wennekes et al., 2010). To improve the selectivity of AMP-DNJ towards GCS the potential that changing stereochemistry could lead to better inhibitors was investigated. Indeed, *N*-Bu-*galacto*-DNJ and *N*-pentyl-*ido*-DNJ had previously been shown to have activity against GCS (Platt et al., 1994b, Weiss et al., 2003). A panel of structural and stereochemical analogues of AMP-DNJ were generated and screened against a range of glycosidases. This included 3 epimers at C-4/C-5 positions (*galacto*, *ido* and *altro*) of AMP-DNJ with a range of *N*-alkyl substituents (Ghisaidoobe et al., 2011).

Ido-AMP-DNJ (Figure 3.10) showed increased specificity towards GCS, compared to *gluco*-AMP-DNJ, with very little inhibitory activity against intestinal glucosidases or sucrase (Wennekes et al., 2010). *Ido*-AMP-DNJ was also 10-fold more specific for GCS over GBA1/2 (Ghisaidoobe et al., 2011). Generation of partially deoxygenated DNJ derivatives revealed the C2 hydroxyl is important for GCS inhibition, whereas the C6 hydroxyl is much less important (Van Den Berg et al., 2011). These guidelines provide a foundation for the development of GCS inhibitors that have lower affinity or other glycoprocessing enzymes.

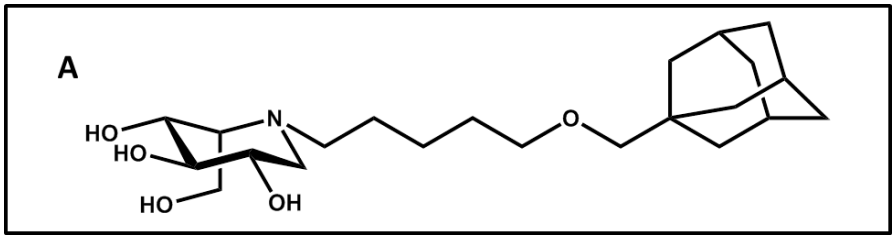

Figure 3.10 The structure potent glucosylceramide synthase inhibitor *Ido*-AMP-DNJ.

Many of the compounds generated by Overkleef and collaborators have been grouped together into a library. This includes iminosugars that cover a large range of C2, C3, C4, C5 stereochemistry alongside numerous *N*-alkyl and deoxygenated derivatives. This is one of the libraries that has been utilised within this study.

3.1.4 The Effects of Iminosugars on Plants

There have been very few studies on the effect of iminosugars on plants. One of the first examples involved castanospermine, this compound acts as a plant growth regulator causing inhibition of root elongation (Stevens and Molyneux, 1988). There is a distinct difference in the effective concentration between monocots and dicots (dicot 300 ppb, monocot 200 ppm)

(Stevens and Molyneux, 1988). The reason for this difference remains unclear. Changes in *N*-linked glycoprotein processing have been reported in castanospermine treated plant cell cultures (Hori, 1984). Glucose trimming was prevented causing accumulation of $Glc_3Man_7GlcNAc_2$. It has not been shown whether the root growth phenotype is directly linked to perturbed glycoprotein processing.

The effect of *N*-hydroxyethyl-DNJ was tested on germinating wheat seeds (Konishi et al., 1994) and mung beans (Konishi, 1998). This produced lower levels of α-glucosidase activity, with accumulation of maltose and a decrease in the rate of starch degradation. This observation was further investigated within our group (Stanley et al., 2011). The effects of the inhibitors DNJ, NB-DNJ, and *N*-hydroxyethyl-DNJ were tested on germinating barley grains. Results showed a decrease in the glucose:maltose ratio implying inhibition of α-glucosidase activity. Starch levels were also elevated in inhibitor treated seeds. All three compounds inhibited root elongation in presence of exogenous sugars. This suggests the inhibitors have a direct effect on proteins in roots and growth inhibition is not simply due to lack of sugar required for growth (Stanley et al., 2011). DNJ in particular inhibited root growth strongly but shoot growth was similar to water treated grains (Figure 3.11). It was concluded the likely targets were enzymes involved in *N*-linked glycoprotein processing.

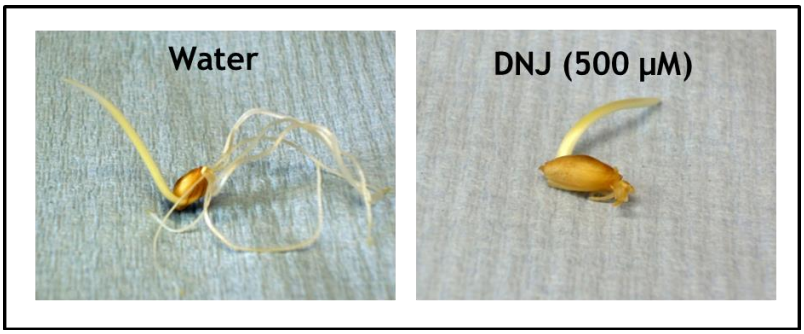

Figure 3.11 The effect of DNJ on germinating barley root and shoot growth.

Mutational analysis of Glucosidase I and II, which trim *N*-linked glycans within the ER, shows that both are required for normal embryo development in Arabidopsis (Burn et al., 2002, Furumizu and Komeda, 2008, Soussillane et al., 2009). In mutants that are capable of germination root growth is retarded (Burn et al., 2002, Furumizu and Komeda, 2008, Soussillane et al., 2009). Iminiosugars have been shown to be capable of inhibiting glucosidases I and II in other plant species (Mega, 2004). Radish leaves treated with DNJ show a correlation between trimming of glucosyl moieties within *N*-linked glycans and retardation of growth (Mega, 2005).

3.2 Aims of this Chapter

Iminosugars have been shown to impact on plant germination, understanding how these molecules interfere with this process is of fundamental interest but also has real world application in the understanding of barley malting for the use in brewing and distilling. The currently identified targets for DNJ are glycosyl hydrolases involved in maltose breakdown and cell wall hydrolysis. There is a need to better understand the other *in vivo* targets for DNJ. Alongside this, the identification of novel inhibitors opens up new avenues for exploration and can be used to compare with existing inhibitors.

This chapter presents the test of iminosugars against Arabidopsis, barley and tef root growth. The effect of DNJ on barley glycoprotein processing is also outlined. The use of Arabidopsis and tef as alternatives to barley has enabled the development of a medium throughput screen to detect compounds capable of inducing a stunted root growth phenotype. Novel iminosugar root growth inhibitors have been identified within a library of compounds developed by Overkleeft et al. Steps towards target identification for these novel inhibitors are also discussed.

3.3 Results

3.3.1 DNJ Inhibits Root Growth in Barley and Arabidopsis in a Concentration Dependent Manner

Previous data generated within our lab shows DNJ to significantly inhibit barley root growth after 10 days in the presence of 500 µM. To confirm this data and explore the effect of different DNJ concentrations, barley grains were germinated in the presence of 5 mM to 10 µM DNJ (Figure 3.12). Root length was measured at 5 dpi (days post imbibition) or 10 dpi. 10 dpi was utilised as this gives a more pronounced phenotype, 5 days was chosen as this is a more relevant time scale to that used in the malting process.

5 mM DNJ blocked almost all root growth in grains grown for both 5 and 10 days, although 200 µM was a high enough concentration of DNJ to significantly inhibit root growth. 100 µM DNJ was a high enough concentration to see a significant difference compared to water treated within the 10 day roots, however the difference at this concentration for 5 day grains is not significant. DNJ has a concentration dependent effect on both 5 day and 10 day samples. 5 days germination gave much smaller root lengths, with a less pronounced growth difference between DNJ concentrations. Measuring growth at 10 dpi increases the likelihood of seeing a difference in growth.

The effect of DNJ was also tested on Arabidopsis to determine whether the observed effects were specific to monocot species. Arabidopsis shows a stunted root phenotype, similar to that of barley. The concentration of DNJ required to elicit 50 % inhibition of root growth, compared to control, is 10-fold lower that is required than barley (20 µM vs 200 µM). The level of variation in root length measurements per condition is much higher with Arabidopsis, growth inhibition is only statistically significant at 200 µM and 500µM.

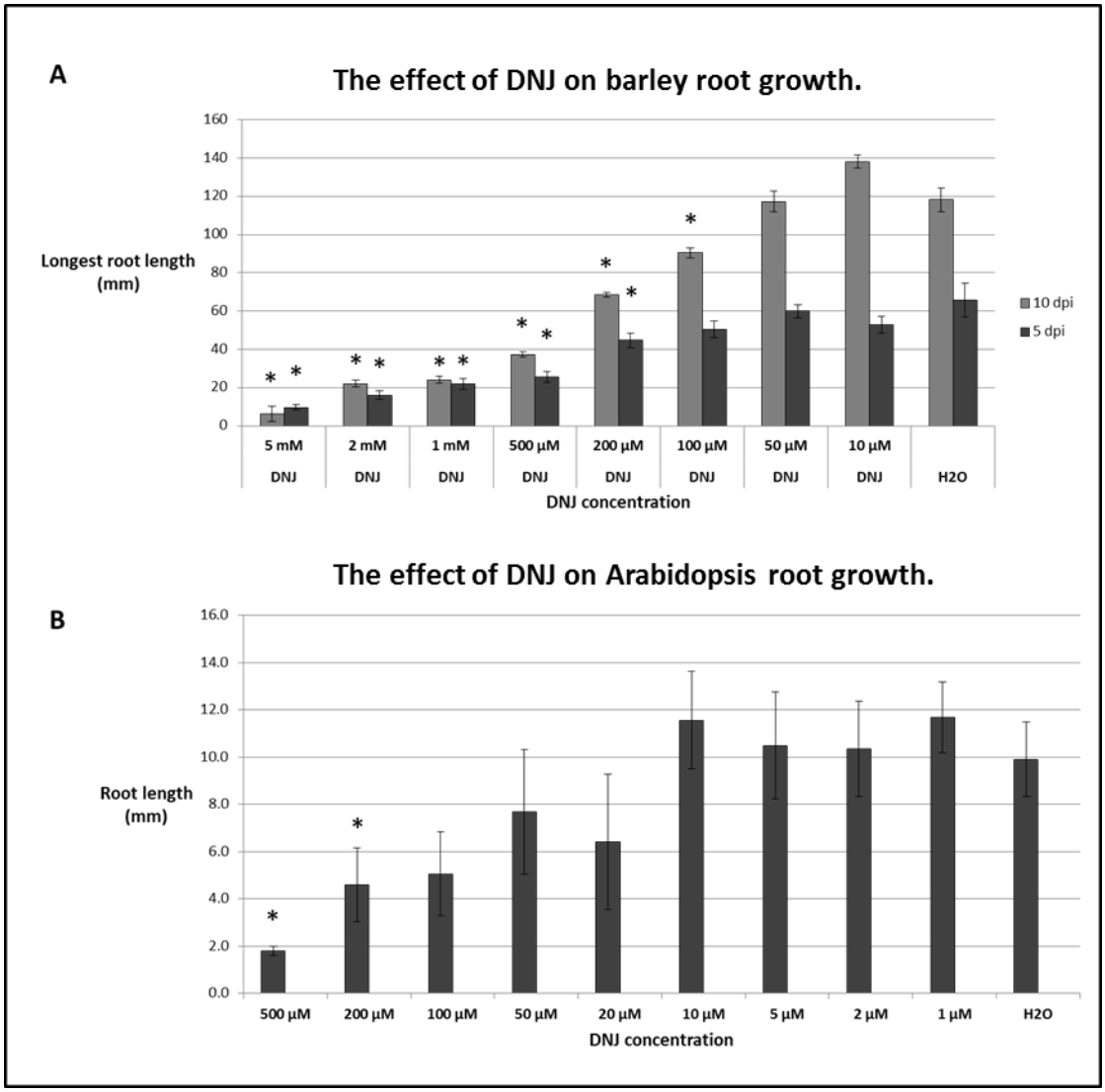

Figure 3.12 Barley and Arabidopsis root growth in the presence of DNJ
A. Grains of barley were grown for 5 or 10 dpi in the presence of water (control) or DNJ. **B.** Arabidopsis was grown for 10 days on ½ MS Agar supplemented with DNJ or water (control). Values of root length shown are the mean value for 10 seedlings. Error bars represent SEM. Values marked with asterisks are statistically significant from the control (water) values (*t*-test, * P <0.05).

3.3.2 Glycoprotein Processing is Specifically Affected in DNJ Treated Barley Roots

DNJ has previously been implicated to interfere with glycoprotein processing. To test whether the stunted root growth of barley grown in the presence of DNJ was associated with modification of *N*-linked glycans, the effect of 200 µM DNJ was analysed on root, shoot and endosperm samples from germinated grain. Soluble protein samples were generated from dissected tissue, treated to release the glycans from glycoproteins, and analysed by MALDI-ToF mass spectrometry.

Two different enzymes were used to cleave *N*-linked glycans from glycoproteins (Figure 3.13): PNGase A, which cleaves the bond between the innermost GlcNAc and an Asn residue, and PNGase F, which cannot cleave when the innermost GlcNAc is linked to an α-1,3 fucose residue, as commonly seen in plant complex glycans.

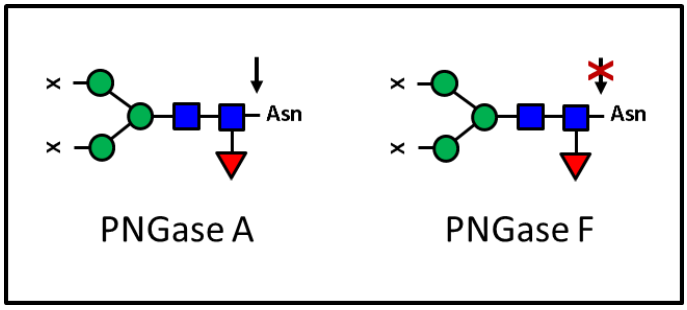

Figure 3.13 The specificity of PNGase A and F on *N*-linked glycans.
Legend detail as for Figure 3.5.

Samples treated using PNGase A showed no distinct differences in the glycan profiles for DNJ or H_2O treated grains (Appendix), complex glycans were detectable within all samples and the relative levels are not affected by DNJ.

When PNGase F was utilised to remove *N*-linked glycans, an a change in the relative intensity of peaks corresponding to masses of 2192 ($Man_8GlcNAc_2$) and 2396 ($Man_9GlcNAc_2$) compared to other peaks was specifically produced in DNJ treated root samples (Figure 3.14). This may be due to increased levels of 2192 ($Man_8GlcNAc_2$) and 2396 ($Man_9GlcNAc_2$) or a decrease in the prevalence of other glycans. No differences were detected between DNJ and H_2O treated shoot or endosperm samples. Comparison of H_2O treated root, shoot and endosperm samples also yielded no extreme differences in the glycan profiles (Appendix). Mannosidase digestion and MS/MS was utilised to confirm the identified masses were high mannose structures and not glucose containing structures of the same mass (Appendix).

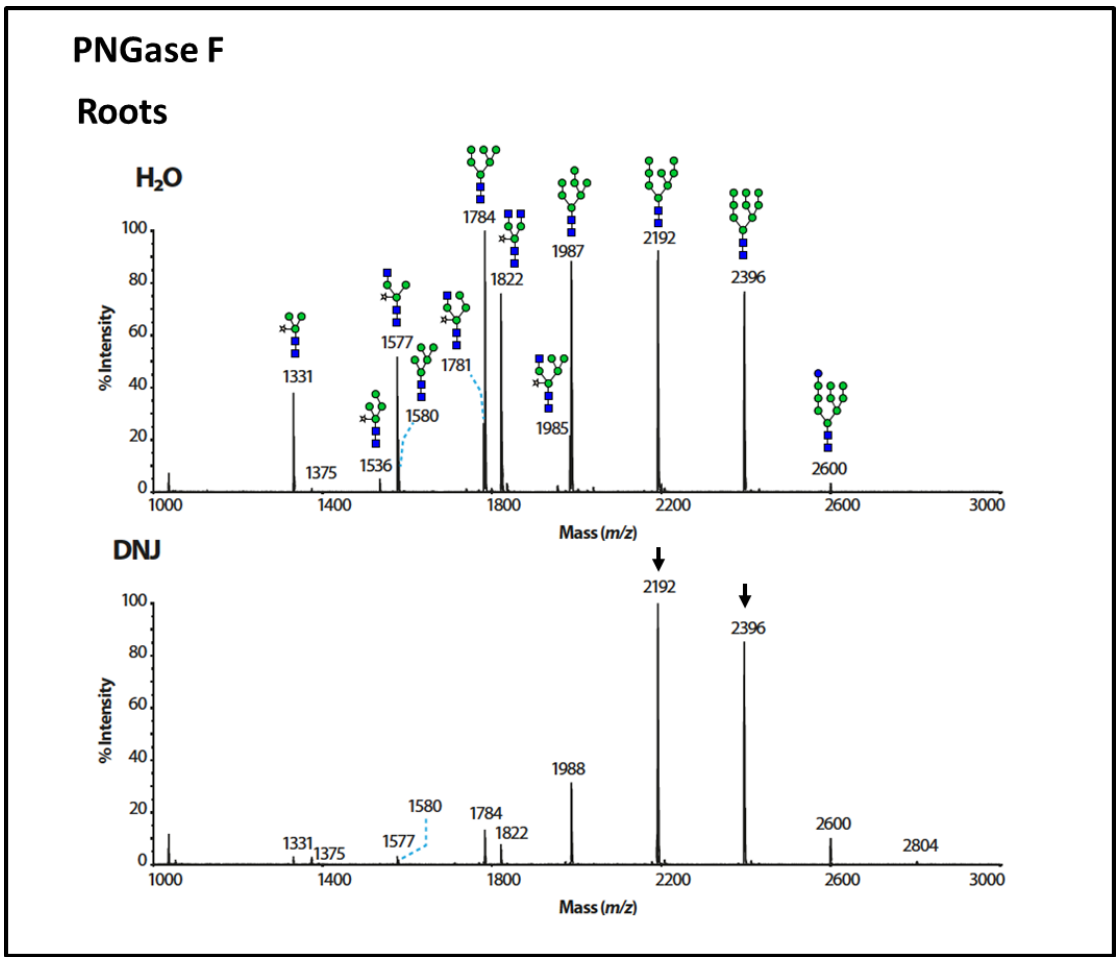

Figure 3.14 Analysis of the glycans present on glycoproteins from barley roots treated with H_2O or DNJ Grains grown in the presence of 200 µM DNJ, 5 dpi. Glycoprotein samples treated with PNGase F. Structures were confirmed by mannosidase digestion and MS/MS experiments.

3.3.3 Screening an Iminosugar Library Against Arabidopsis Identified Novel Inhibitors of Root Growth

The Overkleeft library is a collection of 391 DNJ derivatives with different iminosugar stereochemistry and *N*-substitution. These compounds were designed to be active against glucosylceramide synthase, glucosylceramidase and other glycosidases of medical relevance, including those involved in diabetes.

In an attempt to identify variants of DNJ with a more potent effect on plant growth, this library was blind screened, at a concentration of 10 μM, for perturbation of Arabidopsis root growth. From this library 6 compounds were identified as having a strong effect on root growth; a threshold of 50 % growth, compared to control, was used to define hit compounds, this produced a hit rate of 1.5 %.

Three *ido*-configured sugars were identified from the screen (Figure 3.15). Compound 41 gives almost complete inhibition of root growth (8 % of control), germination occurred as small roots can be seen. This compound is only one carbon different from the potent GCS inhibitor *Ido*-AMP-DNJ: *N*-5-(adamantane-1-yl-methoxy)pentyl-*ido*-DNJ compared to *N*-5-(adamantane-1-yl-ethoxy)pentyl-*ido*-DNJ (*Ido*-AEP-DNJ). The *N*-substituent of this molecule contains 17 carbon molecules making it lipophillic.

Three other *ido* configured compounds were identified within the screen (Figure 3.15). Compound 360, containing a 20 carbon N-substituent, gave 23 % of control. The other two *ido* compounds, 64 and 441, are identical and give 47 % and 36 % growth, respectively, when compared to control. The 11 % difference between these two compounds highlights the variation within the assay but also acts as a good internal control. Castanospermine, a known potent inhibitor of root growth, was also identified, giving 28 % growth, this acts a another internal control.

One gluco configured DNJ variant (523), with a large lipophilic biphenyl group, gave 49 % growth compared to control. Other gluco configured compounds caused significant root inhibition, however these were not below the cut off of 50 % (Appendix). Using a 60 % cut off, 12 extra hits are identified, 11 of these have biphenyl ring system.

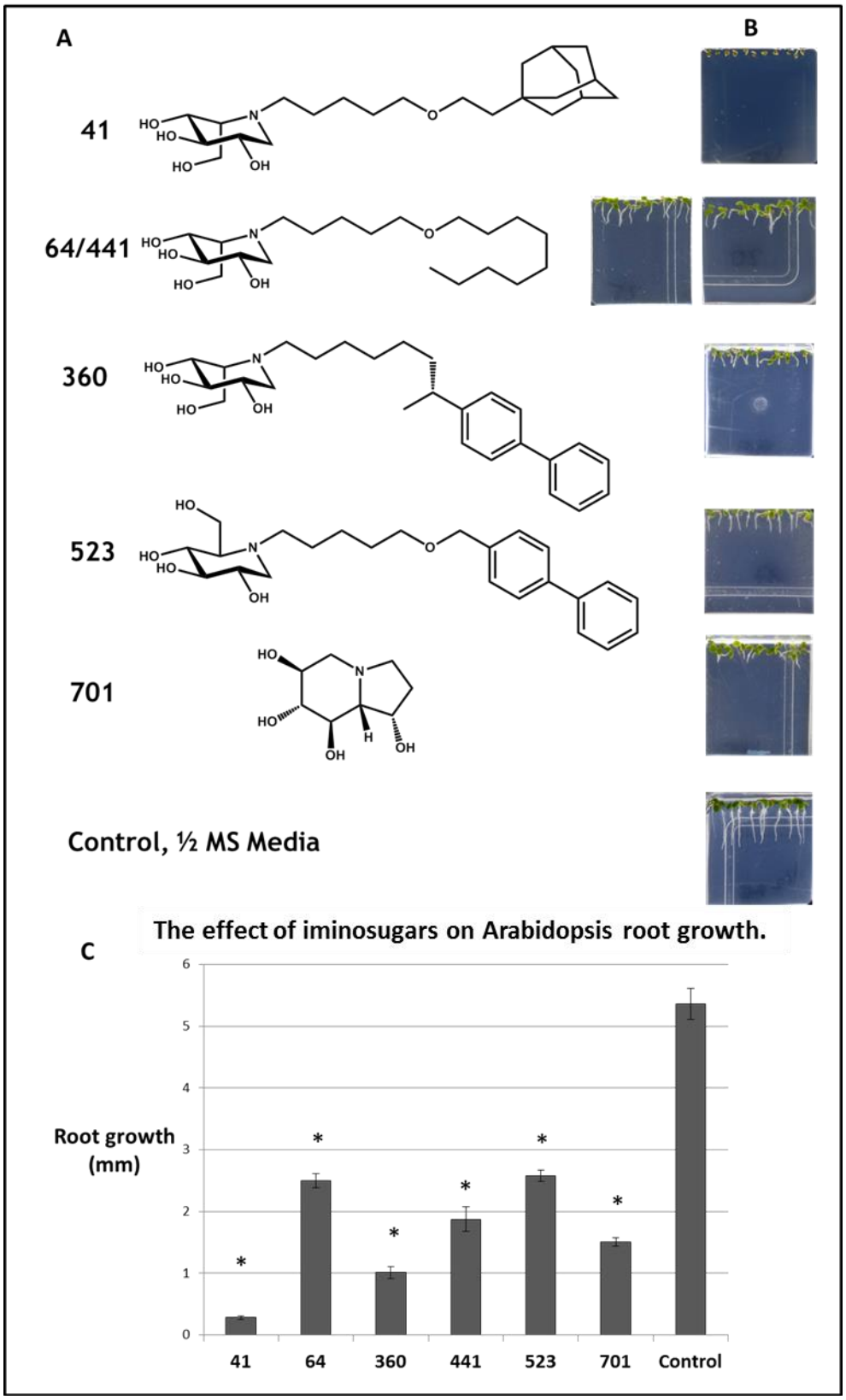

Figure 3.15 Inhibition of Arabidopsis root growth by iminosugars from the Overkleeft library.
A. The structures of compounds which inhibit root growth by more than 50 % of control. **B.** Images of the root growth phenotype. **C.** Mean values of root length in the presence of 10 µM inhibitor. Mean value from 10 plants. Error bars represent SEM. Values marked with asterisks are statistically significant from the control (water) values (t-test, * P <0.05).

3.3.4 *Eragrostis tef*: a Monocot Alternative to Arabidopsis Screening

Arabidopsis does not use starch as the primary energy store within the seed, yet iminosugars are capable of interfering with starch metabolism (Stanley et al., 2011). As such, a monocot alternative for screening was sought. Grains including millet, Brachypodium and *Eragrostis tef* (tef) were tested, of these, tef was found to be the easiest to work with and gave the most reliable germination rates.

The grains of the tef plant are of a very small size making them suitable for medium throughput screening (Figure 3.16) (G. Belay et al., 2009). α-amylase, β- amylase and LD activities have been identified in malted tef (Gebremariam et al., 2012, Gebremariam et al., 2013), making it a good model for other cereals which utilise starch as their main energy reserve. Also the tef genome sequence has recently been published, identifying the closest cultivated relatives as sorghum, foxtail millet and maize (Figure 3.17) (Cannarozzi et al., 2014).

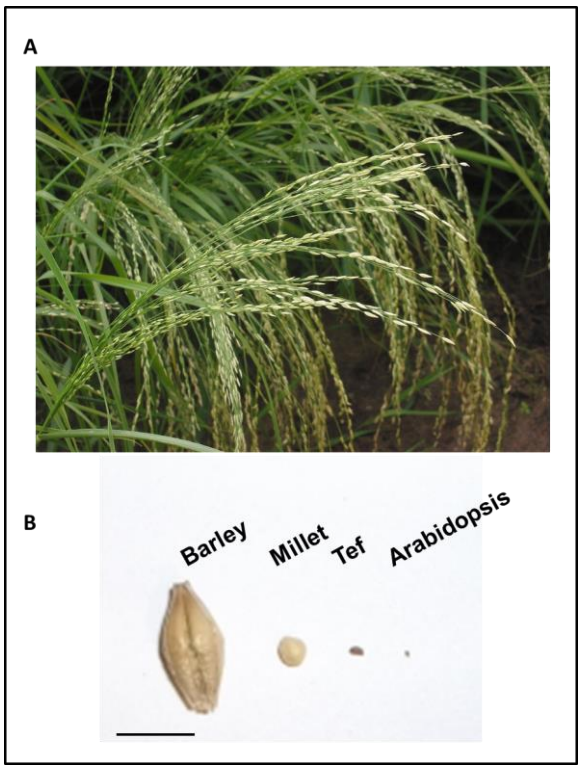

Figure 3.16 *Eragrostis Tef*- the plant and seed size.
A. *Eragrostis tef* plant. **B.** The seed size of: Barley, *Hordeum vulgare*. Millet, *Setaria italica*. Tef, *Eragrostis tef*. Arabidopsis, *Arabidopsis thaliana*. Scale bar: 1 cm.

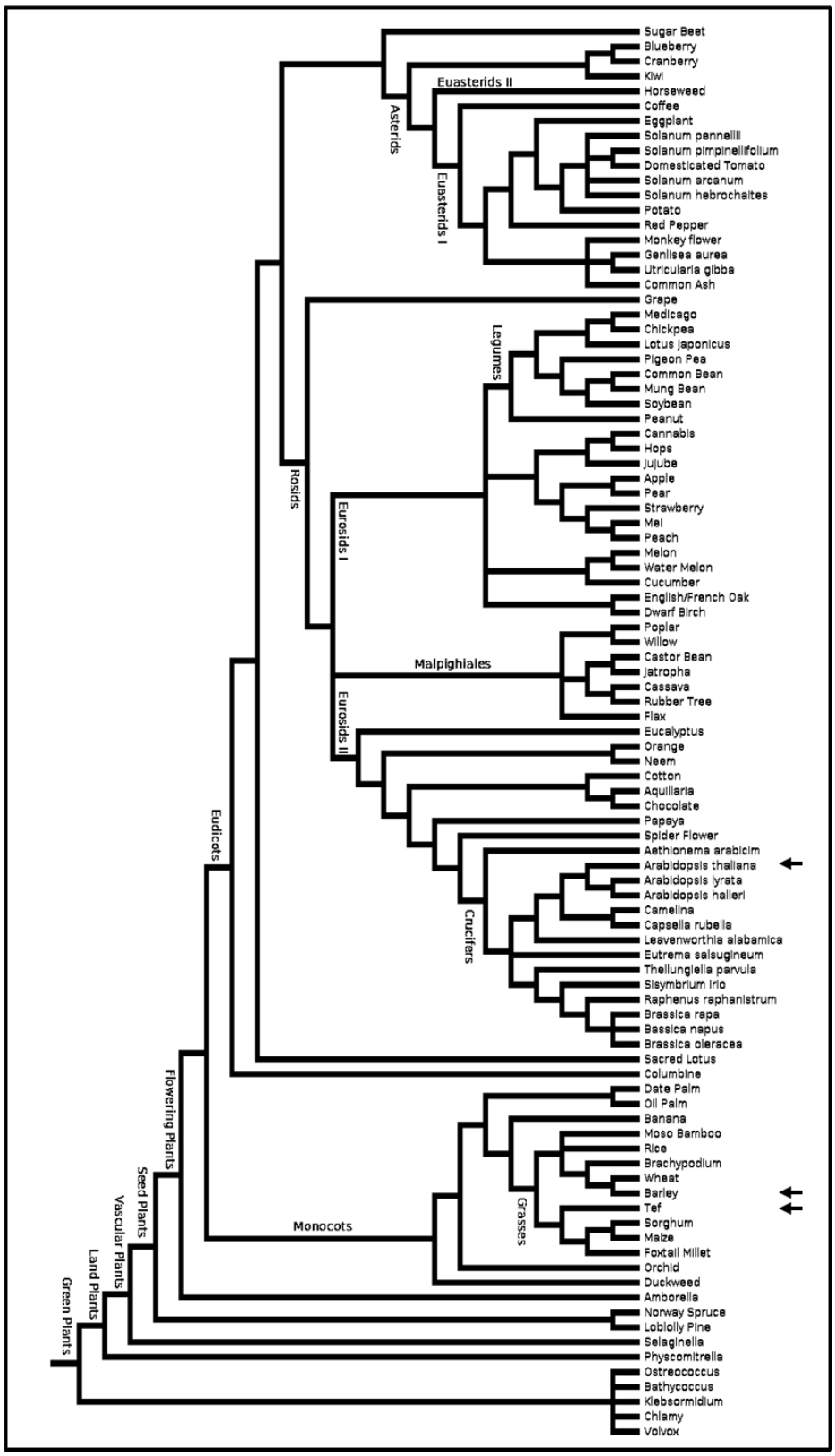

Figure 3.17 Phylogenetic tree of all plants that have sequenced genomes.
Data generated December 2014. Arrows highlight Arabidopsis, barley and tef. Branch lengths are not proportional to anything. Adapted from (Lyons and Freeling, 2008).

3.3.5 Comparison of Chemical Genetic Screens Performed Using Barley, Arabidopsis and Tef

Barley is not amenable to high throughput compound screening, due to the size of the grain screening is limited to using one plate per condition and measuring growth by hand. Arabidopsis offers a convenient model to screen high numbers of compounds (Figure 3.18). 10-12 seeds are grown in a 20 mm x 20 mm well of a 25 well plate, enabling the analysis of many different compounds or concentrations in one experiment. Plates can be digitally imaged and measured manually using a computer. Tef is a monocot that can be treated in same way as Arabidopsis and has similar attributes, however it is 7 days quicker to germinate (Figure 3.18).

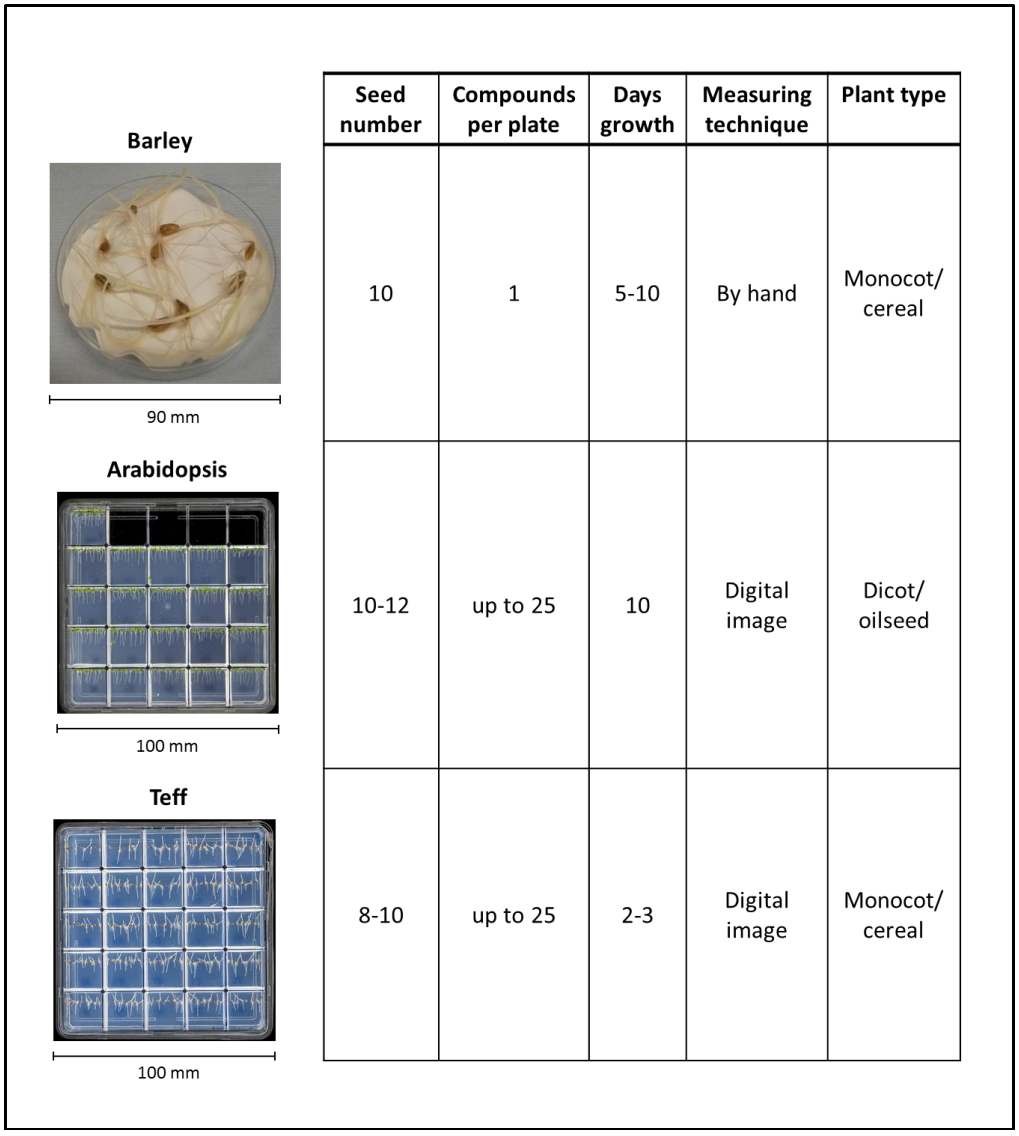

Seed number	Compounds per plate	Days growth	Measuring technique	Plant type
10	1	5-10	By hand	Monocot/ cereal
10-12	up to 25	10	Digital image	Dicot/ oilseed
8-10	up to 25	2-3	Digital image	Monocot/ cereal

Figure 3.18 Comparison of barley, Arabidopsis and Tef for chemical genetic compound screening.

3.3.6 DNJ Inhibits Root Growth in Tef in a Concentration Dependent Manner, Similar to Barley and Arabidopsis

Arabidopsis does not give statistically significant root growth inhibition in the presence of DNJ concentrations below 200 µM. Similar concentrations to this are required to elicit a comparable phenotype in barley, a much larger seed. This indicates a possible difference in the action of DNJ between dicots and monocots. Tef was germinated in the presence of a range of DNJ concentrations to compare growth inhibition with barley and Arabidopsis grown in similar conditions.

Tef produces a similar trend to DNJ-treated barley (Figure 3.19). 50 % root inhibition is achieved at 10 µM, this is a 20-fold lower concentration required to elicit a similar phenotype in barley. At 10 µM DNJ, Arabidopsis root growth is not affected, this indicates a difference in the susceptibility to DNJ between monocots and dicots of similar grain size.

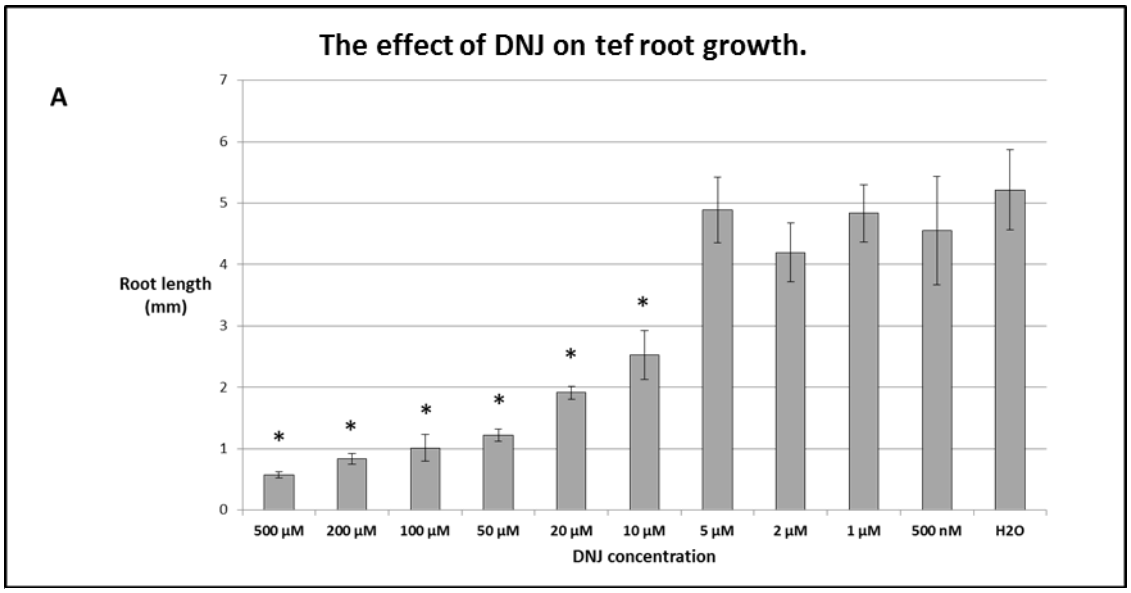

Figure 3.19 Tef root growth in the presence of DNJ.
A. Grains of tef were grown for 3 days on ½ MS Agar supplemented with DNJ or water (control). Values of root length shown are the mean value for 8 seedlings. Error bars represent SEM. Values marked with asterisks are statistically significant from the control (water) values (*t*-test, * *P* <0.05).

3.3.7 Screening an Iminosugar Library Against Tef Identified Inhibitors of Root Growth Similar to those Identified in Arabidopsis

To determine the effect of a range of iminosugars in a monocot system a screen was performed using the Overkleeft library and tef. 391 iminosugar derivatives were screened at a concentration of 10 μM. 8 compounds were identified as hits, using a threshold of 30 % growth, compared to control. This generated a 2 % hit rate.

All hit compounds identified are *ido* configured iminosugars (Figure 3.20). Compounds 41, 514 and 540 (11 %, 27 % and 18 % of control, respectively) all possess an adamantane group with different length linkers. 4 compounds identified had alkoxy groups with lengths differing by 2 carbons: 60, 433, 61/437. Two of these compounds have the same structure and, as with the Arabidopsis screen, act as an internal control. Compound 361 inhibited growth to 15 % of the control, this molecule contains a lipophilic bromophenyl group.

Both the Arabidopsis and tef screens identified compound 41 (*ido*-AEP-DNJ) as the strongest inhibitor, making this a prime candidate for further analysis. When the results of both screens are compared a number of similar criteria are noted: a large proportion of the identified hits are *ido* configured and possess long *N*-substituents containing adamantane or alkoxy functional groups. In contrast castanospermine is not identified as an inhibitor of tef root growth, thus indicating differences between monocots and dicots. A larger number of compounds were found to have an effect on tef root growth, indicating monocots are more susceptible to inhibition by iminosugars. The second round hits, which failed to make the stringent 30 % cut-off, are *gluco*-configured (Appendix).

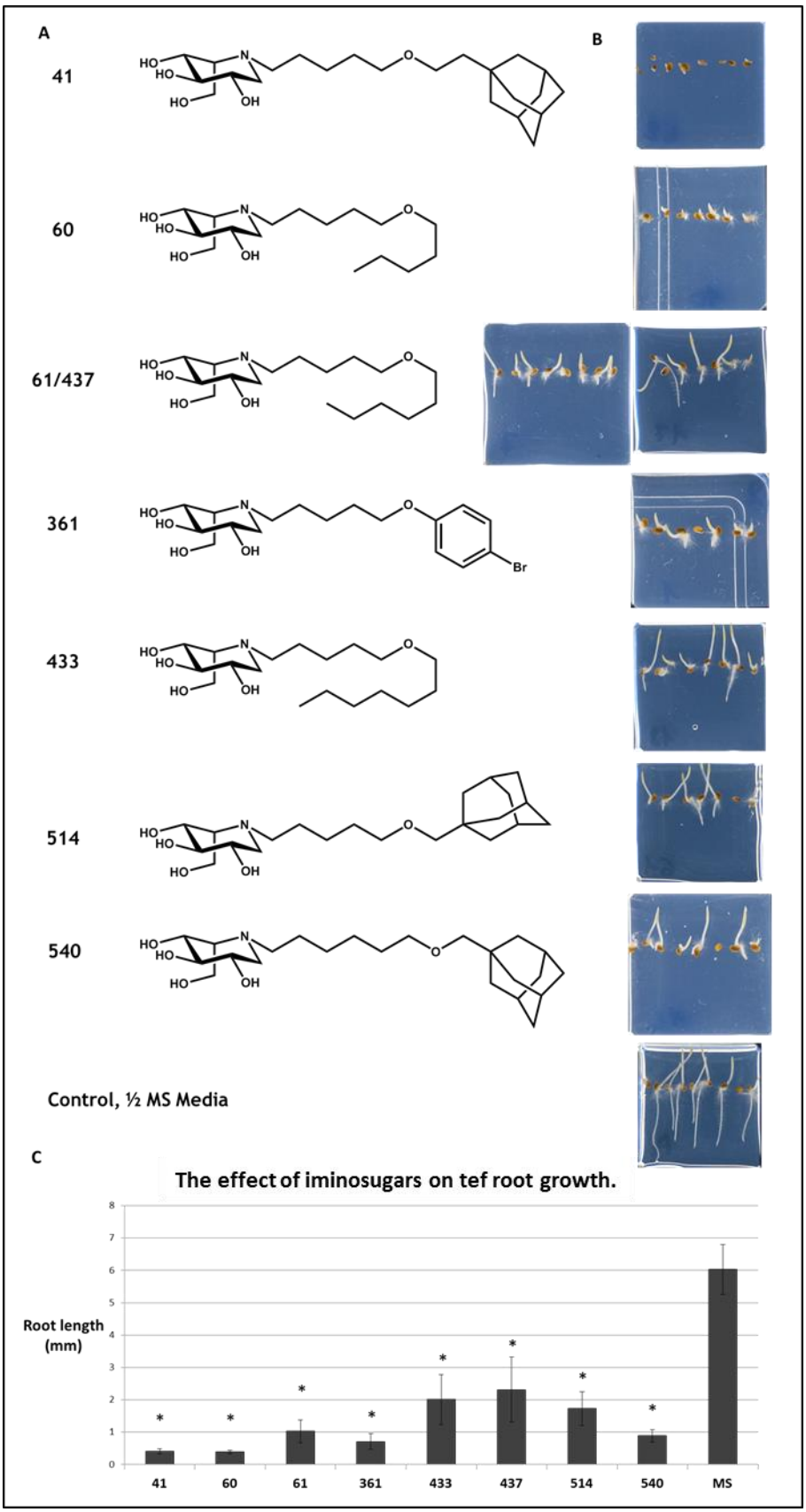

Figure 3.20 Inhibition of Tef root growth by iminosugars from the Overkleeft library.
A. The structures of compounds which inhibit root growth by more than 30 % of control. **B.** Images of the root growth phenotype. **C.** Mean values of root length in the presence of 10 µM inhibitor. Mean value from 8 plants. Error bars represent SEM. Values marked with asterisks are statistically significant from the control (water) values (t-test, * P <0.05).

3.3.8 The Impact of Non-Iminosugar Glucosylceramide Synthase Inhibitors on Arabidopsis and Barley Root Length

As the Overkleeft library was designed against GCS, and the most potent inhibitors identified in both Arabidopsis and tef screens are very similar to the lead compound for GCS inhibition (*ido*-AMP-DNJ) it was hypothesised that the root growth inhibition was due to inhibition of GCS. Other, commercially available, non-iminosugar inhibitors of GCS were tested on Arabidopsis and barley.

At a concentration of 10 µM PDMP (D-threo-1-phenyl-2-decanoylamino-3-morpholino-1-propanol) elicited a similar root growth phenotype to those seen with *ido*-iminosugars on Arabidopsis and tef (Figure 3.21), giving root lengths below 50 % of control. A 10-fold increase in concentration (100 µM) of PDMP (DL-threo-1-Phenyl-2-palmitoylamino-3-morpholino-1-propanol) almost abolishes root growth, this is comparable with compound 41, the strongest *ido*-iminosugar.

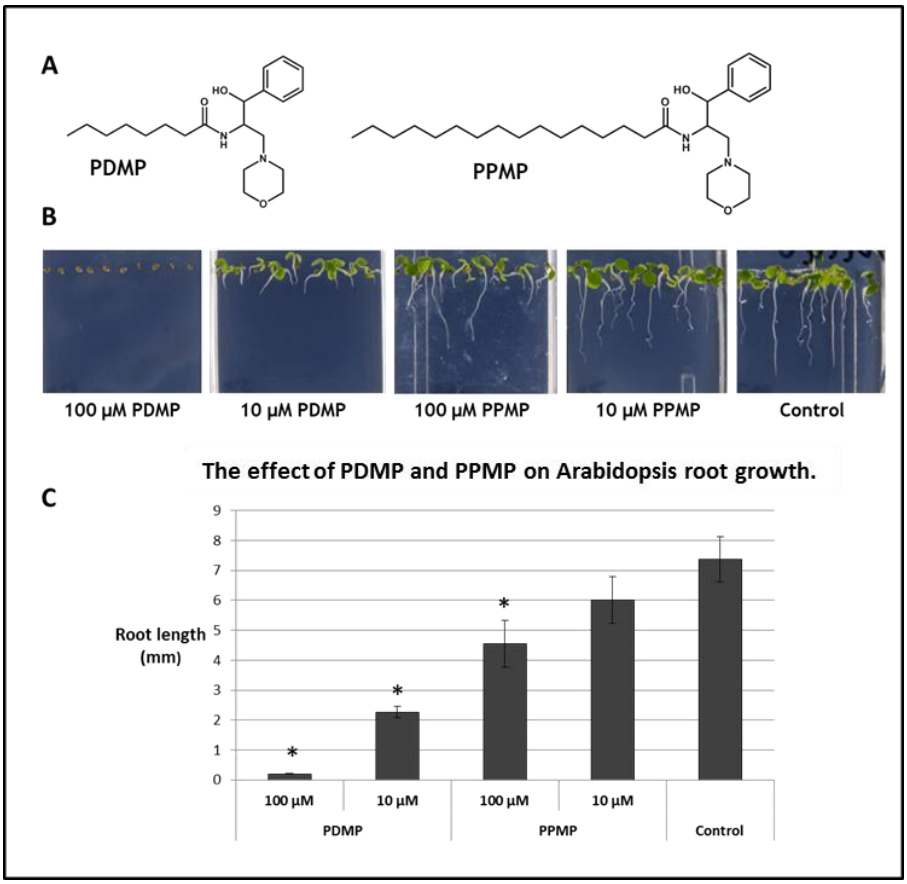

Figure 3.21 Inhibition of Arabidopsis root growth by non-iminosugar glucosylceramide synthase inhibitors.
A. The structures of PDMP and PPMP **B.** Images of the root growth phenotype. **C.** Mean values of root length in the presence of inhibitor. Mean value from 10 plants. Error bars represent SEM. Values marked with asterisks are statistically significant from the control (water) values (t-test, * P <0.05).

The difference in alkyl chain length has an impact on the level of root growth inhibition seen within Arabidopsis. At 10 µM, PPMP (15 C alkyl chain) has small but not significant effect on root growth, this is almost a 3-fold decrease in potency compared to PDMP (7 C alkyl chain) (Figure 3.21). Significant inhibition of root growth is produced using 100 µM PPMP.

When PDMP was tested on germinating barley (Figure 3.22) a concentration of 500 µM was required to elicit a significant phenotype after 5 or 10 day germination. This is 50-fold higher than the concentration required for significant inhibition in Arabidopsis.

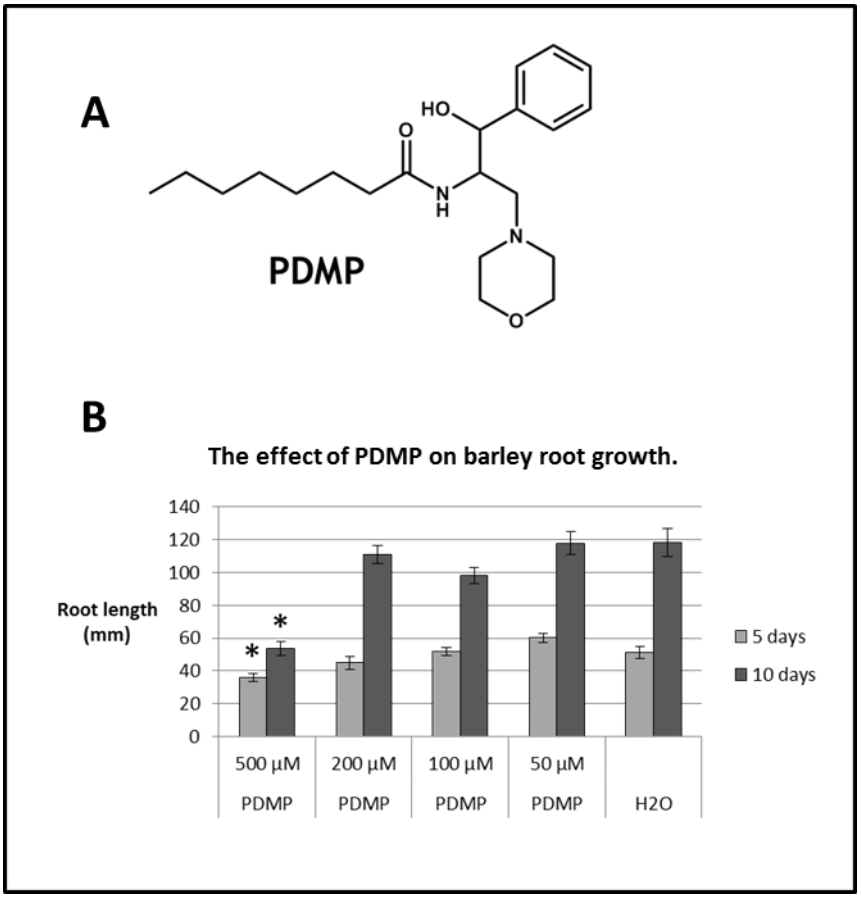

Figure 3.22 The effect of glucosylceramide synthase inhibitor PDMP on barley root growth.
A. The structure of PDMP. **B.** Grains of barley were grown for 5 or 10 dpi in the presence of water (control) or PDMP. Mean values of root length in the presence of inhibitor. Mean value from 10 plants. Error bars represent SEM. Values marked with asterisks are statistically significant from the control (water) values (*t*-test, * P <0.05).

3.4 Discussion

3.4.1 The Effect of DNJ on Glycoprotein Processing

DNJ causes a proportional increase in mannosylated structures (high mannose, $Man_8GlcNAc_2$ and $Man_9GlcNAc_2$) on glycoproteins from barley roots. Mannosidase digestion of these glycans confirms that they are indeed high mannose structures and not other glucosylated glycans. It would be expected that DNJ should act as a glucosidase I/II inhibitor, therefore giving rise to a build-up of glucosylated structures ($Glc_{1-3}Man_9GlcNAc_2$), this does not appear to be the case.

There are two direct ways to increase levels of high mannose glycans: the first is to inhibit their breakdown by preventing the actions of ER and Golgi α-mannosidase. The second would be to inhibit the synthesis of structures that are based upon $Man_9GlcNAc_2$: i.e. block the action of the glycosyltransferases that convert $Man_9GlcNAc_2$ to $Glc_{1-3}Man_9GlcNAc_2$ during synthesis of the dolichol-P-P-linked glycan.

The inhibitory activity of an iminosugar is not always specific with regard to carbohydrate configuration, for example *gluco*-configured DNJ is capable of the *in vitro* inhibition of α-galactosidase, a galactose specific enzyme (Kato et al., 2005). Furthermore 4 *gluco*-configured iminosugars have been shown to be capable of inhibiting α-mannosidase II from Drosophila, three of these compounds- glucoimidazole, *N*-octyl-6-epi-valienamine and gluco-hydroxyiminolactam were low μM inhibitors (Kuntz et al., 2008). There is a possibility that DNJ may be able to inhibit mannosidase in a similar way.

The ER and Golgi mannosidases have been shown to be important for development in Arabidopsis (Liebminger et al., 2009). Three class I mannosidases are required for *N*-glycan processing and root development: ER-mannosidase I (MNS3) and golgi mannosidase I (MNS1 and 2) (Liebminger et al., 2009). A double mutation (*MNS1/MNS2*) causes $Man_8GlcNAc_2$ accumulation and a triple mutant (*MNS1/MNS2/MNS3*) causes the almost exclusive presence of $Man_9GlcNAc_2$. The triple mutant plant has a swollen root and impaired cell wall/pectin biosynthesis. Chemical inhibition with the α-mannosidase inhibitor kifunensine generated a similar phenotype (Liebminger et al., 2009). Mutation of the rice *N*-acetylglucosaminyltransferase has also been shown to cause accumulation of high mannose glycans leading to defective post seedling development, incomplete cell wall biosynthesis and impaired cytokinin signalling (Fanata et al., 2013). These data support the hypothesis that the root growth inhibition caused by DNJ may possibly be due to mannosidase inhibition.

The alternative way to increase the concentration of $Man_9GlcNAc_2$ is to block the synthesis of lipid linked $Glc_3Man_9GlcNAc_2$. Indeed, DNJ has been shown to inhibit the formation of $Glc_3Man_9GlcNAc_2$-P-P-dolichol, leading to higher levels of $Man_9GlcNAc_2$-P-P-dolichol in human epithelial cell culture (Romero et al., 1985). A build-up of Man_8 and Man_9 structures has also been reported in mammalian thyroid slices in which energy deprivation has been induced by chemically uncoupling oxidative phosphorylation. The precise reason for the glycan build-up was not resolved but addition of exogenous glucose did not prevent accumulation (Spiro et al., 1983). It is possible that oligosaccharyltransferase is able to transfer the $Man_9GlcNAc_2$ to proteins allowing for their identification on glycoproteins (Castro et al., 2006). It is not unbelievable that DNJ, a glucose mimic, could interfere with metabolism and induce a state of energy deprivation which leads to the build-up of $Man_9GlcNAc_2$. It remains unclear why the build-up of high mannose structures is restricted to the roots. There is the possibility that roots actively take up DNJ leading to high local concentration or shoots may be unable to take up the compound. DNJ may also be actively exported or metabolised in certain tissues.

3.4.2 Differences in the Effects of Compounds on Barley, Arabidopsis and Tef

The screen of a range of DNJ concentrations against barley, Arabidopsis and tef highlights differences in the susceptibility of monocots and dicots to iminosugars. The data presented herein indicate that Arabidopsis may be more resistant to effects of DNJ, requiring a higher concentration (when compared with tef, a monocot of similar size) in order to elicit a significant root inhibition response. This might be explained as Arabidopsis is a dicot organism which doesn't rely on starch metabolism for germination and seedling growth, whereas DNJ has been shown to impact on starch metabolism in germinating monocots (Stanley et al., 2011). DNJ does, however, affect Arabidopsis root growth indicating a universal mechanism for DNJ action, which exists across monocots and dicots. The effect of castanospermine on Arabidopsis and tef further highlights the difference between monocots and dicots. At a concentration of 10 µM, castanospermine causes significant inhibition of root growth in Arabidopsis but not tef. This phenomenon has previously been noted, with a 1000-fold higher concentration of castanospermine being required to inhibit monocot root growth (Stevens and Molyneux, 1988). These differences highlight why tef is useful as an alternative model for screening for cereal specific effects.

The use of a large library containing similar compounds enables the analysis of structures to help understand how this relates to the function. The structures of similar hit compounds identified in both Arabidopsis and tef screens enable an understanding of the requirements for

potent root growth inhibition. 3 out of 6 hits in Arabidopsis and all of the 8 hits identified in tef are *ido*-configured iminosugars indicating this configuration is important for potent inhibition of root growth. The other recurring theme within the identified compounds is the presence of large, lipid soluble, *N*-substitiuents. These are likely important for compound uptake, enabling diffusion across cell membranes (Kornhuber et al., 2010). A similar phenomenon can be seen with the effect of GCS inhibitors PDMP and PPMP on Arabidopsis and barley root growth. An increase in alkyl chain length by 5 carbon atoms produces a 10-fold drop in the concentration required for effective inhibition. This the reflects the membrane bound nature of GCS.

3.4.3 Glucosylceramide Synthase as a Target for Root Growth Inhibition in Plants

The lead compounds identified from chemical genetic screens are *ido*-AMP-DNJ and *ido*-AEP-DNJ, these compounds are some of the most potent inhibitors of mammalian GCS known (Wennekes et al., 2010, Ghisaidoobe et al., 2011). To test the hypothesis that inhibition of root growth is linked to inhibition of GCS, the effect of PDMP, a known mammalian glucosylceramide synthase inhibitor (Atilla-Gokcumen et al., 2011), was tested on Arabidopsis and barley, this presented a similar phenotype to that generated by *ido*-AMP-DNJ and *ido*-AEP-DNJ.

GCS from cotton and Arabidopsis have been biochemically characterised (Leipelt et al., 2001). To date, there is no literature precedent for the effect of iminosugars on GCS *in planta*. A number of studies have investigated the effect of PDMP on plants. PDMP is able to inhibit overexpressed Arabidopsis GCS both *in vivo* and *in vitro*. When treated with PDMP Golgi morphology and protein secretion are perturbed (Melser et al., 2010). PDMP also affects vacuole morphology in Arabidopsis root cells (Kruger et al., 2013). There is a possibility that GC mediated interference with the membrane structure of subcellular compartments is responsible for the inhibition of root growth. Very recently, mutants of GCS have been reported in Arabidopsis (Msanne et al., 2015). Null mutants were viable as seedlings with strongly reduced size but failed to develop beyond seedling stage. GC was proposed to be important for organ-specific cell differentiation, null mutants had altered Golgi morphology. The inhibited growth phenotype observed in the present study supports the proposal that the root growth inhibition caused by *ido*-AMP-DNJ is mediated by GCS inhibition, but further verification is required

3.4.4 Identification of Other Potential Iminosugar Targets

The effect of an iminosugar is often attributed to inhibition of one or two enzymes within an organism, these are often easily assayed enzymes for which there is literature precedent. However, there can be numerous other targets capable of interacting with iminosugars within complex systems (Cruz et al., 2013). Recently a glycomimetic affinity enrichment proteomics technique (Figure 3.23) was developed to identify binding partners for *N*-Bu-DNJ (Cruz et al., 2013). This drug has been shown to induce reversible, dose-dependent, infertility in certain mouse strains however other strains, with a different genetic background, were insensitive. The known targets for *N*-Bu-DNJ include: β-glucosidase 2, lysosomal acid β-glucosidase and GCS (Cruz et al., 2013). Using this proteomics technique 18 proteins capable of interacting with *N*-Bu-DNJ were identified, these were narrowed down to give 6 strong lead targets (Table 3.2). These previously unidentified targets identify plausible pathways for investigation to identify the cellular target responsible for the infertility side effect (Cruz et al., 2013).

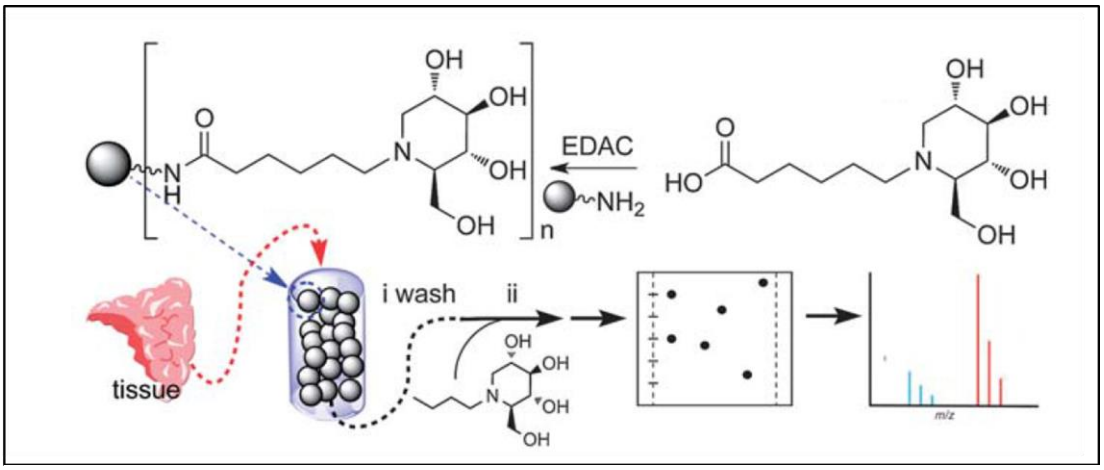

Figure 3.23 Identification of protein targets for iminosugars by glycomimetic affinity enrichment proteomics.
Glycomimetic affinity enrichment proteomics involves the generation of an affinity resin containing the molecule of interest. This is generated by chemical synthesis of an inhibitor derivative containing a carboxylic acid group, which can then be coupled to an amino derivatised resin. Following this, the resin can be used to enrich protein targets from tissue samples. Targets are then identified by 2D-PAGE and mass spectrometry. From (Cruz et al., 2013).

Protein Name	Function	Reference
Hypoxia up-regulated protein 1	Hsp70 protein, directly regulates insulin and vascular endothelial growth factor.	(Kobayashi and Ohta, 2005)
Junction plakoglobulin	Junctional plaque protein involved in formation of tight junctions.	(Kowalczyk et al., 1999)
Heat shock-related 70 kDa protein 2	Hsp70 protein, role during germ cell differentiation and necessary for progression of meiosis.	(Vos et al., 2008)
Acid leucine-rich nuclear phosphoprotein 32 family member A	Implicated in cell cycle progression, differentiation and apoptosis.	(Reilly et al., 2011)
Protein SET (I2PP2A)	Histone chaperone for nucleosome assembly, inhibits multifunctional protein phosphatase PP2A. Binds sphingolipids, including ceramide.	(Saddoughi et al., 2013)
T-complex protein 1 subunit zeta	Chaperone involved in folding of tubulin and actin.	(Gao et al., 1992)

Table 3.2 Targets of *N*-Bu-DNJ in mouse cells.
Data from (Cruz et al., 2013).

BLAST analysis reveals that plant orthologues exist for all of the proteins outlined above. Two of the plant orthologues have been studied: Protein SET and Hsp70. Plant SET/I2PP2A is member of family of nucleosome assembly proteins (NAPs), which plays a similar role to the mammalian protein in the dephosphorylation during heat shock response (Biro et al., 2012). Simultaneous knockout of two Arabidopsis NAPs generates a strong root inhibition phenotype alongside perturbed expression of around 100 genes, including some involved in root cellular organisation (Zhu et al., 2006). Plant 70-kDa HSPs are essential for plant development and thermotolerance in germinating seeds, T-DNA insertion knockout mutants cause impaired root growth, while knockout of the two genes for Hsp70 was lethal (Su and Li, 2008).

Recently, a similar glycomimetic affinity enrichment proteomics technique has been utilised within our group to identify proteins from barley endosperm that are able to bind to DNJ (Andriotis, 2015, submitted to Plant Cell). The proteins, identified using mass spectrometry, were those responsible for hydrolysing barley endosperm cell walls. The identification that these proteins can be partially inhibited by DNJ explains the inhibition of endosperm starch metabolism caused by the iminosugar.

3.5 Future Directions

3.5.1 Understanding the Targets of DNJ Action

It is clear that DNJ causes an effect on glycoprotein processing. However, the mechanism by which this occurs and how this links to inhibition of root growth remains unclear. There is the potential that multiple enzymes in the *N*-linked glycan synthetic pathway are inhibited, DNJ may have effects on α-glucosidase I/II and α-mannosidase with different potency. Changing the concentration of DNJ used in experiments may reveal the concentration dependence of DNJs effect on *N*-linked glycans. Comparison of DNJ with other iminosugars which interfere with glycoprotein processing could be used to dissect the mode of action. The application of DNJ on Arabidopsis at different stages of growth may reveal how DNJ impacts on plant development. Furthermore, a T-DNA mutant library could be screened for enhanced susceptibility or resistance to the effects of DNJ which may help identify targets of inhibition.

Affinity enrichment could be performed on root and shoot protein samples generated in the presence or absence of DNJ, this will enable a comparison which may help determine the reason for root specific effects. It remains likely that DNJ interacts with a number of other proteins within plants, glycomimetic affinity enrichment proteomics offers a useful technique which can be utilised to identify other targets responsible for the DNJ induced phenotype. Putative targets can be overexpressed in heterologous hosts and inhibition can be validated *in vitro.*

3.5.2 Identification of the Target for *Ido*-DNJ Derivatives

It is probable that *ido*-AMP-DNJ targets GCS within plants, which leads to the stunted root growth phenotype. Overexpression of plant GCS and *in vitro* inhibition will help validate GCS as the target for the *ido*-iminosugars identified in chemical screens. Glycomimetic affinity enrichment proteomics using *ido*-DNJ may reveal the specific targets for *ido*-configured iminosugars. Comparison of *gluco*-DNJ and *ido*-DNJ affinity enrichment will help elucidate similar and different protein targets of these molecules.

3.5.3 Further screening using Tef

As tef has proved to be a suitable plant for medium throughput chemical genetic screens, there is scope for the screening of numerous other compound libraries. This will enable comparison of the differences in response to different chemicals by monocots and dicots. The identification of specific growth inhibitors has potential implications in herbicide development and is not only for the malting and brewing scenario.

3.6 References

Aerts, J. M., Hollak, C., Boot, R. & Groener, A. 2003. Biochemistry of glycosphingolipid storage disorders: Implications for therapeutic intervention. *Philosophical Transactions of the Royal Society B: Biological Sciences*, 358, 905-14.

Aerts, J. M., Hollak, C. E., Boot, R. G., Groener, J. E. & Maas, M. 2006. Substrate reduction therapy of glycosphingolipid storage disorders. *Journal of Inherited Metabolic Disease,* 29, 449-56.

Asano, N., Oseki, K., Kizu, H. & Matsui, K. 1994a. Nitrogen-in-the-ring pyranoses and furanoses: Structural basis of inhibition of mammalian glycosidases. *Journal of Medicinal Chemistry,* 37, 3701-3706.

Asano, N., Oseki, K., Tomioka, E., Kizu, H. & Matsui, K. 1994b. N-containing sugars from *Morus alba* and their glycosidase inhibitory activities. *Carbohydrate Research,* 259, 243-55.

Atilla-Gokcumen, G. E., Bedigian, A. V., Sasse, S. & Eggert, U. S. 2011. Inhibition of glycosphingolipid biosynthesis induces cytokinesis failure. *Journal of the American Chemical Society,* 133, 10010-3.

Biro, J., Farkas, I., Domoki, M., Otvos, K., Bottka, S., Dombradi, V. & Feher, A. 2012. The histone phosphatase inhibitory property of plant nucleosome assembly protein-related proteins (nrps). *Plant Physiology Biochemistry,* 52, 162-8.

Borges De Melo, E., Da Silveira Gomes, A. & Carvalho, I. 2006. α- and β-glucosidase inhibitors: Chemical structure and biological activity. *Tetrahedron Letters,* 62, 10277-10302.

Brady, R. O. 2006. Enzyme replacement for lysosomal diseases. *Annual Review of Medicine,* 57, 283-96.

Brady, R. O., Kanfer, J. N., Bradley, R. M. & Shapiro, D. 1966. Demonstration of a deficiency of glucocerebroside-cleaving enzyme in Gaucher's disease. *Journal of Clinical Investigation,* 45, 1112-5.

Burn, J. E., Hurley, U. A., Birch, R. J., Arioli, T., Cork, A. & Williamson, R. E. 2002. The cellulose-deficient arabidopsis mutant rsw3 is defective in a gene encoding a putative glucosidase ii, an enzyme processing N-glycans during er quality control. *The Plant Journal,* 32, 949-960.

Bychkova, V. E. & Ptitsyn, O. B. 1995. Folding intermediates are involved in genetic diseases? *FEBS Letters,* 359, 6-8.

Cannarozzi, G., Plaza-Wuthrich, S., Esfeld, K., Larti, S., Wilson, Y. S., Girma, D., De Castro, E., Chanyalew, S., Blosch, R., Farinelli, L., Lyons, E., Schneider, M., Falquet, L., Kuhlemeier, C., Assefa, K. & Tadele, Z. 2014. Genome and transcriptome sequencing identifies breeding targets in the orphan crop tef (*Eragrostis tef*). *BMC Genomics,* 15, 581.

Castro, O., Movsichoff, F. & Parodi, A. J. 2006. Preferential transfer of the complete glycan is determined by the oligosaccharyltransferase complex and not by the catalytic subunit. *Proceedings of the National Academy of Sciences of the United States of America,* 103, 14756-14760.

Chandrasekar, B., Colby, T., Emran Khan Emon, A., Jiang, J., Hong, T. N., Villamor, J. G., Harzen, A., Overkleeft, H. S. & Van Der Hoorn, R. A. 2014. Broad-range glycosidase activity profiling. *Molecular & Cellular Proteomics,* 13, 2787-800.

Chang, J., Guo, J.-T., Du, Y. & Block, T. 2013. Iminosugar glucosidase inhibitors as broadly active anti-filovirus agents. *Emerging Microbes & Infections,* 2, e77.

Cohen, F. E. & Kelly, J. W. 2003. Therapeutic approaches to protein-misfolding diseases. *Nature,* 426, 905-909.

Compain, P. & Martin, O. R. 2007. *Iminosugars: From synthesis to therapeutic applications*, John Wiley & Sons.

Cook, C. S., Karabatsos, P. J., Schoenhard, G. L. & Karim, A. 1995. Species dependent esterase activities for hydrolysis of an anti-HIV prodrug glycovir and bioavailability of active sc-48334. *Pharmaceutical Research,* 12, 1158-1164.

Cox, T., Lachmann, R., Hollak, C., Aerts, J., Van Weely, S., Hrebicek, M., Platt, F., Butters, T., Dwek, R., Moyses, C., Gow, I., Elstein, D. & Zimran, A. 2000. Novel oral treatment of gaucher's disease with N-butyldeoxynojirimycin (ogt 918) to decrease substrate biosynthesis. *Lancet,* 355, 1481-5.

Cruz, I. N., Barry, C. S., Kramer, H. B., Chuang, C. C., Lloyd, S., Van Der Spoel, A. C., Platt, F. M., Yang, M. & Davis, B. G. 2013. Glycomimetic affinity-enrichment proteomics identifies partners for a clinically-utilized iminosugar. *Chemical Science,* 4, 3442.

Elbein, A. D. 1991. The role of N-linked oligosaccharides in glycoprotein function. *Trends in Biotechnology,* 9, 346-352.

Fan, J.-Q. 2003. A contradictory treatment for lysosomal storage disorders: Inhibitors enhance mutant enzyme activity. *Trends in Pharmacological Sciences,* 24, 355-360.

Fanata, W. I. D., Lee, K. H., Son, B. H., Yoo, J. Y., Harmoko, R., Ko, K. S., Ramasamy, N. K., Kim, K. H., Oh, D.-B., Jung, H. S., Kim, J.-Y., Lee, S. Y. & Lee, K. O. 2013. N-glycan maturation is crucial for cytokinin-mediated development and cellulose synthesis in *Oryza sativa*. *The Plant Journal,* 73, 966-979.

Fischer, P. B., Collin, M., Karlsson, G. B., James, W., Butters, T. D., Davis, S. J., Gordon, S., Dwek, R. A. & Platt, F. M. 1995. The alpha-glucosidase inhibitor N-butyldeoxynojirimycin inhibits human immunodeficiency virus entry at the level of post-cd4 binding. *Journal of Virology,* 69, 5791-7.

Furumizu, C. & Komeda, Y. 2008. A novel mutation in knopf uncovers the role of α-glucosidase i during post-embryonic development in *Arabidopsis thaliana*. *FEBS Letters,* 582, 2237-2241.

G. Belay, A. Zemede, K. Assefa, Metaferia, G. & Tefera, H. 2009. Seed size effect on grain weight and agronomic performance of tef [*Eragrostis tef* (zucc.) trotter]. *African Journal of Agricultural Research*.

Gao, Y., Thomas, J. O., Chow, R. L., Lee, G.-H. & Cowan, N. J. 1992. A cytoplasmic chaperonin that catalyzes β-actin folding. *Cell,* 69, 1043-1050.

Gebremariam, M. M., Zarnkow, M. & Becker, T. 2012. Effect of drying temperature and time on alpha-amylase, beta-amylase, limit dextrinase activities and dimethyl sulphide level of teff (*Eragrostis tef*) malt. *Food and Bioprocess Technology,* 6, 3462-3472.

Gebremariam, M. M., Zarnkow, M. & Becker, T. 2013. Thermal stability of starch degrading enzymes of teff (*Eragrostis tef*) malt during isothermal mashing. *Process Biochemistry,* 48, 1928-1932.

Ghisaidoobe, A., Bikker, P., De Bruijn, A. C. J., Godschalk, F. D., Rogaar, E., Guijt, M. C., Hagens, P., Halma, J. M., Van't Hart, S. M., Luitjens, S. B., Van Rixel, V. H. S., Wijzenbroek, M., Zweegers, T., Donker-Koopman, W. E., Strijland, A., Boot, R., Van Der Marel, G., Overkleeft, H. S., Aerts, J. M. F. G. & Van Den Berg, R. J. B. H. N. 2011. Identification of potent and selective glucosylceramide synthase inhibitors from a library of N-alkylated iminosugars. *ACS Medicinal Chemistry Letters,* 2, 119-123.

Gloster, T. M. & Vocadlo, D. J. 2012. Developing inhibitors of glycan processing enzymes as tools for enabling glycobiology. *Nature Chemical Biology,* 8, 683-694.

Ishida, N., Kumagai, K., Niida, T., Hamamoto, K. & Shomura, T. 1967a. Nojirimycin, a new antibiotic. I. Taxonomy and fermentation. *The Journal of Antibiotics*, *(Tokyo),* 20, 62-5.

Ishida, N., Kumagai, K., Niida, T., Tsuruoka, T. & Yumoto, H. 1967b. Nojirimycin, a new antibiotic. Ii. Isolation, characterization and biological activity. *The Journal of Antibiotics, (Tokyo),* 20, 66-71.

Jacob, J. R., Mansfield, K., You, J. E., Tennant, B. C. & Kim, Y. H. 2007. Natural iminosugar derivatives of 1-deoxynojirimycin inhibit glycosylation of hepatitis viral envelope proteins. *The Journal of Microbiology,* 45, 431-40.

Jones, J. K. N. & Turner, J. C. 1962. 906. 5-acetamido-5-deoxy-l-arabinose: A sugar derivative containing nitrogen as the hetero-atom in the ring. *Journal of the Chemical Society (Resumed)*, 4699-4703.

Kallemeijn, W. W., Li, K. Y., Witte, M. D., Marques, A. R., Aten, J., Scheij, S., Jiang, J., Willems, L. I., Voorn-Brouwer, T. M., Van Roomen, C. P., Ottenhoff, R., Boot, R. G., Van Den Elst, H., Walvoort, M. T., Florea, B. I., Codee, J. D., Van Der Marel, G. A., Aerts, J. M. & Overkleeft, H. S. 2012. Novel activity-based probes for broad-spectrum profiling of retaining beta-exoglucosidases in situ and in vivo. *Angewandte Chemie International Edition,* 51, 12529-33.

Kato, A., Kato, N., Kano, E., Adachi, I., Ikeda, K., Yu, L., Okamoto, T., Banba, Y., Ouchi, H., Takahata, H. & Asano, N. 2005. Biological properties of D- and L-1-deoxyazasugars. *Journal of Medicinal Chemistry,* 48, 2036-44.

Kobayashi, T. & Ohta, Y. 2005. 150-kd oxygen-regulated protein is an essential factor for insulin release. *Pancreas,* 30, 299-306.

Konishi 1998 Effects of bay m 1099, an alpha-glucosidase inhibitor, on starch degradation in germinating mung bean. *Bioscience Biotechnology and Biochemistry*, 62, 142-144.

Konishi, Y., Okamoto, A., Takahashi, J., Aitani, M. & Nakatani, N. 1994. Effects of bay m 1099, an α-glucosidase inhibitor, on starch metabolism in germinating wheat seeds. *Bioscience, Biotechnology, and Biochemistry,* 58, 135-139.

Kornfeld, S. & Mellman, I. 1989. The biogenesis of lysosomes. *Annual Review of Cell Biology,* 5, 483-525.

Kornhuber, J., Henkel, A. W., Groemer, T. W., Stadtler, S., Welzel, O., Tripal, P., Rotter, A., Bleich, S. & Trapp, S. 2010. Lipophilic cationic drugs increase the permeability of lysosomal membranes in a cell culture system. *Journal of Cellular Physiology,* 224, 152-64.

Korschen, H. G., Yildiz, Y., Raju, D. N., Schonauer, S., Bonigk, W., Jansen, V., Kremmer, E., Kaupp, U. B. & Wachten, D. 2013. The non-lysosomal beta-glucosidase gba2 is a non-integral membrane-associated protein at the endoplasmic reticulum (er) and golgi. *Journal of Biological Chemistry,* 288, 3381-93.

Kowalczyk, A. P., Hatzfeld, M., Bornslaeger, E. A., Kopp, D. S., Borgwardt, J. E., Corcoran, C. M., Settler, A. & Green, K. J. 1999. The head domain of plakophilin-1 binds to desmoplakin and enhances its recruitment to desmosomes: Implications for cutaneous disease. *Journal of Biological Chemistry,* 274, 18145-18148.

Kruger, F., Krebs, M., Viotti, C., Langhans, M., Schumacher, K. & Robinson, D. G. 2013. PDMP induces rapid changes in vacuole morphology in arabidopsis root cells. *Journal of Experimental Botany,* 64, 529-40.

Kumar, S., Kumar, V., Rana, M. & Kumar, D. 2012. Enzymes inhibitors from plants: An alternate approach to treat diabetes. *Pharmacognosy Communications,* 2, 18-33.

Kuntz, D. A., Tarling, C. A., Withers, S. G. & Rose, D. R. 2008. Structural analysis of golgi alpha-mannosidase ii inhibitors identified from a focused glycosidase inhibitor screen. *Biochemistry,* 47, 10058-68.

Leipelt, M., Warnecke, D., Zahringer, U., Ott, C., Muller, F., Hube, B. & Heinz, E. 2001. Glucosylceramide synthases, a gene family responsible for the biosynthesis of glucosphingolipids in animals, plants, and fungi. *Journal of Biological Chemistry,* 276, 33621-9.

Lerouge, P., Cabanes-Macheteau, M., Rayon, C., Fischette-Lainé, A.-C., Gomord, V. & Faye, L. 1998. N-glycoprotein biosynthesis in plants: Recent developments and future trends. *Plant Molecular Biology,* 38, 31-48.

Liebminger, E., Hüttner, S., Vavra, U., Fischl, R., Schoberer, J., Grass, J., Blaukopf, C., Seifert, G. J., Altmann, F., Mach, L. & Strasser, R. 2009. Class i α-mannosidases are required for N-glycan processing and root development in arabidopsis thaliana. *The Plant Cell,* 21, 3850-3867.

Liu, P. S. 1987. Total synthesis of 2, 6-dideoxy-2, 6-imino-7-o-(Beta.-d-glucopyranosyl)-D-glycero-L-gulo-heptitol hydrochloride. A potent inhibitor of. Alpha-glucosidases. *The Journal of Organic Chemistry,* 52, 4717-4721.

Lyons, E. & Freeling, M. 2008. How to usefully compare homologous plant genes and chromosomes as DNA sequences. *The Plant Journal,* 53, 661-73.

Mceachern, K. A., Fung, J., Komarnitsky, S., Siegel, C. S., Chuang, W. L., Hutto, E., Shayman, J. A., Grabowski, G. A., Aerts, J. M., Cheng, S. H., Copeland, D. P. & Marshall, J. 2007. A specific and potent inhibitor of glucosylceramide synthase for substrate inhibition therapy of gaucher disease. *Molecular Genetics and Metabolism,* 91, 259-67.

Medzihradszky, K. F. 2008. Characterization of site-specific n-glycosylation. *Methods in Molecular Biology,* 446, 293-316.

Mega, T. 2004. Conversion of the carbohydrate structures of glycoproteins in roots of *Raphanus sativus* using several glycosidase inhibitors. *The Journal of Biochemistry,* 136, 525-31.

Mega, T. 2005. Glucose trimming of N-glycan in endoplasmic reticulum is indispensable for the growth of raphanus sativus seedling (kaiware radish). *Bioscience, Biotechnology, and Biochemistry,* 69, 1353-64.

Mehta, A., Zitzmann, N., Rudd, P. M., Block, T. M. & Dwek, R. A. 1998. A-glucosidase inhibitors as potential broad based anti-viral agents. *FEBS Letters,* 430, 17-22.

Melser, S., Batailler, B., Peypelut, M., Poujol, C., Bellec, Y., Wattelet-Boyer, V., Maneta-Peyret, L., Faure, J. D. & Moreau, P. 2010. Glucosylceramide biosynthesis is involved in golgi morphology and protein secretion in plant cells. *Traffic,* 11, 479-90.

Molyneux, R. J., Roitman, J. N., Dunnheim, G., Szumilo, T. & Elbein, A. D. 1986. 6-epicastanospermine, a novel indolizidine alkaloid that inhibits α-glucosidase. *Archives of Biochemistry and Biophysics,* 251, 450-457.

Msanne, J., Chen, M., Luttgeharm, K. D., Bradley, A. M., Mays, E. S., Paper, J. M., Boyle, D. L., Cahoon, R. E., Schrick, K. & Cahoon, E. B. 2015. Glucosylceramide is critical for cell-type differentiation and organogenesis, but not for cell viability in *Arabidopsis*. *The Plant Journal*, 84, 188-201.

Nash, R. J., Kato, A., Yu, C. Y. & Fleet, G. W. 2011. Iminosugars as therapeutic agents: Recent advances and promising trends. *Future Medicinal Chemistry,* 3, 1513-21.

Overkleeft, H. S., Renkema, G. H., Neele, J., Vianello, P., Hung, I. O., Strijland, A., Van Der Burg, A. M., Koomen, G.-J., Pandit, U. K. & Aerts, J. M. 1998. Generation of specific deoxynojirimycin-type inhibitors of the non-lysosomal glucosylceramidase. *Journal of Biological Chemistry,* 273, 26522-26527.

Palamarczyk, G. & Elbein, A. D. 1985. The effect of castanospermine on the oligosaccharide structures of glycoproteins from lymphoma cell lines. *Biochemical Journal,* 227, 795-804.

Paulsen, H. 1966. Carbohydrates containing nitrogen or sulfur in the “hemiacetal” ring. *Angewandte Chemie International Edition in English,* 5, 495-510.

Paulsen, H. & Todt, K. 1968. Cyclic monosaccharides having nitrogen or sulfur in the ring*. *In:* MELVILLE, L. W. & TIPSON, R. S. (eds.) *Advances in Carbohydrate Chemistry.* Academic Press.

Peyrieras, N., Bause, E., Legler, G., Vasilov, R., Claesson, L., Peterson, P. & Ploegh, H. 1983. Effects of the glucosidase inhibitors nojirimycin and deoxynojirimycin on the biosynthesis of membrane and secretory glycoproteins. *The EMBO Journal,* 2, 823-32.

Platt, F. M., Jeyakumar, M., Andersson, U., Priestman, D. A., Dwek, R. A., Butters, T. D., Cox, T. M., Lachmann, R. H., Hollak, C., Aerts, J. M., Van Weely, S., Hrebicek, M., Moyses, C., Gow, I., Elstein, D. & Zimran, A. 2001. Inhibition of substrate synthesis as a strategy for glycolipid lysosomal storage disease therapy. *Journal of Inherited Metabolic Disease,* 24, 275-90.

Platt, F. M., Neises, G. R., Dwek, R. A. & Butters, T. D. 1994a. N-butyldeoxynojirimycin is a novel inhibitor of glycolipid biosynthesis. Journal of Biological Chemistry, 269, 8362-5.

Platt, F. M., Neises, G. R., Karlsson, G. B., Dwek, R. A. & Butters, T. D. 1994b. N-butyldeoxygalactonojirimycin inhibits glycolipid biosynthesis but does not affect N-linked oligosaccharide processing. *Journal of Biological Chemistry,* 269, 27108-14.

Qu, X., Pan, X., Weidner, J., Yu, W., Alonzi, D., Xu, X., Butters, T., Block, T., Guo, J.-T. & Chang, J. 2011. Inhibitors of endoplasmic reticulum α-glucosidases potently suppress hepatitis C virus virion assembly and release. *Antimicrobial Agents and Chemotherapy,* 55, 1036-1044.

Reilly, P. T., Afzal, S., Gorrini, C., Lui, K., Bukhman, Y. V., Wakeham, A., Haight, J., Ling, T. W., Cheung, C. C., Elia, A. J., Turner, P. V. & Mak, T. W. 2011. Acidic nuclear phosphoprotein 32kda (anp32)b-deficient mouse reveals a hierarchy of anp32 importance in mammalian development. *Proceedings of the National Academy of Sciences of the United States of America,* 108, 10243-8.

Rempel, B. P. & Withers, S. G. 2008. Covalent inhibitors of glycosidases and their applications in biochemistry and biology. *Glycobiology,* 18, 570-86.

Rhinehart, B., Robinson, K. & Liu, P. 1987. Inhibition ofintestinal disaccharidases and suppression of blood glu-cose by a new a-glucohydrolase inhibitor-mdl25, 637. *Journal of Pharmacology and Experimental Therapeutics,* 24, 915-920.

Romero, P. A., Friedlander, P. & Herscovics, A. 1985. Deoxynojirimycin inhibits the formation of $Glc_3Man_9GlcNAc_2$-pp-dolichol in intestinal epithelial cells in culture. *FEBS Letters,* 183, 29-32.

Saddoughi, S. A., Gencer, S., Peterson, Y. K., Ward, K. E., Mukhopadhyay, A., Oaks, J., Bielawski, J., Szulc, Z. M., Thomas, R. J. & Selvam, S. P. 2013. Sphingosine analogue drug fty720 targets i2pp2a/set and mediates lung tumour suppression via activation of pp2a-ripk1-dependent necroptosis. *EMBO Molecular Medicine,* 5, 105-121.

Sasak, V. W., Ordovas, J., Elbein, A. D. & Berninger, R. W. 1985. Castanospermine inhibits glucosidase i and glycoprotein secretion in human hepatoma cells. *Biochemical Journal,* 232, 759-766.

Saul, R., Ghidoni, J. J., Molyneux, R. J. & Elbein, A. D. 1985. Castanospermine inhibits alpha-glucosidase activities and alters glycogen distribution in animals. *Proceedings of the National Academy of Sciences of the United States of America,* 82, 93-97.

Soussillane, P., D’alessio, C., Paccalet, T., Fitchette, A.-C., Parodi, A. J., Williamson, R., Plasson, C., Faye, L. & Gomord, V. 2009. N-glycan trimming by glucosidase ii is essential for arabidopsis development. *Glycoconjugate Journal,* 26, 597-607.

Spiro, R. G., Spiro, M. J. & Bhoyroo, V. D. 1983. Studies on the regulation of the biosynthesis of glucose-containing oligosaccharide-lipids. Effect of energy deprivation. *Journal of Biological Chemistry,* 258, 9469-76.

Stanley, D., Rejzek, M., Naested, H., Smedley, M., Otero, S., Fahy, B., Thorpe, F., Nash, R. J., Harwood, W., Svensson, B., Denyer, K., Field, R. A. & Smith, A. M. 2011. The role of alpha-glucosidase in germinating barley grains. *Plant Physiology,* 155, 932-43.

Stevens, K. L. & Molyneux, R. J. 1988. Castanospermine-a plant growth regulator. *Journal of Chemical Ecology,* 14, 1467-73.

Strasser, R. 2014. Biological significance of complex N-glycans in plants and their impact on plant physiology. *Frontiers in Plant Science,* 5.

Su, P.-H. & Li, H.-M. 2008. Arabidopsis stromal 70-kd heat shock proteins are essential for plant development and important for thermotolerance of germinating seeds. *Plant Physiology,* 146, 1231-1241.

Taylor, D. L., Sunkara, P. S., Liu, P. S., Kang, M. S., Bowlin, T. L. & Tyms, A. S. 1991. 6-0-butanoylcastanospermine (mdl 28,574) inhibits glycoprotein processing and the growth of hivs. *Aids,* 5, 693-698.

Van Den Berg, R. J., Wennekes, T., Ghisaidoobe, A., Donker-Koopman, W. E., Strijland, A., Boot, R. G., Van Der Marel, G. A., Aerts, J. M. & Overkleeft, H. S. 2011. Assessment of partially deoxygenated deoxynojirimycin derivatives as glucosylceramide synthase inhibitors. *ACS Medicinal Chemistry Letters,* 2, 519-522.

Vos, M. J., Hageman, J., Carra, S. & Kampinga, H. H. 2008. Structural and functional diversities between members of the human hspb, hsph, hspa, and dnaj chaperone families. *Biochemistry,* 47, 7001-7011.

Vunnam, R. R. & Radin, N. S. 1980. Analogs of ceramide that inhibit glucocerebroside synthetase in mouse brain. *Chemistry and Physics of Lipids,* 26, 265-78.

Weiss, M., Hettmer, S., Smith, P. & Ladisch, S. 2003. Inhibition of melanoma tumor growth by a novel inhibitor of glucosylceramide synthase. *Cancer Research,* 63, 3654-8.

Wennekes, T., Meijer, A. J., Groen, A. K., Boot, R. G., Groener, J. E., Van Eijk, M., Ottenhoff, R., Bijl, N., Ghauharali, K., Song, H., O'Shea, T. J., Liu, H., Yew, N., Copeland, D., Van Den Berg, R. J., Van Der Marel, G. A., Overkleeft, H. S. & Aerts, J. M. 2010. Dual-action lipophilic iminosugar improves glycemic control in obese rodents by reduction of visceral glycosphingolipids and buffering of carbohydrate assimilation. *Journal of Medicinal Chemistry,* 53, 689-98.

Wennekes, T., Van Den Berg, R. J., Donker, W., Van Der Marel, G. A., Strijland, A., Aerts, J. M. & Overkleeft, H. S. 2007. Development of adamantan-1-yl-methoxy-functionalized 1-deoxynojirimycin derivatives as selective inhibitors of glucosylceramide metabolism in man. *Journal of Organic Chemistry,* 72, 1088-97.

Winchester, B. G. 2009. Iminosugars: From botanical curiosities to licensed drugs. *Tetrahedron: Asymmetry,* 20, 645-651.

Yu, L., Ikeda, K., Kato, A., Adachi, I., Godin, G., Compain, P., Martin, O. & Asano, N. 2006. A-1-c-octyl-1-deoxynojirimycin as a pharmacological chaperone for Gaucher disease. *Bioorganic & medicinal Chemistry,* 14, 7736-7744.

Zeng, Y., Pan, Y., Asano, N., Nash, R. J. & Elbein, A. D. 1997. Homonojirimycin and N-methyl-homonojirimycin inhibit N-iinked oligosaccharide processing. *Glycobiology,* 7, 297-304.

Zhu, Y., Dong, A., Meyer, D., Pichon, O., Renou, J. P., Cao, K. & Shen, W. H. 2006. Arabidopsis nrp1 and nrp2 encode histone chaperones and are required for maintaining postembryonic root growth. *Plant Cell,* 18, 2879-92.

Chapter 4- *In Vitro* Chemical Genetics Reveals Potential Avenues for the Inhibition of Limit Dextrinase

4.1 Introduction

4.1.1 Iminosugars and Other Small Molecule Inhibitors on Barley Enzymes *In vitro*

α-Amylase

The inhibition of amylase has attracted a large amount of attention due to the potential for the treatment of diabetes and reduction of blood glucose levels (Jayaraj et al., 2013). Acarbose (Figure 4.1) is a potent amylase inhibitor from *Actinoplanes* sp. SE50/11 (Müller et al., 1980, Schwientek et al., 2012), this compound is currently marketed as Glucobay, a type II diabetes treatment. A number of compounds similar to acarbose, the acarviostatins, trestatins and amylostatin, have been identified in *Streptomyces* and show potential as amylase inhibitors (Deshpande et al., 1988, Geng et al., 2008). Study of these type of compounds has been transferred from mammalian systems to the study of amylases from other organisms including bacterial plant pathogens and plants. Acarbose and analogues thereof can be prepared by transglycosylation using cyclomaltodextrin glucosyltranferase (Yoon and Robyt, 2003), the products of these types of reaction are μM/nM range inhibitors, depending on the source of the α-amylase being assayed.

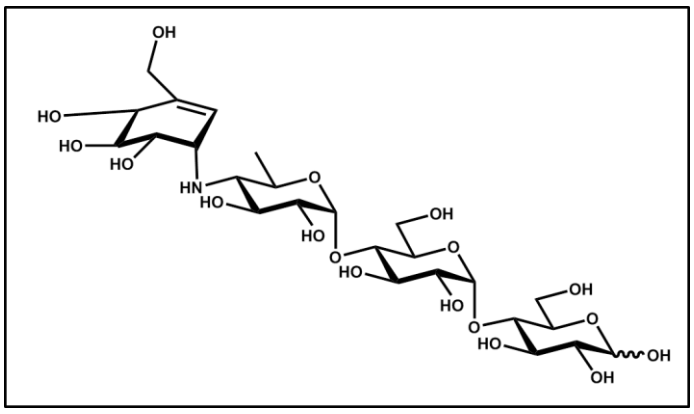

Figure 4.1 The structure of the barley α-amylase inhibitor acarbose.

The crystal structure of barley α-amylase I has been solved in complex with acarbose. The inhibitor was bound within the active site and also on a surface binding site (Kadziola et al., 1998, Mori et al., 2001). The valienamine ring found within acarbose mimics the transition state of the enzymes substrate complex (Gloster and Davies, 2010).

More recently, a new class of amylase inhibitors has been discovered from a screen of 30,000 extracts from terrestrial or marine organisms. This family of three glycosylated acyl-flavonols, named montbretins, inhibit human α-amylase with nM affinity (Tarling et al., 2008). The crystal structures of these compounds bound to α-amylase have been solved, this identified the myricetin (Figure 4.2, M) and caffeic acid (Figure 4.2, CA) moieties as important for forming H-bonds with the catalytic residues (Williams et al., 2015).

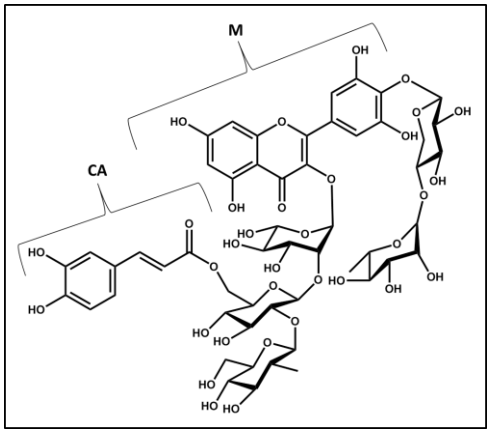

Figure 4.2 The structure of α-amylase inhibitor montbretin A.
M. Myricetin moiety. **CA.** Caffeic acid moiety.

β-Amylase

The irreversible inhibition of β-amylase by 2',3'-epoxypropyl α-D-glucopyranoside (α-EPG) (Figure 4.3, C) was reported some time ago (Isoda et al., 1987). To build upon this a series of chemically synthesised epoxyalkyl α-D-glycopyranosides were screened against barley β-amylase I (Rejzek et al., 2011). The most potent of these compounds was identified to be α-EBG (Figure 4.3, B), giving 100 % inhibition at 25 mM. The most potent non-covalent inhibitor, 4-*O*-α-D-glucopyranosyl moranoline (G1M) (Figure 4.3, A), was identified by screening libraries containing iminosugars, iminosugar glycosides and cyclodextrins. G1M produces 90 % inhibition at 1 mM. These three glycone site binding inhibitors (α-EPG, α-EBG and G1M) have been crystallised in complex with β-amylase (Rejzek et al., 2011).

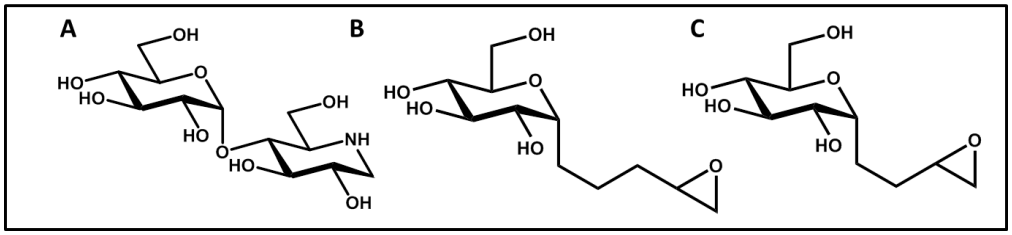

Figure 4.3 The structures of β-amylase inhibitors
A. G1M. **B.** α-EBG. **C.** α-EPG.

α-Glucosidase

In order to identify inhibitors of barley α-glucosidase 2,157 compounds were assayed at 1 µM using a chromogenic substrate (pNP-Glucose), alongside this a range of commercially available α-glucosidase inhibitors were evaluated (Stanley et al., 2011). From these experiments two very potent inhibitors were identified: DNJ and α-homonojirimycin (Figure 4.4). The results of this screen were further extended to look at the effects of similar compounds *in planta*, as discussed in Chapter 3.

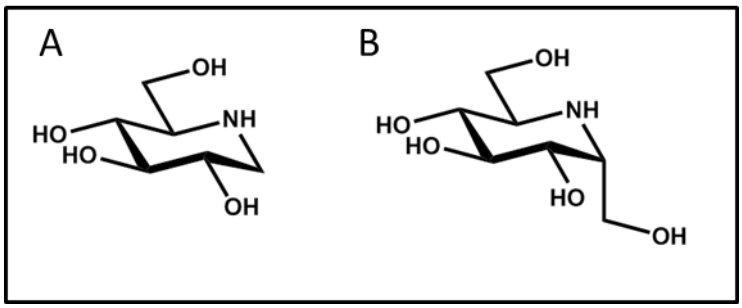

Figure 4.4 The structures of barley α-glucosidase inhibitors.
A. DNJ. **B.** α-homonojirimycin.

Limit Dextrinase

To date, very few potent small molecule inhibitors for LD have been identified. The cyclodextrins are established as the most potent inhibitors of LD, discussed in detail in Chapter 5. The only attempt at generation of an LD inhibitor involved the chemoenzymatic synthesis of hemithiomaltodextrins. Only one of these thio-linked substrate mimics (Figure 4.5) inhibited LD activity, with a K_i of 0.5 mM, an inhibitory concentration similar to that of cyclodextrin (Greffe et al., 2002).

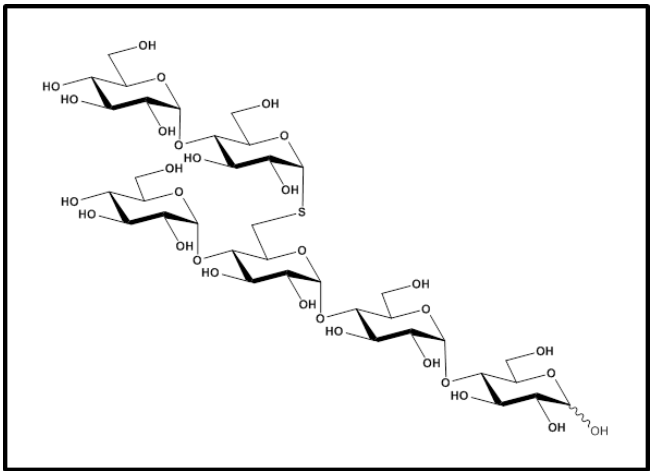

Figure 4.5 Hemithiomaltodextrin inhibitor of limit dextrinase.

4.1.2 Protein and Peptide Inhibitors of Glycosyl Hydrolases

Peptide and protein based inhibitors represent another avenue for the generation of potential inhibitors of LD. Numerous proteinaceous amylase inhibitors exist in nature, these fall into different categories- lectin-like, knottin-like, cereal-type, kunitz-like, gamma-purothionin-like, thaumatin-like (Svensson et al., 2004, Franco et al., 2002) and are found in both plant and non-plant species. Indeed, a proteinaceous inhibitor of LD exists (limit dextrinase inhibitor). This, 14 kDa, protein has been shown to bind LD with picomolar affinity and is discussed further in the results section of this chapter, alongside Chapters 5 and 6. This section focuses on shorter, peptide based glycosyl hydrolase inhibitors.

Tendamistat, an amylase inhibitor from *Streptomyces*, has been the focus of numerous studies due to its potential in treating diabetes. This small protein is able to inhibit porcine pancreatic α-amylase with picomolar affinity (Machius et al., 1996). The crystal structure of this protein complex has been solved (Figure 4.6) (Wiegand et al., 1995), which enabled the rational development of cyclic hexapeptides that mimic tendamistat. All of the peptide mimics contained a WRY amino acid motif, the most effective of these inhibited α-amylase with a K_i of 14 µM (Etzkorn et al., 1994).

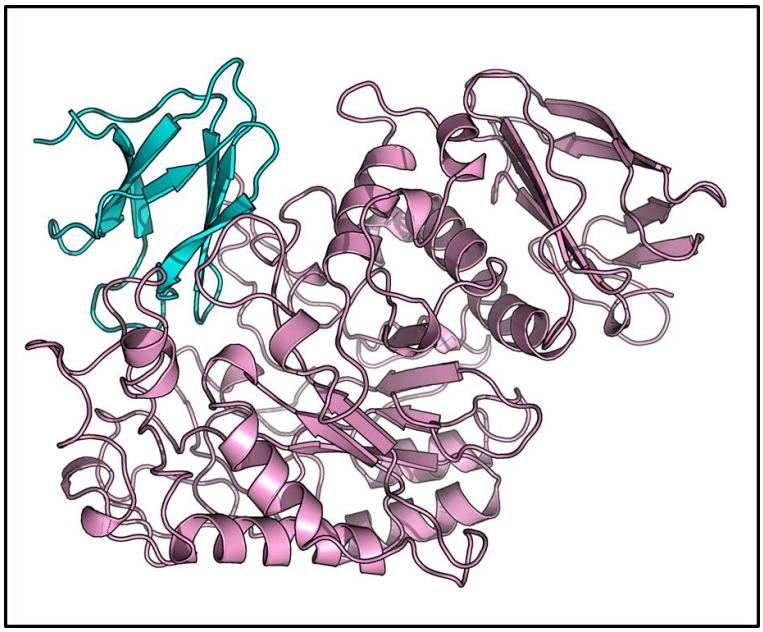

Figure 4.6 The crystal structure of tendamistat bound to α-amylase
Blue: Tendamistat. Pink: porcine α-amylase (PDB: 1BVN).

Other examples of small peptide inhibitors exist within the literature. A 22 amino acid, disulfide linked, peptide (EPCCDSCRCTKSIPPQCHCANI) based on mung bean trypsin inhibitor has been crystallised in complex with bovine trypsin (Li et al., 1994). Peptides based on the N-terminal domain of ragi alpha-amylase/trypsin inhibitor (RATI) (SVGTSCIPGMA) show competitive inhibition in amylase assays (Alam et al., 2001). Optimisation studies of these types of inhibitors shows further potential for rational and *de novo* design of peptide inhibitors for GHs (Heyl et al., 2005).

Modelling inhibitors based on known structures requires prior knowledge of existing structures. Combinatorial chemistry is another method that is used to access a broad range of chemical space not utilised by nature, the *de novo* α-amylase inhibitor designated PAMI was identified using this method (Figure 4.7) (Doleckova-Maresova et al., 2005). This peptide inhibits α-amylase and α-glucosidase enzymes from a range of sources including human, pig, *Bacillus*, *Saccharomyces* and *Aspergillus*. A lead hexapeptide containing a HWXXXX motif was optimised by iterative rounds of synthesis and screening to produce a peptide with the sequence GHWYYRCW that gave IC_{50} values at low μM level. The PAMI peptide has been further optimised to give RHWYYRYW. Docking simulation with the active site of PPA revealed the importance of the WYY motif (Ochiai et al., 2012). These inhibitors have been shown to bind in, or near to the active site however there is the possibility that they may also bind elsewhere on the proteins.

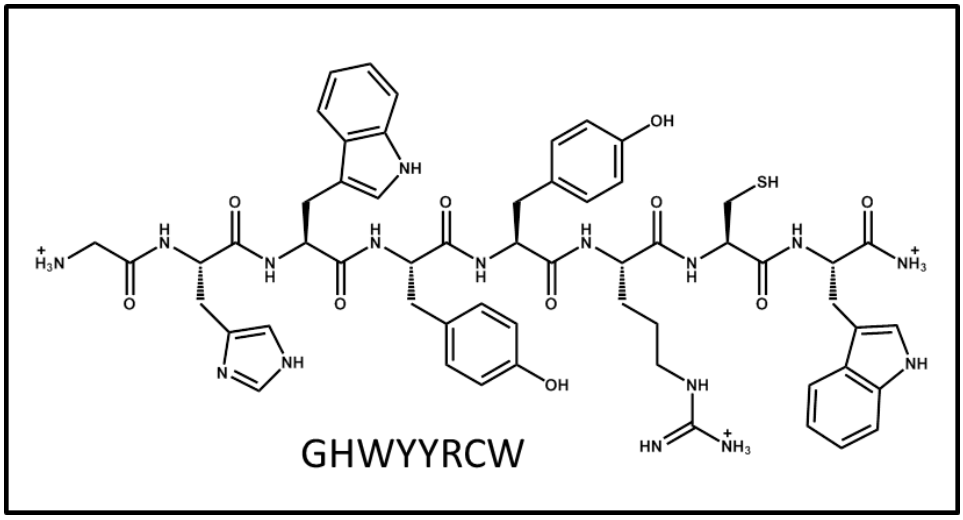

Figure 4.7 The structure of α-amylase and α-glucosidase inhibitor PAMI.
Note the C-terminal end is protected with an amino group to prevent degradation by peptidases (Doleckova-Maresova et al., 2005).

4.1.3 Biochemical Assays of Limit Dextrinase

Limit dextrinase was originally assayed using limit dextrins (Manners and Rowe, 1971). Since this point numerous assays have been developed utilising different substrates and analytical methods. The most commonly used assays can be divided into two categories: reducing end assays and chromophore based assays.

Reducing End Assays

The reducing end assay is used for analysis of numerous glycosyl hydrolases, the substrate used within this assay determines the specificity. Pullulan is utilised as the substrate for LD. The reducing ends released by hydrolysis are measured using BCA (Figure 4.8) or DNS (Figure 4.9) methods (Doner and Irwin, 1992, Wood et al., 2012). Both methods have been shown to work on LD, however BCA produces more reliable results (Gusakov et al., 2011), suffers from fewer background issues and is more amenable to miniaturisation (Green et al., 1989). Issues do however occur when using complex protein samples, as reduction by peptide backbones can affect these assays (Doner and Irwin, 1992).

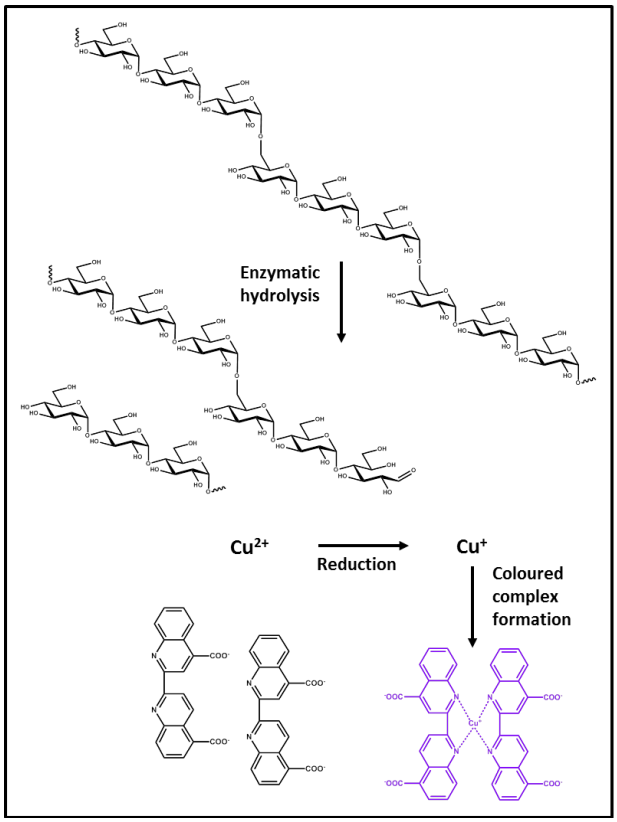

Figure 4.8 The bicinchoninic acid reducing end assay.
Pullulan is hydrolysed by the activity of limit dextrinase or another 1,6-debranching enzyme. This generates reducing ends which in turn reduce Cu^{2+} to Cu^{+}. Bicinchoninic acid is able to form a lavender coloured complex with Cu^{+}. The absorbance of this complex is measured at 565 nm.

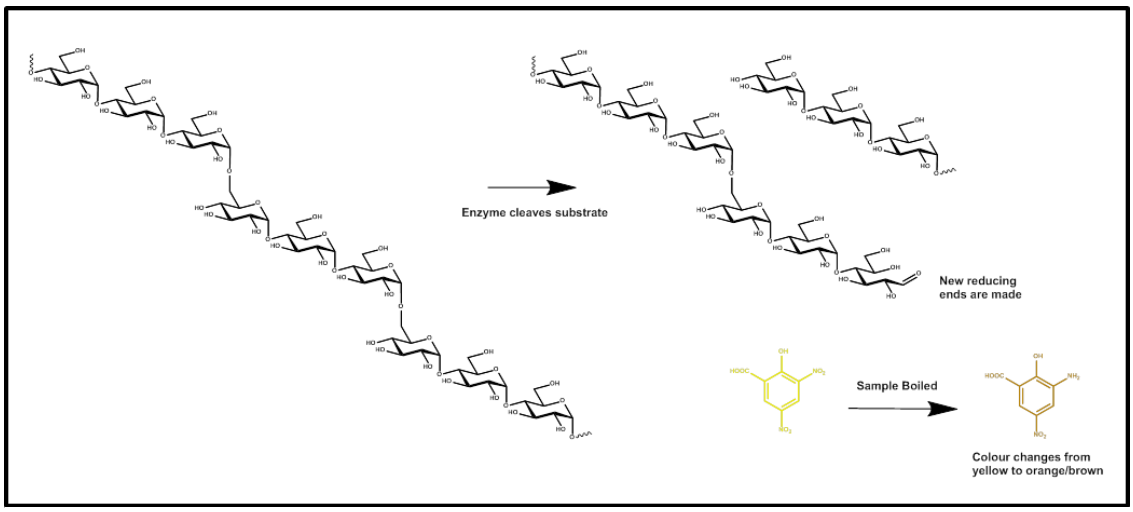

Figure 4.9 The dinitrosalicylic acid reducing end assay.
Pullulan is hydrolysed by the activity of limit dextrinase or another 1,6-debranching enzyme. This generates reducing ends. When DNS is boiled in the presence of a reducing agent the colour changes from yellow to orange/brown. The absorbance of this compound is measured at 540 nm.

Chromophore Based Assays

The chromophore based assays (Figure 4.10) utilise pullulan- both the red pullulan and limit dextrizyme assays were developed by Megazyme (Mccleary, 1992) and utilise procion red MX-5B linked pullulan and azurine crosslinked pullulan, respectively. The red pullulan can also be used in substrate-in-gel electrophoresis (zymography) (Furegon et al., 1994). The assays based on reducing ends and chromophores each have their own drawbacks. These chromophore based methods require either high quantities of LD or long incubation times due to the relatively low level/activity of LD in malt.

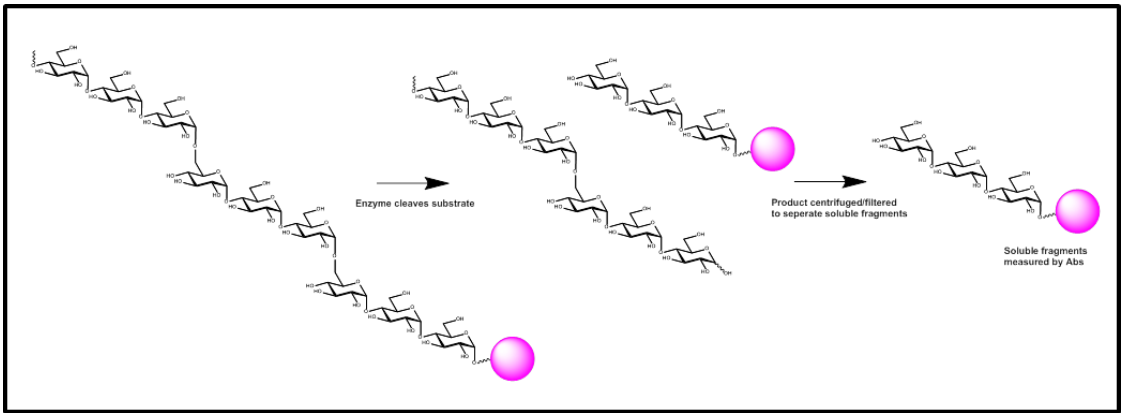

Figure 4.10 The red pullulan and limit dextrizyme chromophore based assays.
The chromophore linked pullulan is hydrolysed by limit dextrinase or another 1,6-debranching enzyme. This releases soluble chromophore linked fragments. These can be extracted and measured at 510 nm (procion red MX-5B) or 590 nm (azurine). Pink circle represents chromophore.

Advances in technology and synthetic methods have led to the development of new substrates for the assay of LD. A FRET based assay has been reported (Bøjstrup et al., 2012) however this is not commercially available. More recently, colourimetric/fluorimetric assay methods have been independently implemented by two groups for assay of pullulanase (PUL) and LD (Bojstrup et al., 2014, Mccleary et al., 2014). Both of these assays are based on maltotriosyl-maltotriose derivatives, which are more similar in structure to the proposed natural substrate of LD (Figure 4.11). Mangan et al developed a non-reducing end blocked substrate, benzylidine-maltotriosyl-maltotriose, which is resistant to hydrolysis by exo-acting enzymes (Mangan et al., 2015). These substrates have been shown to be sensitive and specific for the activity of PUL and LD and are applicable to high throughput, miniaturised assays. Furthermore they are believed to be unaffected by transglycosylation (Mangan et al., 2015, Mccleary et al., 2014).

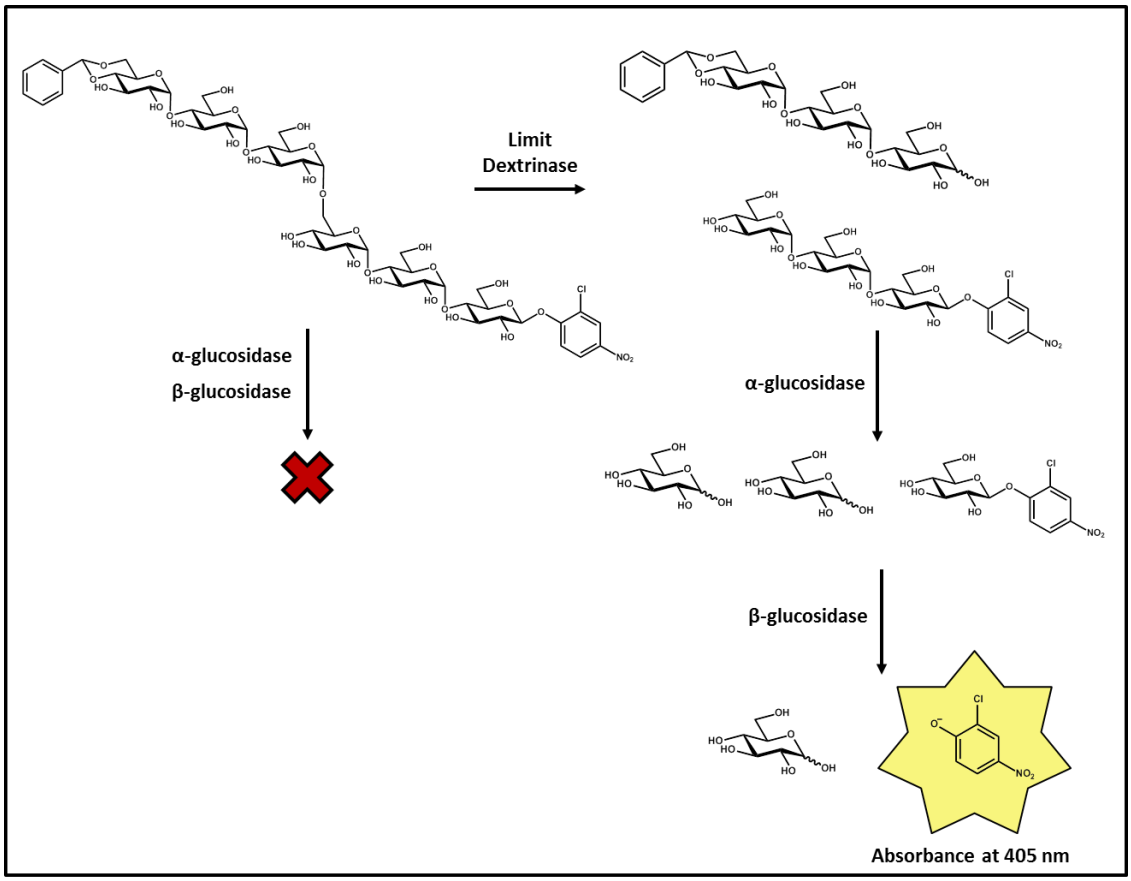

Figure 4.11 The hexachrom maltotriosyl-maltotriose assay of limit dextrinase.
This assay involves the cleavage of a 1,6-linkage present in 4-nitrophenyl-6^3-α-D- maltotriosyl-maltotriose. This opens the substrate up to breakdown by glucosidses which release the nitrophenyl group that is measured at 405 nm. A fluorescent, methylumbelliferyl, variant of the substrate is also available.

4.2 Aims of this Chapter

Recent work on the inhibition of barley glycosyl hydrolases has identified a number of potent inhibitors for α-amylase, β-amylase and α-glucosidase. These inhibitors have been used as tools, alongside genetics, to dissect the role of enzymes in carbohydrate metabolism during grain germination. To date, no potent (μM/nM) small molecule inhibitors have been identified for LD.

Currently the only known inhibitors for LD are cyclodextrins and thio-oligosaccharides. Iminosugars may have the potential to inhibit LD but have not been studied in any great detail. Proteinaceous inhibitors exist for numerous amylases and other GHs and represent another potential avenue for the development of novel inhibitors. As LD plays an important role in the hydrolysis of 1,6-glucans during malting and mashing the potential to inhibit or chaperone the protein may enable regulation of 1,6 branched glucan levels. It is also possible that an inhibitor could prevent the interaction between LD and LDI. A specific inhibitor would prove a useful tool to understand the biochemical role of LD during germination and starch synthesis, this would complement the genetic knock-down approach outlined in Chapter 6. The objectives of this chapter were twofold: firstly, to identify the effects iminosugars have on LD activity, secondly, to develop peptide inhibitors capable of inhibiting LD.

4.3 Results

4.3.1 Limit Dextrinase is Strongly Inhibited by Cyclodextrins but not Iminosugars DNJ and G1M

Preliminary screens performed using recombinant LD expressed in *Pichia pastoris* (Vester-Christensen, 2010) were performed using an in-house library of iminosugars with potential activity against amylases and glucosidases (Appendix) (carried out by Malene Vester-Christensen). This screen identified only two compounds that were capable of inhibiting LD activity by more than 20 % at a concentration of 1 mM, G1M- a glucosylated variant of DNJ and a glucose linked to a triazole amine (SD93). DNJ was screened within this assay and gave no inhibition; α-, β- and γ- CD were used as the positive controls within the screen.

Recombinant LD was utilised in a BCA assay in order to confirm the effect of cyclodextrins, DNJ and G1M. SD93 was not further pursued due to limited compound availability. The data from an assay performed with 1 mM of inhibitor produced the results in Figure 4.12. β-CD was the strongest inhibitor of the three cyclodextrins tested, giving 95 % inhibition of LD activity. α-CD and γ-CD gave around 85 % inhibition. The iminosugar DNJ showed almost no inhibitory effect (5 % inhibition) whereas G1M, the α-1,4-glucosylated form of DNJ gave 30 % inhibition, indicating that extension of the iminosugar is a potential way enhance enzyme inhibition.

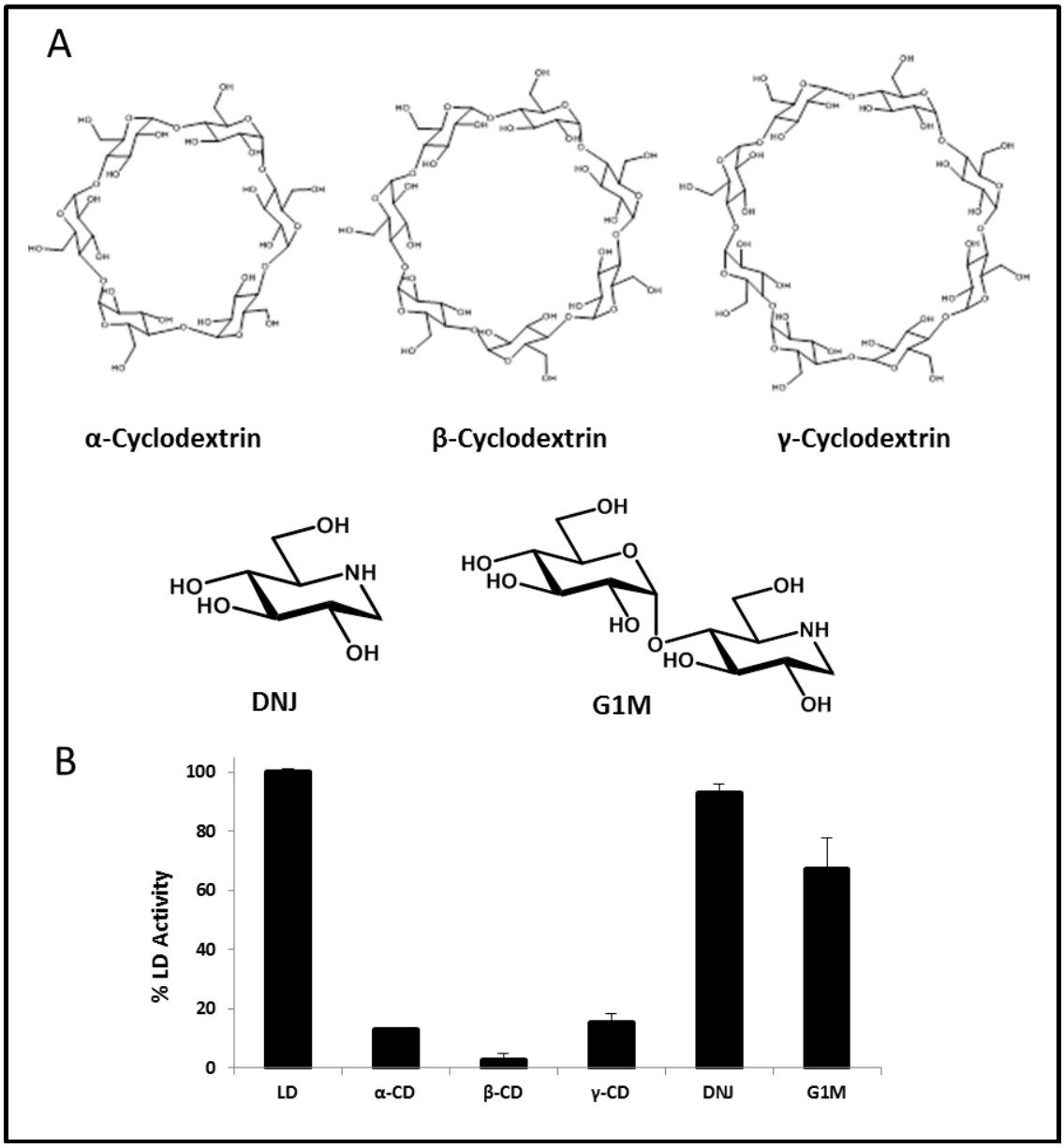

Figure 4.12 Percentage inhibition assay of limit dextrinase in the presence of cyclodextrins and iminosugars.

A. Structures of inhibitors used in the assay. **B.** All compounds tested at 1 mM. Assay was incubated at 30 °C for 30 min, 0.1 mg/mL pullulan, 4 nM recombinant LD. Reactions were monitored by BCA assay. Error bars show SEM calculated from three replicates.

4.3.2 Iminosugar Inhibitors have an Inhibitory Effect on Pullulanase and Limit Dextrinase Activity at High Concentrations

The iminosugars G1M and G2M were synthesised by enzymatic transglycosylation using DPE1 and DPE2 from Arabidopsis. (Latousakis, 2013, Tantanarat et al., 2014). These compounds were tested in a BCA assay for their ability to inhibit LD and *Klebsiella planticola* pullulanase (*Kp*PUL). LD and *Kp*PUL show similar patterns of inhibition, some differences arose due to the differences in specificity of each enzyme. At lower concentrations of inhibitor (0.001-0.1 mM) enzyme activity was high (above 60 %) (Figure 4.13). As the concentration of inhibitor increased enzyme inhibition became more pronounced, with G2M inhibiting LD and *Kp*PUL by 90 % and 95 %, respectively at 1 mM (Figure 4.13, B and C). β-CD shows inhibition one order of magnitude stronger than the iminosugars for LD whereas within the *Kp*PUL assay G2M and G1M are stronger inhibitors than β-CD.

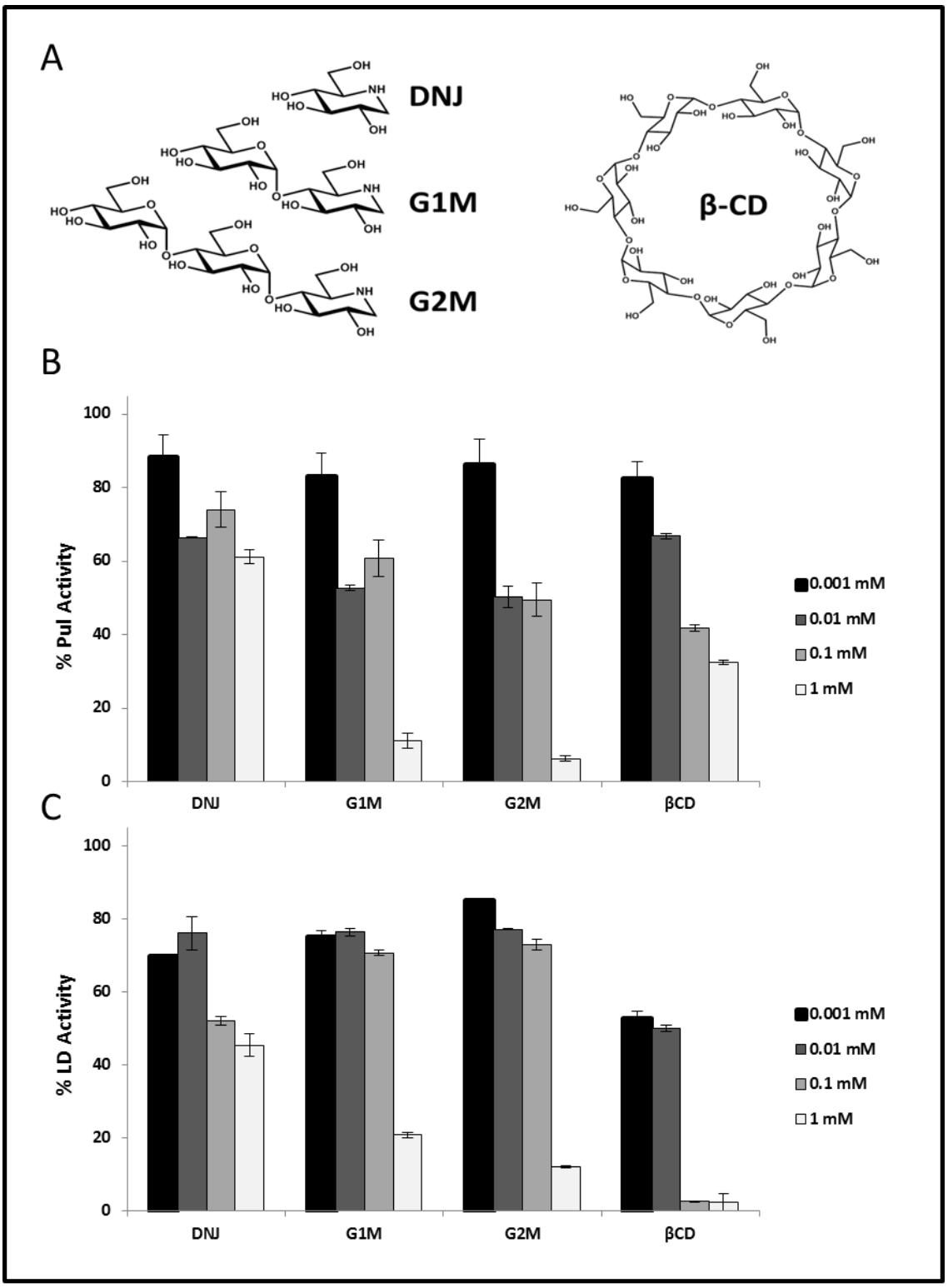

Figure 4.13 Inhibitory assay with pullulanase and limit dextrinase using iminosugars of different length.

A. Structures of the inhibitors tested in this assay. Assay performed with **B.** *Kp*PUL, 0.1 U. and **C.** LD, 4 nM. Assay reactions were incubated at 30 °C for 30 min, 0.1 mg/mL pullulan. Reaction was monitored by BCA assay. Error bars show SEM calculated from three replicates.

4.3.3 Peptide Amylase Inhibitor is able to Inhibit Limit Dextrinase Activity

The peptide based inhibitor (PAMI, sequence- GHWYYRCW-NH_2), discussed in the introduction, has previously been shown to inhibit mammalian and bacterial α-amylase. This peptide was tested for the ability to inhibit LD. PAMI produced an IC_{50} of around 250 µM (Figure 4.14), making this one of the strongest inhibitors of LD identified so far. The inhibition is within a similar (µM) range to the strongest known LD inhibitor, β-CD, however there is still a distinct two fold difference in their inhibitory ability (Figure 4.14).

The concentration of LD used in this assay was increased to 10 nM to help overcome issues caused by high background, caused by the reducing potential of the peptide backbone of PAMI, this explains the difference in the inhibitory ability of β-CD when compared to other assays.

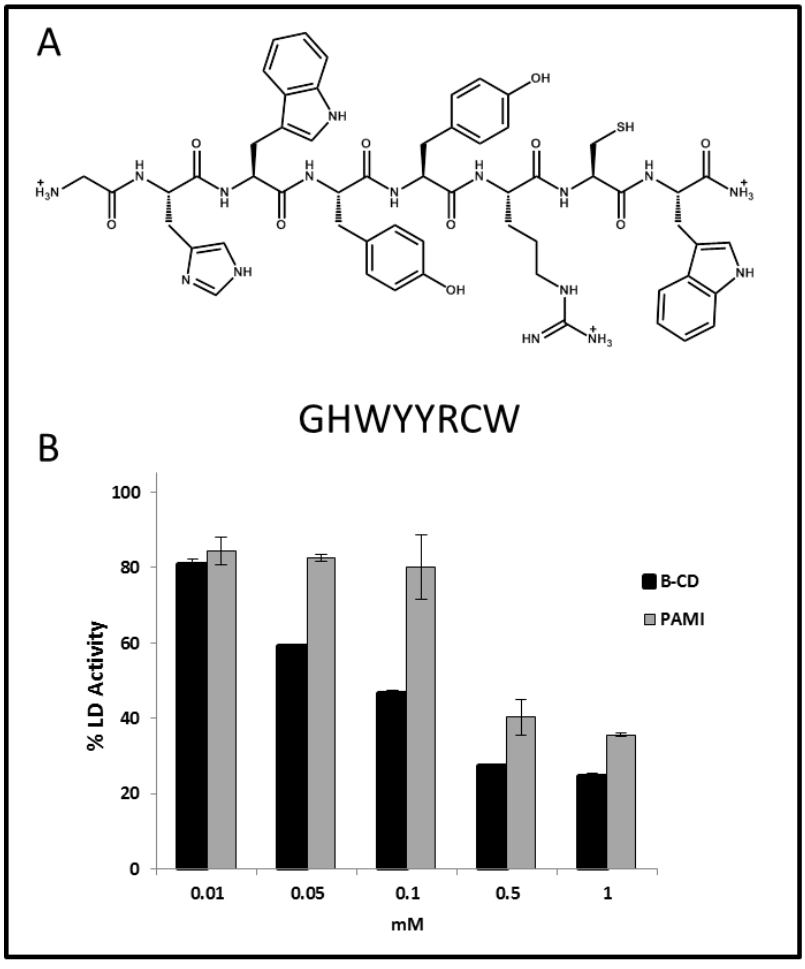

Figure 4.14 LD inhibitory assay comparing the effects of PAMI and β-CD
A. Structure pf PAMI inhibitor peptide. **B.** BCA assay was incubated at 30 °C for 30 min, 10 nM LD and 0.1 mg/mL pullulan. Reaction was monitored by BCA assay. Error bars show SEM calculated from three replicates.

4.3.4 Attempts to Crystallise Limit Dextrinase in Complex with PAMI

Attempts to obtain a crystal structure of LD in complex with PAMI were made with support from collaborators (Marie Møller, DTU). Crystals were formed by hanging drop vapour diffusion and soaked with 1 mM PAMI. Crystals were obtained and successfully diffracted to 4 Å resolution, however, due to problems with the collection of diffraction data, a full dataset could not be obtained.

4.3.5 Peptides Based on the Sequence of Limit Dextrinase Inhibitor show Partial Inhibitory Activity Against Limit Dextrinase

Prior to the publication of the LD/LDI complex crystal structure, data regarding the residues involved in the interaction was shared in the form of an interaction diagram (Figure 4.15, Figure 4.16) (Møller et al., 2015a). The interacting residues are highlighted within the entire protein structures in Figure 4.15. The information on the amino acid contacts was used to inform the design of peptide inhibitors of LD based on the structure of LDI. A patch of 12 amino acids (RGPSRPMLVKER, corresponding to residues 34-45 of the LDI crystal structure) within LDI was found to be responsible for almost half of the interactions with LD, these interactions were composed of a selection of ionic, hydrogen bonding and hydrophobic contacts (Figure 4.15). A dodecapeptide (LDI_{12}) based on this sequence was purchased, alongside hexameric (LDI6) synthetic truncations of the peptide covering residues 1-6, 4-9 and 7-12 of the dodecapeptide (Figure 4.17, A 1-5) (LDI_{1-6}, LDI_{4-9}, LDI_{7-12}). The hexameric truncations were generated in an attempt to infer which residues of the dodecapeptide may confer inhibitory activity. An L8W mutant was also generated (LDI_{4-9W}), the corresponding LDI (L42W) mutant for this was reported to have stronger binding to LD than wild type LDI (Marie Møller, personal communication).

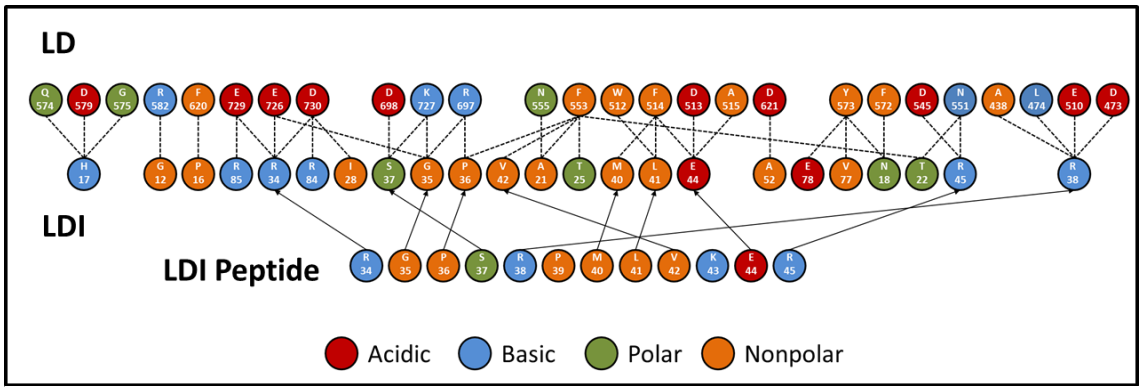

Figure 4.15 Map of the interactions within the limit dextrinase/limit dextrinase inhibitor complex.
LD and LDI complex interface contacts, including salt bridges, H bonds and hydrophobic contacts within 4.0 Å (dotted line). LDI peptide is also represented, corresponding amino acids are shown by arrows. There are 41 interactions in total. Numbering corresponds to that found in the crystal structure (Møller et al., 2015a).

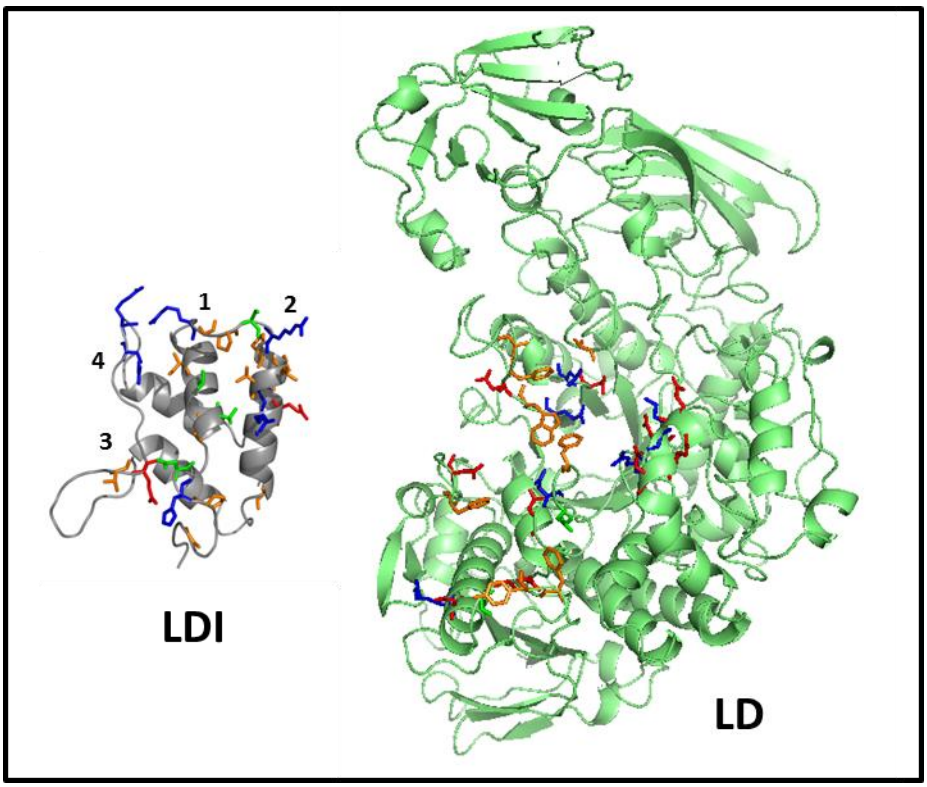

Figure 4.16 3-D structures of limit dextrinase and limit dextrinase inhibitor and the residues involved in their interaction.
Residues within a 4 Å distance were deemed as interacting. Amino acid side chain labelling: Red- Acidic. Blue- Basic. Green-polar. Orange- Nonpolar. Numbering represents the LDI helices in order from N to C terminus.

The peptide inhibitors were tested in a BCA assay and showed partial inhibition of LD (10-30 % inhibition) at 1 mM concentrations (Figure 4.17). RGPSRP (Figure 4.17, A 1) gives the strongest inhibition (30 %) of the five peptides. The dodecapeptide (Figure 4.17, A 5) gives 20 % inhibition. The tryptophan containing 'mutant' peptide gives stronger inhibition than the corresponding leucine containing compound, with a difference of 10 % (Figure 4.17, A 2 vs 4). None of the peptides gave inhibition comparable to PAMI and β-CD, which give 75 % and 80 % inhibition of LD, within this assay.

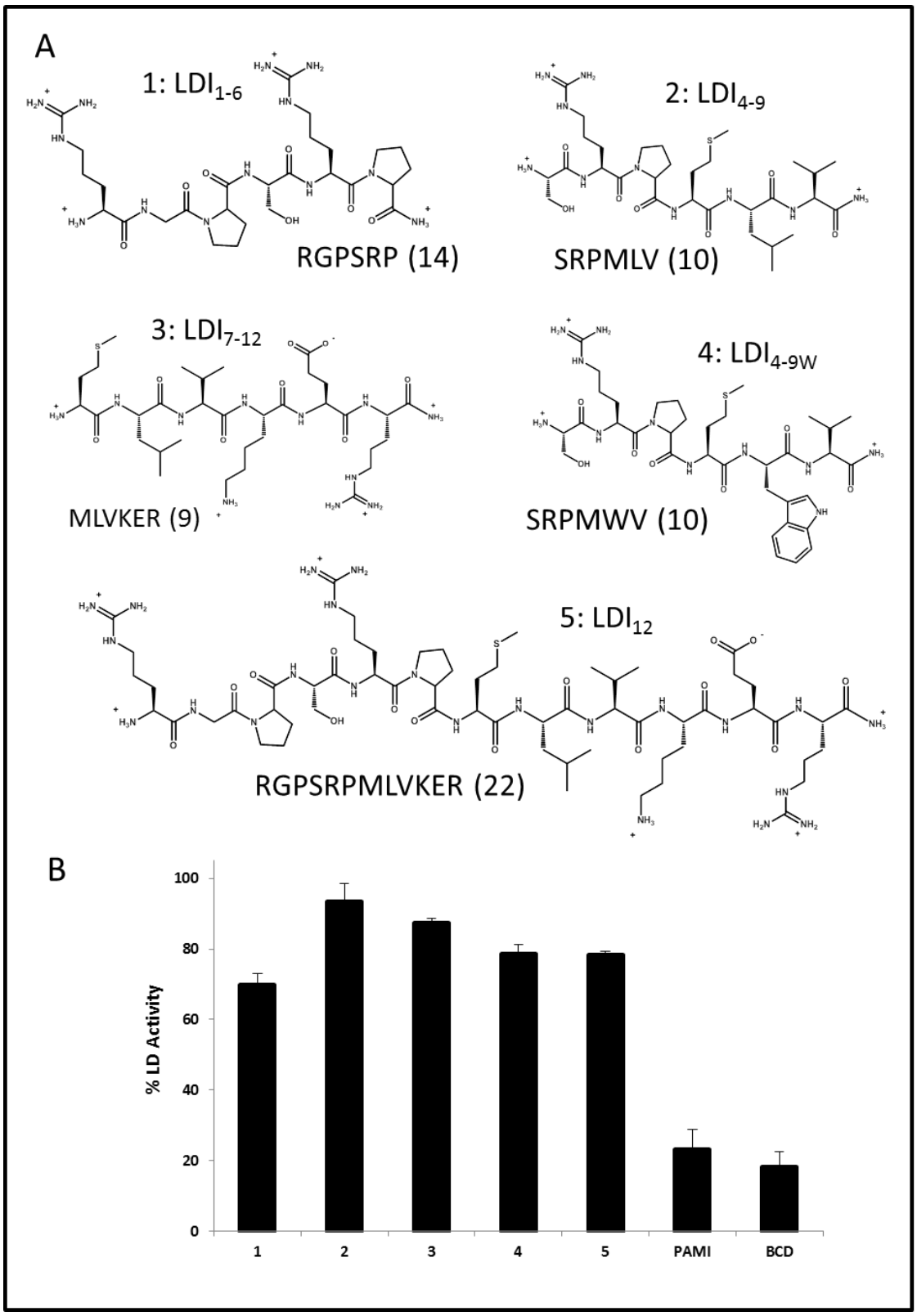

Figure 4.17 Limit dextrinase BCA activity assay in the presence of limit dextrinase inhibitor peptides. **A.** Structures of the LDI peptides. Numbers in brackets represent the number of interactions the peptide contributes to the binding of LDI to LD within the crystal structure. **B.** BCA assay of LD with LDI peptides, designed using the structure of LDI. Assay was incubated at 30 °C for 30 min, buffer 0.1 mg/mL pullulan, 4 nM LD. Inhibitors were at 1 mM. Reaction was monitored by BCA assay. Error bars show SEM calculated from three replicates.

4.3.6 Molecular Modelling Reveals that Peptide Inhibitors have a Flexible Structure

Previous work on peptide inhibitors of glycosyl hydrolases has revealed that secondary structure is important to the inhibitory activity of peptides (Etzkorn et al., 1994). Both PAMI and the LDI peptides show potential as inhibitors but may, however, not possess the optimal spatial orientation to bind LD with high affinity. The length of the inhibitors may be an important factor; longer peptides tend to form stable secondary structures, whereas small peptides are often of a more flexible nature (Huang and Nau, 2003). Secondary structure has implications in presenting amino acid side chains in the correct orientation to give optimal binding.

To assess their secondary structures, the sequences for PAMI and LDI peptides were analysed using peptide folding modelling software which generates the 5 best predicted structural models. An additional glycine residue was added to make the PAMI peptide a suitable length for secondary structure prediction, a minimum of 9 amino acids are required by the program. Of the 5 models generated for PAMI (Figure 4.18, A), only one has a secondary structural element, a short helix. It is likely that PAMI has a flexible loop like structure.

The LDI hexapeptides were too short to be modelled, the addition of three extra amino acids was considered too much of a deviation from the original short sequences. Two of the five predicted models for the LDI_{12} peptide have a helical structure (Figure 4.18, B), these two structures superimpose well. When the backbone of best model for LDI_{12} (Figure 4.18, green) is overlaid on the corresponding residues within the LDI crystal structure the short helix overlaps with the helix of LDI that interfaces with LD. However the helix of LDI_{12} extends beyond that of LDI by two amino acids this may lead to incorrect presentation of amino acid side chains and act to prevent optimal binding to LD. The other models generated have a much less defined structure, meaning there is a chance that LDI_{12} does not form a helix in solution.

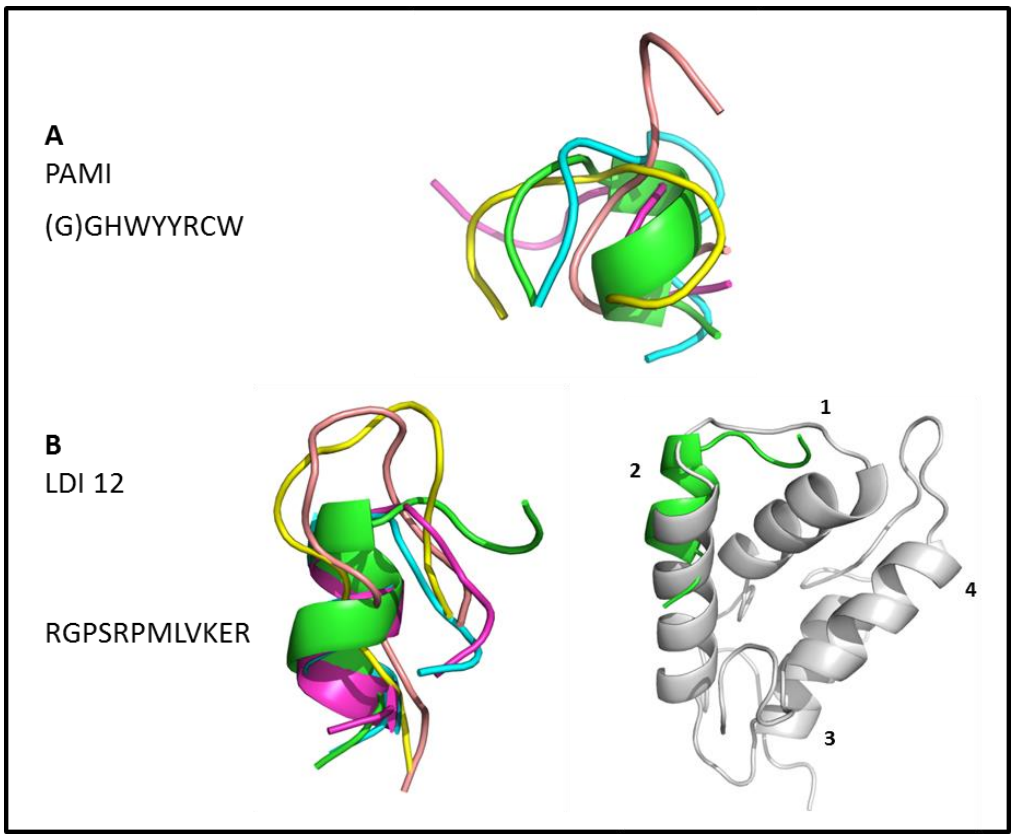

Figure 4.18 Molecular modelling of the 3-D structures of limit dextrinase inhibitor peptide and PAMI
A. PAMI, the 5 strongest molecular models superimposed. **B.** LDI12 peptide **Left,** the 5 strongest molecular models superimposed. **Right,** the best model superimposed on the corresponding residues of limit dextrinase inhibitor (PDB: 4CVW) RSMD= 4.516. Numbering represents the helices in order from N to C terminus.

4.3.7 Molecular Modelling Based on the Structure of Limit Dextrinase Inhibitor

The publication of the LD/LDI structure enabled further modelling studies. Using the LDI crystal structure as a guide, a number of peptides were designed and modelled to compare their predicted structure to that of LDI. A core helix dodecamer (LDI_{Helix}) and an extended helix ($LDI_{HelixEx}$) were first analysed. The extended helix peptide includes the LDI_{12} peptide that was previously tested (Figure 4.17) and shown to partially inhibit LD. The models generated for both peptides all contain helical structural elements with the best models overlapping neatly with the backbone of LDI (Figure 4.20, C and D).

The LDI crystal structure indicates that disulfide bonds are important linkers which hold the 4 helices of LDI in shape. There is potential that the disulfides can be used to generate truncated peptides that maintain the native conformation of LDI.

The sequence of LDI helixes 1 and 2, linked by a native disulfide, was first chosen as a potential peptide (LDI_{35C-C}). The models produced using this sequence, with disulfides linked, indicate a β-sheet type structure that has no similarity to the LDI structure (Figure 4.20, A). A non-disulfide linked variant of this sequence (LDI_{35}) was also modelled, this too had a β-sheet type structure and does not mimic the structure of LDI (Figure 4.20, B).

A larger disulfide linked peptide (LDI_{35C-C}) was designed to test the hypothesis that a second helix (helix 1, Figure 4.18) within LDI may be important for holding helix 2 in the correct conformation. The close proximity of two cystine residues within the LDI structure led to the design of a non-native disulfide linkage between Cys 2 and 6 (Figure 4.19). The models generated using this peptide all possess a two helical structure. The best of these models overlays extremely well with LDI. A non-disulfide linked variant (LDI_{35}) also overlays well with LDI but has a less rigid structure compared to the disulfide linked variant.

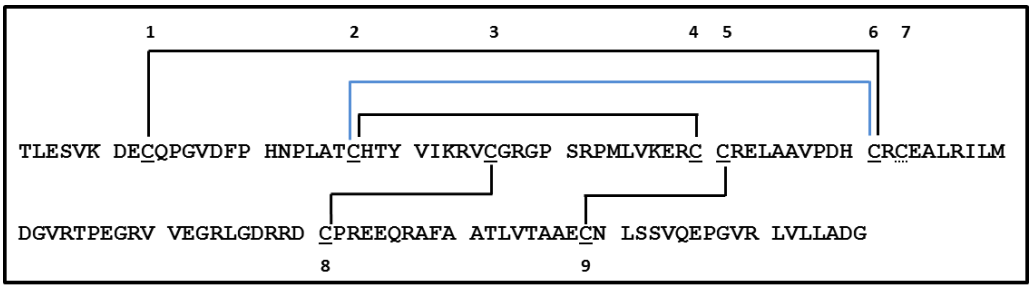

Figure 4.19 Cysteine and cystine residues present in barley limit dextrinase inhibitor.
Cystine disulfide bonds (solid underline) are formed between cys residues 1-6, 2-4, 3-8, 5-9. cysteine 7 (dashed underline) is found coupled to either a free cysteine or glutathione *via* a disulfide bond. The non-native, 2-6, disulfide used in the LDI_{35C-C} peptide is shown in blue.

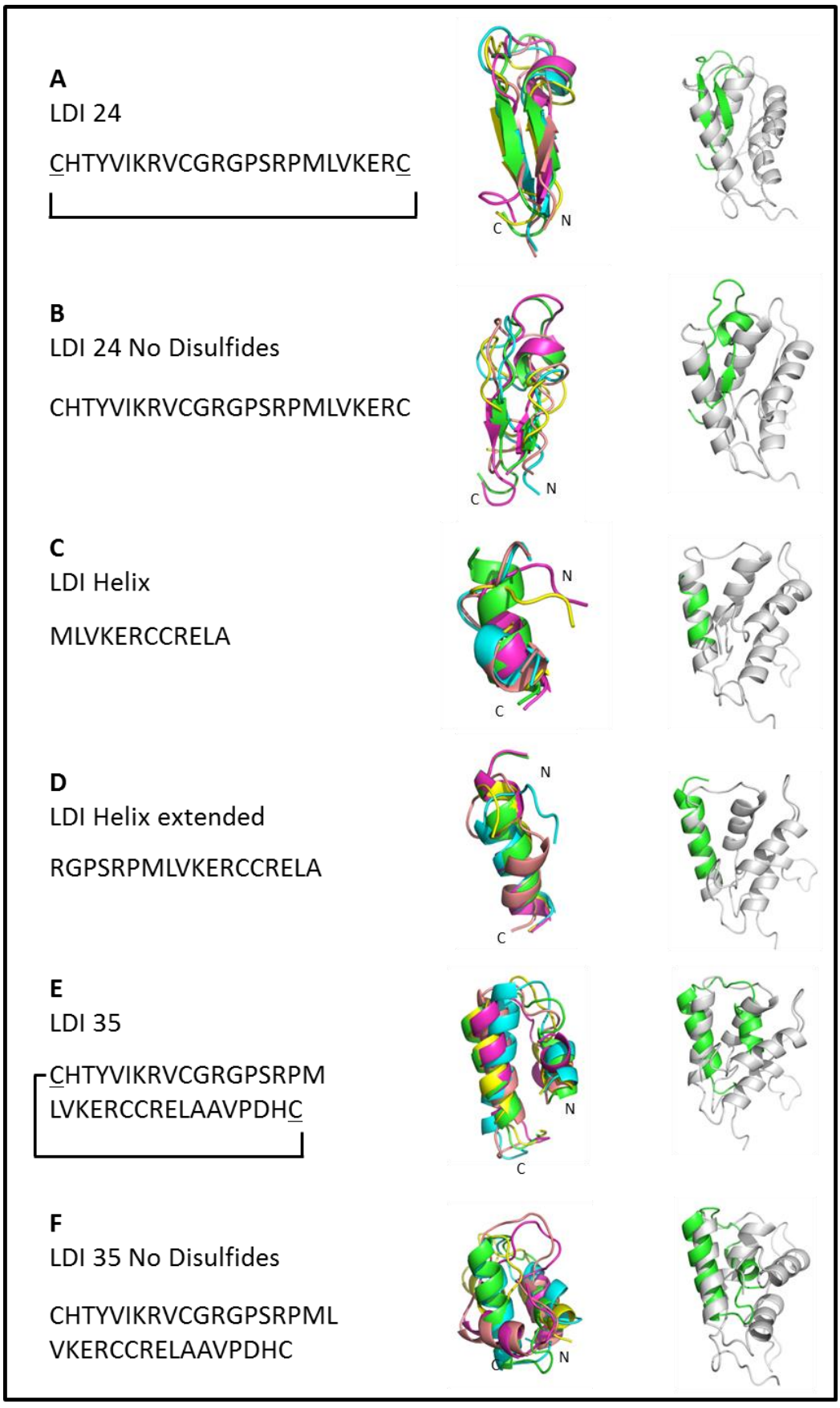

Figure 4.20 The sequences and 3-D structural models of potential limit dextrinase inhibitory peptides. **Left.** Sequence of peptides designed using the sequence of LDI. **Middle.** Overlay of the 5 strongest peptide models. **Right.** The structure of the best model superimposed with LDI. RSMD values: **A.** 7.146, **B.** 7.599, **C.** 0.553, **D.** 1.092, **E.** 6.638, **F.** 7.451.

4.4 Discussion

4.4.1 Inhibition of Limit Dextrinase by Iminosugars

Iminosugars inhibit numerous glycosyl hydrolases at low (pM to μM) concentration. These compounds have been utilised to gain a deeper fundamental understanding of this class of enzymes, as well as having established commercial application as therapeutic agents (Nash et al., 2011). No iminosugar type inhibitors have been developed against α-1,6-linked glucose acting enzymes from plants. This chapter outlines the first example of the strong inhibition of LD by an iminosugar.

Preliminary screens revealed that very few compounds within a library of synthetic and natural molecules, directed against starch active enzymes, appear able to inhibit LD at concentrations lower than 1 mM. DNJ, one of the compounds present in this library, showed no inhibitory activity towards LD, for instance. G1M, a glucosylated derivative of DNJ, however, showed potential as one of the only compounds capable of LD inhibition, albeit at a relatively high concentration of 1 mM. The inhibition of LD activity by G1M is likely indicative of binding to the active site as iminosugars act as transition state analogues; the imino group is protonated to form a structure that mimics an oxocarbenium ion. Within a crystal structure of barley β-amylase, G1M was bound at subsites -1 and -2 within the substrate binding site (Rejzek et al., 2011). LD is capable of performing transglycosylation reactions using a matlosyl fluoride donor and G1M as an acceptor to generate maltosyl-1,6-G1M this indicates likely binding at the +1, +2 subsites (Vester-Christensen, 2010). The precise binding site of G1M within the LD substrate binding site remains unclear.

The extension of G1M *via* transglycosylation, mediated by Arabidopsis disproportionating enzyme (DPE 1), generated G2M. G2M is a stronger inhibitor of LD than G1M, this higher level of inhibition is likely due to the presence of an extra glycosyl moiety which increases the number of potential interactions that can form between inhibitor and enzyme. As with G1M, it is likely that G2M binds within the substrate binding site thus blocking substrate binding. There is potential for binding in the -1 to -3 or +1 to +3 subsites (Figure 4.21).

G2M gives stronger LD inhibition than seen with any other iminosugar, associated with the observation that maltodextrins of higher DP are more effective inhibitors of LD (Dunn and Manners 1975). The increase in inhibition by increasing iminosugar length, as seen within this study, confirms this observation and supports the proposal that LD has a binding preference

for fragments of four/five glucose units in length (Manners and Yellowlees, 1971). Crystal structures of LD bound to maltotetraose have been solved confirming that molecules of these sizes can fit in the active site of LD (Møller et al., 2015b). Crystal soaks with different concentrations of maltotetraose revealed both high and low affinity sites binding sites, at a low concentration (25 mM), maltotetraose is seen in the main chain binding subsites (0', +1, +2, +3) Figure 4.21. Wereas at high concentration (300 mM) glucose residues can also be fitted in to density seen within the branch chain binding site (-2, -3, -4) (Møller et al., 2015b). It is therefore likely that G2M binds within the main chain binding site at the concentrations used within this study.

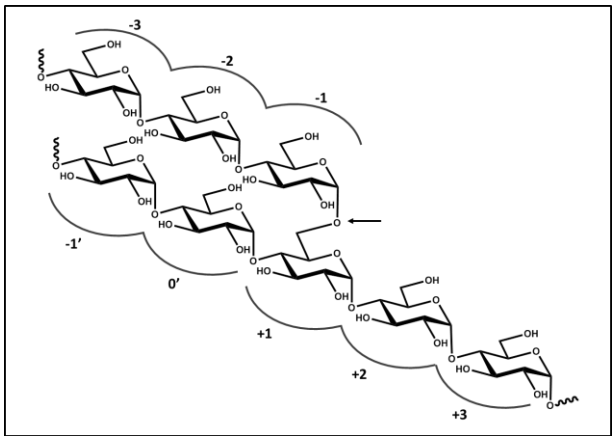

Figure 4.21 The sub-site numbering of the limit dextrinase binding cleft.
The hydrolysed bond is indicated by an arrow. Numbering follows the rules set out by (Davies et al., 1997). The non-main chain (side chain) is identified by (').

LD catalyses both transglycosylation alongside hydrolysis, as is identified by the generation of higher Mw products when maltotriosyl-APTS is incubated with LD in the presence of pullulan (Mcdougall et al., 2004). There is therefore potential for transglycosylation to mask true inhibition values by transferring an inhibitor onto to other glucans, this activity can also interfere with the release of reducing ends that are measured in the BCA assay used herein.

β-CD was used as a positive control throughout the assays reported herein and remains one of the strongest identified LD inhibitors. The crystal structure of LD in complex with α and β-cyclodextrin revealed these molecules bind at the +1 and +2 sub-sites (Vester-Christensen et al., 2010a). Cyclodextrins are proposed to mimic the structure of an α-glucan helix (Vester-Christensen et al., 2010a). It is not fully understood how the intricate differences between α, β γ CDs relate to LD binding preferences. The differences in β-CD inhibition level between LD and PUL arise because of differences within the enzymes active sites (Manners and Yellowlees, 1971).

4.4.2 Inhibition of Limit Dextrinase by PAMI

Peptide amylase inhibitor (PAMI) is a good general inhibitor of a number of glycosyl hydrolases within CAZy database family GH13, it has also been shown herein to be a good inhibitor of LD. Analysis of the PAMI inhibition of α-amylase showed a non-competitive mode of inhibition which suggests that some of the active site is blocked by the molecule (Doleckova-Maresova et al., 2005). Hydrophobic interactions, aromatic stacking and ionic/polar interactions were also important for the binding. A similar combination of interactions may be involved in the inhibition of LD. LD belongs to the same CAZy family (GH13) as α-amylase and shares some structural similarities, including acidic catalytic residues. The arginine residue of PAMI may be important for interacting with these amino acids, as is seen with barley amylase-subtilisin inhibitor (BASI) in complex with α-amylase (Abe et al., 1993) and LDI in complex with LD (Møller et al., 2015a). Hydrophobic residues (WYF) are also implicated as being important between peptide inhibitors and their targets, these residues are seen in high levels in numerous peptide based amylase inhibitors (Etzkorn et al., 1994, Wong et al., 1999, Heyl et al., 2005, Ochiai et al., 2012).

The molecular modelling reported herein indicates PAMI has a flexible structure, how the structure of this peptide relates to binding is unknown. The generation of a crystal structure with PAMI bound to LD could have answered some of these questions, crystallography was attempted, however, during the collection of diffraction data the crystal collapsed and the quality decreased beyond use.

4.4.3 Inhibition of Limit Dextrinase by Peptides Based on the Sequence of Limit Dextrinase Inhibitor

Peptides designed based on the LDI sequence were generated without knowledge of the LDI 3-D structure, only details on the amino acid interactions were available at the time. As such, peptides containing the amino acids contributing highest number of interactions were chosen for analysis. Of the 5 peptides generated, LDI_{1-6} gives the highest inhibition. This peptide contains two arginine residues which account for 7 interactions with the residues of LD, including the catalytic acid residues, within the LD/LDI crystal strucutre. The three other hexameric peptides give weaker inhibition of LD, these peptides have a higher proportion of residues involved in LDI helix 2, and may potentially contain a small helix which could cause incorrect presentation of an arginine residue. The LDI hexapeptides are too short to model, however, alpha helical conformations have been seen in other peptides of this length (Esteve et al., 2001).

The mutation of LDI residues L41D and V42D causes an almost 500,000 fold decrease in LD binding affinity, determined using SPR (Møller et al., 2015a), is not clear that these residues are important in the peptides used in this study. The peptide based on an LDI L42W mutant ($LDI_{4\text{-}9W}$) has slightly stronger inhibitory activity, which would be expected given that the corresponding LDI mutant binds to LD with higher affinity than the wild type (Marie Møller, personal communication).

The LDI_{12} peptide would be expected to give stronger inhibition than the hexamers due to the presence of more interacting residues, however, this is not the case. A possible reason for the weaker inhibitory ability of LDI_{12} compared to $LDI_{1\text{-}6}$ may be that the larger peptide forms a secondary structure which hinders binding. To test this hypothesis the structure of LDI_{12} was modelled which revealed a potential helical element that was seen to extend beyond helix 2 of LDI when overlaid (Figure 4.18). The extension of the helix may place residues important for the interaction with LD in an incorrect orientation.

4.4.4 Molecular Modelling for the Design of Potential Peptide Inhibitors of Limit Dextrinase

The publication of the LDI structure in complex with LD enabled better design of potential inhibitors using molecular modelling. The majority of the interacting residues of LDI lie within helix 2 and the loop linking this and helix 1 (Figure 4.16), this is the region on which LDI_{12} was based.

It was believed that the precise helical nature of LDI is important to achieve correct presentation of the amino acids required for interaction with LD. To analyse this, a peptide including the residues of helix 2 was modelled (LDI_{Helix}), an extended version of this peptide was also analysed ($LDI_{HelixEx}$). The short helix formed an almost perfect match with the LDI structure whereas the extended helix shows extension beyond that of LDI, as seen within the LDI_{12} peptide.

From analysis of the LDI structure it can be proposed that helix 1 is important for ensuring the correct residue presentation of helix 2 and acts to break the helix at the correct point. Helix 1 and 2 are linked by a disulfide bond between cysteine residues number 2 and 4; the LDI sequence between these two residues, when modelled, generates a β-sheet structure with ($LDI_{24C\text{-}C}$) (Figure 4.20) or without a disulfide (LDI_{24}) (Figure 4.20). This indicates that other

elements (other helices or disulfides) are important in maintaining the correct conformation of LDI helices 1 and 2.

Due to the observed close proximity of cysteine residues number 2 and 6, a peptide containing a non-native disulfide bond was designed ($LDI_{35C\text{-}C}$) (Figure 4.20). The model generated from this sequence had a high similarity to LDI structure, with a break in helix 2 at the correct point. This indicates the use of non-native disulfides may be a novel way to generate a suitable LDI mimic. Modelling of the same peptide without disulfide bonds (LDI_{35}) indicates the non-native disulfide may be a way to decrease flexibility and force the peptide to form two helices. A more rigid, disulfide linked, molecule avoids loss of conformation entropy upon binding and may generate a better inhibitor (Dekker et al., 2003). These peptide models represent the starting point of a rational design process to create a high affinity peptide based inhibitor.

4.4.5 The Potential of the Inhibitors *In Planta*

The potential of compounds from this chapter to affect plant growth was tested using barley, Arabidopsis or tef. Due to the high concentration, and therefore high quantities, required for inhibition there was insufficient G2M to test on plants. G1M was previously tested on barely and showed inhibition of endosperm starch metabolism alongside α-glucosidase inhibition (Stanley et al., 2011). Interestingly, no inhibition of root or shoot growth occurred, as seen with DNJ. The reasons for this are unclear, however, G1M may not be capable of inhibiting the target(s) of DNJ responsible for stunted root growth by virtue of its *in situ* hydrolysis, thus releasing DNJ (Field group, unpublished data).

When tested on barley, Arabidopsis and tef, the peptides, $LDI_{1\text{-}6}$, $LDI_{4\text{-}9}$, $LDI_{7\text{-}12}$, $LDI_{4\text{-}9W}$ and LDI_{12} showed no effect on growth (Data not shown). This is likely due to degradation by proteases or inability to reach the correct cellular concentration or location to be effective. Peptides have been shown to be able to penetrate tissues within mammalian systems (Futaki et al., 2007) If the peptides were to reach and inhibit LD it is questionable as to whether a visible growth phenotype would be generated (discussed further in Chapter 6).

α-, β- and γ-cyclodextrins were tested for their ability to affect barley germination, when applied at concentrations above 100 µM the cyclodextrins had a distinct effect on grain germination and seedling growth (data not shown). This is proposed to be due to interference with hormone metabolism and signalling, cyclodextrins are known to complex hydrophobic

molecules within their hydrophobic core (Szejtli, 1983, Salminen et al., 1990, Del Valle, 2004). The impact on hormone metabolism can have many downstream effects, the precise mechanism of action is unclear and would require much work to clarify. It is possible cyclodextrins are able to enter the endosperm and impact directly on the enzymes involved in starch metabolism however this is masked by the interference with hormone metabolism which is required for the correct activation and release of these enzymes (discussed in Chapter 6).

4.5 Future Directions

4.5.1 Further Analysis of the Interactions between Inhibitors and Limit Dextrinase

Further characterisation of the inhibitors outlined within this chapter could be achieved by biochemical analysis of their interactions with LD by methods such as isothermal titration calorimetry (ITC) and surface plasmon resonance (SPR), which yield precise details on binding affinity. Detailed kinetic assays could be performed to generate Michaelis-Menten, Lineweaver-Burk or similar plots to determine the mode of action as competitive, uncompetitive or non-competitive. Structural analyses, including crystallography, could also be employed to determine how these molecules interact. The majority of these experiments are dependent on having sufficient quantities of recombinant LD, as outlined in Chapter 5.

4.5.2 The Identification of Other Iminosugar Inhibitors of Limit Dextrinase

Only a small proportion of the existing iminosugars have been screened against LD. Due to the large diversity of existing compounds there is scope that high throughput screening (HTS) of existing compound libraries could identify a strong, nanomolar Kd, inhibitor. The Overkleeft library (Chapter 3) is one potential library, though many other synthetic chemical and natural product libraries exist. Furthermore there are a number of avenues by which novel iminosugars can be generated, for example the transglycosylation mediated extension. Recent generation of a new assay for LD which utilises a soluble chromophoric substrate, specific for LD, enables convenient HTS of compounds against LD (Mangan et al., 2015).

4.5.3 Screening of Peptide Libraries against Limit Dextrinase

Peptide libraries offer the opportunity to screen a large number of compounds for binding or inhibitory activity. The display of random peptide libraries on bacteriophage (phage display) is one method to access large numbers of peptides (Matsubara, 2012). Peptide ligands that bind to pancreatic alpha-amylase were isolated from libraries displaying random 15-mer peptides. The lead peptide from this screen (TRWLVYFSRPYLVAT) bound barley alpha-amylase with a 4.4

μM affinity (Wong et al., 1998, Wong et al., 1999), a similar approach could be applied to LD. The other approach to generating a peptide library involves iterative rounds of combinatorial synthetic chemistry and screening, these are the methods by which PAMI was generated (Doleckova-Maresova et al., 2005). Peptide arrays offer similar opportunities with the benefit of the peptides being synthesised immobilised to a plate, making high throughput analysis convenient (Min and Mrksich, 2004). There is also scope for further rational design of peptides using *in silico* methods such as molecular docking (Li et al., 2014, Kurcinski et al., 2015).

4.6 References

Abe, J., Sidenius, U. & Svensson, B. 1993. Arginine is essential for the alpha-amylase inhibitory activity of the alpha-amylase/subtilisin inhibitor (basi) from barley seeds. *Biochemical Journal,* 293 (Pt 1), 151-5.

Alam, N., Gourinath, S., Dey, S., Srinivasan, A. & Singh, T. P. 2001. Substrate-inhibitor interactions in the kinetics of alpha-amylase inhibition by ragi alpha-amylase/trypsin inhibitor (rati) and its various N-terminal fragments. *Biochemistry,* 40, 4229-33.

Bøjstrup, M., Christensen, C. E., Windahl, M. S., Henriksen, A. & Hindsgaul, O. 2014. A chromogenic assay for limit dextrinase and pullulanase activity. *Analytical Biochemistry,* 449, 45-51.

Bøjstrup, M., Windahl, M. S., Johannesen, S. A., Henriksen, A. & Hindsgaul, O. 2012. A fluorescence resonance energy transfer (fret) based assay for the starch debranching enzyme limit dextrinase. Unpublished

Davies, G. J., Wilson, K. S. & Henrissat, B. 1997. Nomenclature for sugar-binding subsites in glycosyl hydrolases. *Biochemical Journal,* 321, 557-559.

Dekker, F. J., De Mol, N. J., Bultinck, P., Kemmink, J., Hilbers, H. W. & Liskamp, R. M. J. 2003. Role of solution conformation and flexibility of short peptide ligands that bind to the p56lck sh2 domain. *Bioorganic & Medicinal Chemistry,* 11, 941-949.

Del Valle, E. M. M. 2004. Cyclodextrins and their uses: A review. *Process Biochemistry,* 39, 1033-1046.

Deshpande, B. S., Ambedkar, S. S. & Shewale, J. G. 1988. Biologically active secondary metabolites from streptomyces. *Enzyme and Microbial Technology,* 10, 455-473.

Doleckova-Maresova, L., Pavlik, M., Horn, M. & Mares, M. 2005. De novo design of alpha-amylase inhibitor: A small linear mimetic of macromolecular proteinaceous ligands. *Chemistry and Biology,* 12, 1349-57.

Doner, L. W. & Irwin, P. L. 1992. Assay of reducing end-groups in oligosaccharide homologues with 2,2'-bicinchoninate. *Analytical Biochemistry,* 202, 50-3.

Esteve, V., Blondelle, S., Celda, B. & Perez-Paya, E. 2001. Stabilization of an alpha-helical conformation in an isolated hexapeptide inhibitor of calmodulin. *Biopolymers,* 59, 467-76.

Etzkorn, F. A., Guo, T., Lipton, M. A., Goldberg, S. D. & Bartlett, P. A. 1994. Cyclic hexapeptides and chimeric peptides as mimics of tendamistat. *Journal of the American Chemical Society,* 116, 10412-10425.

Franco, O. L., Rigden, D. J., Melo, F. R. & Grossi-De-Sa, M. F. 2002. Plant alpha-amylase inhibitors and their interaction with insect alpha-amylases. *European Journal of Biochemistry,* 269, 397-412.

Furegon, L., Curioni, A. & Peruffo, A. D. 1994. Direct detection of pullulanase activity in electrophoretic polyacrylamide gels. *Analytical Biochemistry,* 221, 200-1.

Futaki, S., Nakase, I., Tadokoro, A., Takeuchi, T., Jones, A.T. 2007. Arginine-rich peptides and their internalization mechanisms. *Biochem Society Transactions*, 35, 784-787.

Geng, P., Qiu, F., Zhu, Y. & Bai, G. 2008. Four acarviosin-containing oligosaccharides identified from streptomyces coelicoflavus zg0656 are potent inhibitors of α-amylase. *Carbohydrate Research,* 343, 882-892.

Gloster, T. M. & Davies, G. J. 2010. Glycosidase inhibition: Assessing mimicry of the transition state. *Organic & Biomolecular Chemistry,* 8, 305-320.

Green, F., 3rd, Clausen, C. A. & Highley, T. L. 1989. Adaptation of the nelson-somogyi reducing-sugar assay to a microassay using microtiter plates. *Analytical Biochemistry,* 182, 197-9.

Greffe, L., Jensen, M. T., Chang-Pi-Hin, F., Fruchard, S., O'Donohue, M. J., Svensson, B. & Driguez, H. 2002. Chemoenzymatic syntheses of linear and branched hemithiomaltodextrins as potential inhibitors for starch-debranching enzymes. *Chemistry,* 8, 5447-55.

Gusakov, A. V., Kondratyeva, G. & Sinitsyn, A. P. 2011. Comparison of two methods for assaying reducing sugars in the determination of carbohydrase activities. *International Journal of Analytical Chemistry*.

Heyl, D. L., Tobwala, S., Lucas, L. S., Nandanie, A. D., Himm, R. W., Kappler, H. J., Blaney, E. J., Groom, J., Asbill, J., Nzoma, J. K., Jarosz, C., Palamma, H. & Schullery, S. E. 2005. Peptide inhibitors of alpha-amylase based on tendamistat: Development of analogues with omega-amino acids linking critical binding segments. *Protein & Peptide Letters,* 12, 275-80.

Huang, F. & Nau, W. M. 2003. A conformational flexibility scale for amino acids in peptides. *Angewandte Chemie International Edition,* 42, 2269-2272.

Isoda, Y., Asanami, S., Takeo, K. I. & Nitta, Y. 1987. Attempt at affinity labeling of. Alpha.-and. Beta.-amylases by. Alpha.-and. Beta.-d-glucopyranosides and. Alpha.-and. Beta.-maltooligosaccharides with 2, 3-epoxypropyl residue as aglycone: Specific inactivation of. Beta.-amylases. *Agricultural and Biological Chemistry,* 51, 3223-3229.

Jayaraj, S., Suresh, S. & Kadeppagari, R.-K. 2013. Amylase inhibitors and their biomedical applications. *Starch - Stärke,* 65, 535-542.

Kadziola, A., Sogaard, M., Svensson, B. & Haser, R. 1998. Molecular structure of a barley alpha-amylase-inhibitor complex: Implications for starch binding and catalysis. *Journal of Molecular Biology,* 278, 205-17.

Kurcinski, M., Jamroz, M., Blaszczyk, M., Kolinski, A. & Kmiecik, S. 2015. Cabs-dock web server for the flexible docking of peptides to proteins without prior knowledge of the binding site. *Nucleic Acids Research,* 43, W419-W424.

Li, H., Lu, L., Chen, R., Quan, L., Xia, X. & Lü, Q. 2014. Paflexpepdock: Parallel ab-initio docking of peptides onto their receptors with full flexibility based on rosetta. *PLoS ONE,* 9, e94769.

Li, Y., Huang, Q., Zhang, S., Liu, S., Chi, C. & Tang, Y. 1994. Studies on an artificial trypsin inhibitor peptide derived from the mung bean trypsin inhibitor: Chemical synthesis, refolding, and crystallographic analysis of its complex with trypsin. *The Journal of Biological Chemistry,* 116, 18-25.

Machius, M., Vertesy, L., Huber, R. & Wiegand, G. 1996. Carbohydrate and protein-based inhibitors of porcine pancreatic alpha-amylase: Structure analysis and comparison of their binding characteristics. *Journal of Molecular Biology,* 260, 409-21.

Mangan, D., Mccleary, B. V., Cornaggia, C., Ivory, R., Rooney, E. & Mckie, V. 2015. Colourimetric and fluorimetric substrates for the assay of limit dextrinase. *Journal of Cereal Science,* 62, 50-57.

Manners, D. & Rowe, K. L. 1971. Studies on carbohydrate-metabolizing enzymes part xxv. The debranching enzyme system in germinated barley. *Journal of the Institute of Brewing,* 77, 358-365.

Manners, D. J. & Yellowlees, D. 1971. Studies on carbohydrate metabolising enzymes. Part xxvi. The limit dextrinase from germinated barley. *Starch - Stärke,* 23, 228-234.

Matsubara, T. 2012. Potential of peptides as inhibitors and mimotopes: Selection of carbohydrate-mimetic peptides from phage display libraries. *Journal of Nucleic Acids,* 2012, 740982.

Mccleary, B. V. 1992. Measurement of the content of limit-dextrinase in cereal flours. *Carbohydrate Research,* 227, 257-268.

Mccleary, B. V., Mangan, D., Mckie, V., Cornaggia, C., Ivory, R. & Rooney, E. 2014. Colourimetric and fluorometric substrates for measurement of pullulanase activity. *Carbohydrate Research,* 393, 60-9.

Mcdougall, G. J., Ross, H. A., Swanston, J. S. & Davies, H. V. 2004. Limit dextrinase from germinating barley has endotransglycosylase activity, which explains its activation by maltodextrins. *Planta,* 218, 542-51.

Min, D. H. & Mrksich, M. 2004. Peptide arrays: Towards routine implementation. *Current Opinions in Chemical Biology,* 8, 554-8.

Møller, M. S., Vester-Christensen, M. B., Jensen, J. M., Abou Hachem, M., Henriksen, A. & Svensson, B. 2015a. Crystal structure of barley limit dextrinase:Limit dextrinase inhibitor (ld:Ldi) complex reveals insights into mechanism and diversity of cereal-type inhibitors. *The Journal of Biological Chemistry*.

Møller, M. S., Windahl, M. S., Sim, L., Bojstrup, M., Abou Hachem, M., Hindsgaul, O., Palcic, M., Svensson, B. & Henriksen, A. 2015b. Oligosaccharide and substrate binding in the starch debranching enzyme barley limit dextrinase. *Journal of Molecular Biology,* 427, 1263-77.

Mori, H., Bak-Jensen, K. S., Gottschalk, T. E., Motawia, M. S., Damager, I., Møller, B. L. & Svensson, B. 2001. Modulation of activity and substrate binding modes by mutation of single and double subsites +1/+2 and -5/-6 of barley alpha-amylase 1. *European Journal of Biochemistry,* 268, 6545-58.

Müller, L., Junge, B., Frommer, W., Schmidt, D. & Truscheit, E. 1980. Acarbose (bay g 5421) and homologous α-glucosidase inhibitors from actinoplanaceae. *Enzyme inhibitors. Verlag Chemie, Weinheim*, 109-122.

Nash, R. J., Kato, A., Yu, C. Y. & Fleet, G. W. 2011. Iminosugars as therapeutic agents: Recent advances and promising trends. *Future Medicinal Chemistry,* 3, 1513-21.

Ochiai, T., Sugita, T., Kato, R., Okochi, M. & Honda, H. 2012. Screening of an alpha-amylase inhibitor peptide by photolinker-peptide array. *Biosci Biotechnol Biochem,* 76, 819-24.

Rejzek, M., Stevenson, C. E., Southard, A. M., Stanley, D., Denyer, K., Smith, A. M., Naldrett, M. J., Lawson, D. M. & Field, R. A. 2011. Chemical genetics and cereal starch metabolism: Structural basis of the non-covalent and covalent inhibition of barley beta-amylase. *Molecular Biosystems,* 7, 718-30.

Salminen, L., Uosukainen, M., Mattsson, P. & Korpela, T. 1990. Action of cyclodextrins on germinating seeds and on micropropagated plants. *Starch - Stärke,* 42, 350-353.

Schwientek, P., Szczepanowski, R., Ruckert, C., Kalinowski, J., Klein, A., Selber, K., Wehmeier, U. F., Stoye, J. & Puhler, A. 2012. The complete genome sequence of the acarbose producer actinoplanes sp. Se50/110. *BMC Genomics,* 13, 112.

Stanley, D., Rejzek, M., Naested, H., Smedley, M., Otero, S., Fahy, B., Thorpe, F., Nash, R. J., Harwood, W., Svensson, B., Denyer, K., Field, R. A. & Smith, A. M. 2011. The role of alpha-glucosidase in germinating barley grains. *Plant Physiology,* 155, 932-43.

Svensson, B., Fukuda, K., Nielsen, P. K. & Bonsager, B. C. 2004. Proteinaceous alpha-amylase inhibitors. *Biochimica et Biophysica Acta,* 1696, 145-56.

Szejtli, J. 1983. Physiological effects of cyclodextrins on plants. *Starch - Stärke,* 35, 433-438.

Tarling, C. A., Woods, K., Zhang, R., Brastianos, H. C., Brayer, G. D., Andersen, R. J. & Withers, S. G. 2008. The search for novel human pancreatic alpha-amylase inhibitors: High-throughput screening of terrestrial and marine natural product extracts. *Chembiochem,* 9, 433-8.

Vester-Christensen, M. B. 2010. *Glycoside hydrolase family 31. Functional analysis and biotechnological development*, PhD Thesis. Technical University of Denmark (DTU).

Vester-Christensen, M. B., Abou Hachem, M., Svensson, B. & Henriksen, A. 2010a. Crystal structure of an essential enzyme in seed starch degradation: Barley limit dextrinase in complex with cyclodextrins. *Journal of Molecular Biology,* 403, 739-50.

Vester-Christensen, M. B., Hachem, M. A., Naested, H. & Svensson, B. 2010b. Secretory expression of functional barley limit dextrinase by pichia pastoris using high cell-density fermentation. *Protein Expression and Purification,* 69, 112-9.

Wiegand, G., Epp, O. & Huber, R. 1995. The crystal structure of porcine pancreatic alpha-amylase in complex with the microbial inhibitor tendamistat. *Journal of Molecular Biology,* 247, 99-110.

Williams, L. K., Zhang, X., Caner, S., Tysoe, C., Nguyen, N. T., Wicki, J., Williams, D. E., Coleman, J., Mcneill, J. H., Yuen, V., Andersen, R. J., Withers, S. G. & Brayer, G. D. 2015. The amylase inhibitor montbretin a reveals a new glycosidase inhibition motif. *Nature Chemical Biology,* advance online publication.

Wong, D., Robertson, G., Tillin, S. & Wong, C. 1998. Identifying peptide ligands for barley α-amylase 1 using combinatorial phage display libraries. *Journal of Agricultural and Food Chemistry,* 46, 3852-3857.

Wong, D. W. S., Robertson, G. H., Tillin, S. J. & Wong, C. 1999. Phage-displayed peptide ligands for pancreatic α-amylase cross-react with barley α-amylase. *Journal of Agricultural and Food Chemistry,* 47, 3934-3937.

Wood, I. P., Elliston, A., Ryden, P., Bancroft, I., Roberts, I. N. & Waldron, K. W. 2012. Rapid quantification of reducing sugars in biomass hydrolysates: Improving the speed and precision of the dinitrosalicylic acid assay. *Biomass and Bioenergy,* 44, 117-121.

Yoon, S.-H. & Robyt, J. F. 2003. Study of the inhibition of four alpha amylases by acarbose and its 4iv-α-maltohexaosyl and 4iv-α-maltododecaosyl analogues. *Carbohydrate Research,* 338, 1969-1980.

Chapter 5- Cloning, Heterologous Expression and Purification of Barley Limit Dextrinase and Limit Dextrinase Inhibitor

5.1 Introduction

5.1.1 Limit Dextrinase

Limit dextrinase (LD), also known as plant pullulanase, has been implicated as the sole enzyme responsible for the debranching of starch during grain germination i.e. isoamylase is not involved (Burton et al., 1999). LD acts to cleave the α-1,6-glucosidic linkages present in α- and β-limit dextrins derived by the activities of the other starch catabolising glycoside hydrolases. LD has only a low activity towards amylopectin (Manners and Yellowlees, 1971) and therefore requires the hydrolysis of starch *via* the concerted action of α-amylase and β-amylase to produce smaller soluble and branched glucans that are capable of serving as a substrate. As well as functioning during germination, LD has also been shown to be capable of functioning during leaf starch biosynthesis (Streb et al., 2012) and it is proposed to be involved with the pre-amylopectin trimming model of starch synthesis, alongside ISA (Sim et al., 2014, Martin and Smith, 1995, Streb et al., 2008).

5.1.2 Previous Purification of Limit Dextrinase

LD activity was first identified in barley malt in 1948 (Kneen and Spoerl, 1948). Following this, the first partial purification of a debranching enzyme capable of hydrolysing β-limit dextrin was performed using potato and broad bean (Hobson et al., 1950). To date, LD has been identified and characterised, on both proteome and genome levels, from numerous plant sources including both dicots and monocots (Table 5.1).

	Common Name	Latin Name	Reference
Dicots	Arabidopsis	*Arabidopsis thaliana*	(Zeeman et al., 1998)
	Potato	*Solanum tuberosum*	(Hobson et al., 1950)
	Broad bean	*Vicia faba*	(Hobson et al., 1950)
	Pea	*Pisum sativum*	(Zhu et al., 1998)
	Spinach	*Spinacia oleracea*	(Renz et al., 1998, Ludwig et al., 1984)
	Sugar Beet	*Beta vulgaris*	(Li et al., 1992)
Monocots	Barley	*Hordeum vulgare*	(Manners and Yellowlees, 1973, Macgregor et al., 1994a)
	Maize	*Zea mays*	(Beatty et al., 1999, Wu et al., 2002, Dinges, 2003)
	Oat	*Avena sativa*	(Manners and Yellowlees, 1973)
	Proso millet	*Panicum miliaceum*	(Zarnkow et al., 2010)
	Rice	*Oryza sativa*	(Nakamura et al., 1996, Li et al., 2009)
	Rye	*Secale cereal*	(Manners and Yellowlees, 1973)
	Sorghum	*Sorghum bicolor*	(Hardie et al., 1976)
	Tef	*Eragrosits tef*	(Gebremariam et al., 2012)
	Wheat	*Triticum aestivum*	(Kruger and Marchylo, 1978, Repellin et al., 2008)

Table 5.1 Plants confirmed to contain limit dextrinase.

The primary sequences of cereal LDs are highly conserved within maize, rice, barley and wheat- having protein sequence identities of 70-95 %. Comparison of barley LD with that of Arabidopsis produces an overall protein sequence identity of 58 %, highlighting the phylogenetic distance between the monocots and dicots.

H.v	ID				
T.a	94.8	ID			
O.s	71.7	71.9	ID		
Z.m	75.3	74.8	70.8	ID	
A.t	57.9	57.8	54.7	57.5	ID
	H.v	***T.a***	***O.s***	***Z.m***	***A.t***

Table 5.2 Percentage identity between protein sequences for cereal and Arabidopsis limit dextrinase. Alignment performed using BioEdit software. *H.v- Hordeum vulgare* (barley), Acc. AAD34347.1. *T.a- Triticum aestivum* (wheat), Acc. ABL84490.1. *O.s- Oryza sativa* (rice), Acc. BAA09167.1. *Z.m- Zea mays* (maize), Acc. XP_008668612.1. *A.t- Arabidopsis thaliana,* Acc. AED90732.1.

The most focused and lengthy studies have been performed on the barley enzyme because of its important commercial role in the malting and mashing processes of beer and spirit production (Sissons et al., 1995). The first LD purified to homogeneity from barley malt was by Sissons et al. One kg of malt yielded 0.37 mg of LD purified by 4 steps (Sissons et al., 1992a). Further purification schemes were soon established, all of which included a combination of ammonium sulfate precipitation, anion and cation exchange, size exclusion and affinity chromatography (Sissons et al., 1992b, Sissons et al., 1992a, Macgregor et al., 1994a). An improved purification procedure gave higher yields of LD by heat treatment at 65 °C to release LD into a buffer including a divalent cation and a reducing agent (Kristensen et al., 1998). This produced 9 mg of LD per kg of malt.

Further to purification from plant sources, attempts at production of recombinant LD from maize (Wu et al., 2002), spinach (Renz et al., 1998) and wheat (Repellin et al., 2008) have been carried out. All expression attempts resulted in relatively poor yields when compared to expected protein levels usually produced by *E. coli* (Tegel et al., 2011). Proposed reasons for these low levels include protein degradation, premature termination of translation, issues with codon usage or misfolding and targeting to inclusion bodies (Francis and Page, 2010). A codon-optimised barley LD has reportedly been produced in *E. coli*, purified and used for X-ray crystallography analyses, however details regarding yield and activity were not disclosed (Møller et al., 2015b). The highest reported levels of pure, catalytically active, LD have been produced by a high-cell density fermentation system using *Pichia pastoris* secretion, followed by purification with β-cyclodextrin-Sepharose and gel filtration (Vester-Christensen et al., 2010b). This enabled the multi-mg production of LD and its crystallisation in complex with numerous substrate analogues (Møller et al., 2015b).

5.1.3 The Structure of Limit Dextrinase and Other Pullulanases

LD, also described as plant pullulanase, belongs to the glycoside hydrolase (GH) family 13 (Cantarel et al., 2009), a diverse group of enzymes, containing nearly 26,000 members, characterised by a retaining catalytic mechanism, a catalytic Asp base and a Glu proton donor (Svensson et al., 2002). This family includes, amongst others, α-amylase, α-glucosidase, isoamylase, neopullulanase and cyclomaltodextrinase (Jespersen et al., 1993). GH13 members belong to the CAZy clan-H, a group that all share the same $(\beta/\alpha)_8$ barrel catalytic domain (Cantarel et al., 2009). LD is further grouped into the GH13 subfamily 13 (GH13_13, bacteria and eukaryote) with other pullulanases being assigned to subfamilies 12 (GH13_12, firmicutes) and 14 (GH13_14, bacteria) depending on their sequence and phylogenetic origin (Cantarel et al., 2009, Stam et al., 2006). The majority of well characterised pullulanases are of microbial origin, from organisms such as *Bacillus subtilis* (*Bs*), *Bacillus acidopullulyticus* (*Ba*) and *Klebsiella pneumonia* (*Kp*). Sequence alignment of barley LD with microbial pullulanases shows sequence identities around 30 % (Vester-Christensen et al., 2010b).

Carbohydrate binding modules (CBMs) are protein sequences that fold into a structurally discrete module. The N-terminal domain of LD possesses structural similarity to CBM21 of *Rhizopus oryzae* glucoamylase and is speculated to be involved in protein-substrate/surface interactions (Møller et al., 2012). A mutant of sorghum LD has been identified which possesses two missense mutations in the N-terminal domain (Gilding et al., 2013). These mutations lead to increased LD activity and increased *in vitro* starch digestibility and have no deleterious trade off. It is proposed that the mutation is a reversion to a sequence nearer to that of barley. These observations support the idea that the N-terminal domain is related to substrate binding or catalytic activity. The plant LD and isoamylases only contain a single annotated CBM (CBM48) (Machovič and Janeček, 2008) in comparison to the structures of *Kp*PUL and *Ba*PUL which show two N-terminal CBMs (CBM41 and CBM48) (Figure 5.1, red domains) (Mikami et al., 2006, Turkenburg et al., 2009). There are still other domains that exist within these proteins that have an undefined function (Figure 5.1, purple domains).

The N-terminal domain is followed by the $(\beta/\alpha)_8$ barrel catalytic domain that is common to all GH13 enzymes (Figure 5.1, blue domains) (Kuriki and Imanaka, 1999). A C-terminal domain follows the catalytic domain, this consists of a two-sheet β-sandwich motif (Matsuura et al., 1984) (Figure 5.1, green domains).

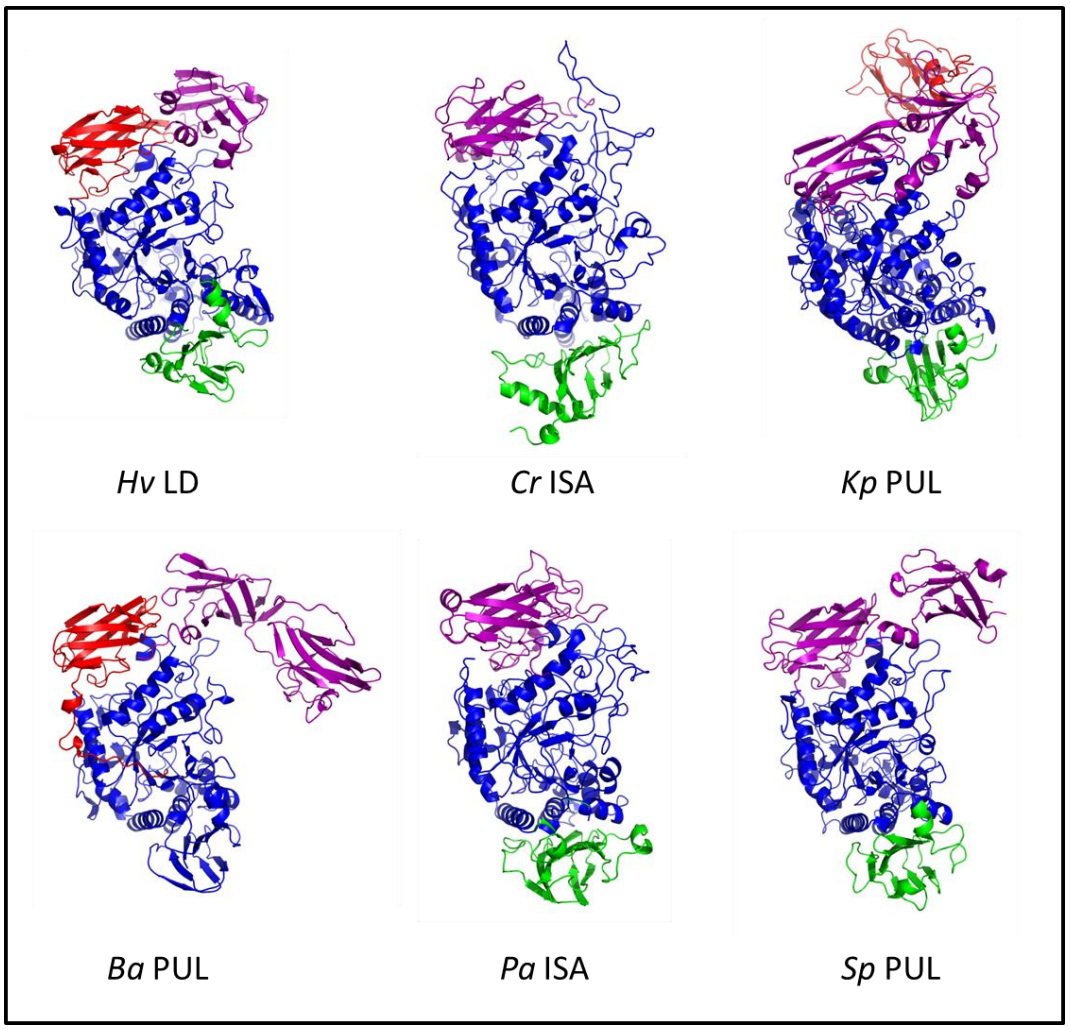

Figure 5.1 Domain organisation of limit dextrinase, isoamylase and pullulanase.
Structures solved by crystallography. *Hv*LD- *Hordeum vulgare* limit dextrinase (4AIO) (Moller et al., 2012), *Ba*PUL *Bacillus acidopullulyticus* pullulanase (2WAN) (Givens et al., 2004), *Cr*ISA *Chlamydomonas reinhardtii* isoamylase (4J7R) (Shu et al., 2014), *Pa*ISA *Pseudomonas amyloderamosa* isoamylase (1BF2) (Katsuya et al., 1998), *Kp*PUL *Klebsiella pneumoniae* (2FHB) (Mikami et al., 2006), *Sa*PUL *Streptococcus pneumonia* pullulanase (3FAW) (Gourlay et al., 2009). Colours refer to domains: purple- N-terminal, red- CBMs, blue- catalytic domain and green- C-terminal.

The α-1,6 acting enzymes, including LD (EC3.2.1.142), pullulanase (EC 3.2.1.41) from bacteria, and isoamylase (EC 3.2.1.68,) are all composed of a similar domain organisation (Figure 5.1). At the N-terminus is a domain of varying length that can contain structural features such as carbohydrate binding modules (Figure 5.1, red and purple domains) (Vester-Christensen et al., 2010b).

The interaction of barley LD (recombinant, expressed in *Pichia*) with different size cyclodextrins reveal affinities (K_d) of 27.2, 0.7 and 34.7 μM for α-, β- and γ-CD, respectively (Vester-Christensen et al., 2010a). The distinct differences in binding to the different CDs indicates a higher level of plasticity within the substrate binding site of LD, which enables

optimisation of substrate binding when compared to pullulanase (Vester-Christensen et al., 2010a). β-CD is the preferred ligand for LD and its resemblance to the positioning of glucose within the glucan helices of amylopectin fits with the role of LD (Figure 5.2). A study on *Ba*PUL revealed that the protein structure, observed by circular dichroism, decreased in helix and increased in sheet content, upon binding β-CD; this change was associated with loss of catalytic activity and supports the suggestion that conformational changes may be important for catalytic activity.

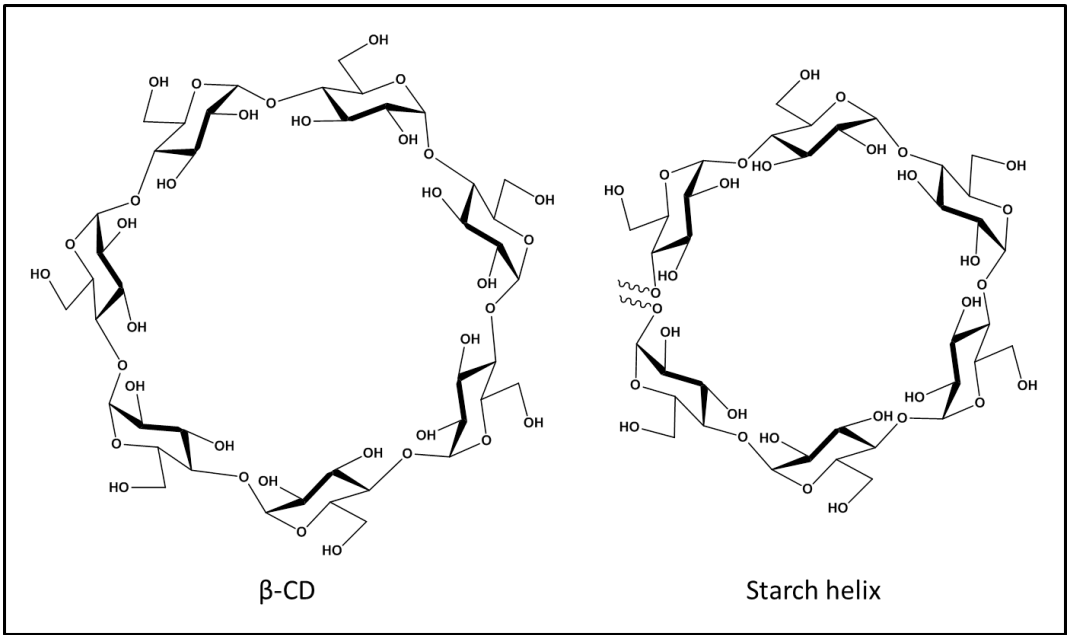

Figure 5.2 Representative structures of β-cyclodextrin and an amylose helix from starch.
Cyclodextrins are constrained to a semi-rigid form because of their cyclic nature, however, β-cyclodextrin can have an internal diameter between 5.40 and 8.34 Å, depending on its conformation (Pinjari et al., 2010). The helixes found within starch vary in width depending on conformation (Hancock and Tarbet, 2000). β-cyclodextrin represents the preferred shape for binding to the LD active site, as concluded by SPR studies (Vester-Christensen et al., 2010b), crystallography (Vester-Christensen et al., 2010a) and inhibition studies (Chapter 4).

The ability to generate high levels of pure protein (Vester-Christensen et al., 2010b) has enabled crystallisation of LD in complex with competitive inhibitors α- or β-cyclodextrin bound within the active site (Vester-Christensen et al., 2010a). The crystal structures of these complexes were solved to 2.5 Å and 2.1 Å, respectively, with the cyclodextrins occupying the active site carbohydrate binding sites +1 and +2 (Figure 5.3) and a glycerol and three water molecules mimicking a glucose residue at sub-site -1, thereby identifying the residues involved in catalysis as Asp^{473} and Glu^{510} (Figure 5.3). A catalytically inactive mutant of Glu^{510} (E510A) has been generated therefore confirming the role of this residue in catalysis (Møller et al., 2015b).

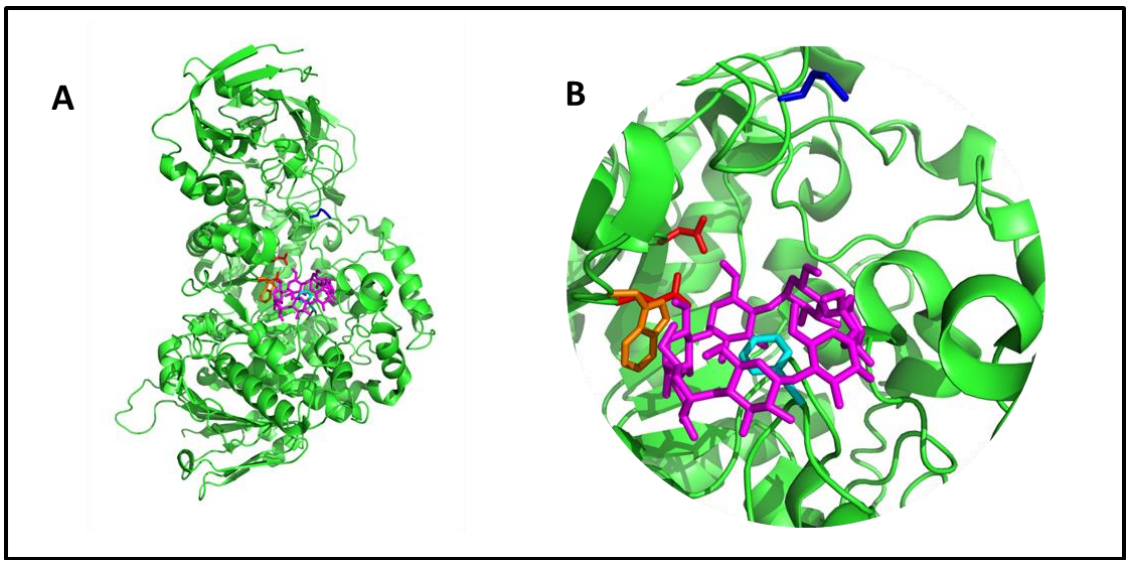

Figure 5.3 The structure of limit dextrinase in complex with β-cyclodextrin
A&B LD and β-CD complex (2X4B). β-CD (purple). Asp^{473} and Glu^{510} (red) are the catalytic residues in active site. Met^{440} (blue) blocks the binding of long polymers.

5.1.4 The Mechanism of Limit Dextrinase-Catalysed Hydrolysis and Transglycosylation

The α-1,6-glucoside hydrolysis reaction catalysed by LD occurs by general acid catalysis, which utilises a proton donor (Asp^{473}) and a nucleophile/base (Glu^{510}). A third acid residue is required for catalysis by LD and other GH13 enzymes (Macgregor, 2005) this residue is involved in distortion of the substrate *via* hydrogen bonding (Uitdehaag et al., 1999). Cleavage of the glycosidic bond results in retention of anomeric configuration around the anomeric carbon, taking place *via* a double displacement mechanism that is common to all GH13 family members. The reaction (Figure 5.4) occurs in two steps, beginning with nucleophilic attack of the substrate by the deprotonated Asp^{473} (Figure 5.4, A) to form a covalent β-glucosyl-enzyme intermediate and simultaneous protonation of the leaving aglycone by Glu^{510} (Figure 5.4, B). Stabilization of the oxocarbonium ion-like transition state is believed to be mediated several conserved amino acids, in particular His^{404} and His^{641} (Vester-Christensen et al., 2010a). Once deprotonated, Glu^{510} acts as a base, abstracting a proton from an activated acceptor which goes on to attack the anomeric carbon (Figure 5.4, C). The acceptor can be either a water molecule (hydrolysis) or the primary C6 hydroxyl group of a non-reducing glucose terminus of a glucan (transglycosylation). Hydrolysis occurs at the 1,6-linkage between glucose units at sub-sites -1 and +1 (Figure 5.5) (Davies et al., 1997, Bissaro et al., 2015).

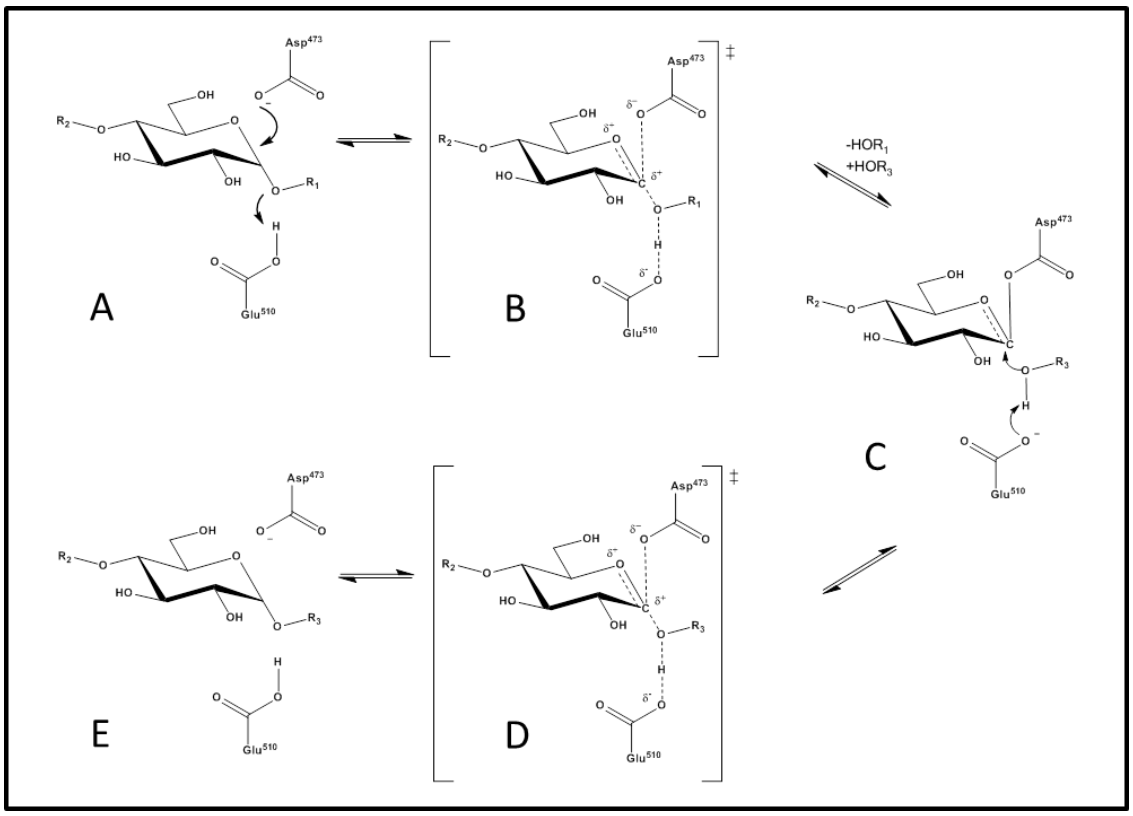

Figure 5.4 The catalytic mechanism of limit dextrinase and other retaining hydrolases.
The catalytic process is explained in the text. Adapted from (Macgregor et al., 2001, Bissaro et al., 2015). R1 and R2 represent residues within the polymeric substrate- pullulan or dextrin. R3 represents either a H, in the case of hydrolysis, or the C6 position of a glucose residue of another glucan, in the case of transglycosylation.

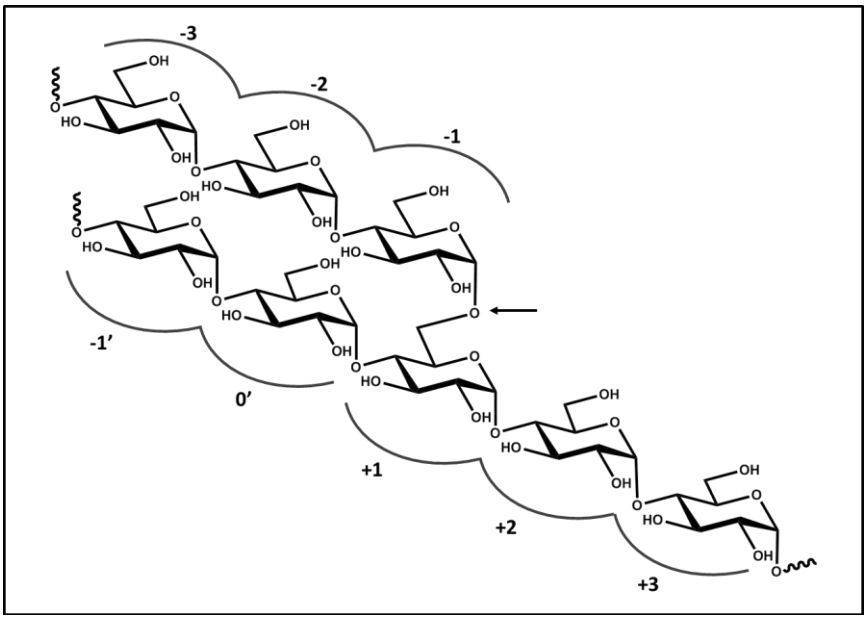

Figure 5.5 The sub-site numbering of the limit dextrinase binding cleft.
Other α-1,6 debranching enzymes sub-sites are numbered in the same way but may possess more or fewer sub-sites. The hydrolysed bond is indicated by an arrow. Numbering follows the rules set out by (Davies et al., 1997). The non-main chain (side chain) is identified by (').

5.1.5 The Substrate Specificity of Limit Dextrinase

The GH13 family has diverse substrate specificities. LD specifically hydrolyses α-1,6 bonds found within branched dextrins created during starch catabolism. It also shows activity towards the α-1,6 bonds of the α-1,4, α-1,6 glucose polymer pullulan (Manners and Yellowlees, 1971). The relative rates of LD, *Kp*PUL and *Ps*ISA, when compared (Table 5.3), show that the pullulanase type debranching enzymes have a preference for short oligosaccharides over polymeric substrates. Long substrates, other than pullulan, cause a distinct drop in rate of hydrolysis (Greffe et al., 2003, Kainuma et al., 1978). In comparison, isoamylase has a preference for polymeric substrates, having a high activity towards amylopectin (Kainuma et al., 1978). α-Maltosylmaltotetraose is the preferred main chain length for LD (Manners and Yellowlees, 1971). The hydrolysis rate increase associated with the change from α-maltosyl to α-maltotriosyl indicates that the optimum side chain length is three glucose units long (Manners and Yellowlees, 1971). Neither LD nor *Kp*PUL show activity with smaller di- and tri-saccharides and are incapable of cleaving α-1,6 linkages between a single glucose residue attached to either a linear or cyclic oligosaccharide (Manners and Yellowlees, 1971, Greffe et al., 2003, Abdullah et al., 1966). It is worthwhile noting that the specificity of debranching enzymes from microbial origin, outlined in Table 5.3, do not precisely compare to those of plant limit dextrinase and isoamylase.

Substrate	**Relative Rates**			
	LD[a]	**LD[b]**	***Kp*PUL[c]**	***Ps*ISA[d]**
6^3-α-maltosylmaltotriose	-	13	49	3
6^3-α-maltosylmaltotetraose	-	123	169	7
6^3-α-maltotriosylmaltotriose	-	129	90	10
6^3-α-maltotriosylmaltotetraose	358	243	123	33
Nonasaccharide from pullulan	-	114	-	-
Pullulan	100	100	100	<1
Amylopectin β-limit dextrin	-	68	-	-
Amylopectin	-	<<1	-	100
Glycogen	-	0	-	-

Table 5.3 Substrate preferences for limit dextrinase and other debranching enzymes.
Data combined from the following references. a. (Greffe et al., 2003). **b.** (Manners and Yellowlees, 1971). **c.** (Abdullah et al., 1966). **d.** (Kainuma et al., 1978).

The crystal structure of LD has implicated a number of residues in the specificity of LD action (Vester-Christensen et al., 2010a). The bulky Met^{440} (Figure 5.6, blue) is a residue in a position unique to LD that obstructs sub-site -4; it is proposed that the steric hindrance may affect the specificity of LD and be the cause of low activity towards amylopectin. Further to this, an extended loop (Asp^{513}-Asn^{520}) within the catalytic domain also appears to influence substrate specificity (Vester-Christensen et al., 2010a). LD has been crystallised in complex with a number of substrates and substrate analogues (Figure 5.7) (Møller et al., 2015b). This has revealed that 2 glucose units at the main chain non-reducing end of the substrate are required for optimal binding in the active site sub-sites -1 and -2. Sub-sites +1 and +2 are also important for substrate binding, these are the same sites in which CD was bound in the first LD crystal structures solved (Vester-Christensen et al., 2010a). All of these findings are in agreement with LD catalytic substrate preferences. The preference for 1,6 linkages is driven by Trp^{512} and Phe^{553} that flank the catalytic cleft and keep non-branched substrates away from the active site, but position 1,6-branched substrates correctly (Møller et al., 2015b) (Figure 5.6, orange and cyan residues). This study confirmed that GH13 proteins recognise their substrates based on shape and size, it is the combined effect of shape and interactions over a polymeric substrate that drives specificity.

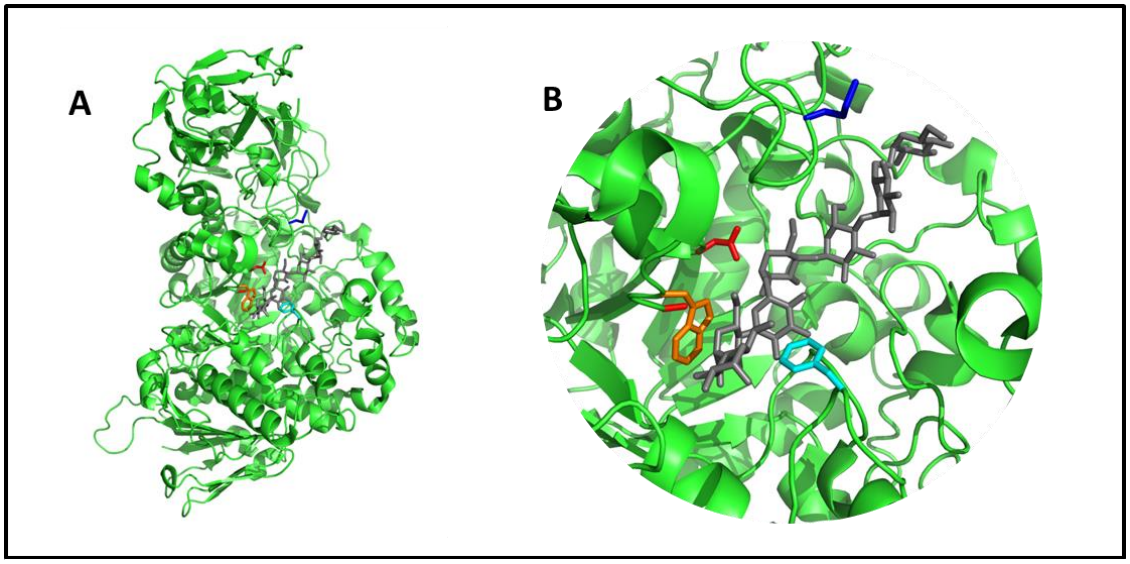

Figure 5.6 The structure of limit dextrinase in complex with 6^3-α-glucosyl-maltotriosylmaltotriose.
A&B LD and 6^3-α-glucosyl-maltotriosylmaltotriose (4J3X). 6^3-α-glucosyl-maltotriosylmaltotriose (grey). Asp^{473} and Glu^{510} (red) are the catalytic residues in active site. Met^{440} (blue) blocks the binding of long polymers. Phe^{553} (magenta) and Trp^{512} (orange) flank the catalytic cleft and prevent binding of non-branched substrates.

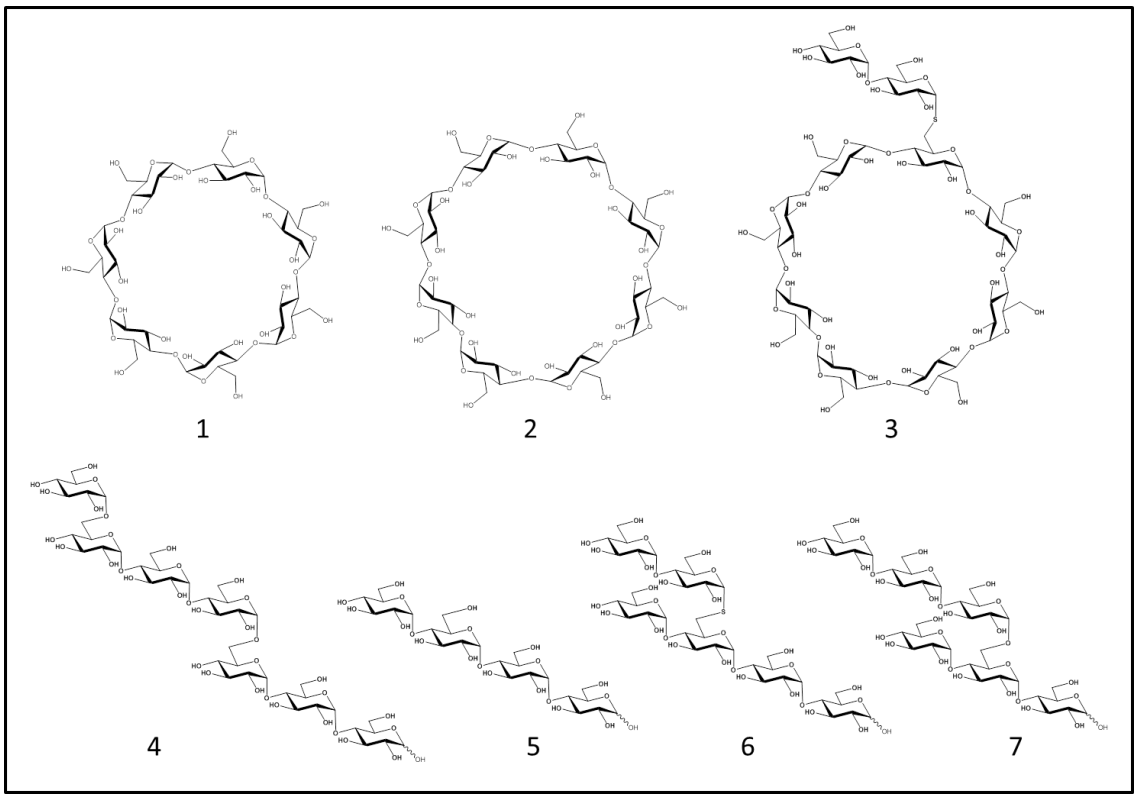

Figure 5.7 Substrates bound to limit dextrinase in published crystal structures.
1. α-cyclodextrin (2X4C). **2.** β-cyclodextrin (2X4B). **3.** maltosyl-S-β-cyclodextrin (4J3U). **4.** 6^3-α-glucosyl-maltotriosylmaltotriose (1J3V). **5.** maltotetraose (4J3T, 4J3S). **6.** 6^3-o-α-maltosylmaltotetraose (4J3X). **7.** 6^2-α-maltotriosylmaltotriose (4J3W).

LD, *Sulfolobus solfataricus* debranching enzyme and *Pa*ISA have been shown to display transglycosylation activity (Abe et al., 1988, Svensson et al., 2002, Mcdougall et al., 2004, Yamasaki et al., 2008, Kang et al., 2008, Nguyen et al., 2014). Maximum LD transglycosylation activity has been seen with maltotriose, confirming that the optimum subsite chain length is three glucose units long (Mcdougall et al., 2004).

Transglycosylation activity is dependent on donor and acceptor molecules (Mcdougall et al., 2004). Further to this maltose to maltoheptose are capable of activation of LD at concentrations between 5 mM-12.5 mM. High levels of dextrins can cause inhibition of the enzyme (Macgregor et al., 2002, Mcdougall et al., 2004). The mechanisms of inhibition and activation are unknown. The effect of dextrins on LD can cause issues with interpretation of previous assay data if samples were not cleared of small glucans. Samples can be cleared by size exclusion or treatment with amyloglucosidase to hydrolyse glucans to produce glucose, which shows no inhibitory activity towards LD. Transglycosylation activity can be utilised for the synthesis of novel compounds, often requiring much less time than traditional chemical synthesis, examples of transglycosylation reactions catalysed by similar enzymes are outlined

in Figure 5.8 (Kang et al., 2008, Kang et al., 2011, Leong et al., 2007, Abe et al., 1988, Shimura et al., 2011). The *in planta* of role of transglycosylation is not yet clear, it may be relevant to pre-amylopectin trimming and/or granule initiation (Mcdougall et al., 2004, Streb et al., 2008).

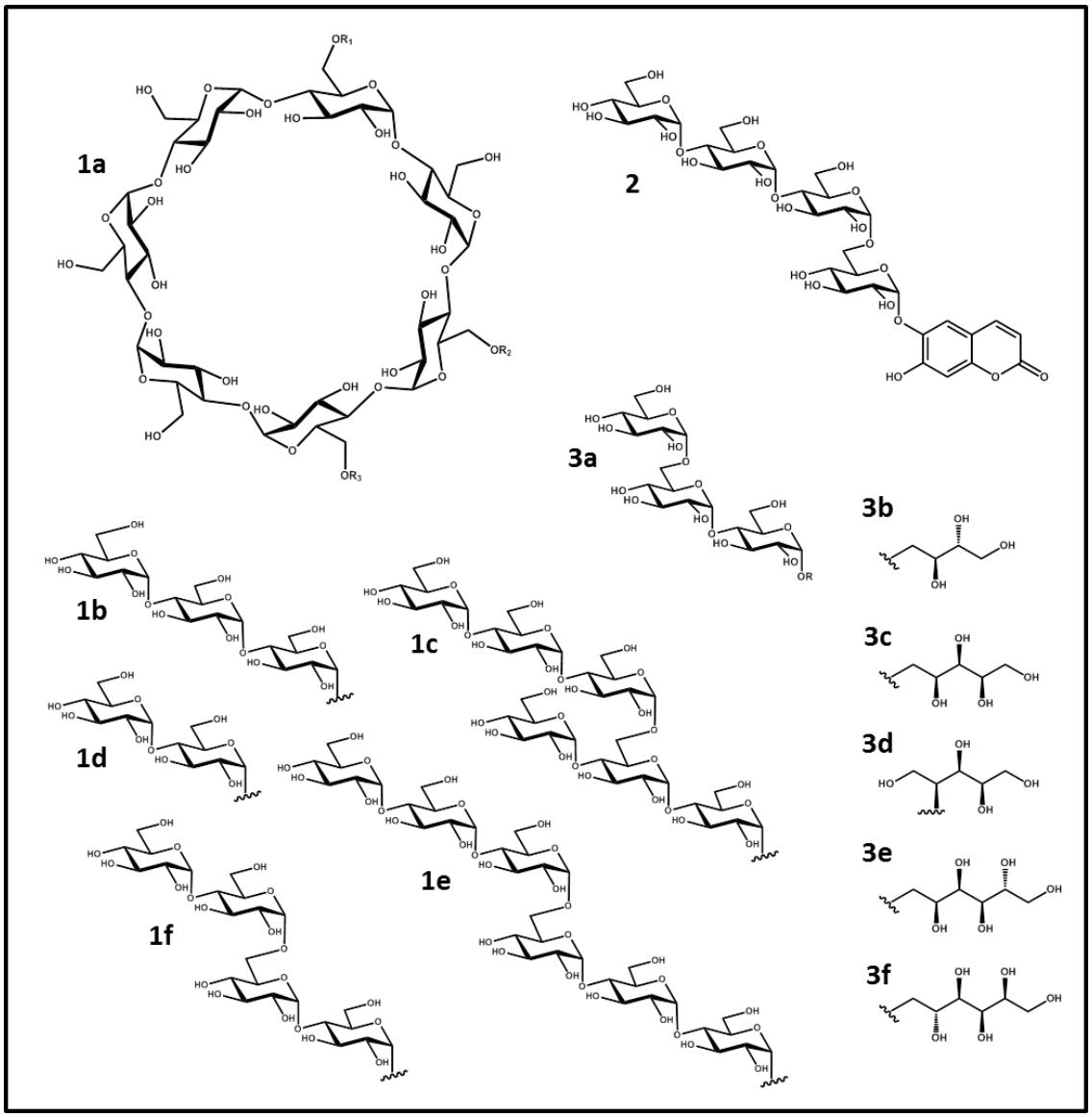

Figure 5.8 Products created by transglycosylation catalysed by proteins similar to limit dextrinase.
1. The following compounds were generated using *Pa*ISA and glycosyl-β-CD, diglucosyl-β-CD, maltosyl-β-CD or maltotriosyl-β-CD: 6^A,6^D-di-*o*-α-maltosyl-β-CD (1a: R1-1d, R2-H, R3-1d). 6-*o*-α-(6^2-o-α-maltosyl)maltosyl-β-CD (1a: R1-1f, R2-H, R3-H). 6^A,6^D-di-*o*-α-maltotriosyl-β-CD (1a: R1-1b, R2-H, R3-1H). 6-*o*-α-(6^3-o-α-maltotriosyl)maltotriosyl-β-CD (1a: R1-1e, R2-H, R3-H). 6-*o*-α-(6^2-o-α-maltotriosyl)maltotriosyl-β-CD (1a: R1-1c, R2-H, R3-H). *Sulfolobus sulfataricus* was used to generate 6^A,6^D-di-*o*-α-maltosyl-β-CD (1a: R1-1d, R2-H, R3-1d) and 6^A,6^c-di-*o*-α-maltosyl-β-CD (1a: R1-1d, R2-1d, R3-1H) from maltosyl-β-cyclodextrin (Abe et al., 1988, Kang et al., 2008). **2.** Maltotriosyl-aesculin was produced using pullulan and aesculin, catalysed using *Thermatoga neapolitana* PUL (Kang et al., 2011).
3. 1-o-α-panosylerythritol (3a, R-3b). 1-o-α-panosylxylitol (3a, R-3c). 2-o-α-panosylxylitol (3a, R-3d). 1-o-α-panosylsorbitol (3a, R-3e). 6-o-α-panosylsorbitol (3a, R-3f) were produced from pullulan and the respective sugar alcohols (3b-f) using *Thermoactinomyces vulgaris* pullulan hydrolysing amylase (Shimura et al., 2011).

5.1.6 Limit Dextrinase Inhibitor

The identification of limit dextrinase inhibitor (LDI) as the protein potentially responsible for low levels of LD activity during malting occurred alongside the studies of LD. LD inhibitory activity was first identified in cereal extracts (Yamada, 1981), where incubation of LD in the presence of a reducing agent was required for complete extraction and full LD activity (Mccleary, 1992). LD purified from barley malt was found to be in active (free) and inactive (bound) forms (Longstaff and Bryce, 1993). It was proposed that LD is bound to a protein that is affected by proteases or reducing agents. Two forms of LDI, which differed in migration in isoelectric focusing, were identified in barley malt. These two forms had identical amino acid sequences but differed in the attachment of glutathione or cysteine to a cysteine residue (Macri et al., 1993). The interaction between LD and LDI has been well studied *in vitro*, with the two proteins interacting with picomolar affinity (Møller et al., 2015a). It has been proposed that LDI is a specific inhibitor (Macgregor, 2004) controlling LD activity during germination and it is suggested to be responsible for low levels of LD during mashing, though these proposals are yet to be confirmed experimentally *in planta* (Macgregor, 2004).

5.1.7 Previous Purification of Limit Dextrinase Inhibitor and Related Proteins

LDI belongs to a family of CM proteins, which are named so as they can be extracted from cereal flour using chloroform-methanol because of their hydrophobicity. Analysis of this fraction reveals a complex mix of small proteins with a range of functions including: cereal type inhibitors (CTIs), lipid transfer proteins, stress enzymes and storage proteins (Wong et al., 2004). The precise function of many of these proteins remains unclear. CTIs consist of a common protein fold utilised in widespread processes including: regulation of endogenous hydrolases (both carbohydrate and protein, sometimes with dual action), defence against pathogens and pests- fungi and insects, seed storage proteins that provide amino acids for germinating plants, lipid transfer and maintenance of cell wall structure (Svensson et al., 2004, Jose-Estanyol et al., 2004).

Functional recombinant CTIs have proved extremely challenging to produce in high yields. Only a handful of these types of proteins have been expressed with success - α-amylase inhibitor from rye (Dias et al., 2005), wheat monomeric α-amylase inhibitor 0.28 (WMAI-1) (Garcia-Maroto et al., 1991), allergenic wheat CM16 protein (Lullienpellerin et al., 1994), ragi bifunctional α-amylase/trypsin inhibitor (RBI) (Sen and Dutta, 2012), α-amylase inhibitor from wheat kernel (Okuda et al., 1997) and Hageman factor inhibitor from corn (CHFI) (Chen et al., 1999, Hazegh-Azam et al., 1998). All of these proteins have been overexpressed in *E. coli,* and

in most cases purified from the insoluble fraction and refolded. Whilst the processes of expression, cell lysis, inclusion body preparation and solubilisation are all similar, precise conditions are required for each protein refolding procedure (Burgess, 2009). One commonly used refolding method for disulfide rich proteins involves dilution with a suitable redox system to catalyse disulfide bond exchange (Kohno et al., 1990). However, in general, low levels of active protein are often obtained following refolding.

Recently LDI has been identified on a sequence level in wheat, rice and brachypodium (*Brachypodium distachyon*) (Møller et al., 2015a). These proteins have not been confirmed experimentally. The sequence identities between these proteins are outlined in Table 5.4. LDI has only been purified and analysed from barley grain. LDI consists of two forms of a 114 amino acid protein. The two forms of LDI were found to differ in a thiol linked residue, having either cysteine or glutathione attached (position 7 in Figure 5.9), both forms were capable of inhibiting LD (Macgregor et al., 1994b, Macgregor et al., 2000). Modelling the sequence of LDI against known family member ragi amylase-trypsin inhibitor predicted four alpha-helices held together by four disulfide bridges (Figure 5.1) (Macgregor et al., 2000). A 1:1 ratio of LD:LDI caused complete inhibition of activity, their proposed stoichiometry was confirmed by ESI-MS (Macgregor et al., 2003). LDI has been tested against various bacterial, plant, mammalian and insect enzymes- pullulanase and isoamylase from *Aerobacter aerogenes*, isoamylase from *Pseudomonas amyloderamosa,* pullulanase from *Bacillus acidopullulyticus* (Macgregor et al., 1994b), trypsin and α-amylase from *Sus scrofa*, barley malt α-amylase and α-amylase from *Tenebrio molitor* (Macgregor et al., 2000): no inhibitory activity against any of these proteins was identified.

H.v	ID			
T.a	77.5	ID		
B.d	55.4	54.3	ID	
O.s	45.0	44.7	43.1	ID
	H.v	***T.a***	***B.d***	***O.s***

Table 5.4 Percentage identities between protein sequences for cereal limit dextrinase inhibitors.
Alignment performed using BioEdit software. *H.v- Hordeum vulgare* (barley), Acc.ABB885733. *T.a- Triticum aestivum* (wheat), Acc. CAA68248. *B.d- Brachypodium distachyon,* Acc. XP_003561291. *O.s- Oryza sativa* (rice), Acc. ABK34477.

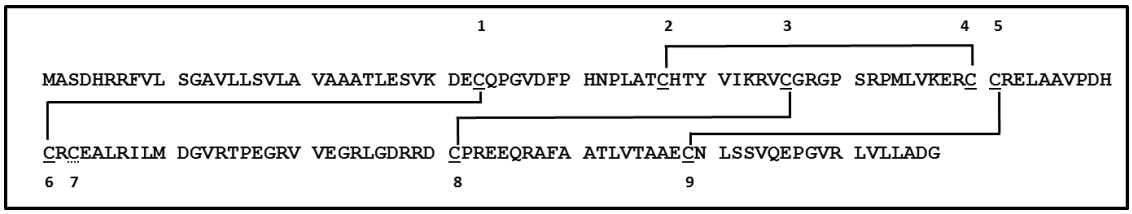

Figure 5.9 Cysteine and cystine residues present in barley limit dextrinase inhibitor.
Cystine disulfide bonds (solid underline) are formed between cys residues 1-6, 2-4, 3-8, 5-9. cysteine 7 (dashed underline) is found coupled to either a free cysteine or glutathione *via* a disulfide bond.

Attempts at producing LDI in *E. coli* and *Lactococcus lactis* have been reported (Bønsager et al., 2007). Expression of a His_6-tagged fusion protein construct yielded no soluble or insoluble protein. N-terminal fusion of thioredoxin to LDI yielded some soluble protein in *E. coli*, however cleavage of the thioredoxin tag caused a drop in LDI activity assessed by LD activity assay. Secretory expression of LDI in *Pichia pastoris* high cell density batch-fed fermentation, followed by nickel affinity chromatography and gel filtration produced high amounts of protein. This protein had twofold stronger inhibitory activity than barley LDI purified from grain (Jensen et al., 2011).

5.1.8 The Structure of Limit Dextrinase Inhibitor and Other Cereal Type Inhibitor Proteins

There are only 4 CTI protein structures that have been solved to date - ragi bifunctional α-amylase/trypsin inhibitor (RBI) (Strobl et al., 1995), Hageman factor inhibitor from corn (CHFI), α-amylase inhibitor from wheat (WAI) (Oda et al., 1997) and LDI (Møller et al., 2015a). The structure of RBI bound to yellow mealworm α-amylase have also been solved (Strobl et al., 1998). Further to this, CHFI has been shown capable of inhibiting mammalian trypsin, Hageman blood coagulation factor and α-amylases from insects (Behnke et al., 1998). LDI is the only known debranching enzyme inhibitor in this protein family and has been shown to inhibit LD specifically; many other known and unknown sources of possible targets for LDI have yet to be tested. All of these inhibitors possess a common fold of four alpha helices connected by short loops and held together *via* four disulfide bonds which are conserved (Jose-Estanyol et al., 2004, Juge and Svensson, 2006). The disulfide bridges are responsible for maintaining the tertiary structure of the helical core whilst the loops are variable, dependent on the necessary function (Figure 5.10, orange residues).

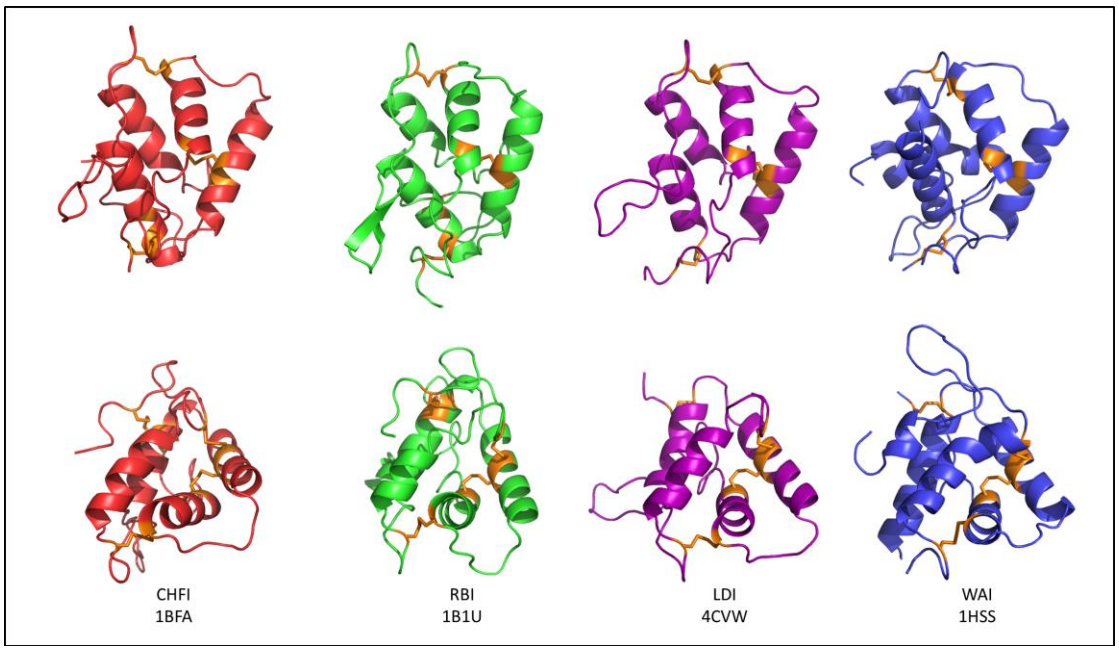

Figure 5.10 The three dimensional structures of four cereal type inhibitor proteins.
Hageman factor inhibitor from corn (CHFI)- red, ragi bifunctional α-amylase/trypsin inhibitor (RBI)- green, LDI- purple, α-amylase inhibitor from wheat (WAI)- blue. **Top row.** The common four helix structures with variable loops are visible. **Bottom row.** 90° rotation on the z-axis. The four disulfide bonds are highlighted in orange. PDB codes are shown below the abbreviated protein names.

5.1.9 The Structure and Interactions of Limit Dextrinase-Limit Dextrinase Inhibitor

The successful expression of both LD and LDI using *Pichia pastoris* has enabled the structure of their complex to be solved to a 2.7 Å resolution (Møller et al., 2015a). The LD structure within the complex is identical to previous structures solved (Vester-Christensen et al., 2010a).

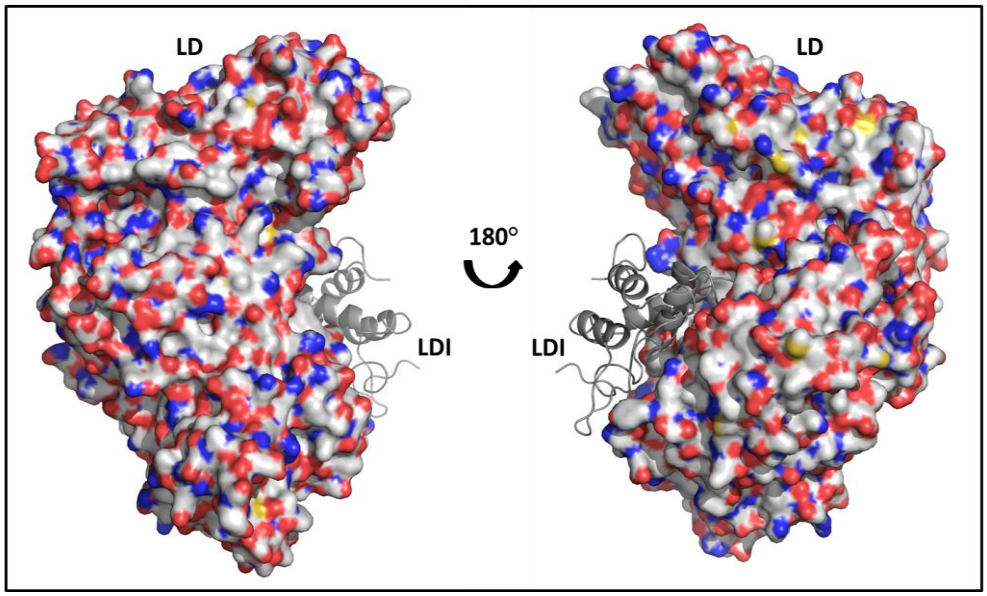

Figure 5.11 The structure of the limit dextrinase-limit dextrinase inhibitor complex.
LDI (dark gray) binds in the active site cleft of LD (carbon- light gray, oxygen- red, nitrogen- blue, sulfur- yellow).

Analysis of the complex revealed that hydrophobic cluster and ionic interactions are vital for the affinity of the LD-LDI interactions. The catalytic Asp, Glu and Asp were in the same conformation in all structures, this active site is buried by LDI complexation. Key residues at the protein:protein interface were studied by site directed mutagenesis (SDM) followed by surface plasmon resonance (SPR) analysis (Table 5.5). LDI Arg^{34} contacts Glu^{729} and Asp^{730} in LD at the entrance to the active site and LDI Arg^{38} forms ionic interactions with the catalytic nucleophile Asp^{473} and acid/base catalyst Glu^{510}. LDI Leu^{41} and Val^{42} are perhaps the most important residues that form a hydrophobic cluster with LD Trp^{512}, Phe^{514} and Phe^{553}.

Variant		Relative K_d
	WT	1
LDI	R34A	22
	R38A	33
	R38W	12
	L41G	100
	L41W	1.8
	V42D	4,048
	L41G-V42D	476,190
LD	D730W	7.9
	D730R	171

Table 5.5 Binding affinity (K_d) between recombinant mutants of limit dextrinase and limit dextrinase inhibitor generated using surface plasmon resonance.
Values from (Møller et al., 2015a). The importance of L41 and V42 is highlighted by the drastic change in affinity caused by mutation of these residues.

The interaction between LD and LDI occurs at an affinity of 30 pM, with a pH optimum of 6.5. The LD: LDI complex has a thermal stability peak of 77 °C, this is 11 °C higher than LD alone. LDI is extremely thermally stable, alone it has a thermal stability peak of 97.4 °C and a half-life over 50 min at 90 °C (Møller et al., 2015a). The thermal stability that LDI confers to LD may well be relevant to the mashing step during brewing (Yang et al., 2008, Evans et al., 2010).

5.2 Aims of this Chapter

Recent work on LD and LDI has centred on *in vitro* analysis of the proteins and their interactions. A large amount of structural data has been gathered and used to explain how LD and LDI interact. However there are still questions about the *in planta* roles of LD and LDI left to be answered. These include the subcellular localisation of LD and LDI, the temporal expression of both proteins and the question of whether LD and LDI actually interact *in planta*, during the processes of germination or endosperm starch synthesis.

The genes and proteins for both LD and LDI are required in order to perform experiments that can answer these questions. Currently both proteins are produced by a lengthy and expensive procedure utilising *P. pastoris* as the expression host, where ideally *E. coli* would be used as the expression host. Recombinant protein is required for continuation of *in vitro* inhibition studies. Further to this, protein expression will enable the production of antibodies, which alongside the newly developed assays for LD (Mangan et al., 2015) will enable a more in depth analysis of LD and LDI within plants.

The first objective of the current study was the cloning of the genes encoding LD and LDI from barley into entry vectors compatible with Gateway cloning. This cloning system enables easy sub-cloning into vectors for different end uses. The second objective was to overexpress both LD and LDI in *E. coli* and develop purification strategies that produce homogeneous proteins. A further objective was the utilisation of the recombinant proteins to raise polyclonal antibodies specific for LD and LDI, which could be utilised to gain a better understanding of LD, LDI and their interaction *in planta*.

5.3 Results

5.3.1 Full length Limit Dextrinase Could Not be Cloned from Barley

Total RNA was purified from tissue samples taken from whole grain (0 dpi), endosperm (3 dpi and 5 dpi), aleurone (3 dpi) and leaf tissue (21 dpi). cDNA was synthesised from this RNA and used in a PCR, no samples yielded amplicons corresponding to full length LD (2889 bp). To check cDNA quality, a fragment of barley housekeeping gene GAPDH (604 bp) was successfully PCR amplified (Figure 5.12, A) (Burton et al., 1999). The same RNA was further used in an RT-PCR which also proved unsuccessful. Alongside a small amplicon of 900 bp, leaf RNA gave also a weak amplification product of around 2900 bp, possibly corresponding to full length LD (Figure 5.12, B), however further optimisation of this reaction proved unfruitful.

To test for the presence of LD in the RNA samples an RT-PCR was performed using primers previously used to identify the presence of LD (Burton et al., 1999) and cDNA produced using 21 dpi leaf RNA, 3 dpi endosperm RNA, and 3 dpi aleurone RNA. Amplicons of the correct size (621 bp) (Figure 5.12, C) were generated indicating that LD cDNA was present in all samples, however, the full length transcript was not present.

A fragment based cloning methodology was devised in an attempt to clone parts of the LD sequence, followed by ligation to produce the full length gene. A GC rich PCR on 3 dpi aleurone cDNA was performed in an attempt to generate three independent PCR products (1-1443 bp, 2-859 bp and 3-587 bp, (Figure 5.13). However the PCR yielded no amplicons of the correct size (Figure 5.12, D).

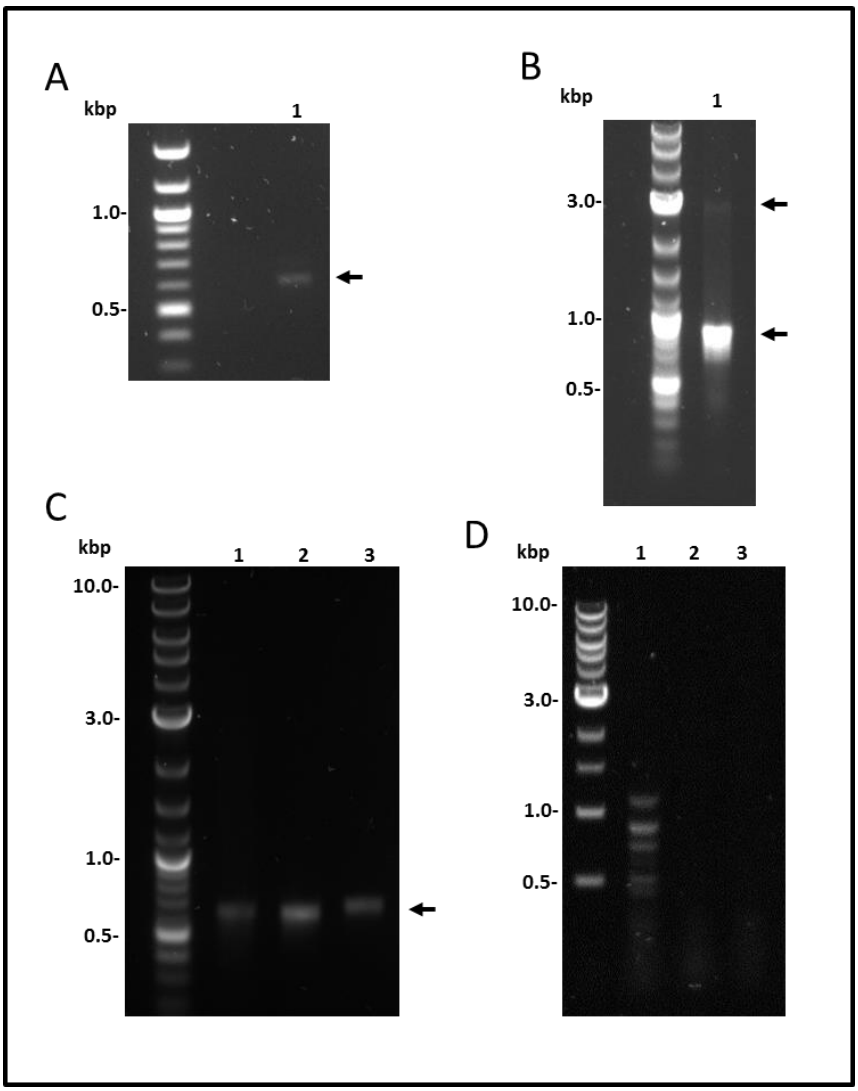

Figure 5.12 Agarose gels from attempted cloning of limit dextrinase.
A. PCR product, using cDNA prepared from 3 dpi aleurone layers, for housekeeping gene GAPDH, amplicon of correct size (604 bp) indicated by arrow. **B**. RT-PCR product, for full length LD, on 21 dpi leaf RNA, amplicons of ~2900 bp and ~900 bp indicated by arrows. **C**. PCR product, LD fragment probe, performed on cDNA from (**1**) 21 dpi leaf RNA, (**2**) 3 dpi endosperm RNA, and (**3**) 3 dpi endosperm, expected amplicons (621 bp) indicated by arrow. **D**. Agarose gel of PCR for LD cloning fragments, using cDNA prepared from 3 dpi aleurone layers (**1**) Fragment 1 (**2**) Fragment 2 (**3**) Fragment 3- see Figure 5.13.

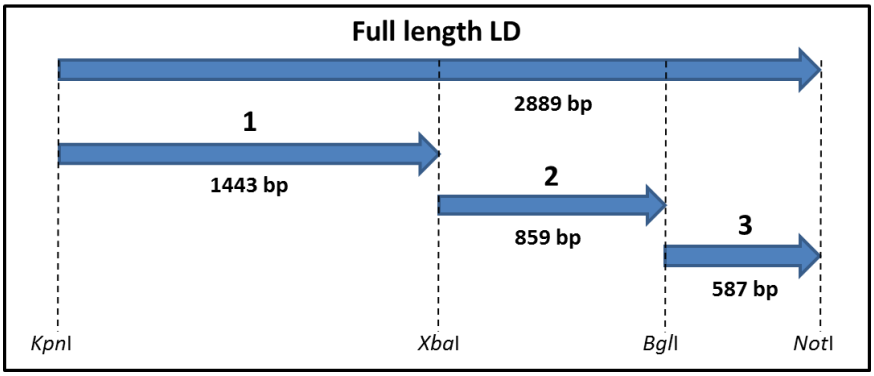

Figure 5.13 Map showing gene fragments designed for cloning limit dextrinase.

5.3.2 The Gene Encoding Limit Dextrinase was Obtained by Gene Synthesis

Due to the problems obtaining a full length gene, cloning was abandoned in favour of gene synthesis. Full length cDNA encoding LD (Genbank: AF122049.1) was ordered from Gene Art Gene Synthesis (Life Technologies, Carlsbad, CA, USA). A non-codon optimised version of the gene was chosen so that the native cDNA could be used for a number of final purposes. During the gene synthesis procedure the company experienced unforeseen problems with the synthesis, which caused a major delay in production. The full length gene was subdivided into four smaller sub-fragments (Figure 5.14, A, B, C and D) to be assembled separately and then ligated step by step in order to obtain the full-length construct. Problems arose with the synthesis of the 3' part of fragment C (bps 1434-2046), multiple *E. coli* clones screened by sequencing showed mutations within the same region, beginning at position 1491. This region (gttcctgggtac) contained either an insertion of 1 or 2 nucleotides or a deletion of 7, all of which would cause a frame shift when translated. Other codon optimisation options were considered for fragment C (Figure 5.15, A-D) however all options had relatively similar GC/AT levels. The 5' end of full length LD has extremely high GC content (Figure 5.15, E) which hindered the gene synthesis process. Finally, the full length sequence for fragment C was obtained in one colony. DNA from this colony and other LD gene fragments were ligated together to give the full length sequence for LD (2889 bp). The gene was cloned into a pOK vector (details in Appendix). This gene was sequenced and shown to be correct.

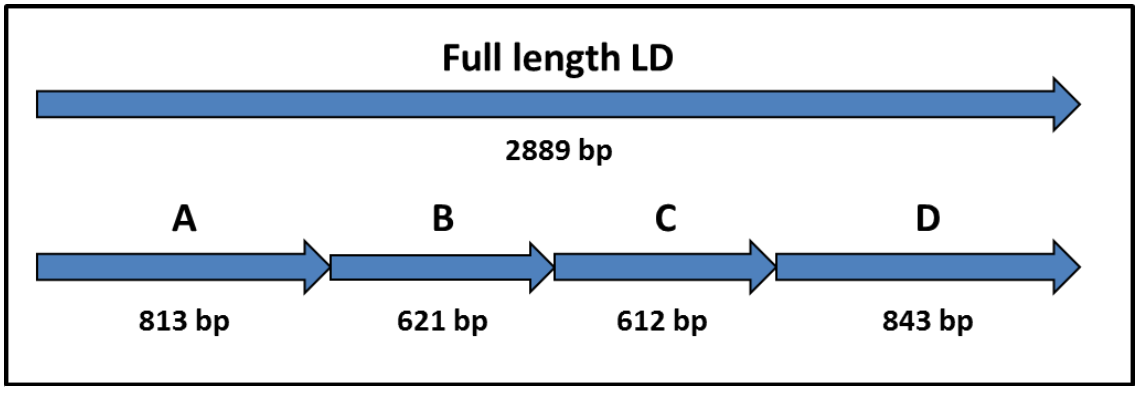

Figure 5.14 Map showing gene fragments used for gene synthesis of limit dextrinase.

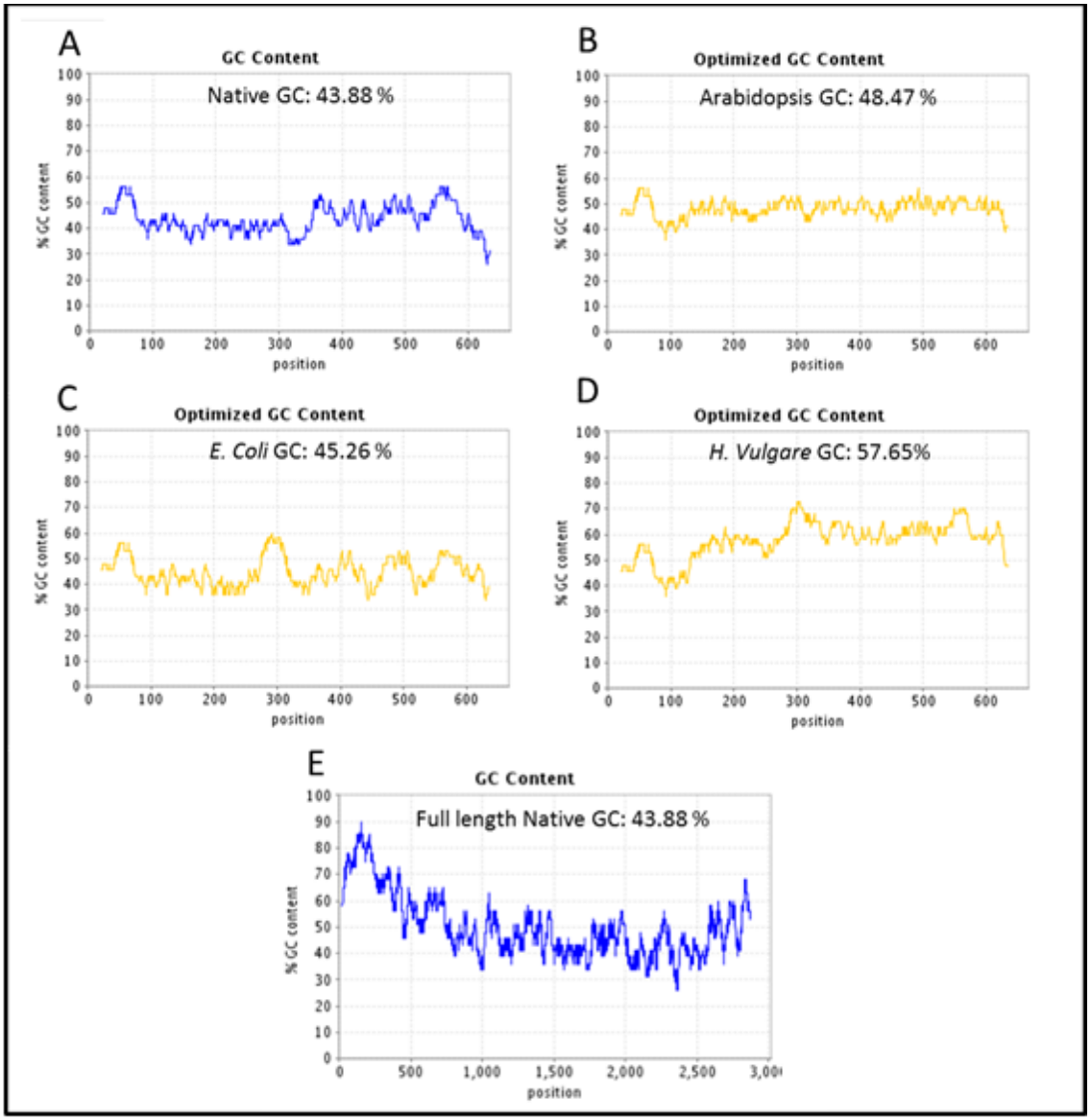

Figure 5.15 GC base content of full length limit dextrinase and fragment gene sequences.
A. GC Content of native LD bps 1434-2046 **B**. GC Content of LD bps 1434-2046 optimised for Arabidopsis codon usage. **C**. GC Content of LD bps 1434-2046 optimised for *E. coli* codon usage. **D**. GC Content of LD bps 1434-2046 optimised for Barley codon usage. **E**. GC Content of full length native Barley LD.

5.3.3 Limit Dextrinase was Successfully Cloned into Gateway Entry Vectors

Previous literature suggests that barley LD has a putative transit peptide (Burton et al., 1999, Kristensen et al., 1999b). Mature barley LD has been shown, by N-terminal sequencing, to start at sequence ATQ, however 50 % of sequenced LD lacked the residues ATQ and began with the amino acids AFM (Figure 5.16, orange letters, dotted line) (Kristensen et al., 1998). Kristensen suggested MAV as the start point of the amino acid sequence (Figure 5.16, blue letters, dashed line) (Kristensen et al., 1999b), however this gene is shorter than that identified by Burton who proposed the protein to begin with MPM (Figure 5.16, green letters, solid line) (Burton et al., 1999). Interestingly the first exon in the barley LD gene codes from residues MPM to ATQ (Figure 5.16, green and orange codons) however a methionine residue would be required as the first residue for translation if this first exon was to be skipped, this is not the case.

Figure 5.16 DNA and corresponding protein sequence of the N-terminal section of limit dextrinase. Green letters and solid line corresponds to the starting Met proposed by Burton. Blue letters and dashed line shows start the starting Met proposed by Kristensen. Orange letters and dotted line show the N-terminal amino acids of mature LD identified by MS. (*) indicates the proposed N-terminal transit peptide cleavage sites identified by ChloroP software.

The gene for full length LD cDNA was subjected to analysis using sub-cellular localisation (Protein Prowler) (Bodén and Hawkins, 2005), secretion (SignalP-4.1) (Petersen et al., 2011) and chloroplast (ChloroP-1.1) (Emanuelsson et al., 1999) prediction software in order to determine the point at which to truncate the DNA to give a truncated protein product. SignalP predicted no secretory peptide present in the N-terminal domain of full length LD (Figure 5.17, A). Prowler indicated that that there was a 63 % chance that the transit peptide encoded a chloroplast targeting sequence (Figure 5.17, B). The peak of the chloroplast targeting sequence was the M residue present in the MAV sequence. ChloroP predicted a chloroplast targeting sequence with a length of 68 amino acids when the full length LD was analysed. The truncated, LD sequence, starting MAV, gave no strong prediction for any specific localisation. Other plants sequences for LD show the presence of the putative transit peptide (Table 5.6). In Arabidopsis LD has been shown to be plastid localised using proteomics (Zybailov et al., 2008). Alignment of the first 90 amino acids of barley and Arabidopsis LD shows 22 % identity meaning the two sequences are not considered significantly similar. There are, however, common features that are similar between both sequences including the presence of a semi-conserved consensus sequence for chloroplast transit peptide cleavage (Gavel and Von Heijne, 1990, Zybailov et al., 2008). This motif, (V/I)-X-(A/C)-A, is present in the barley LD N-terminal sequence- VSAA (Figure 5.16, *). The whole LD protein sequences for barley and Arabidopsis have 58 % identity when aligned. The MAV sequence was chosen as the point of truncation as this was sufficient to stop predicted chloroplast targeting in ChloroP and has previously been successfully expressed in *Pichia pastoris* (Vester-Christensen et al., 2010b).

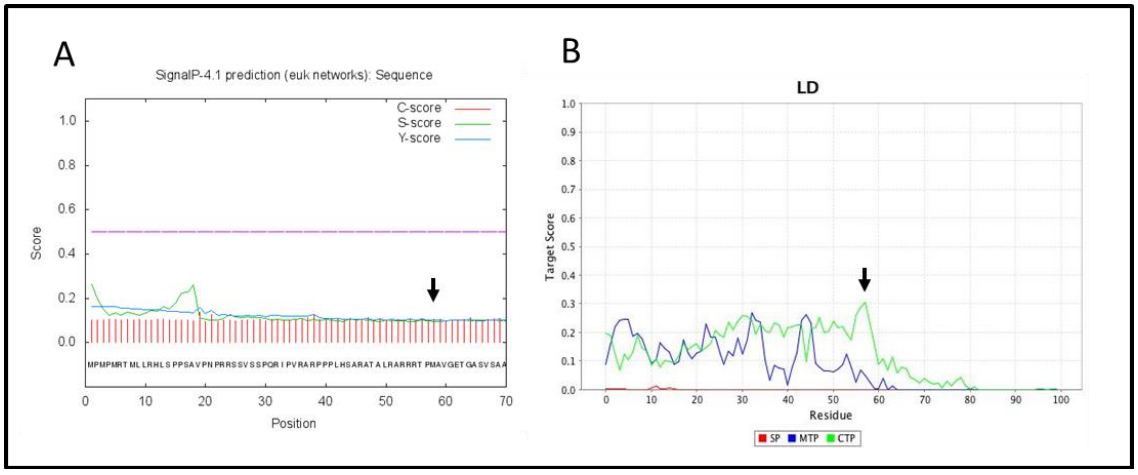

Figure 5.17 Subcellular localisation signal prediction for limit dextrinase.
A. Protein secretion signal prediction performed on the full length LD sequence using SignalP software shows no sign of a secretory peptide. **B.** Protein subcellular localisation prediction performed on the full length LD sequence using Prowler shows that the N-terminus likely encodes a plastid transit peptide. SP- signal peptide, MTP- mitochondrial transit peptide, CTP- chloroplast transit peptide. Arrow indicates proposed truncation point.

Organism	Accession	Length	Score	cTP	cTP- length
Triticum aestivum	ABL84490.1	963	0.585	Yes	69
Oryza sativa	BAA09167.1	986	0.577	Yes	73
Arabidopsis thaliana	AED90732.1	965	0.585	Yes	62
Setaria italica	XP_004975057.1	958	0.585	Yes	45
Sorghum bicolor	EES10414.1	966	0.59	Yes	47
Vitis vinifera	XP_002271820.3	956	0.588	Yes	46
Hordeum vulgare	AAD34347.1	962	0.588	Yes	68

Table 5.6 Analysis of plant limit dextrinase protein sequences for the presence of N-terminal chloroplast transit peptides.
Calculated using ChloroP software. cTP- chloroplast transit peptide.

A PCR, using gene synthesis LD DNA as a template, was performed to amplify LD with and without the putative transit peptide, variations of these were created with and without stop codons. The correct amplicon sizes were obtained (Table 5.7 and Figure 5.18). Further to this, the putative transit peptide alone was also PCR amplified- LD transit peptide 171 bp (gel not shown). These five PCR products were cloned into entry vector pCR8-TOPO-GW (Figure 5.18). This set of gene variations enables cloning into Gateway compatible vectors for different purposes. Constructs containing the correct sequences were obtained after a number of screening rounds.

Name	Abbreviation	Size (bp)	Primers
Full length LD	LD-FL	2889	MR3, MR4
Full length LD with no stop codon	LD-NS	2886	MR3, MR9
LD with no transit peptide	LD-NP	2718	MR 12, MR4
LD with no transit peptide with no stop codon	LD-NPNS	2715	MR12, MR9
LD transit peptide with no stop codon	LD-TP	171	MR3, MR46

Table 5.7 Limit dextrinase gene constructs created by PCR.

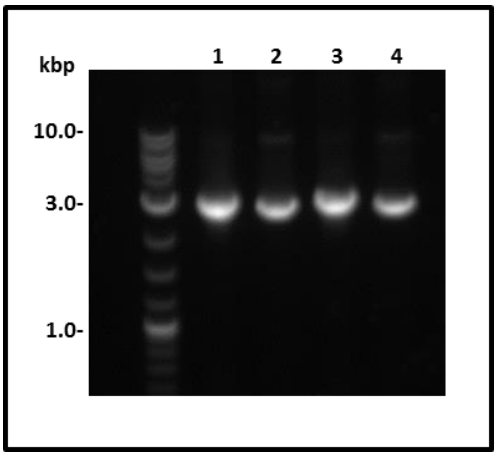

Figure 5.18 Agarose gel of PCR of gene variants of limit dextrinase for cloning.
Agarose gel of LD PCR products. Lane 1 LD-FL, lane 2 LD-NS, lane 3 LD-NP, lane 4 LD-NPNS (see for full details of genes).

5.3.4 Limit Dextrinase was Cloned into Protein Expression Plasmids and Overexpression in *E. coli* was Optimised

LD-FL and LD-NP were sub-cloned into vectors pDEST17 and pETG-10A which encode N-terminal hexahistidine fusion proteins. Sub-cloning was performed using Gateway LR clonase which utilises site specific recombination. The plasmid recombination products were expressed in Rosetta and SoluBL21 *E. coli* hosts. The ability of the strains to produce LD in whole cells was tested by SDS-PAGE, to determine the best vector and gene combination for expression. The optimal conditions for expression of protein in whole cells, was LD with no transit peptide (LD-NP) in pDEST17 expressed using SoluBL21 with induction using 0.2 mM IPTG and growth overnight at 28 °C (Figure 5.19, lane 4).

The solubility of LD in the *E. coli* was next investigated. Soluble and insoluble protein fractions were produced and analysed by SDS-PAGE and anti-His_6 western blot. Strain SoluBL21 gave the best expression of soluble LD (Figure 5.19, lanes 5 and 6) according to western blot. Further details on the optimisation of soluble expression are given in the Appendix.

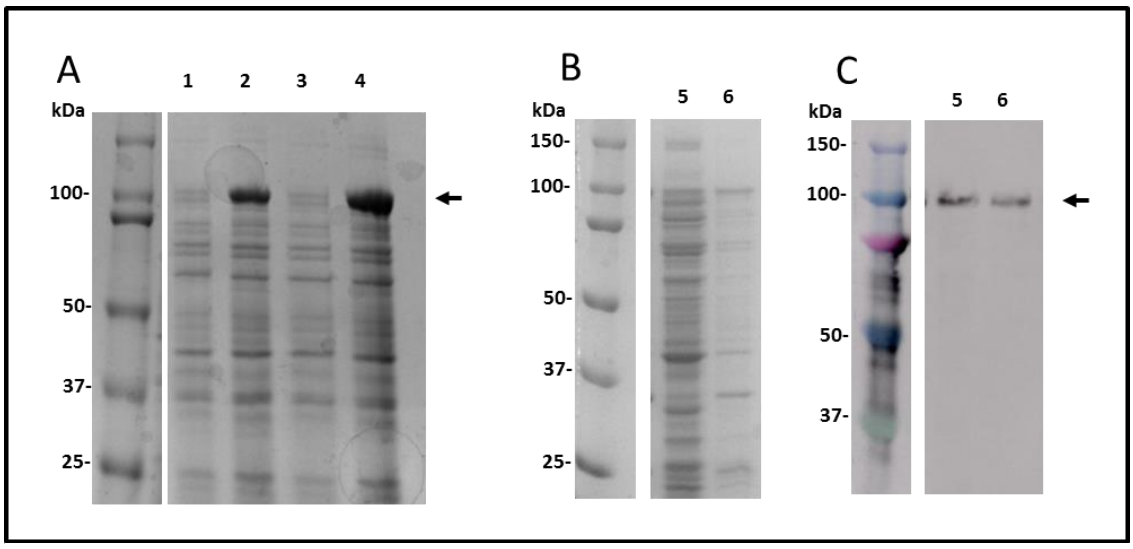

Figure 5.19 Example of limit dextrinase overexpression and solubility screening in *E. coli*.
A. pDEST17 constructs in SoluBL21. Lanes 1&2 correspond to LD-FL, lanes 3&4 correspond to LD-NT expressed at 28 °C overnight. 1&3 are uninduced, 2&4 are induced with 1 mM IPTG. All lanes loaded with the same volume of whole cells. **B.** SDS-PAGE and **C.** Western blot with anti-His_6 antibody of pDEST17-LD-NT construct expressed at 28 °C overnight. 5&6 SoluBL21 strain. 5- soluble fraction, 6- insoluble fraction. LD-NT (101,974 Da) is indicated by an arrows.

5.3.5 Limit Dextrinase was Overexpressed and Purified by Nickel Affinity, β-Cyclodextrin Affinity and Gel Filtration Chromatography

Nickel Affinity Chromatography

LD was cloned into a pDEST17 vector that encodes an N-terminal His_6 tag, thereby enabling purification by nickel affinity chromatography. Protein was expressed in SoluBL21, 8 L cultures of *E. coil*. Soluble protein extract was added to the nickel resin. Non-binding proteins were washed away, small traces of LD were seen in both the flow through and wash (Figure 5.20, A, B, lanes 3-5) this is possibly due to weak binding to the nickel column or column overloading. Bound proteins eluted in one sharp peak upon addition of 500 mM imidazole (Figure 5.20, B). Fractions from purification were analysed by SDS-PAGE and western blot. A band corresponding to the correct mass for His_6-LD (101,974 Da) is present, although degradation products and other proteins appear to have bound to the nickel column. Degradation occurred during the purification process, as whole cell extracts show no signs of degradation. Other proteins may be bound to the resin because the low level of LD produced leaves capacity on the column for other proteins to bind. Activity of LD was shown using RP zymography (Figure 5.20, D)- LD was highly active in elutions from the nickel column.

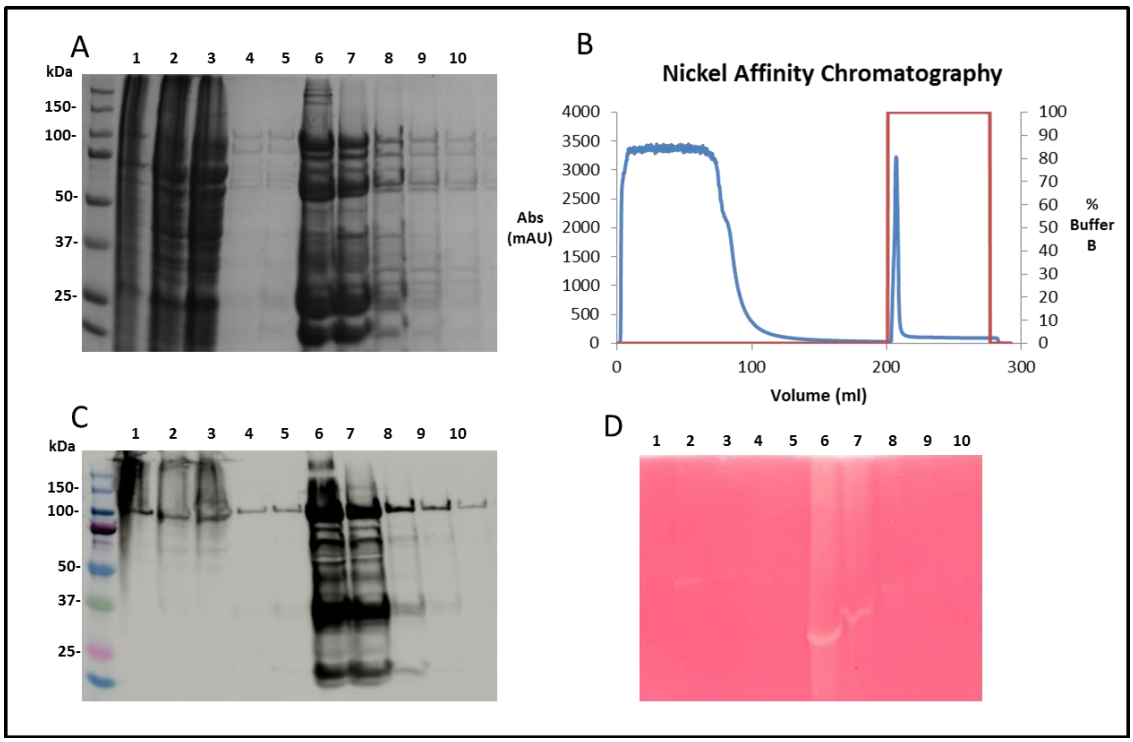

Figure 5.20 Nickel Affinity Chromatography Purification of His-limit dextrinase.
A. SDS-PAGE 12 % gel showing fractions. **B.** Chromatogram showing UV trace and corresponding elution from the column. Purification performed using 5 mL HisTrap column (GE), elution was performed with 500 mM imidazole. 1 CV = 5 mL **C.** Western blot with anti-His_6 antibody. **D.** Red Pullulan zymogram. Lanes: 1- soluble lysate 2- insoluble fraction 3- column flow through, 4&5- wash steps, 6-10- elutions.

Anion Exchange and β-Cyclodextrin Affinity Chromatography

MonoQ anion exchange was attempted to further purify LD from nickel affinity purification however contaminating proteins were not removed, further details are in the Appendix.

The product from nickel affinity chromatography was further purified by β-CD affinity chromatography. A β-CD affinity column was prepared by chemical modification of β-CD to give 6-deoxy-6-amino-β-cyclodextrin (amino-β-CD) and conjugation to NHS-activated Sepharose resin *via* the free amino group of amino-β-CD.

Protein from nickel affinity chromatography was loaded onto the β-CD Sepharose resin. The flow through contained only a very small amount of LD, this is likely mis-folded protein that is not able to bind β-CD (Figure 5.21, A, lane 1). The flow through also contained a large number of other proteins with masses smaller than 100 kDa that had not been removed by the nickel affinity purification step (Figure 5.21, B, lane 2). The column was washed with prior to elution, this was sufficient to remove any traces of non-binding proteins as seen by the absorbance of zero on the chromatogram (Figure 5.21, between 25 mL and 75 mL). LD was eluted from the column by the addition of 7 mM β-CD. Bound protein elutes after 1 CV and eluted over 1 CV as one sharp peak. LD containing elution fractions were combined and buffer exchanged to remove traces of β-CD, which would otherwise inhibit the protein. The β-CD affinity purification process removed the vast majority of contaminating proteins.

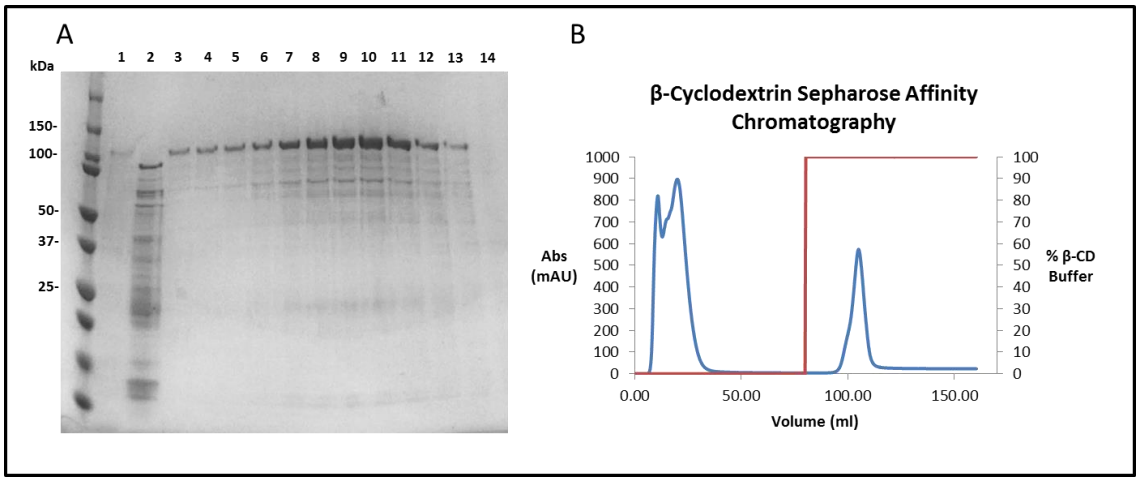

Figure 5.21 β-Cyclodextrin Affinity chromatography of limit dextrinase from nickel affinity purification.
A. SDS-PAGE 12 % gel showing fractions from purification. 1-2- flow through fractions. 3-14- elution fractions. **B.** Chromatogram showing UV trace and elutions. Elution performed with 7 mM β-CD. 1 CV = 25 mL

Gel Filtration

The product from β-CD affinity purification was concentrated and applied to a Superdex S200 gel filtration column. Protein eluted between 75 and 125 mL as one sharp peak (Figure 5.22, B). There is little indication of other proteins on the chromatogram, small peaks at 135 mL and 300 mL can be seen (Figure 5.1, A) however when analysed by SDS-PAGE no protein was identified because the protein concentration was too low. LD eluted over a volume of 50 mL, fractions were combined and concentrated.

A band at 25 kDa is visible by SDS-PAGE (Figure 5.22, A), this has occurred throughout all purification steps. The smaller protein fragment should have been removed by gel filtration and therefore it can be concluded that this fragment is a thermal degradation product produced during the heating step in preparation of samples for SDS-PAGE. Gel filtration was a successful method to obtain pure LD, there is little sign of other proteins on GF elution.

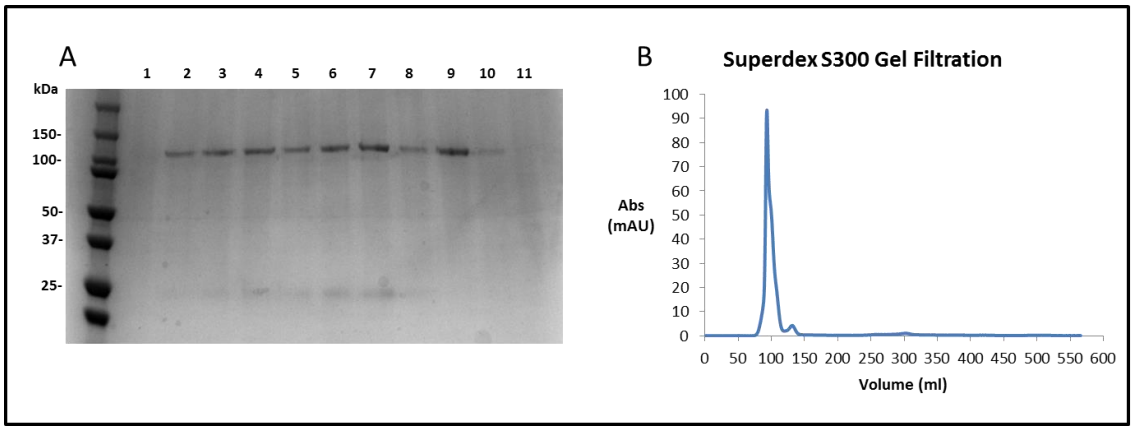

Figure 5.22 Size Exclusion Chromatography on limit dextrinase.
A. SDS-PAGE 12 % gel showing fractions from purification. 1- elution after 50 mL. 2-11- elutions corresponding to 75-125 mL. 1 CV = 320 mL **B.** Chromatogram showing UV trace and elutions fractions were collected when abs went above 0.2 mAU.

5.3.6 Overall Purification of Recombinant Limit Dextrinase to Homogeneity

The overall protein purification procedure is summarised in Table 5.8. The procedure involved expression of LD-NT, harvesting and lysis of cells to produce a soluble lysate which was applied to a nickel affinity column. Proteins eluted from this were added to a β-CD affinity column and further purified. LD was then purified to homogeneity by gel filtration. The activity of LD was analysed throughout the procedure using the Limit Dextrizyme assay (Megazyme). The overall purification procedure enriched LD 75.4 fold.

A large amount of protein was present in the soluble lysate however only a small proportion of this was LD, as identified by activity and SDS-PAGE. A large amount of the LD expressed in *E. coli* is found in the inclusion bodies. The process of nickel affinity chromatography purified the protein 42.3 fold, giving a highly enriched LD sample although numerous contaminating proteins remained present (Figure 5.23, lane). β-CD affinity chromatography produced a 70.5-fold enrichment of LD, producing almost pure protein. Gel filtration removed the trace contaminants left over from β-CD affinity purification, however a large amount of total activity is lost with only a small increase in specific activity. It is possible that the contaminants present after β-CD affinity purification are fragments of LD that possess some form of activity. Nickel affinity purification gives good recovery (94 %) with only 10 % of total activity being lost. During β-CD purification a large, ten-fold, amount of total LD activity is lost. The protein may have been lost during concentration and buffer exchange steps during which some protein can be lost to aggregation or nonspecific binding to membranes. Protein products from each step were visualised by SDS-PAGE and western blot, an increase in LD purity can be seen throughout the purification procedure. The specific activity increases as purity increases (Table 5.1). A band at 25 kDa can be seen throughout the procedure. The presence of LD was confirmed by MS on the SDS-PAGE bands at 101974 Da from β-CD and GF.

Step	Total Protein (mg)	Total Activity (U)	Recovery (%)	Specific Activity (U/mg)	Purification (fold)
Soluble Lysate	1832.40	111.36	100.0	0.1	1.0
HisTrap	40.89	105.19	94.5	2.6	42.3
β-CD-Sepharose	2.36	10.12	9.1	4.3	70.5
Gel Filtration	1.44	6.61	5.9	4.6	75.4

Table 5.8 Purification Table for Recombinant limit dextrinase expressed in *E. coli*
LD activity was analysed using the Limit Dextrizyme assay, following manufacturer's (Megazyme) instructions. Total protein was quantified by Bradford assay with BSA a standard.

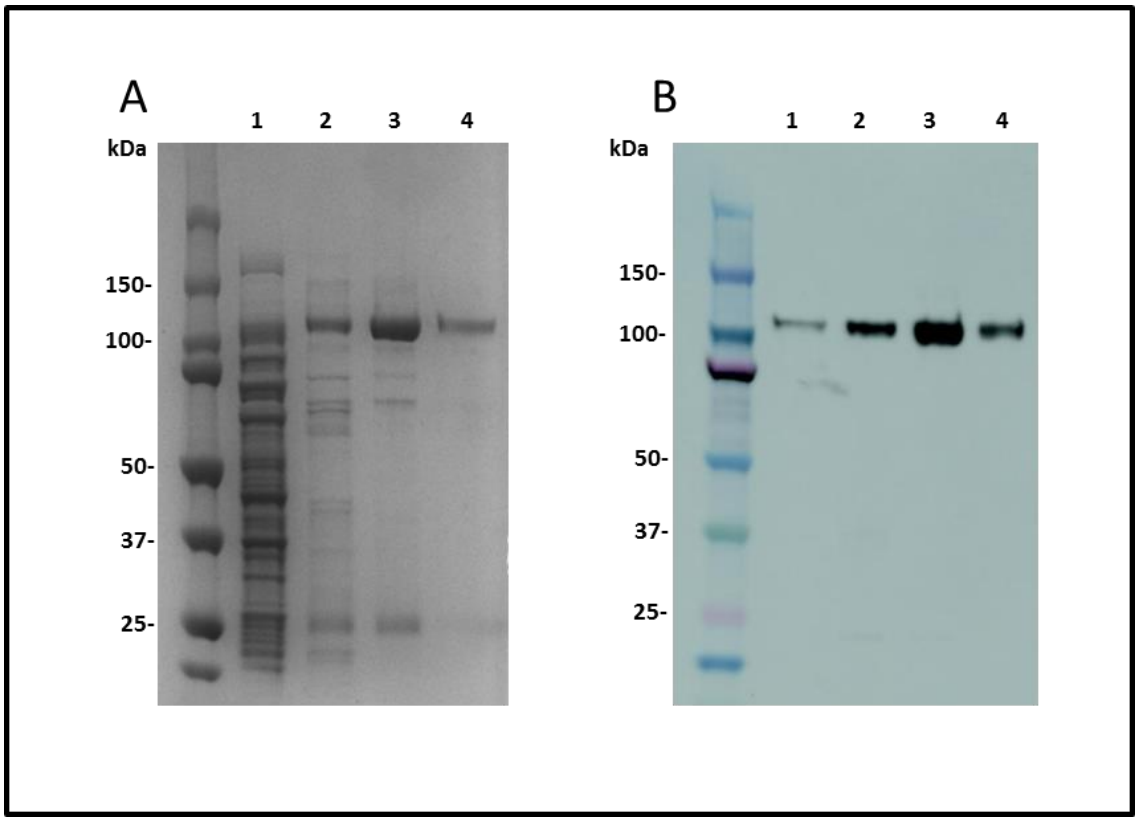

Figure 5.23 Overall purification of His-tagged limit dextrinase.
A. SDS-PAGE 12 % gel showing products from purification steps. **B.** Western blot with anti-His_6 antibody. 1- Soluble lysate from *E. coli*. 2- Product from nickel affinity chromatography. 3- Product from β-CD affinity chromatography. 4- Product from gel filtration.

5.3.7 Production of Polyclonal Antibodies against Limit Dextrinase

Antibodies were raised using recombinant LD produced in *E. coli*. Antibody production was performed in two rabbits (Eurogentec). Four immunisations were performed at days 0, 14, 28, 56. Four bleeds were taken at days 0 (pre-immune), 38 (small bleed), 66 (large bleed), 87 (final bleed). An ELISA was performed on the bleed samples from both rabbits. LD was adsorbed to an ELISA plate, blocked to prevent non-specific binding, incubated with sera dilutions, then incubated with anti-rabbit HRP conjugate secondary antibody. Figure 5.24 demonstrates that the sera raised against LD has activity against the recombinant protein bound to the surface of the ELISA plate. Pre-immune sera from both rabbits shows little activity towards LD. These sera represent the background binding of rabbit sera prior to immunisation and show that the polyclonal antibodies lack pre-existing activity. Any activity observed by the sera following immunisation represents specific activity of the antibodies towards LD. Small bleed and final bleed sera from both rabbits show a strong activity at high to medium concentrations. Rabbit 03 shows an increase in response between the small bleed (38 d) and final bleed (87 d) this is due to an increased antigen exposure time leading to a stronger immune response. The anti-LD sera from both rabbits have good affinity for LD and can be utilised in further analyses.

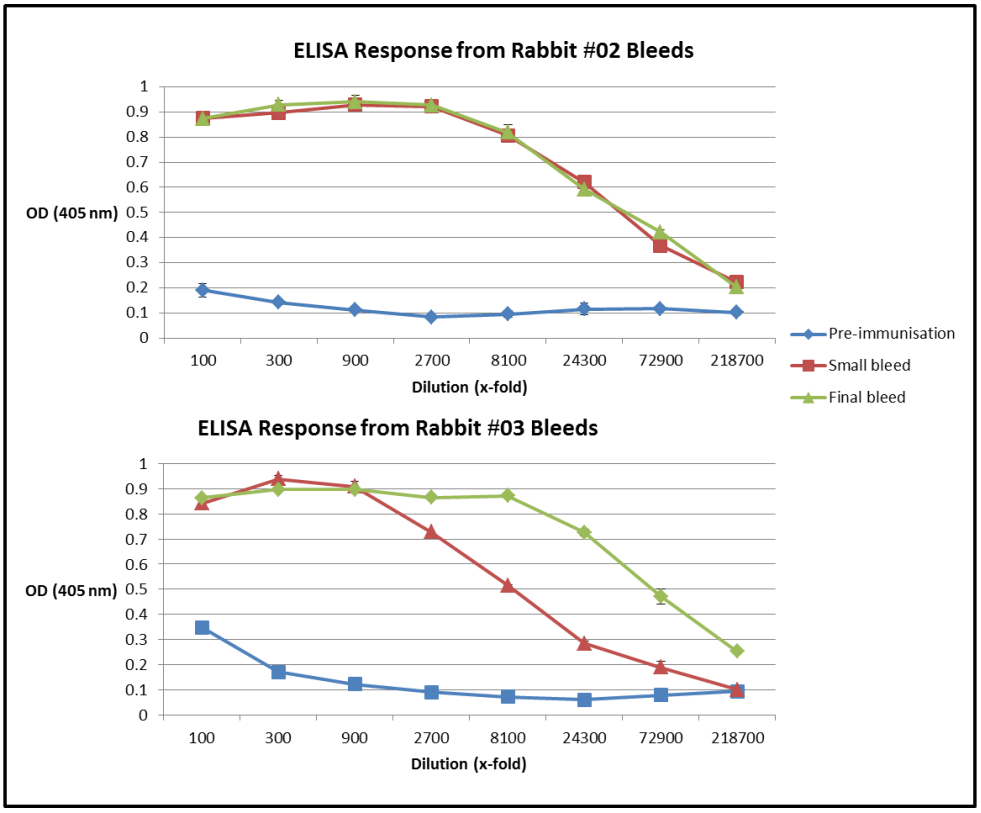

Figure 5.24 ELISA of rabbit sera activity against recombinant limit dextrinase produced in *E. coli*. Blue- preimmune sera (0 d), red- small bleed (38 d) green- final bleed (87d). Data was recoded in triplicate using ELISA protocol.

The following section describes the work performed on the proteinaceous inhibitor of limit dextrinase- LDI. This protein is proposed to be responsible for low levels of LD activity. To analyse the interaction between the two proteins *in planta* recombinant protein was generated used and raise antibodies.

5.3.8 The Gene Encoding Limit Dextrinase Inhibitor was Detected in Barley

The total barley RNA samples used for the attempted cloning of LD were utilised for the cloning of LDI. RNA from 0 dpi and 3 dpi endosperm were utilised in an RT-PCR to successfully amplify the 444 bp gene encoding LDI (
Figure 5.25, lanes 1&2).

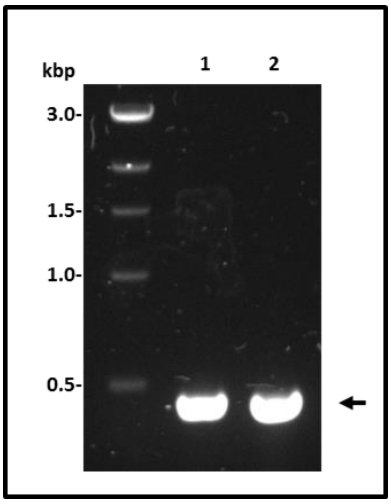

Figure 5.25 Agarose Gel of PCR amplified limit dextrinase inhibitor from barley mRNA.
Amplicons produced using mRNA from, Lane 1- 0 dpi endosperm, Lane 2- 3 dpi endosperm.

5.3.9 Limit Dextrinase Inhibitor was Cloned from Barley mRNA into Gateway Compatible Entry Plasmids

The LDI sequence (acc. DQ285564.1) was analysed using SignalP-4.1, Protein Prowler and ChloroP-1.1 software to identify the presence of any localisation signal. A secretion signal was identified when full length LDI was analysed by SignalP (Figure 5.27, A). The cleavage site identified was VAAA/TLE (Figure 5.27, arrows). This cleavage point has been experimentally validated by N-terminal sequencing of mature LDI from barley (Figure 5.26) (Macgregor et al., 2000). The cleavage product, beginning TLE when re-analysed with SignalP produces no indication of a secretion signal. Protein prowler analysis supports the SignalP prediction (Figure

5.27). ChloroP showed no indication of a chloroplast transit peptide. TLE was chosen as the cleavage point for the production of LDI genes with and without secretory peptide.

```
atggcatccgaccatcgtcgcttcgtcctctccggcgccgtcttgctctcggtcctcgcc
 M  A  S  D  H  R  R  F  V  L  S  G  A  V  L  L  S  V  L  A
gtcgccgccgccacgctggagagcgtcaaggacgagtgccaaccaggggtggacttcccg
 V  A  A  A  T  L  E  S  V  K  D  E  C  Q  P  G  V  D  F  P
cataacccgttagccacctgccacacctacgtgataaaacgggtctgcggccgcggtccc
 H  N  P  L  A  T  C  H  T  Y  V  I  K  R  V  C  G  R  G  P
agccggcccatgctggtgaaggagcggtgctgccgggagctggcggccgtcccggatcac
 S  R  P  M  L  V  K  E  R  C  C  R  E  L  A  A  V  P  D  H
tgccggtgcgaggcgctgcgcatcctcatggacggggtgcgcacgccggagggccgcgtg
 C  R  C  E  A  L  R  I  L  M  D  G  V  R  T  P  E  G  R  V
gttgagggacggctcggtgacaggcgtgactgcccgagggaggagcagagggcgttcgcc
 V  E  G  R  L  G  D  R  R  D  C  P  R  E  E  Q  R  A  F  A
gccacgcttgtcacggcggcggagtgcaacctatcgtccgtccaggagccgggagtacgc
 A  T  L  V  T  A  A  E  C  N  L  S  S  V  Q  E  P  G  V  R
ttggtgctactggcagatggatga
 L  V  L  L  A  D  G  -
```

Figure 5.26 DNA and protein sequence of limit dextrinase inhibitor.
Green letters and solid line correspond to the starting Met proposed by (Stahl et al., 2007). Blue letters and dashed line represents the cleavage site of the proposed secretory peptide (Macgregor et al., 2000).

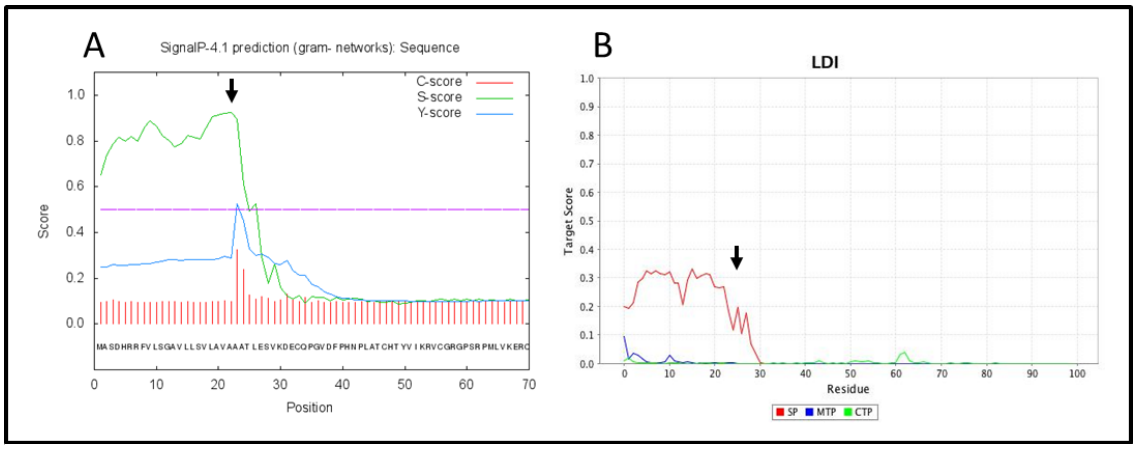

Figure 5.27 Subcellular Localisation Signal Prediction for limit dextrinase inhibitor.
Protein secretion signal prediction performed on the full length LDI sequence using **A.** SignalP software, **B.** Protein Prowler, SP- signal peptide. MTP- mitochondrial transit peptide, CTP- chloroplast transit peptide. Arrow shows predicted secretory peptide cleavage point.

An RT-PCR reaction was performed, using 0 dpi endosperm RNA as the template. The LDI gene with and without putative secretory sequence were amplified with and without stop codons (Table 5.9). The product of the PCR for each gene can be seen in, D. The secretion signal alone was also amplified however this amplicon is small (69 bp) and not easily visualised by agarose gel electrophoresis. The five PCR products were cloned into pCR8-TOPO-GW using TOPO cloning. Constructs containing the correct sequences were obtained after screening. Sequencing revealed one natural polymorphism (C62T) when compared with accession DQ285564.1. This causes a V21A change to the protein sequence. SNPs similar to this have been identified in LDI genes from numerous wild barley cultivars (Huang et al., 2014).

Name	Abbreviation	Size (bp)	Primers
Full length LDI	LDI-FL	444	MR5, MR6
Full length LDI with no stop codon	LDI-NS	441	MR5, MR10
LDI with no secretion peptide	LDI-NP	375	MR13, MR6
LDI with no secretion peptide with no stop codon	LDI-NPNS	372	MR13, MR10
LDI secretion peptide with no stop codon	LDI-SP	69	MR5, MR36/37

Table 5.9 Limit dextrinase inhibitor gene constructs created by PCR.

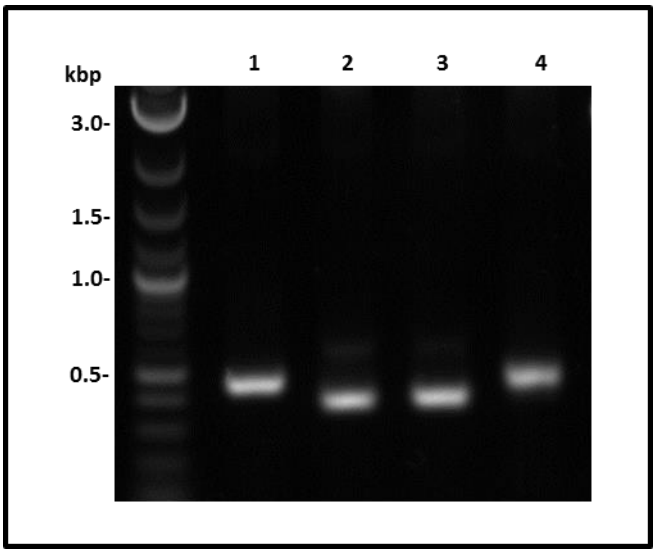

Figure 5.28 PCR of limit dextrinase inhibitor gene variants for cloning.
Agarose gel of LDI PCR products. Lane 1 LDI-FL, lane 2 LDI-NS, lane 3 LDI-NP, lane 4 LDI-NPNS (see Table 5.9).

5.3.10 Limit Dextrinase Inhibitor was Cloned into Protein Expression Vectors and Insoluble Protein was Expressed

LDI-FL and LDI-NS were sub-cloned into hexahistidine fusion vectors pDEST17 and pETG-10A. Sub-cloning was performed by Gateway LR cloning. Vectors harbouring the correct sequences were transformed into Rosetta and SoluBL21 *E. coli* expression hosts. The strains ability to express LDI in whole cells was tested by SDS-PAGE, to determine the best vector and gene combination for expression alongside the optimal IPTG concentration and growth temperature. The optimal conditions for expression, in whole cells, was LDI-NS in pDEST17 expressed using SoluBL21 at 28 °C overnight (Figure 5.29, A, lane 4).

The solubility of LDI in *E. coli* strains was next investigated. Soluble and insoluble protein fractions were generated and analysed using SDS-PAGE and anti-His_6 western blot (Figure 5.29, B and C). No soluble LDI was identified in any *E. coli* strains. Further details on expression screening are in the Appendix.

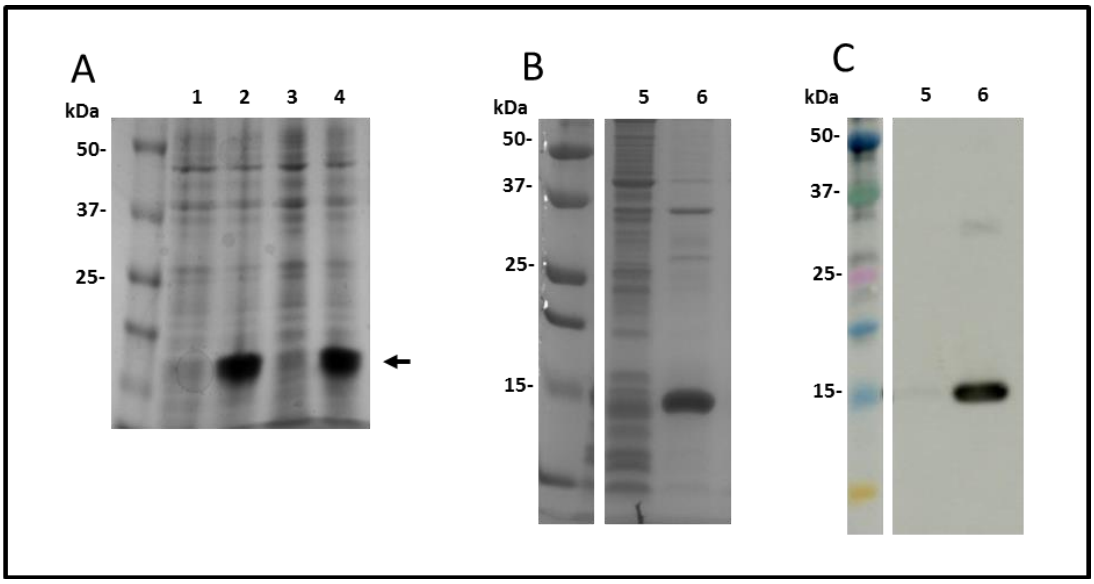

Figure 5.29 Example of limit dextrinase inhibitor overexpression and solubility screening in *E. coli*.
A. pDEST17 constructs in SoluBL21. SDS-PAGE. Lanes 1&2 correspond to LDI-FL (18624 Da), lanes 3&4 correspond to LDI-NS (16318 Da) all expressed at 28 °C overnight. 1&3 are uninduced, 2&4 are induced with 1 mM IPTG. All lanes loaded with the same volume of whole cells. **B&C.** pDEST17- LDI-NS construct expressed in SoluBL21 at 28 °C overnight. **B.** SDS-PAGE **C.** Western blot with anti-His_6 antibody. Lane 5- soluble fraction. Lane 6- insoluble fraction. Lanes loaded with the same volume of cell lysate.

5.3.11 Attempted Expression of Limit Dextrinase Inhibitor as a Secretory Protein

As no soluble protein was produced by cytosolic expression, protein secretion to the periplasmic space was attempted. First secretion was attempted using the secretory peptide present in full length LDI. The previously cloned LDI-NS was cloned into pDEST42 which encodes a C-terminal His_6 tag. Expression was performed in strains Rosetta and SoluBL21. These strains are compatible with periplasmic expression as they lack the plysS lysozyme system which can interfere with secretion. Periplasmic protein fractions were created using cold osmotic shock. The osmotic shock and whole cell fractions were analysed by SDS-PAGE and western blot (Figure 5.30). LDI (20726 Da) could only be identified in the whole cell fractions meaning it had not been secreted. The LDI signal peptide was not sufficient to drive protein secretion in *E. coli*.

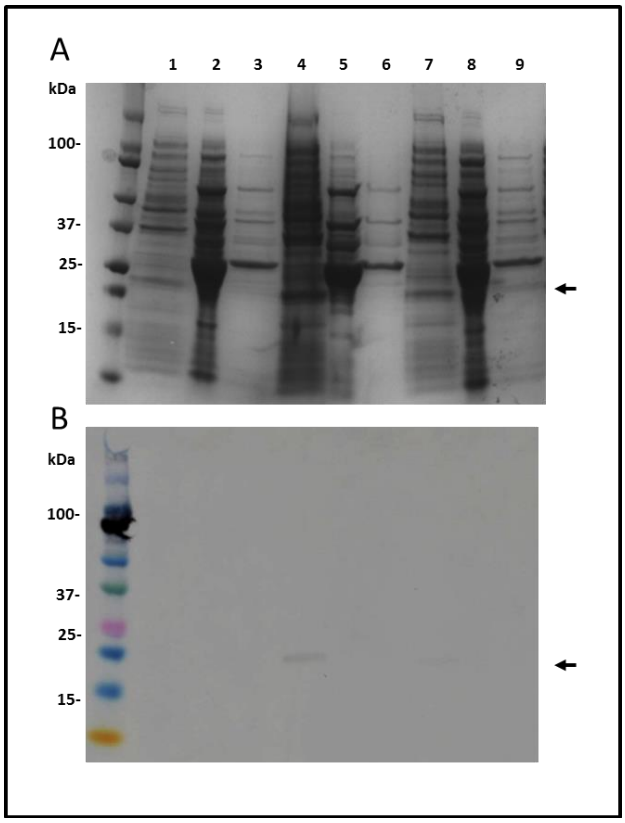

Figure 5.30 Gel of attempted periplasmic expression of limit dextrinase inhibitor using the native plant secretory peptide.
A. SDS-PAGE **B.** Western blot with anti-His_6 antibody. Lanes correspond to the following: 1-6 SoluBL21 and 7-9 Rosetta. Lanes 1, 4, 7- whole cells. 2, 5, 8- concentrated periplasmic fraction. 3, 6, 9 dilute periplasmic fraction LDI (20726 Da) is only present in whole cells according to western blot.

As LDIs own secretion signal was not sufficient to enable periplasmic expression LDI-FL was cloned into pOPIN27b- a derivative of pET27b that encodes a PelB secretion signal as well as a C-terminal His_6 tag. Expression was performed in Rosetta and SoluBL21. Whole cell, concentrated and dilute periplasmic fractions were analysed by SDS-PAGE and western blot

Figure 5.31. No expression could be seen at the correct size (16,318 Da). LDI could not be targeted to the periplasmic fraction using the PelB secretion signal.

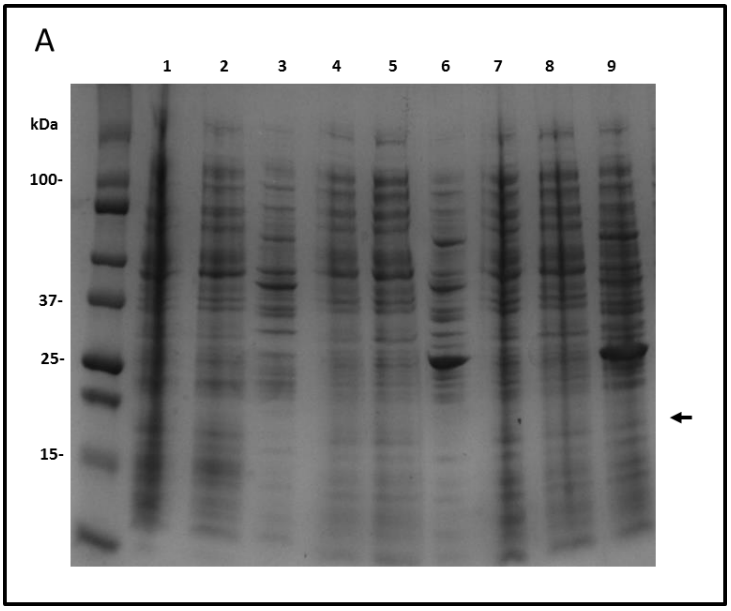

Figure 5.31 SDS-PAGE gel of attempted periplasmic expression of limit dextrinase inhibitor in *E. coli* using the PelB secretory peptide.

SDS-PAGE gel. Lanes correspond to the following: 1-6 SoluBL21 and 7-9 Rosetta. Lanes 1, 4, 7- uninduced whole cells. 2, 5, 8- induced whole cells. 3, 6, 9 dilute periplasmic fraction LDI (20726 Da) is not present according to western blot (not shown). Arrow indicates where LDI should be seen.

5.3.12 Insoluble Limit Dextrinase Inhibitor was Purified and Refolded

Purification and refolding by dilution in redox buffer

As no method for producing soluble LDI was achieved, a protocol for solubilisation, purification and refolding was established. Insoluble LDI was produced in SoluBL21 and solubilised using urea and β-ME. The solubilised sample was refolded by dilution in a cysteine-cystine redox system that catalyses disulfide exchange and therefore rearranges the linkages found within the protein. Soluble product was concentrated by nickel affinity chromatography. The elution from the nickel column was subjected to SDS-PAGE in both reducing and non-reducing conditions. Non-reducing conditions reveal the existence of three separate species (Figure 5.32, A, arrows) with masses ranging from ~13-18 kDa. These bands correspond to different intramolecular disulfide linkage combinations. A 32 kDa dimer is also present alongside higher order multimers corresponding to inter protein disulfide bonds or covalent multimers. The different species became one diffuse band under reducing conditions (Figure 5.32, B), the breakdown of disulfide bonds produces only one species of unfolded and reduced LDI. The gels show that the refolding process generated a number of soluble forms that represent misfolded LDI. The LDI from this procedure was tested in a Limit Dextizyme assay however it showed no inhibitory activity.

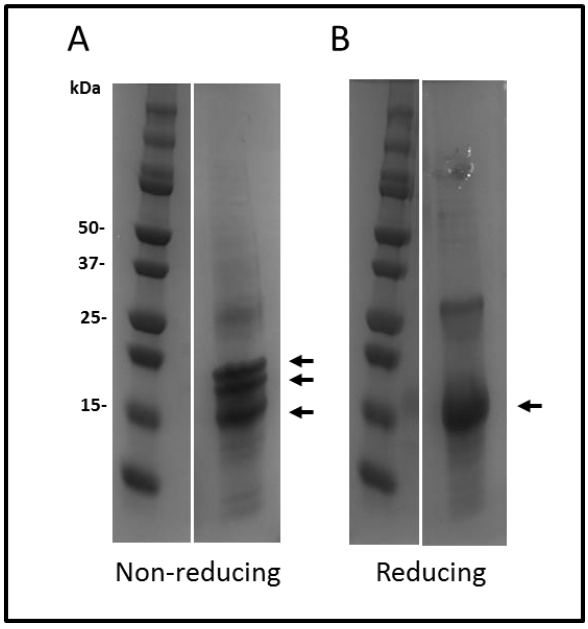

Figure 5.32 SDS-PAGE gel showing refolded limit dextrinase inhibitor.
A. Non-reducing gel **B.** Reducing gel. Arrows indicate forms of LDI.

On-column refolding

As multiple forms of LDI were produced using the refolding by dilution method, an on-column folding method was attempted. β-ME solubilised LDI was loaded directly onto a HisTrap column. The column was washed to remove non-specifically bound proteins. Buffer was slowly added to the column to allow the concentration of β-ME to slowly decrease to support refolding of LDI. Proteins were eluted using 500 mM imidazole. The latter elution fractions contain monomeric and dimeric LDI forms (Figure 5.33, lanes 14-15). LDI is already relatively pure prior to affinity column purification, this method helps refold LDI to the monomeric form which can be seen by the decrease in larger proteins in the elution and the increase in LDI protein at 16 kDa (Figure 5.33, lanes 13-15). LDI containing fractions were combined and concentrated. Refolding on HisTrap column produced some protein that remained in solution however most protein was prone to aggregation. LDI refolding using a QuickFold protein refolding kit was attempted with the product from on column refolding. Analysis of 15 different refolding buffers showed no enhancement of folding and solubility (Appendix).

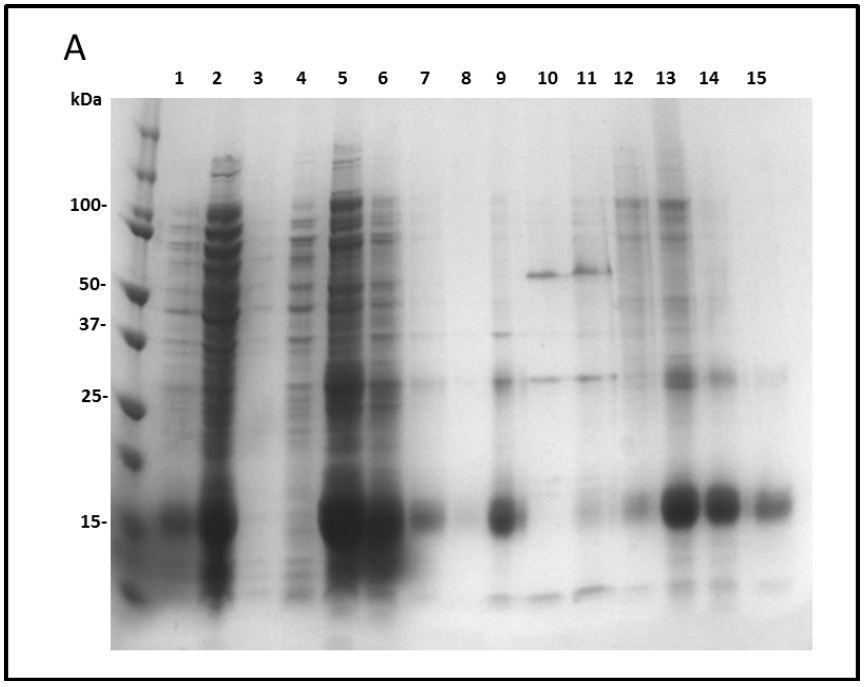

Figure 5.33 Solubilisation and nickel affinity chromatography purification of limit dextrinase inhibitor. SDS-PAGE 12 % gel showing purification fractions. Monomeric form of the protein can be seen at 16 kDa. Lanes 1-6 pre-loading onto nickel resin, 7-9 flow though, 10-11 wash steps 12-15 elution steps.

MonoQ anion exchange chromatography was attempted to further purify LDI from on column refolding (Appendix). The protein added to the MonoQ column and the elutions were almost identical, only one large peak was produced. It was therefore concluded that LDI had been purified to homogeneity by the previous steps.

5.3.13 Overall Purification and Solubilisation of Limit Dextrinase Inhibitor

LDI was purified by an overall procedure involving extraction of insoluble material from *E. coli* followed by solubilisation of the disulfide linked aggregate using β-ME. The solubilised LDI was concentrated and refolded using column assisted refolding with a nickel affinity resin. Protein quantification was hampered by the lack of any aromatic residues within the protein, alongside the tendency to aggregate. Estimates of protein concentration were made using densitometry on an SDS-PAGE gel alongside BSA standards of known concentration. It was estimated that 4 mg of protein were purified from 4 L of *E. coli* culture.

The LDI produced by this procedure is prone to aggregation. Incubation at room temperature leads to the reformation of aggregates (Figure 5.34, A, lane 2) with sizes which correspond to multiples of LDI (16, 32, 48, 64, 80, 94 kDa). Some LDI remained soluble and could be separated from insoluble material by centrifugation. This protein was used for the generation of antibodies for LDI. Inclusion of this protein in a limit dextrizyme assay for LD resulted in no inhibition.

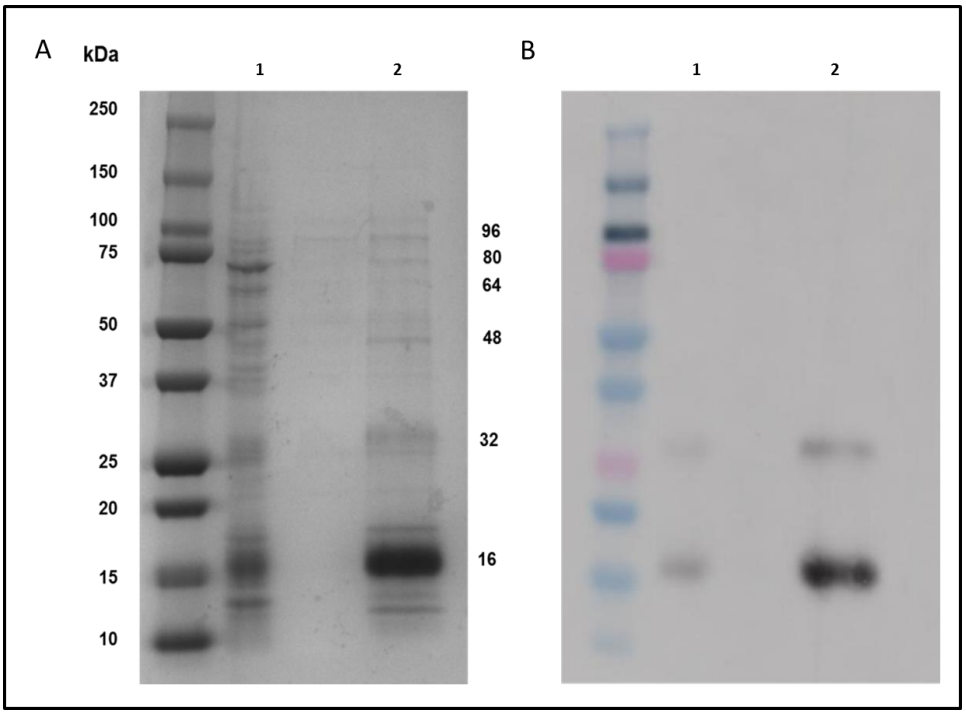

Figure 5.34 Purification of His-tagged limit dextrinase inhibitor.
A. SDS-PAGE 12 % gel. **B.** Western blot with anti-His_6 antibody. Lanes correspond to, 1- Protein from solubilisation using β-mercaptoethanol. 2- Protein following purification using nickel affinity chromatography and incubation at room temperature for 2 days.

5.3.14 Production of Antibodies for Limit Dextrinase Inhibitor

Antibodies were raised using recombinant refolded LDI produced in *E. coli*. Protein was combined with adjuvant and administered to two rabbits over a period of three months. Antibody production was performed by Eurogentec. Four immunisations were performed on days 0, 14, 28, 56. Four bleed samples were taken at days 0 (pre-immune), 38 (small bleed), 66 (large bleed), 87 (final bleed). An ELISA was attempted on the bleed samples from both rabbits however issues arose due to the insoluble nature of recombinant LDI. The protein would not adsorb to the ELISA plate and therefore gave low immunogenic readings. To overcome the insolubility issues caused by recombinant LDI a western blot was performed using recombinant LDI, blot slices were incubated with different sera at different concentrations. Both rabbits produce sera that is able to detect LDI, whereas the pre-immune sera does not detect LDI Figure 5.35.

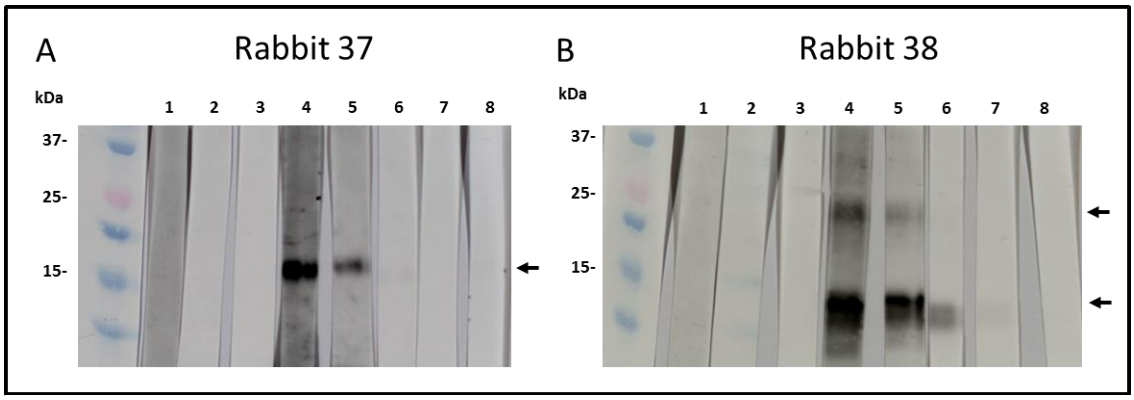

Figure 5.35 Western blot on limit dextrinase inhibitor produced in *E. coli*. using rabbit sera antibodies raised against the recombinant protein
Strips from western blot were incubated with different concentrations of sera. Lanes: Pre- immune 1. 1/100. 2. 1/1000. 3. 1/10000. Large bleed 4. 1/10. 5. 1/100. 6. 1/1000. 7. 1/10000. 8. No primary control.

5.4 Discussion

This chapter presents the first detailed outline of the production of recombinant LD and LDI in *E. coli*. In order to achieve this, the genes encoding LD and LDI were obtained by gene synthesis and cloning, respectively. The genes were cloned into *E. coli* expression vectors and protein expression was optimised. The proteins were purified and utilised for the generation of polyclonal antibodies.

5.4.1 The Gene Encoding Limit Dextrinase

The large gene, encoding LD was produced by Gene synthesis. Methods to obtain the full length gene from germinating barley grains failed. Previous cloning of the full length gene outlined in the literature involved lengthy efforts which utilised cDNA libraries or fragment based cloning and ligation (Kristensen et al., 1999a). Strategies similar to these were attempted but yielded only fragments of the cDNA sequence. LD is a large gene (11 kbp) with 27 introns that are spliced to produce a cDNA of 2,889 bp (Burton et al., 1999). The struggle in cloning was likely due to a combination of the length of the gene and the high number of introns. The LD gene has a high GC content which may form secondary structures that can block polymerase activity and prevent amplification. Low transcript levels may also contribute to the inability to amplify full length LD.

Gene synthesis of the cDNA for native barley (i.e. non-codon optimised) LD was hampered as the sequence was not well tolerated by *E. coli*, with one gene section giving repeated mutations in independent transformants. The portion of the gene causing mutations was analysed, however, there was no obvious explanation for the mutations. Furthermore, extremes of GC/AT content, as seen within the LD gene, can cause issues during gene synthesis. A correct LD sequence was obtained in one colony and the gene was successfully synthesised. A codon optimised version of the gene would likely make gene synthesis easier and may be better for *E. coli* expression. However, due to length of the gene, synthesis was costly and it was decided that the native barley gene would be of more use for expression in other hosts.

A putative chloroplast transit peptide has been identified within the N-terminal protein sequence of LD, the significance of this targeting sequencing has not yet been studied within plants. The generation of vector constructs containing LD with and without the putative cTP now enables experiments to gain a better understanding of LD localisation.

5.4.2 The Gene Encoding Limit Dextrinase Inhibitor

The gene encoding LDI was easily amplified from barley mRNA, this is likely due to its small size (444 bp) and the absence of introns within its gene sequence (Stahl et al., 2007). Others have reported the cloning of LDI, the procedures described suggest cloning was problem free (Jensen et al., 2011, Stahl et al., 2007). The LDI transcript is present in endosperm mRNA at both 0 and 3 dpi. It has been proposed that the LDI transcript is not expressed during germination (Stahl et al., 2007). However, there is a possibility that small amounts of transcript remain present from grain filling, these can be amplified by RT-PCR.

To date LDI has only been identified in the gene sequence data for wheat, brachypodium, rice and barley. Searches performed with the full length protein or gene sequences against other plant genomes transcriptomes and proteomes, including sorghum, tef, and millet, yielded no significant hits. There is a possibility that LDI is only found within a small group of closely related grasses. LD has been identified in both dicot and monocot species, as such it is not clear why some plants would require LDI when others do not. The protein family to which LDI belongs has a common fold which is used for multiple purposes including antimicrobial defence, cell wall metabolism and signal transduction (Svensson et al., 2004, Yeats and Rose, 2008, Maldonado et al., 2002, Liu et al., 2015). It is possible that this protein fold acts as a general scaffold with variable loops that have evolved to perform a range of functions (Jang et al., 2008).

5.4.3 The Heterologous Overexpression and Purification on Limit Dextrinase

A recent publication, published whilst this work was ongoing, outlined the use of *E. coli* for the production of pure LD for the use in crystallography (Møller et al., 2015b). However, no details on expression optimisation and conditions were given, except that a codon-optimised version of the LD gene was used. Within this study a non-codon optimised (i.e. the native barley sequence) gene for LD was utilised to generate soluble protein.

When expressed in *E. coli*, a large proportion of the LD produced is found in an insoluble form, although low levels of active soluble protein are present and can be purified. The insolubility issues were overcome to some extent by using SoluBL21, an *E. coli* strain developed to give better soluble expression. The likely explanation for the insolubility of LD in *E. coli* is that it is a large, multi-domain protein, which is prone to incorrect folding. Expression at 37 °C does not give high yield of active protein and produces higher levels of aggregated and precipitated protein. Decreasing the growth temperature from 37 °C to 28 °C and reducing the IPTG

concentration used for induction of protein synthesis, from 1 mM to 0.2 mM, generated increased levels of soluble protein. Furthermore, expression of genes containing high levels of rare codons can deplete the *E. coli* tRNA pools and lead to sub-optimal translation that can cause protein misfolding. This issue can be overcome by the use of strains that contain extra tRNAs for rare codons as outlined in this study, however the gold standard for expression is the use of a gene that is codon optimised for expression in *E. coli*.

Previous purification of LD, expressed using *Pichia*, involved an untagged protein which was purified by β-CD affinity and GF (Vester-Christensen et al., 2010b). This simple two step purification method was enabled by the secretion of the protein into the culture supernatant which therefore enriched the protein sample before purification. The purification of LD outlined within this work involved an additional nickel affinity purification step, this was due to the large number of protein contaminants seen within the cytosol of *E. coli*. It is likely that β-CD affinity chromatography and GF would not be sufficient to remove all contaminants. However, if the *E. coli* crude protein was applied directly to the β-CD the CD coupled to the resin may be hydrolysed or modified by *E. coli* proteins therefore degrading the column.

Anion exchange was attempted as an alternative separation method following a nickel affinity purification step. This procedure gave poor separation of LD, with contaminant proteins from *E. coli* eluting alongside LD. Anion exchange performed on LD following β-CD affinity purification revealed the existence of multiple forms of LD. This type of microhetereogeneity has been described previously with spinach and wheat enzyme (Schindler et al., 2001, Renz et al., 1998, Repellin et al., 2008). This is the first evidence for similar behaviour in the barley protein.

A high level of LD degradation products are present following nickel affinity purification the expected cause of this is proteolysis enabled by incorrect folding. β-CD affinity chromatography works well to remove most contaminants left over from the nickel affinity step, and GF effectively removes all contaminants to produce very pure LD. Throughout the purification procedure a band is seen at 25 kDa, this band is likely a product of LD thermal degradation as it remains present in all samples and is proportional to the amount of LD loaded on a gel. LD has a thermal stability of 65 °C (Møller et al., 2015a), during sample preparation for SDS-PAGE a temperature of 70 °C is used, therefore supporting this argument.

When analysed using the limit dextrizyme assay or red pullulan zymography, the activity of LD expressed in *E. coli* is much lower when compared with *the P. pastoris* expression system. This may arise because of a difference in protein folding within the different hosts, although the longer purification process also introduces more points for loss of protein activity. In terms of quantity *E. coli* produces similar protein levels to *Pichia* grown in regular culture conditions, it is only when fed batch production is used that multi-mg quantities are produced (Vester-Christensen et al., 2010b). *E. coli* does, however, generate higher quantities of LD than purification from barley malt which would be the alternative to recombinant expression.

5.4.4 The Heterologous Overexpression of Limit Dextrinase Inhibitor

LDI was insoluble in all *E. coli* expression conditions tested. Previous expressions of LDI in *E. coli* encountered similar problems, yielding only low levels of insoluble protein. As the protein contains 9 cysteine residues, 8 of which form disulfides, it is likely that incorrect disulfide folding is the reason LDI does not form soluble protein (Trivedi et al., 2009). Evidence for covalent disulfide multimers are seen in non-reducing SDS-PAGE. A covalent dimer is also generated which is resistant to disulfide cleavage using β-ME. Covalent dimers can also form by oxidation of thiol groups (Figure 5.36) (Trivedi et al., 2009) and has been previously identified in this type of protein (Chen et al., 1999, Yoo et al., 2003).When expressed in *Pichia*, secretion and batch feeding enabled the production of high levels of correctly folded LDI, the yeast extracellular environment is conducive to the generation of correctly linked disulfides.

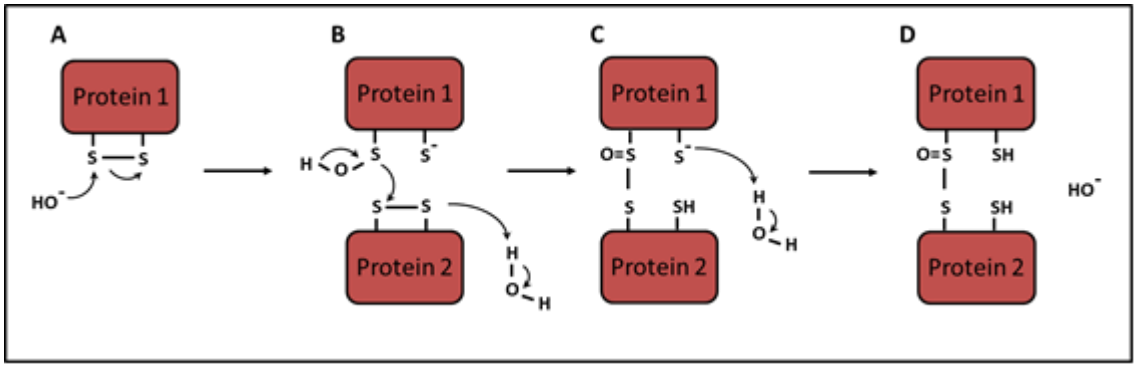

Figure 5.36 The generation of covalent dimers in disulfide containg proteins
A hydroxyl attacks a disulfide bond (**A**) generating sulfinic acid and a thiolate ion (**B**), this can undergo an intermolecular reaction between the sulfur atom of the sulfinic acid group and a disulfide present in another molecule thus producing an intermediate dimer (**C**). This intermediate can form a dimer molecule containing two free thiols (**D**).

The role of the secretion peptide within the LDI protein sequence is unclear. The peptide is yet to be proven to direct secretion however the mature form of LDI found in barley lacks the peptide, implying it is cleaved (Macgregor et al., 2000). Generation of gene constructs with and without the secretory peptide enabled demonstration that the secretory peptide is unable to direct secretion within *E. coli.* It would not necessarily be expected that a Eukaryotic secretion signal could direct protein secretion within a Prokaryote, however there is precedent for crossover between the two systems (Hall et al., 1990, Moeller et al., 2009). Secretion of LDI using the native *E. coli* PelB secretion signal also yielded no recombinant protein in the periplasmic fraction.

A procedure for the solubilisation of insoluble LDI using urea and β-ME was developed. This procedure produced relatively pure LDI because the inclusion bodies of *E. coli* contain high levels of the expressed protein and the extraction process removed the majority of other urea soluble proteins. This solubilised protein was used in refolding experiments by dialysis, dilution or on-column refolding. All methods yielded LDI that would remain in solution for short periods of time however precipitation occurred upon storage for days. There is no overarching method by way to refold proteins and one can easily become embroiled in process of testing numerous different methods. Other disulfide containing proteins, similar to LDI, have been produced in an insoluble form in *E. coli* and refolded in many different ways (Okuda et al., 1997, Lullienpellerin et al., 1994, Dias et al., 2005), though the analysis of refolding yield is limited by analytical techniques. With this type of inhibitor proteins there is no way to easily asses folding. Assays utilise either inhibition of another enzymes activity or the use in variable biological assays. Neither of which give a direct and definitive indication of correct folding. Optimisation of soluble expression within a host or changing host can be much simpler than the protein refolding process.

5.4.5 The Generation of Polyclonal Antibodies Specific for Limit Dextrinase and Limit Dextrinase Inhibitor

The immunisation of rabbits with recombinant LD and LDI enabled the production of protein-specific polyclonal antibodies. When tested in an ELISA the LD antibodies show strong specific binding to recombinant antigen. The LDI antibodies give a good response to recombinant LDI in western blot although issues caused by insolubility give an imprecise result and hamper the use of an ELISA. Both sets of antibodies show a specific response at a 1 in 1000 dilution of sera, when compared to pre-immune sera of the same concentration. There are slight differences

between the binding capability of the sera produced in different rabbits however all are capable of detecting the protein they have been raised against. The antibodies are a useful tool for further studies of LD and LDI *in planta*. Other antibodies have previously been produced for LDI, however these were generated decades ago and have been passed between researchers to the point that their origins have become untraceable (Stahl et al., 2007).

5.5 Future Directions

5.5.1 Understanding the Genes Encoding Limit Dextrinase and Limit Dextrinase Inhibitor

It remains unclear why LD possesses many introns and exons, and how this relates to its function. Only the LD cDNA has been generated and utilised within this study. There may be potential to better understand the gene and its expression by analysis of the promoter, flanking regions and splice sites.

It is yet to be determined whether the putative chloroplast transit peptide of LD and secretory peptide of LDI are important for their function in cereals in the context of the aleurone layer and the leaf. As both genes for LD and LDI were cloned into Gateway compatible entry vectors, cloning into other expression vectors, in order to answer these questions, will be convenient.

5.5.2 Further Optimisation of Limit Dextrinase Protein Expression

There is scope for further optimisation of LD expression and purification to obtain more soluble protein. An *E. coli* codon optimised version of the gene may generate more soluble protein. IPTG concentration, batch induction, additional of osmolytes, growth temperature and other growth media are all avenues for potential optimisation.

Periplasmic expression of pullulanase alongside the addition of betaine and a detergent to the growth media has also been reported to produce high quantity of active protein (Duan et al., 2013, Duan et al., 2015). Periplasmic secretion would also enable a streamlined purification procedure as fewer potential contaminant proteins are present in the periplasmic space compared to inside the cell.

5.5.3 Expression of Limit Dextrinase Inhibitor Protein in a Soluble Form

There are a number of other avenues that can be explored in an attempt to generate correctly folded, soluble, LDI. Further opportunities for optimisation in *E. coli* include the use of other peptides for secretion, the use of disulfide folding strains and the generation of thioredoxin fusion proteins to aid the generation of correct disulfide linkages (Kong and Guo, 2014, De Marco, 2009).

There is already precedent for the production of LDI in *Pichia*, however this expression system requires an expensive batch bioreactor to yield high levels of protein. Expression in another bacterial host which can be easily cultured (in a way similar to *E. coli*) may be possible. One potential host may be *Streptomyces*, which is known to secrete a number of enzymes, and has been used for the secretory expression of disulfide linked heterologous proteins (Tremblay et al., 2002, Lussier et al., 2010). There is also the possibility of expression in plants (*N. benthamiana*) using the pEAQ-HT overexpression system developed at John Innes Centre (Peyret and Lomonossoff, 2013).

5.5.4 Use of Antibodies

Both sets of antibodies have been shown to be able to detect the proteins they have been raised against. This result suggests that the antibodies will be useful for further analysis of native and recombinant-fusion proteins, *in planta*, using techniques such as Co-IP, immunolocalisation and western blots.

5.6 References

Abdullah, M., Catley, B. J., Lee, E. Y. C., Robyt, J., Wallenfe.K & Whelan, W. J. 1966. Mechanism of carbohydrase action .11. Pullulanase an enzyme specific for hydrolysis of alpha-1,6-bonds in amylaceous oligo- and polysaccharides. *Cereal Chemistry,* 43, 111-&.

Abe, J.-I., Hizukuri, S., Koizumi, K., Kubota, Y. & Utamura, T. 1988. Enzymic syntheses of doubly branched cyclomaltoheptaoses through the reverse action of pseudomonas isoamylase. *Carbohydrate Research,* 176, 87-95.

Beatty, M. K., Rahman, A., Cao, H., Woodman, W., Lee, M., Myers, A. M. & James, M. G. 1999. Purification and molecular genetic characterization of zpu1, a pullulanase-type starch-debranching enzyme from maize. *Plant Physiology,* 119, 255-266.

Behnke, C. A., Yee, V. C., Trong, I. L., Pedersen, L. C., Stenkamp, R. E., Kim, S. S., Reeck, G. R. & Teller, D. C. 1998. Structural determinants of the bifunctional corn hageman factor inhibitor: X-ray crystal structure at 1.95 a resolution. *Biochemistry,* 37, 15277-88.

Bissaro, B., Monsan, P., Faure, R. & O'Donohue, M. J. 2015. Glycosynthesis in a waterworld: New insight into the molecular basis of transglycosylation in retaining glycoside hydrolases. *Biochemical Journal,* 467, 17-35.

Bodén, M. & Hawkins, J. 2005. Prediction of subcellular localization using sequence-biased recurrent networks. *Bioinformatics,* 21, 2279-2286.

Bønsager, B., Svensson, B. & Finnie, C. 2007. *Proteome analysis of dissected barley seed tissue during germination and radicle elongation: Heterologous expression of barley limit dextrinase inhibitor.* Ph.D. Thesis. Danish Technical University.

Burgess, R. R. 2009. Refolding solubilized inclusion body proteins. *Methods in Enzymology,* 463, 259-82.

Burton, R. A., Zhang, X. Q., Hrmova, M. & Fincher, G. B. 1999. A single limit dextrinase gene is expressed both in the developing endosperm and in germinated grains of barley. *Plant Physiology,* 119, 859-71.

Cantarel, B. L., Coutinho, P. M., Rancurel, C., Bernard, T., Lombard, V. & Henrissat, B. 2009. The carbohydrate-active enzymes database (CAZy): An expert resource for glycogenomics. *Nucleic Acids Research,* 37, D233-8.

Chen, Z.-Y., Brown, R. L., Lax, A. R., Cleveland, T. E. & Russin, J. S. 1999. Inhibition of plant-pathogenic fungi by a corn trypsin inhibitor overexpressed in *Escherichia coli*. *Applied and Environmental Microbiology,* 65, 1320-1324.

Davies, G. J., Wilson, K. S. & Henrissat, B. 1997. Nomenclature for sugar-binding subsites in glycosyl hydrolases. *Biochemical Journal,* 321, 557-559.

De Marco, A. 2009. Strategies for successful recombinant expression of disulfide bond-dependent proteins in escherichia coli. *Microbial Cell Factories,* 8, 26.

Dias, S. C., Franco, O. L., Magalhaes, C. P., De Oliveira-Neto, O. B., Laumann, R. A., Figueira, E. L., Melo, F. R. & Grossi-De-Sa, M. F. 2005. Molecular cloning and expression of an alpha-amylase inhibitor from rye with potential for controlling insect pests. *The Protein Journal,* 24, 113-23.

Dinges, J. R. 2003. Mutational analysis of the pullulanase-type debranching enzyme of maize indicates multiple functions in starch metabolism. *The Plant Cell,* 15, 666-680.

Duan, X., Chen, J. & Wu, J. 2013. Optimization of pullulanase production in escherichia coli by regulation of process conditions and supplement with natural osmolytes. *Bioresource Technology,* 146, 379-85.

Duan, X., Zou, C. & Wu, J. 2015. Triton x-100 enhances the solubility and secretion ratio of aggregation-prone pullulanase produced in *Escherichia coli*. *Bioresource Technology,* 194, 137-143.

Emanuelsson, O., Nielsen, H. & Von Heijne, G. 1999. Chlorop, a neural network-based method for predicting chloroplast transit peptides and their cleavage sites. *Protein Science,* 8, 978-984.

Evans, D. E., Dambergs, R., Ratkowsky, D., Li, C., Harasymow, S., Roumeliotis, S. & Eglinton, J. K. 2010. Refining the prediction of potential malt fermentability by including an assessment of limit dextrinase thermostability and additional measures of malt modification, using two different methods for multivariate model development. *Journal of the Institute of Brewing,* 116, 86-96.

Francis, D. M. & Page, R. 2010. Strategies to optimize protein expression in *E. coli*. *Current Protocols in Protein Science,* Chapter 5, Unit 5 24 1-29.

Garcia-Maroto, F., Carbonero, P. & Garcia-Olmedo, F. 1991. Site-directed mutagenesis and expression in escherichia coli of wmai-1, a wheat monomeric inhibitor of insect alpha-amylase. *Plant Molecular Biology,* 17, 1005-11.

Gavel, Y. & Von Heijne, G. 1990. A conserved cleavage-site motif in chloroplast transit peptides. *FEBS Letters,* 261, 455-458.

Gebremariam, M. M., Zarnkow, M. & Becker, T. 2012. Effect of drying temperature and time on alpha-amylase, beta-amylase, limit dextrinase activities and dimethyl sulphide level of teff (*Eragrostis tef*) malt. *Food and Bioprocess Technology,* 6, 3462-3472.

Gilding, E. K., Frere, C. H., Cruickshank, A., Rada, A. K., Prentis, P. J., Mudge, A. M., Mace, E. S., Jordan, D. R. & Godwin, I. D. 2013. Allelic variation at a single gene increases food value in a drought-tolerant staple cereal. *Nature Communications,* 4, 1483.

Givens, D. I., Davies, T. W. & Laverick, R. M. 2004. Effect of variety, nitrogen fertiliser and various agronomic factors on the nutritive value of husked and naked oats grain. *Animal Feed Science and Technology,* 113, 169-181.

Gourlay, L. J., Santi, I., Pezzicoli, A., Grandi, G., Soriani, M. & Bolognesi, M. 2009. Group B streptococcus pullulanase crystal structures in the context of a novel strategy for vaccine development. *Journal of Bacteriology,* 191, 3544-52.

Greffe, L., Jensen, M. T., Bosso, C., Svensson, B. & Driguez, H. 2003. Chemoenzymatic synthesis of branched oligo- and polysaccharides as potential substrates for starch active enzymes. *Chembiochem,* 4, 1307-11.

Hall, J., Hazlewood, G. P., Surani, M. A., Hirst, B. H. & Gilbert, H. J. 1990. Eukaryotic and prokaryotic signal peptides direct secretion of a bacterial endoglucanase by mammalian cells. *Journal of Biology and Chemistry,* 265, 19996-9.

Hancock, R. D. & Tarbet, B. J. 2000. The other double helix—the fascinating chemistry of starch. *Journal of Chemical Education,* 77, 988.

Hardie, D. G., Manners, D. J. & Yellowlees, D. 1976. The limit dextrinase from malted sorghum (Sorghum vulgare). *Carbohydrate Research,* 50, 75-85.

Hazegh-Azam, M., Kim, S. S., Masoud, S., Andersson, L., White, F., Johnson, L., Muthukrishnan, S. & Reeck, G. 1998. The corn inhibitor of activated hageman factor: Purification and properties of two recombinant forms of the protein. *Protein Expression and Purification,* 13, 143-9.

Hobson, P. N., Whelan, W. J. & Peat, S. 1950. A 'de-branching' enzyme in bean and potato. *Biochemical Journal,* 47, xxxix.

Huang, Y., Cai, S., Ye, L., Han, Y., Wu, D., Dai, F., Li, C. & Zhang, G. 2014. Genetic architecture of limit dextrinase inhibitor (LDI) activity in tibetan wild barley. *BMC Plant Biology,* 14, 117.

Jang, C. S., Yim, W. C., Moon, J. C., Hung, J. H., Lee, T. G., Lim, S. D., Cho, S. H., Lee, K. K., Kim, W., Seo, Y. W. & Lee, B. M. 2008. Evolution of non-specific lipid transfer protein (nsltp) genes in the poaceae family: Their duplication and diversity. *Molecular Genetics and Genomics,* 279, 481-97.

Jensen, J. M., Vester-Christensen, M. B., Møller, M. S., Bonsager, B. C., Christensen, H. E., Hachem, M. A. & Svensson, B. 2011. Efficient secretory expression of functional barley limit dextrinase inhibitor by high cell-density fermentation of *Pichia pastoris*. *Protein Expression and Purification,* 79, 217-22.

Jespersen, H. M., Macgregor, E. A., Henrissat, B., Sierks, M. R. & Svensson, B. 1993. Starch- and glycogen-debranching and branching enzymes: Prediction of structural features of the catalytic (beta/alpha)8-barrel domain and evolutionary relationship to other amylolytic enzymes. *The Protein Journal,* 12, 791-805.

Jose-Estanyol, M., Gomis-Ruth, F. X. & Puigdomenech, P. 2004. The eight-cysteine motif, a versatile structure in plant proteins. *Plant Physiology and Biochemistry,* 42, 355-65.

Juge, N. & Svensson, B. 2006. Proteinaceous inhibitors of carbohydrate-active enzymes in cereals: Implication in agriculture, cereal processing and nutrition. *Journal of the Science of Food and Agriculture,* 86, 1573-1586.

Kainuma, K., Kobayashi, S. & Harada, T. 1978. Action of pseudomonas isoamylase on various branched oligo and poly-saccharides. *Carbohydrate Research,* 61, 345-57.

Kang, H. K., Cha, H., Yang, T. J., Park, J. T., Lee, S., Kim, Y. W., Auh, J. H., Okada, Y., Kim, J. W., Cha, J., Kim, C. H. & Park, K. H. 2008. Enzymatic synthesis of dimaltosyl-beta-cyclodextrin via a transglycosylation reaction using trex, a sulfolobus solfataricus p2 debranching enzyme. *Biochemical and Biophysical Research Communications,* 366, 98-103.

Kang, J., Park, K. M., Choi, K. H., Park, C. S., Kim, G. E., Kim, D. & Cha, J. 2011. Molecular cloning and biochemical characterization of a heat-stable type i pullulanase from *Thermotoga neapolitana*. *Enzyme and Microbial Technology,* 48, 260-6.

Katsuya, Y., Mezaki, Y., Kubota, M. & Matsuura, Y. 1998. Three-dimensional structure of *Pseudomonas* isoamylase at 2.2 a resolution. *Journal of Molecular Biology,* 281, 885-97.

Kneen & Spoerl 1948. The limit dextrinase activity of barley malt. *Proceedings of the Annual Meeting of the American Society of Brewing Chemists*, 20.

Kohno, T., Carmichael, D. F., Sommer, A. & Thompson, R. C. 1990. Refolding of recombinant proteins. *Methods in Enzymology,* 185, 187-95.

Kong, B. & Guo, G. L. 2014. Soluble expression of disulfide bond containing proteins fgf15 and fgf19 in the cytoplasm of Escherichia coli. *PLoS One,* 9, e85890.

Kristensen, M., Lok, F., Planchot, V., Svendsen, I., Leah, R. & Svensson, B. 1999a. Isolation and characterization of the gene encoding the starch debranching enzyme limit dextrinase from germinating barley. *Biochimica et Biophysica Acta,* 1431, 538-546.

Kristensen, M., Planchot, V., Abe, J.-I. & Svensson, B. 1998. Large-scale purification and characterization of barley limit dextrinase, a member of the α-amylase structural family. *Cereal Chemistry Journal,* 75, 473-479.

Kruger, J. E. & Marchylo, B. 1978. Note on the presence of debranching enzymes in immature wheat kernels. *Cereal Chemistry,* 55, 529-533.

Kuriki, T. & Imanaka, T. 1999. The concept of the alpha-amylase family: Structural similarity and common catalytic mechanism. *Journal of Bioscience and Bioengineering,* 87, 557-65.

Leong, Y. H., Karim, A. A. & Norziah, M. H. 2007. Effect of pullulanase debranching of sago (*Metroxylon sagu*) starch at subgelatinization temperature on the yield of resistant starch. *Starch - Stärke,* 59, 21-32.

Li, B., Servaites, J. C. & Geiger, D. R. 1992. Characterization and subcellular localization of debranching enzyme and endoamylase from leaves of sugar beet. *Plant Physiology,* 98, 1277-84.

Li, Q. F., Zhang, G. Y., Dong, Z. W., Yu, H. X., Gu, M. H., Sun, S. S. & Liu, Q. Q. 2009. Characterization of expression of the ospul gene encoding a pullulanase-type debranching enzyme during seed development and germination in rice. *Plant Physiology and Biochemistry,* 47, 351-8.

Liu, F., Zhang, X., Lu, C., Zeng, X., Li, Y., Fu, D. & Wu, G. 2015. Non-specific lipid transfer proteins in plants: Presenting new advances and an integrated functional analysis. *Journal of Experimental Botany*.

Longstaff, M. A. & Bryce, J. H. 1993. Development of limit dextrinase in germinated barley (*Hordeum vulgare*) (evidence of proteolytic activation). *Plant Physiology,* 101, 881-889.

Ludwig, I., Ziegler, P. & Beck, E. 1984. Purification and properties of spinach leaf debranching enzyme. *Plant Physiology,* 74, 856-861.

Lullienpellerin, V., Gavalda, S., Joudrier, P. & Gautier, M. F. 1994. Expression of a cDNA encoding the wheat cm 16 protein in escherichia coli. *Protein Expression and Purification,* 5, 218-224.

Lussier, F.-X., Denis, F. & Shareck, F. 2010. Adaptation of the highly productive t7 expression system to *Streptomyces lividans*. *Applied and Environmental Microbiology,* 76, 967-970.

Macgregor, A. W., Bazin, S. L. & Schroeder, S. W. 2002. Effect of starch hydrolysis products on the determination of limit dextrinase and limit dextrinase inhibitors in barley and malt. *Journal of Cereal Science,* 35, 17-28.

Macgregor, A. W., Donald, L. J., Macgregor, E. A. & Duckworth, H. W. 2003. Stoichiometry of the complex formed by barley limit dextrinase with its endogenous inhibitor. Determination by electrospray time-of-flight mass spectrometry. *Journal of Cereal Science,* 37, 357-362.

Macgregor, A. W., Macri, L. J., Schroeder, S. W. & Bazin, S. L. 1994a. Limit dextrinase from malted barley: Extraction, purification, and characterization. *Cereal Chemistry*, 71, 610-617.

Macgregor, A. W., Macri, L. J., Schroeder, S. W. & Bazin, S. L. 1994b. Purification and characterisation of limit dextrinase inhibitors from barley. *Journal of Cereal Science,* 20, 33-41.

Macgregor, E. A. 2004. The proteinaceous inhibitor of limit dextrinase in barley and malt. *Biochimica et Biophysica Acta,* 1696, 165-70.

Macgregor, E. A. 2005. An overview of clan gh-h and distantly-related families. *Biologia Bratislava,* 60, 5-12.

Macgregor, E. A., Bazin, S. L., Ens, E. W., Lahnstein, J., Macri, L. J., Shirley, N. J. & Macgregor, A. W. 2000. Structural models of limit dextrinase inhibitors from barley. *Journal of Cereal Science,* 31, 79-90.

Macgregor, E. A., Janecek, S. & Svensson, B. 2001. Relationship of sequence and structure to specificity in the alpha-amylase family of enzymes. *Biochimica et Biophysica Acta,* 1546, 1-20.

Machovič, M. & Janeček, Š. 2008. Domain evolution in the gh13 pullulanase subfamily with focus on the carbohydrate-binding module family 48. *Biologia,* 63, 1057-1068.

Macri, L. J., Macgregor, A. W., Schroeder, S. W. & Bazin, S. L. 1993. Detection of a limit dextrinase inhibitor in barley. *Journal of Cereal Science,* 18, 103-106.

Maldonado, A. M., Doerner, P., Dixon, R. A., Lamb, C. J. & Cameron, R. K. 2002. A putative lipid transfer protein involved in systemic resistance signalling in *Arabidopsis*. *Nature,* 419, 399-403.

Mangan, D., Mccleary, B. V., Cornaggia, C., Ivory, R., Rooney, E. & Mckie, V. 2015. Colourimetric and fluorimetric substrates for the assay of limit dextrinase. *Journal of Cereal Science,* 62, 50-57.

Manners, D. J. & Yellowlees, D. 1971. Studies on carbohydrate metabolising enzymes. Part xxvi. The limit dextrinase from germinated barley. *Starch - Stärke,* 23, 228-234.

Manners, D. J. & Yellowlees, D. 1973. Studies on debranching enzymes. Part i the limit dextrinase activity of extracts of certain higher plants and commercial malts. *Journal of the Institute of Brewing,* 79, 377-385.

Martin, C. & Smith, A. M. 1995. Starch biosynthesis. *The Plant Cell,* 7, 971-985.

Matsuura, Y., Kusunoki, M., Harada, W. & Kakudo, M. 1984. Structure and possible catalytic residues of taka-amylase a. *Journal of Biochemistry,* 95, 697-702.

Mccleary, B. V. 1992. Measurement of the content of limit-dextrinase in cereal flours. *Carbohydrate Research,* 227, 257-268.

Mcdougall, G. J., Ross, H. A., Swanston, J. S. & Davies, H. V. 2004. Limit dextrinase from germinating barley has endotransglycosylase activity, which explains its activation by maltodextrins. *Planta,* 218, 542-51.

Mikami, B., Iwamoto, H., Malle, D., Yoon, H. J., Demirkan-Sarikaya, E., Mezaki, Y. & Katsuya, Y. 2006. Crystal structure of pullulanase: Evidence for parallel binding of oligosaccharides in the active site. *Journal of Molecular Biology,* 359, 690-707.

Moeller, L., Gan, Q. & Wang, K. 2009. A bacterial signal peptide is functional in plants and directs proteins to the secretory pathway. *Journal of Experimental Botany,* 60, 3337-3352.

Møller, M. S., Abou Hachem, M., Svensson, B. & Henriksen, A. 2012. Structure of the starch-debranching enzyme barley limit dextrinase reveals homology of the N-terminal domain to CBM21. *Structural Biology and Crystallization Communications,* 68, 1008-12.

Møller, M. S., Vester-Christensen, M. B., Jensen, J. M., Abou Hachem, M., Henriksen, A. & Svensson, B. 2015a. Crystal structure of barley limit dextrinase:Limit dextrinase inhibitor (LD:LDI) complex reveals insights into mechanism and diversity of cereal-type inhibitors. *Journal of Biology and Chemistry*.

Møller, M. S., Windahl, M. S., Sim, L., Bojstrup, M., Abou Hachem, M., Hindsgaul, O., Palcic, M., Svensson, B. & Henriksen, A. 2015b. Oligosaccharide and substrate binding in the starch debranching enzyme barley limit dextrinase. *Journal of Molecular Biology,* 427, 1263-77.

Nakamura, Y., Umemoto, T., Ogata, N., Kuboki, Y., Yano, M. & Sasaki, T. 1996. Starch debranching enzyme (r-enzyme or pullulanase) from developing rice endosperm: Purification, cDNA and chromosomal localization of the gene. *Planta,* 199, 209-218.

Nguyen, D. H., Park, J. T., Shim, J. H., Tran, P. L., Oktavina, E. F., Nguyen, T. L., Lee, S. J., Park, C. S., Li, D., Park, S. H., Stapleton, D., Lee, J. S. & Park, K. H. 2014. Reaction kinetics of substrate transglycosylation catalyzed by TreX of *Sulfolobus solfataricus* and effects on glycogen breakdown. *Journal of Bacteriology,* 196, 1941-9.

Oda, Y., Matsunaga, T., Fukuyama, K., Miyazaki, T. & Morimoto, T. 1997. Tertiary and quaternary structures of 0.19 alpha-amylase inhibitor from wheat kernel determined by x-ray analysis at 2.06 a resolution. *Biochemistry,* 36, 13503-11.

Okuda, M., Satoh, T., Sakurai, N., Shibuya, K., Kaji, H. & Samejima, T. 1997. Overexpression in *Escherichia coli* of chemically synthesized gene for active 0.19 alpha-amylase inhibitor from wheat kernel. *Journal of Biochemistry,* 122, 918-26.

Petersen, T. N., Brunak, S., Von Heijne, G. & Nielsen, H. 2011. Signalp 4.0: Discriminating signal peptides from transmembrane regions. *Nature Methods,* 8, 785-786.

Peyret, H. & Lomonossoff, G. P. 2013. The peaq vector series: The easy and quick way to produce recombinant proteins in plants. *Plant Molecular Biology,* 83, 51-8.

Pinjari, R., Khedkar, J. & Gejji, S. 2010. Cavity diameter and height of cyclodextrins and cucurbit[n]urils from the molecular electrostatic potential topography. *Journal of Inclusion Phenomena and Macrocyclic Chemistry,* 66, 371-380.

Renz, A., Schikora, S., Schmid, R., Kossmann, J. & Beck, E. 1998. Cdna sequence and heterologous expression of monomeric spinach pullulanase: Multiple isomeric forms arise from the same polypeptide. *Biochemical Journal,* 331, 937-945.

Repellin, A., Båga, M. & Chibbar, R. N. 2008. In vitro pullulanase activity of wheat (triticum aestivum l.) limit-dextrinase type starch debranching enzyme is modulated by redox conditions. *Journal of Cereal Science,* 47, 302-309.

Schindler, I., Renz, A., Schmid, F. X. & Beck, E. 2001. Activation of spinach pullulanase by reduction results in a decrease in the number of isomeric forms. *Biochimica et Biophysica Acta,* 1548, 175-86.

Sen, S. & Dutta, S. 2012. Cloning, expression and characterization of biotic stress inducible ragi bifunctional inhibitor (rbi) gene from *Eleusine coracana* gaertn. *Journal of Plant Biochemistry and Biotechnology,* 21, 66-76.

Shimura, Y., Oh, K., Kon, M., Yamamoto, E., Mizuno, Y., Adachi, T., Abe, T., Tamogami, S., Fukushima, J., Inamoto, T. & Tonozuka, T. 2011. Enzymatic synthesis of novel branched sugar alcohols mediated by the transglycosylation reaction of pullulan-hydrolyzing amylase ii (tva ii) cloned from *Thermoactinomyces vulgaris* r-47. *Carbohydrate Research,* 346, 1842-7.

Shu, X., Sun, J. & Wu, D. 2014. Effects of grain development on formation of resistant starch in rice. *Food Chemistry,* 164, 89-97.

Sim, L., Beeren, S. R., Findinier, J., Dauvillee, D., Ball, S. G., Henriksen, A. & Palcic, M. M. 2014. Crystal structure of the *Chlamydomonas* starch debranching enzyme isoamylase isa1 reveals insights into the mechanism of branch trimming and complex assembly. *Journal of Biology and Chemistry,* 289, 22991-3003.

Sissons, M., Taylor, M. & Proudlove, M. 1995. Barley malt limit dextrinase - its extraction, heat-stability, and activity during malting and mashing. *Journal of the American Society of Brewing Chemists,* 53, 104-110.

Sissons, M. J., Lance, R. C. M. & Sparrow, D. H. B. 1992a. Studies on limit dextrinase in barley i. Purification of malt limit dextrinase and production of monospecific antibodies. *Journal of Cereal Science,* 16, 107-116.

Sissons, M. J., Lance, R. C. M. & Sparrow, D. H. B. 1992b. Studies on limit dextrinase in barley ii. Application of an elisa and immunoblotting to studies of genetic variability and malting effects. *Journal of Cereal Science,* 16, 117-128.

Stahl, Y., R. D., Coates, S., Bryce, J. H., Morris, P. C. 2004. Antisense downregulation of the barley limit dextrinase inhibitor modulates starch granule size distribution, starch composition and amylopectin structure. *The Plant Journal*, 39, 599–611

Stahl, Y., Alexander, R. D., Coates, S., Bryce, J. H., Jenkinson, H. R. & Morris, P. C. 2007. The barley limit dextrinase inhibitor: Gene expression, protein location and interaction with 14-3-3 protein. *Plant Science,* 172, 452-461.

Stam, M. R., Danchin, E. G., Rancurel, C., Coutinho, P. M. & Henrissat, B. 2006. Dividing the large glycoside hydrolase family 13 into subfamilies: Towards improved functional annotations of alpha-amylase-related proteins. *Protein Engineering, Design & Selection,* 19, 555-62.

Streb, S., Delatte, T., Umhang, M., Eicke, S., Schorderet, M., Reinhardt, D. & Zeeman, S. C. 2008. Starch granule biosynthesis in arabidopsis is abolished by removal of all debranching enzymes but restored by the subsequent removal of an endoamylase. *Plant Cell,* 20, 3448-66.

Streb, S., Eicke, S. & Zeeman, S. C. 2012. The simultaneous abolition of three starch hydrolases blocks transient starch breakdown in arabidopsis. *Journal of Biology and Chemistry,* 287, 41745-56.

Strobl, S., Maskos, K., Wiegand, G., Huber, R., Gomis-Ruth, F. X. & Glockshuber, R. 1998. A novel strategy for inhibition of alpha-amylases: Yellow meal worm alpha-amylase in complex with the ragi bifunctional inhibitor at 2.5 Å resolution. *Structure,* 6, 911-21.

Strobl, S., Muhlhahn, P., Bernstein, R., Wiltscheck, R., Maskos, K., Wunderlich, M., Huber, R., Glockshuber, R. & Holak, T. A. 1995. Determination of the three-dimensional structure of the bifunctional alpha-amylase/trypsin inhibitor from ragi seeds by nmr spectroscopy. *Biochemistry,* 34, 8281-93.

Svensson, B., Fukuda, K., Nielsen, P. K. & Bonsager, B. C. 2004. Proteinaceous alpha-amylase inhibitors. *Biochimica et Biophysica Acta,* 1696, 145-56.

Svensson, B., Jensen, M. T., Mori, H., Bak-Jensen, K. S., Bønsager, B., Nielsen, P. K., Prætorius-Ibba, M., Nøhr, J., Juge, N., Greffe, L., Williamson, G. & Driguez, H. 2002. Fascinating facets of function and structure of amylolytic enzymes of glycoside hydrolase family. *Biologia Bratislava,* 57, 1-9.

Tegel, H., Ottosson, J. & Hober, S. 2011. Enhancing the protein production levels in *Escherichia coli* with a strong promoter. *FEBS Journal,* 278, 729-739.

Tremblay, D., Lemay, J., Gilbert, M., Chapdelaine, Y., Dupont, C. & Morosoli, R. 2002. High-level heterologous expression and secretion in *Streptomyces lividans* of two major antigenic proteins from *Mycobacterium tuberculosis*. *Canadian Journal of Microbiology,* 48, 43-8.

Trivedi, M. V., Laurence, J. S. & Siahaan, T. J. 2009. The role of thiols and disulfides in protein chemical and physical stability. *Current Protein & Peptide Science,* 10, 614-625.

Turkenburg, J. P., Brzozowski, A. M., Svendsen, A., Borchert, T. V., Davies, G. J. & Wilson, K. S. 2009. Structure of a pullulanase from *Bacillus acidopullulyticus*. *Proteins: Structure, Function, and Bioinformatics,* 76, 516-519.

Uitdehaag, J. C., Mosi, R., Kalk, K. H., Van Der Veen, B. A., Dijkhuizen, L., Withers, S. G. & Dijkstra, B. W. 1999. X-ray structures along the reaction pathway of cyclodextrin glycosyltransferase elucidate catalysis in the alpha-amylase family. *Nature Structural & Molecular Biology,* 6, 432-6.

Vester-Christensen, M. B., Abou Hachem, M., Svensson, B. & Henriksen, A. 2010a. Crystal structure of an essential enzyme in seed starch degradation: Barley limit dextrinase in complex with cyclodextrins. *Journal of Molecular Biology,* 403, 739-50.

Vester-Christensen, M. B., Hachem, M. A., Naested, H. & Svensson, B. 2010b. Secretory expression of functional barley limit dextrinase by *Pichia pastoris* using high cell-density fermentation. *Protein Expression and Purification,* 69, 112-9.

Wong, J. H., Cai, N., Tanaka, C. K., Vensel, W. H., Hurkman, W. J. & Buchanan, B. B. 2004. Thioredoxin reduction alters the solubility of proteins of wheat starchy endosperm: An early event in cereal germination. *Plant Cell Physiology,* 45, 407-15.

Wu, C., Colleoni, C., Myers, A. M. & James, M. G. 2002. Enzymatic properties and regulation of zpu1, the maize pullulanase-type starch debranching enzyme. *Archives of Biochemistry and Biophysics,* 406, 21-32.

Yamada, J. 1981. Purification of oat debranching enzyme and occurrence of inactive debranching enzyme in cereals. *Agricultural and Biological Chemistry,* 45, 1013-1015.

Yamasaki, Y., Nakashima, S. & Konno, H. 2008. Pullulanase from rice endosperm. *Acta Biochimica Polonica,* 55, 507-10.

Yang, X., Westcott, S., Gong, X., Evans, E., Zhang, X.-Q., Lance, R. C. M. & Li, C. 2008. Amino acid substitutions of the limit dextrinase gene in barley are associated with enzyme thermostability. *Molecular Breeding,* 23, 61-74.

Yeats, T. H. & Rose, J. K. 2008. The biochemistry and biology of extracellular plant lipid-transfer proteins (LTPs). *Protein Science,* 17, 191-8.

Yoo, E. M., Wims, L. A., Chan, L. A. & Morrison, S. L. 2003. Human IgG2 can form covalent dimers. *Journal of Immunology,* 170, 3134-8.

Zarnkow, M., Keßler, M., Back, W., Arendt, E. K. & Gastl, M. 2010. Optimisation of the mashing procedure for 100 % malted proso millet (Panicum miliaceum l.) as a raw material for gluten-free beverages and beers. *Journal of the Institute of Brewing,* 116, 141-150.

Zeeman, S. C., Northrop, F., Smith, A. M. & Rees, T. 1998. A starch-accumulating mutant of *Arabidopsis thaliana* deficient in a chloroplastic starch-hydrolysing enzyme. The *Plant Journal,* 15, 357-65.

Zhu, Z.-P., Hylton, C. M., Rössner, U. & Smith, A. M. 1998. Characterization of starch-debranching enzymes in pea embryos. *Plant Physiology,* 118, 581-590.

Zybailov, B., Rutschow, H., Friso, G., Rudella, A., Emanuelsson, O., Sun, Q. & Van Wijk, K. J. 2008. Sorting signals, N-terminal modifications and abundance of the chloroplast proteome. *PLoS One,* 3, e1994.

Chapter 6- Steps Towards Understanding the *in Planta* Roles of Limit Dextrinase and Limit Dextrinase Inhibitor

6.1 Introduction

6.1.1 The Release of Starch Active Enzymes During Germination

Temporal and spatial control over carbohydrate active enzymes during germination is essential for plant growth. Proteomics on grain tissues has identified that a large number of the proteins present during germination are glycosyl hydrolases (Finnie et al., 2011). Changes in the protein profile occurs as early as 4 h after the onset of germination (or GA addition in culture) which indicates that some processes involved in germination are pre-programmed into the grain during seed maturation. Other processes including the hydrolytic action of proteases, activation by redox and programmed cell death (PCD) of the aleurone act to regulate and control the process of germination (Finnie et al., 2011).

β-Amylase

β-Amylase is synthesised in the endosperm during grain filling. Upon germination the protein is released from an inactive "bound" form. The "free" form of β-amylase can be generated by incubation with reducing agents (Buttimer and Briggs, 2000, Duke et al., 2012). Both serine and cysteine proteases are capable of producing active β-amylase (Guerin et al., 1992, Schmitt and Marinac, 2008) (Figure 6.2). β-amylase in maize is reported to not be involved in starch degradation. The protein is synthesised and retained in the aleurone layer and is therefore proposed to be unimportant for germination (Wang et al., 2004, Wang et al., 1997, Subbarao et al., 1998).

α-Glucosidase

α-Glucosidase is proposed to be released from the aleurone in a way similar to α-amylase. mRNA levels increase strongly after the application of GA, with a similar pattern to that exhibited by α-amylase (Tibbot and Skadsen, 1996). Little else is known about the role of glucosidases, however knockdown of the main isoform *AGL97* does not have dramatic effects on germination (Stanley et al., 2011, Frandsen et al., 2000).

α-Amylase

The release of α-amylase from the aleurone layer in response to GA has long been studied using isolated aleurone layers in liquid culture (Chrispeels and Varner, 1967, Locy and Kende, 1978, Ranki and Sopanen, 1984) (Figure 6.2). Cultured aleurone layers produce comparable α-

amylase levels to GA treated deembryonated half grains (Chrispeels and Varner, 1967). Indeed, GA responsive elements have been identified in the promoter of the barley α-amylase gene (Gubler and Jacobsen, 1992). Ca^{2+} also stimulates the release of amylase, although the mechanism of action is yet to be elucidated (Bush et al., 1986). Cyclic guanosine monophosphate (cGMP) is required for GA induced gene expression in barley. LY83583, a small molecule inhibitor of guanylate cyclase prevents GA induced α-amylase synthesis and secretion (Penson et al., 1996). α-amylase production is blocked when protein and RNA synthesis are inhibited, indicating the protein is synthesised *de novo* by the aleurone layer (Chrispeels and Varner, 1967). During the first 24 h of germination the enzyme is retained within the aleurone cells. Protein and RNA synthesis inhibitors added at 24 h prevent formation of the release mechanism, indicating it is likely protein based (Chrispeels and Varner, 1967). It is suggested that a breakdown of the aleurone cell walls is responsible for the release of α-amylase (Gubler et al., 1987).

It is not clear how all of these processes come together to control the release and activity of α-amylase though it is a tightly regulated process. Timing of germination is essential to a seedlings survival. Germination at the wrong time, as is seen during pre-harvest sprouting (PHS), can have dire consequences for both the growing plant and farmers (Figure 6.1) (Ren et al., 2012). It is likely that other glycosyl hydrolases within the aleurone and endosperm are under similar control, however, details regarding this are scarce.

Figure 6.1 Pre-harvest sprouting in wheat
Upper. Sprouted heads which have undergone pre-harvest sprouting. **Lower.** Non-sprouted heads. Adapted from (Ren et al., 2012).

6.1.2 The Release of Limit Dextrinase During Germination

In barley, expression of the sole gene encoding for LD is induced by GA during grain germination by GA (Hardie, 1975, Shahpiri et al., 2015) (Figure 6.2). Transcripts corresponding to LD can be identified within the aleurone layer as early as 12 h after the onset of germination. However, LD activity isn't present at high levels until two days post imbibition, with activity increasing almost tenfold from day 2 to day 5 (Burton et al., 1999, Schroeder and Macgregor, 1998, Macgregor et al., 1994). The activity and precise timing of LD release depends on germination conditions and variety (Ross et al., 2003).

Transcripts for LD are also present during grain development. RT-PCR shows LD mRNA is present in the endosperm at low levels during early stages (1-10 days post anthesis, dpa) and increases steadily until 24 dpa (Radchuk et al., 2009, Burton et al., 1999). LD activity is present at very low levels in ungerminated grain, this is likely to be protein that is carried over from grain filling (Macgregor et al., 1994, Schroeder and Macgregor, 1998). Interestingly, LD in rice and peas has been shown to be present in a mature, active form within the endosperm of dormant seeds (Vlodawsky et al., 1971, Yamada, 1981, Mangan et al., 2015).

The slow release of LD is not fully understood. LD has no signal peptide to direct secretion and has a putative plastid transit peptide as discussed in Chapter 5. It is unclear what role this plays and whether LD is directed to plastids within the aleurone. There is very little recent information on plastids in the aleurone layer (Wise, 2006). LDI, cell wall metabolism, proteases, cell death and redox have all been linked to LD release and activity levels.

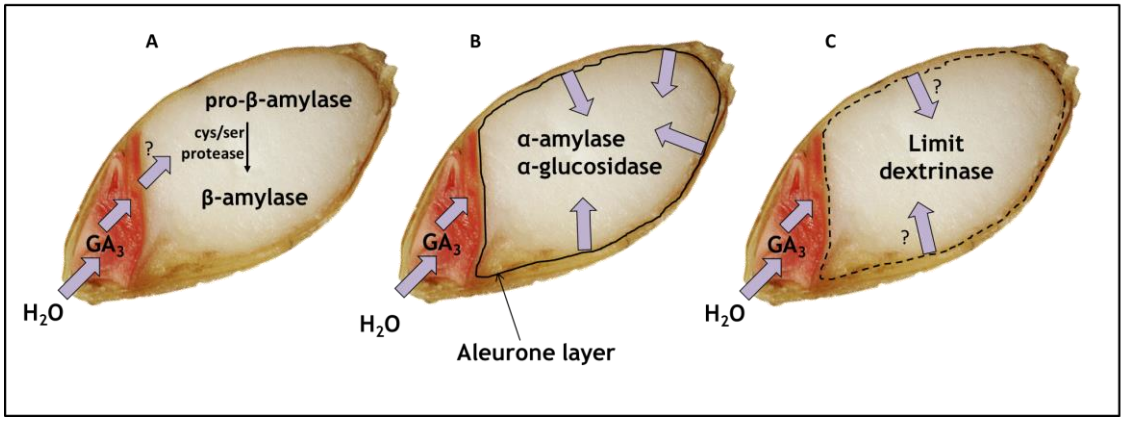

Figure 6.2 The release of starch active enzymes during barley grain germination.
A. β-Amylase is activated by proteolysis. **B.** α-Amylase and α-glucosidase are secreted from the aleurone layer. **C.** The precise mode of limit dextrinase release remains unknown.

Limit Dextrinase Inhibitor

When extracted from germinating barley grains LD is found in a "bound", inactive from as well as a "free" enzymatically active form (Longstaff and Bryce, 1993). The inactive form of LD has been proposed be in complex with the endogenous inhibitor LDI (Mccafferty et al., 2004). No LDI activity has been identified in maize, pearl millet, sorghum or rice (Macgregor 2004).

Barley LDI is encoded by a small multigene family (giving at least 3 bands by Southern blot). Transcripts encoding LDI are only detected in starchy endosperm during grain development, 2 and 4 weeks post anthesis; no expression is seen in germinating grains or vegetative tissue by northern blot (Stahl et al., 2007). The expression of LDI is controlled by an endosperm specific promoter (Morris and Stahl, 2004). Western blot shows LDI protein in developing and germinating grain (Stahl et al., 2007). During germination the protein is present for the first 1-3 days but is not detectable by day 4 (Stahl et al. 2007)**.** LDI is purified from ungerminated grain supporting the proposal that it is only produced in the developing endosperm (Macgregor 1994).

A 14-3-3 protein interaction motif (RGPSRP) has been identified within LDI and the proteins have been shown to interact (Stahl et al., 2007)**.** 14-3-3 proteins are involved in regulation of metabolism by phosphorylation. The interaction motif is the same residues that are seen binding LD within the solved crystal complex (Møller et al., 2015). The inaccessibility of 14-3-3 proteins to LDI when bound to LD may be important for regulation.

Cell Wall Degradation

Cell wall breakdown is one of the main hydrolytic events within the germinating grain, alongside starch hydrolysis and protein degradation (Jamar et al., 2011). The cell walls act as a physical barrier which can prevent the release and movement of hydrolytic enzymes required for seedling establishment (Gianinetti et al., 2007, Gibbons, 1980). The degradation of cell walls is also important in malting and brewing as problems with viscosity and haze can arise due to incomplete cell wall hydrolysis (Jamar et al., 2011, Burton et al., 2010). A large proportion of the cell wall material in the endosperm and aleurone is either heteroxylan or 1,3-1,4-β-glucan (Table 6.1) (Bacic and Stone, 1981, Wilson et al., 2012).

Glucan	Aleurone (%)	Endosperm (%)
Arabinoxylan	71	20
(1-3,1-4)-β-D-glucans	26	75
Cellulose	2	2
Glucomannan	1	2

Table 6.1 The composition of cell walls found within germinating barley.
Data from (Bacic and Stone, 1981, Wilson et al., 2012).

The model for starchy endosperm cell wall architecture proposed by Bamforth and Kanauchi suggests that arabinoxylan masks β-glucan, making it inaccessible to enzymatic attack (Kanauchi and Bamforth, 2002). The actions of arabinofuranosidase and endoxylanases are required to allow the action of endo-β-glucanases on the β-glucan (Bamforth, 2009). Endo-β-1,4-xylanase alongside β-xylopyranosidase and α-arabinofuranosidase have all been shown to be stimulated by GA (Taiz and Honigman, 1976). These enzymes have been implicated in enabling the release of enzymes from the aleurone layer (Figure 6.1, AL) by digesting the cell wall (Taiz and Honigman, 1976, Eastwell and Spencer, 1982). The cell wall composition can be determined by stepwise fractionation into different solvents followed by hydrolysis, separation and identification of the components by chromatography techniques, more recently gas chromatography-mass spectrometry has been implemented (Pettolino et al., 2012).

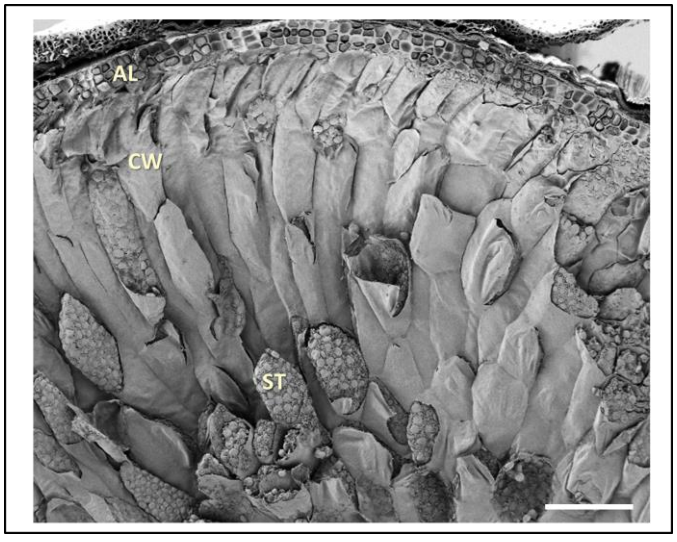

Figure 6.3 Cross section of a barley grain visualised by scanning electron microscopy.
AL. Aleurone layer. **CW.** Cell wall. **ST.** Starch granules. Courtesy of Vasilios Andriotis and Elaine Braclay. Scale bar: 200 µm

More recently, an endo-β-1,4-xylanase has been studied in more detail (Caspers et al., 2001). This enzyme is expressed as a inactive precursor with N-and C-terminal pro-peptides. The enzyme remains in the cytoplasm of aleurone cells and only become active at a late stage of germination, when the aleurone has ceased to secrete hydrolases. Cysteine proteases are responsible for cleaving the pro-peptides to yield active enzyme, this processing can be enhanced by DTT. The processing and release of this xylanase coincide with PCD associated loss of plasma membrane integrity.

Endo-β-1,4-xylanase is not involved in the degradation of the aleurone layer outer cell wall (Caspers et al., 2001). This process, which is proposed to facilitate hydrolase secretion, is catalysed by other enzymes (Figure 6.4, A&B). Once the outer cell wall is degraded, cysteine proteases are able to enter the aleurone and activate the breakdown on the inner cell wall *via* endo-β-1,4-xylanase (Figure 6.4, C&D) (Caspers et al., 2001). It is possible that this pathway plays a role in releasing "trapped" intra-cellular hydrolases such as LD (Figure 6.4, E). The delay in aleurone breakdown is important as integrity is required to allow hydrolase production and secretion (Fincher and Shewry, 1992).

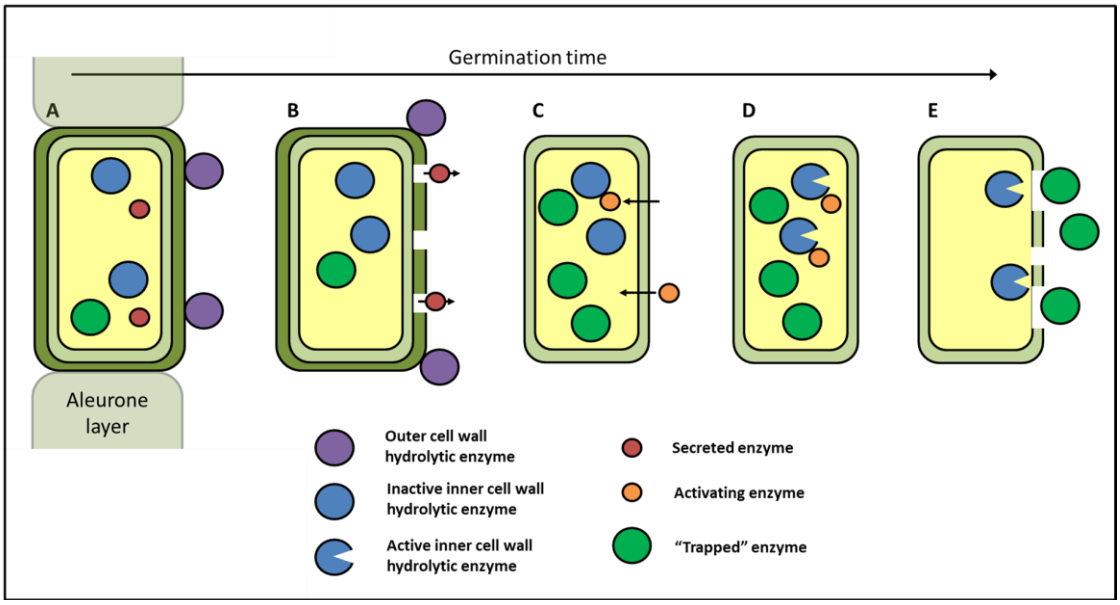

Figure 6.4 The control of protein release from the aleurone layer.
A. Degradation of the aleurone layer outer cell wall enables **B.** the release of secretory enzymes. Further cell wall metabolism enables the activating enzymes to cross the inner cell wall and **C.** enter the aleurone cells. **D.** Activated hydrolytic enzymes can attach the inner cell wall, enabling **E.** the release of trapped enzymes.

Cell Death of the Aleurone Layer

Apoptosis is important for many processes in plants, being an integral part of plant growth, development and death (Domínguez and Cejudo, 2014). Programmed cell death (PCD) is controlled by cellular oxidation status, phytohormones and DNA methylation. PCD occurs within cultured aleurone protoplasts, triggered by GA (Bethke et al., 1999). 4 to 8 days following GA treatment 70 % of protoplasts were dead. ABA treated aleurone protoplasts, however, are viable in liquid culture up to 3 weeks. The protoplasts undergoing PCD become highly vacuolated and lose plasma membrane integrity, alongside this α-amylase production ceases. Cell death can be prevented by guanylate cyclase inhibitor LY83583 which interferes with GA signalling (Bethke et al., 1999). Reactive oxygen species (ROS) also play an important role in GA induced cell death (Bethke and Jones, 2001).

Proteases

Barley contains a complex set of proteases that differ in temporal and spatial expression (Wrobel and Jones, 1992). Numerous proteases have been characterised within the germinating grain: cysteine, metallo, aspartic and serine proteases have all been identified (Koehler and Ho, 1990, Jones, 2003, Jones and Budde, 2005). Some of these proteases have been associated with storage protein proteolysis and cell death (He and Kermode, 2003).

Longstaff has proposed that proteolysis plays a role in the activation of LD, as addition of protease inhibitors, antipain and leupeptin to barley protein extracts prevented LD activation. The proteolytic activity was kept active or activated by DTT (Longstaff and Bryce, 1993). Extraction under reducing conditions produces higher levels of active LD leading to the suggestion that LDI may be regulated by thioredoxin although it is not yet clear that this is the case, degradation of LDI by proteases has also been suggested (Macgregor et al., 1994, Heisner and Bamforth, 2008).

Redox and Thioredoxin

The *redox environment* of a linked set of redox couples as found in a biological fluid, organelle, cell, or tissue is the summation of the products of the reduction potential and reducing capacity of the linked redox couples present.

The redox environment of a cell is the summation of the products of reduction potential and reducing capacity of the redox active molecules. Redox is an important process in all organisms: driving respiration and photosynthesis. Key players in cellular redox are thioredoxin (Trx) and glutaredoxin proteins, disulfide reductases which possess similar structural fold and

mechanism (Figure 6.5) (Meyer et al., 2008). Starch active enzymes from different species have also been shown to be affected by redox (Blennow and Svensson, 2009). BAM1 (Sparla et al., 2006), GWD (Mikkelsen et al., 2005) and SEX4 (Silver et al., 2013) from crop plants are all redox sensitive. Starch metabolic enzymes have also been shown to be regulated by redox conditions in Arabidopsis (Kotting et al., 2010). These include: ISA1/2, LD, SS1, SS3, SBE2 and likely β-amylase (BAM3) and α-amylase (AMY3) (Glaring et al., 2012).

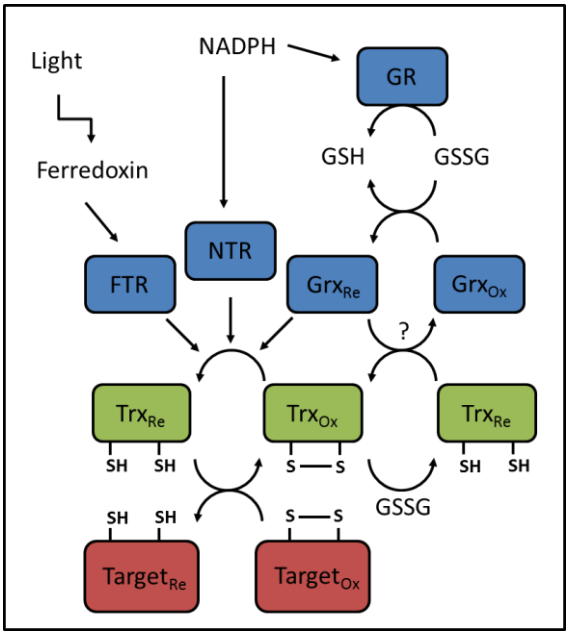

Figure 6.5 Pathways for thioredoxin catalysed reduction.
Reduction within the chloroplast involves ferredoxin-thioredoxin reductase (FTR). NADP-thioredoxin reductase (NTR) is believed to reduce thioredoxins in the mitochondria and cytoplasm. Certain thioredoxins are also reduced vi glutathione (GSH/GSSG)/glutaredoxin (Grx) (Gelhaye et al., 2005).

The Effect of Thioredoxin on Limit Dextrinase and Limit Dextrinase Inhibitor

Limit dextrinase was one of the first starch active enzymes identified as linked to redox. Thioredoxin *h* (Trx *h*) overexpression in barley endosperm produced enhanced limit dextrinase activity (Cho et al., 1999). It was speculated that LDI was not linked to the LD activity in this study as protein extracts were generated at a time point after LDI became inactive. The same overexpression lines were further studied and revealed that Trx *h* accelerated germination rate, with α-amylase activity increasing 1 day earlier than control. This was proposed to be linked to GA *via* the embryo, but deembryonated half grains treated with GA also produced amylase at a faster rate, highlighting an embryo independent pathway (Wong et al., 2002).

The role of thioredoxin with regard to releasing LD during malting and brewing was investigated (Heisner and Bamforth, 2008). Recombinant Trx *h* had no direct effect on LD activity or release in protein extracts produced following a malting regime. LD was, however, activated by reducing agents (DTT) and pH change (Heisner and Bamforth, 2008). It is possible that the thioredoxin is linked to LD activity by an indirect process. In contradiction to the barley study, maize leaf LD activity is increased twofold by direct interaction with Trx *h*. There is no evidence for LDI in maize and recombinant barley LDI tested against maize LD has no effect (Wu et al., 2002).

Direct or indirect LD sensitivity to redox has been identified in Arabidopsis, wheat, spinach, maize and barley (Renz et al., 1998, Repellin et al., 2008). DTT is required for full activity of the enzyme in all cases. Three surface exposed cysteine residues were proposed to be involved in microheterogeneity in spinach and Arabidopsis, however the residues are a significant distance apart, meaning a large conformational change would be required to form disulfide bridges (Glaring et al., 2012). It is likely that an alternative mechanism is responsible for the effect of Trx and DTT on LD (Glaring et al., 2012). DTT effects on protein activity that are not linked to disulfide modulation have been reported, although the alternate mechanism of action is not clear (Alliegro, 2000).

Experiments involving incubation of recombinant LD, LDI and Trx *h* revealed inactivation of barley LDI can be catalysed by disulfide reduction (Jensen et al., 2012). Trx *h* progressively reduced LDI disulfides which was accompanied by loss of LDI activity. LDI bound to LD was not affected by Trx *h*, meaning Trx is not directly responsible for the dissociation of the LD/LDI complex. It was proposed that Trx aids conformational destabilisation of LDI which may support cysteine protease activity (Longstaff and Bryce, 1993). Thioredoxin has independent effects on LD and LDI. There is a large gap in the knowledge relating to the effect of redox on these proteins.

6.1.3 Genetic Manipulation of Carbohydrate Active Enzymes in Crop Species

Introduction

Mutation in Arabidopsis can be useful to dissect the role of enzymes within the context of a dicot, however metabolic pathways can often differ between species, in particular between dicots and monocots. Dicots utilise lipid reserves within their seed as opposed to cereals which utilise starch as their primary energy reserve for germination (Raven et al., 2005). Differences also exist in the way monocots and dicots synthesise and degrade starch (Morell et al., 2003, Zhu et al., 2015). As such, to identify the precise role of proteins within a monocot crop species, genetic manipulation of the organism of interest is required. Alternative models to Arabidopsis have been proposed, such as Brachypodium and rice, however there can still be distinct differences between these model organisms and the crop being studied (Goff, 1999, Opanowicz et al., 2011, Guillon et al., 2012, Tanackovic et al., 2014). The increasing power of molecular genomics, plant transformation and growth facilities enables the production of transgenic non-model species, allowing work to be carried out in the organism of interest (Morrell et al., 2012). With advances in technology the lines between model and non-model species are becoming blurred.

Traditional breeding techniques and genetic mapping have long been the paradigm for the identification of novel traits (Varshney et al., 2014). More recently Target Induced Local Lesions IN Genomes (TILLING) has enabled a leap forward in the generation of mutants within crop species (Mccallum et al., 2000, Talame et al., 2008, Mrizova et al., 2014). TILLING populations avoid issues with genetic modification (GM) and remain a useful tool to complement GM in research (Kurowska et al., 2011). However backcrossing is required to "clean up" induced mutations and lines may need crossing into elite cultivars which can be expensive and time consuming (Mccallum et al., 2000).

The discovery of gene silencing in plants (Baulcombe, 1996) and animals (Fire et al., 1998) led to the development of RNA interference (RNAi) (Figure 6.6). This technique was heralded as the next genetics revolution (Wasi, 2003) and has indeed proved a useful technique. There are numerous examples of the genetic manipulation of many different targets within cereals (Table 6.2) (Goedeke, 2007, Mcginnis, 2010, Mrizova et al., 2014). It is this technique that is utilised to generate knockdown lines for LD and LDI within this study.

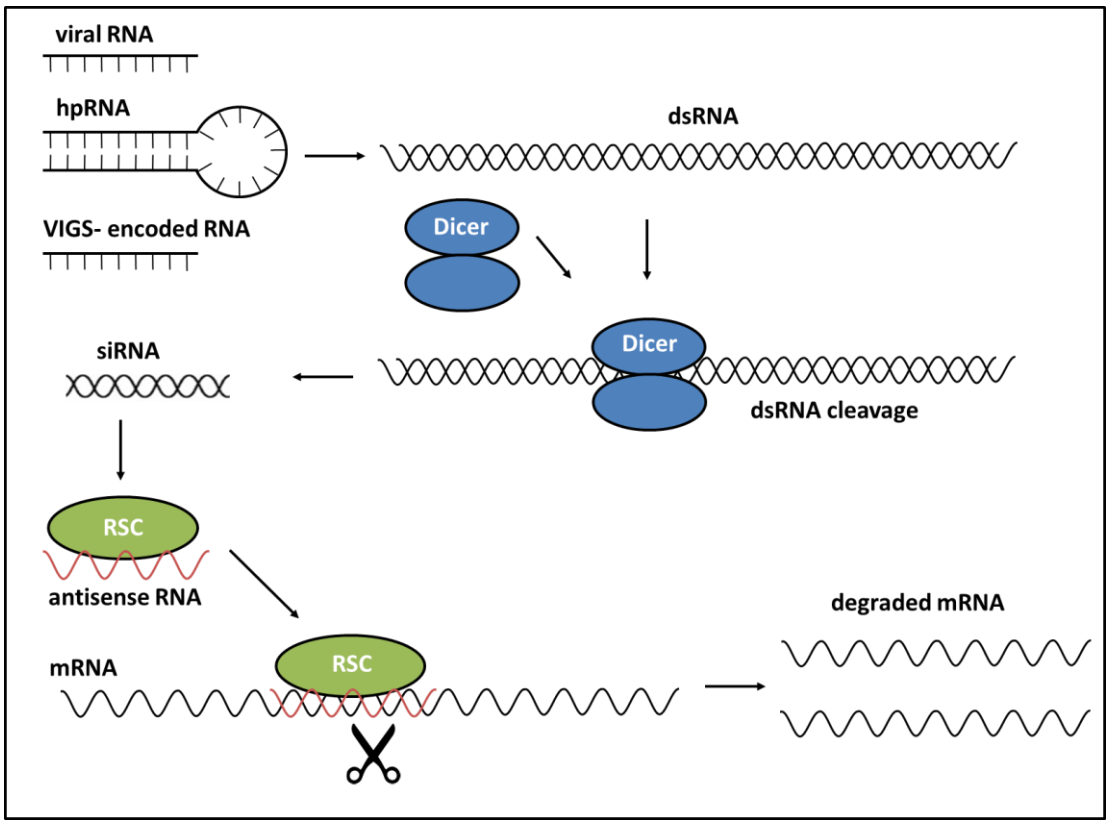

Figure 6.6 The process of RNAi
RNAi initiated by the Dicer enzyme complex which processes double-stranded RNA into ~22- nucleotide small interfering RNAs. These siRNAs are incorporated into the multicomponent nuclease RSC (RNA-induced silencing complex). RSC the nunwinds the siRNA and used the unwind sequence as a guide for substrate selection. Substrates, endogenous mRNA in the case of RNAi, are then degraded.

Gene of interest	Comments	Reference
GWD	RNAi mediated GWD downregulation increased vegetative growth and seed mass in wheat.	(Ral et al., 2012)
β-AMY1, GBSSI, LD, SSI and SSII	Barley TILLING lines. Starches with different features generated. Modified amylose/amylopectin ratios. Different A:B granule ratios.	(Bovina et al., 2011, Sparla et al., 2014)
SBE IIa and b	Barley RNAi. Grains possessed a high amylose phenotype. Reduced branching frequency in amylopectin.	(Regina et al., 2010)
Amylopullulanase	Overexpression of a bi-functional and thermostable amylopullulanase in transgenic rice seeds led to autohydrolysis and altered composition of starch.	(Chiang et al., 2005)
α-amylase and α-glucosidase	Overexpression in barley. Introgressed into an elite cultivar, amylase gave no effect, glucosidase levels were higher.	(Matthews and Jacobsen, 2001)
β-1,3-1,4 glucanase	Overexpression in barley under α-amylase (secretion) or D hordein (endosperm storage) promoters. Barley has low nutritional value in poultry as β-glucan limits nutrient uptake. Grains were tested and showed benefits to poultry nutrition.	(Jensen et al., 1996, Horvath et al., 2000, Von Wettstein et al., 2000)
GWD	Overexpression of GWD in barley endosperm generated hyperphosphorylated starch, plants exhibited no severe phenotype. When germinated, grains degraded starch similarly to wild type.	(Carciofi et al., 2011, Shaik et al., 2014)
SBE I, SBE IIa and SBE IIb	Simultaneous suppression of all three starch branching enzymes by RNAi produced amylose only starch granules.	(Carciofi et al., 2012)
α-amylase	Endosperm specific overexpression of AMY3 generated no significant impact on starch content.	(Whan et al., 2014)

Table 6.2 Selected examples of genetic modification and TILLING in carbohydrate metabolism in crop species
GWD. Glucan water dikinase. SS. Starch synthase. SBE. Starch branching enzyme.

Mutants of Limit Dextrinase and Limit Dextrinase Inhibitor

TILLING mutants have been identified for LD within barley. No truncation or nonsense mutations, which would decrease or knock out LD activity, were generated (Bovina et al., 2011, Sparla et al., 2014). A missense V270I mutant was associated with a higher percentage of small B-granules (Sparla et al., 2014). It was proposed that the enzyme plays a role in starch granule initiation. The possibility that modification of LD activity has a pleiotropic effect on other enzymes involved in starch granule biogenesis was not analysed.

Null mutation of LD has been reported in maize (Dinges, 2003). Homozygous plants were impaired in transient and storage starch degradation. The developing endosperm accumulated branched maltooligosaccharides and were deficient in linear maltooligosaccharides suggesting that LD functions in glucan hydrolysis during kernel starch formation. Knockout of LD affected the levels of other starch metabolic enzymes (SBE and BAM) (Dinges, 2003). Germination of LD mutant grains was briefly analysed. The number of kernels that germinated was the same as wild type. Cotyledon emergence was, however, 1 day later in mutant lines. There are differences between maize and barley LD. LDI does not appear present in the maize genome and recombinant LDI has no effect on maize LD (Wu et al., 2002).

A rice LD insertion knockout mutation has been generated and analysed (Fujita et al., 2009). Knockout of LD had no effect on other enzymes in starch biosynthesis. Levels of short chain amylopectin were increased in the mutant, however, amylose, amylopectin and water soluble polysaccharide (wsp) were almost identical to wild type. Germination of the rice LD mutants was not analysed.

There is only one case of the genetic manipulation of LDI. Transgenic antisense RNA barley lines were generated by bombardment (Stahl, 2004). LDI levels were analysed by western blot and LD inhibitory assay. LDI was present in all western blot samples albeit at different levels. Inhibitory assay showed some lines which have lower inhibitory activity on LD, however the replicates gave large levels of variation. The knockdown of LDI was suggested to have a pleotropic effect on α and β-amylase, which increased in activity in developing endosperm (14 dpa) (Stahl, 2004). The importance of this is questionable as neither enzyme is directly involved in starch synthesis. No effect was seen on SBE and only a small effect on SS activity. The main conclusion from this study was that knockdown of LDI largely impacted on the A/B ratio of starch granules, with a reduced number of B type being generated.

6.2 Aims of this Chapter

Questions arise regarding the importance of LD in starch degradation in barley endosperm as it is reported that the newly synthesised enzyme is not released from the aleurone layer until germination is well underway (3-5 dpi) (Burton et al., 1999, Schroeder and Macgregor, 1998). The levels of LD activity within the endosperm during germination remain unclear. The endogenous, proteinaceous inhibitor of LD, limit dextrinase inhibitor (LDI) has been shown to tightly bind LD *in vitro* (Jensen et al., 2011) This inhibitor is present in ungerminated cereals however its importance in grain germination remains unclear. LD and LDI have never been shown to interact within a plant.

The aims of this chapter were to develop techniques which can be utilised to study the temporal and spatial separation of LD and LDI *in planta*, in order to gain a better understanding of the roles of these proteins during germination and how this relates to their functions during malting and beer manufacture. Antibodies were generated against recombinant LD (Chapter 5) showed the ability to detect barley LD within crude extracts, with the presence of LD being proportional to its activity. Sub-cellular localisation studies using LD and LDI GFP fusions expressed in *N. benthamiana* indicate these proteins may be localised to the plastid and the apoplast, respectively. Homozygous transgenic barley lines containing an RNAi cassette for the knockdown of LD or LDI were also generated using *Agrobacterium* transformation.

6.3 Results

6.3.1 The Antibodies Generated Against Recombinant Protein Specifically Detect Limit Dextrinase in Grain Extracts

In order to gain a better understanding of LD release and activation *in planta* antibodies were generated against recombinant protein. This enables the observation of LD at a protein level, rather than analysing activity, which can be variable depending on the extraction method and assay used. Protein samples from grain at 0, 3, 5, 7 and 9 dpi were analysed using SDS-PAGE, western blot and red pullulan zymography. LD cannot be seen by SDS-PAGE (Figure 6.7, A). The antibodies specifically detect a protein of the correct mass, ~104 kDa, for LD (Figure 6.7, B). The western blot shows an increase in the amount of LD throughout germination. Only trace levels of LD are detected in 0 dpi grain. An increase in LD activity can be seen over the time course (Figure 6.7, C), this correlates well with the protein levels identified by western blot. When incubated with DDT for 16 h a second pullulan degrading activity band appears within the zymogram (Figure 6.7, D).

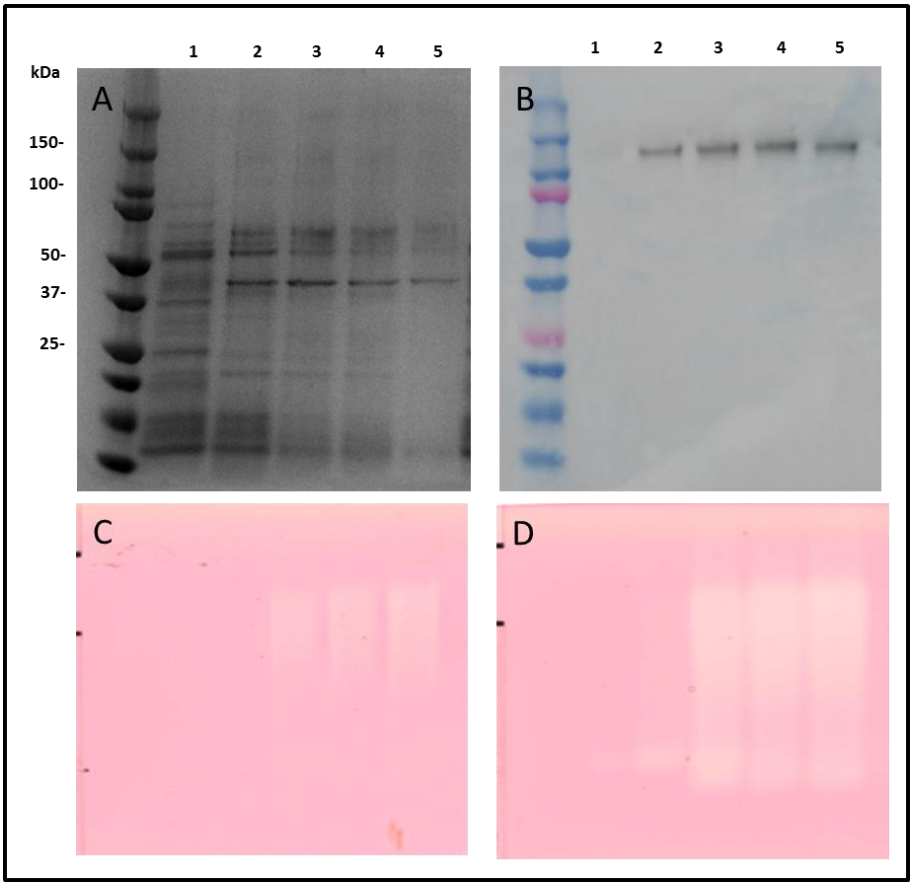

Figure 6.7 Analysis of protein extracts from barley for limit dextrinase
Lanes **1**- 0 dpi. **2**- 3 dpi. **3**- 5 dpi. **4**- 7 dpi. **5**- 9 dpi. **A.** SDS-PAGE **B.** Anti-LD western blot. **C.** Red pullulan zymogram for LD activity, 2 h incubation**. D.** 16 h incubation.

6.3.2 Subcellular Localisation of Limit Dextrinase and Limit Dextrinase Inhibitor GFP-Fusion Proteins

In order to determine the importance of the LD chloroplast transit peptides (cTP) and the LDI signal peptide (SP), discussed in Chapter 5, the genes encoding LD and LDI with and without targeting sequences were cloned into C-terminal GFP fusion protein vectors for plant expression. Agrobacterium harbouring the expression plasmids was infiltrated in to *N. benthamiana* leaves. The expression of GFP fusion proteins was analysed by confocal microscopy. Protein expression is analysed in leaf epidermal cells. Cytosolic proteins appear around the edge of a cell due to the presence of a large vacuole that pushes the cell contents up against the cell wall (Figure 6.8, Left). A gap corresponding to the cell wall and apoplastic space can often be seen between cells. Secreted or cell wall associated proteins appear ase a green band following the shape of a cell (Figure 6.8, middle). Chloroplasts autofluoresce when excited at the wavelength used to detect GFP, as such plastid localised proteins are seen as an orange colour in defined structures (Figure 6.8, right).

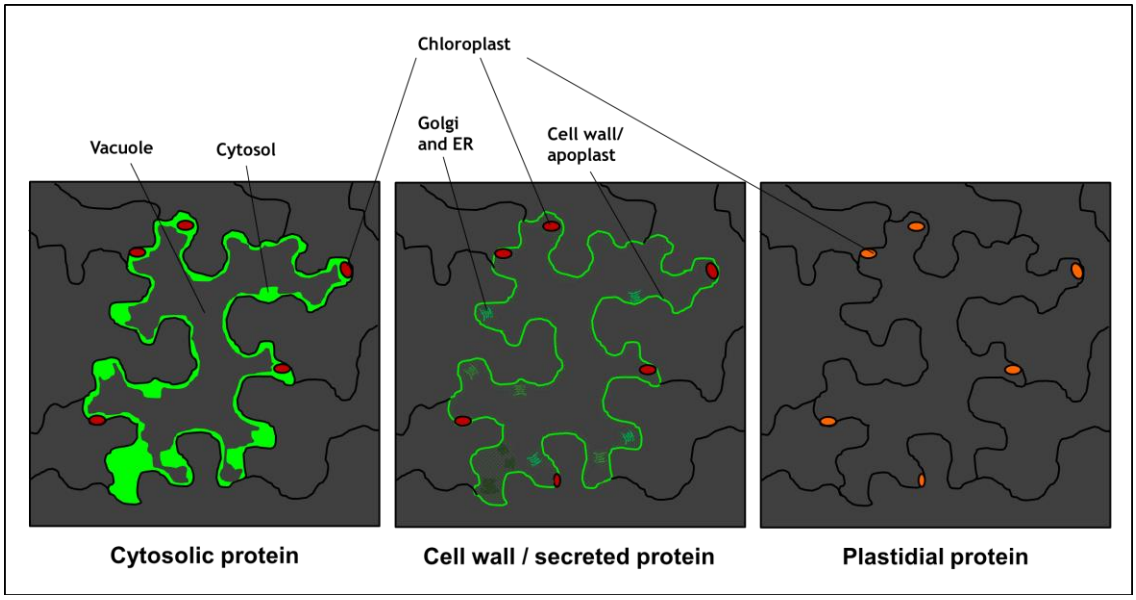

Figure 6.8 Cartoon representation of subcellular localisation analysis using GFP

Expression of SP-LDI-GFP in *N. benthamiana* generated a GFP-tagged protein that appears to localise to the cell wall or apoplast, as would be expected in the presence of the secretion signal peptide. Deletion of the signal peptide and expression of ΔSP-LDI-GFP led to the generation of large aggregate structures (Figure 6.9, D, star), furthermore a distinct line can be identified between the cells, likely indicating the cell walls (Figure 6.9, D, arrow).

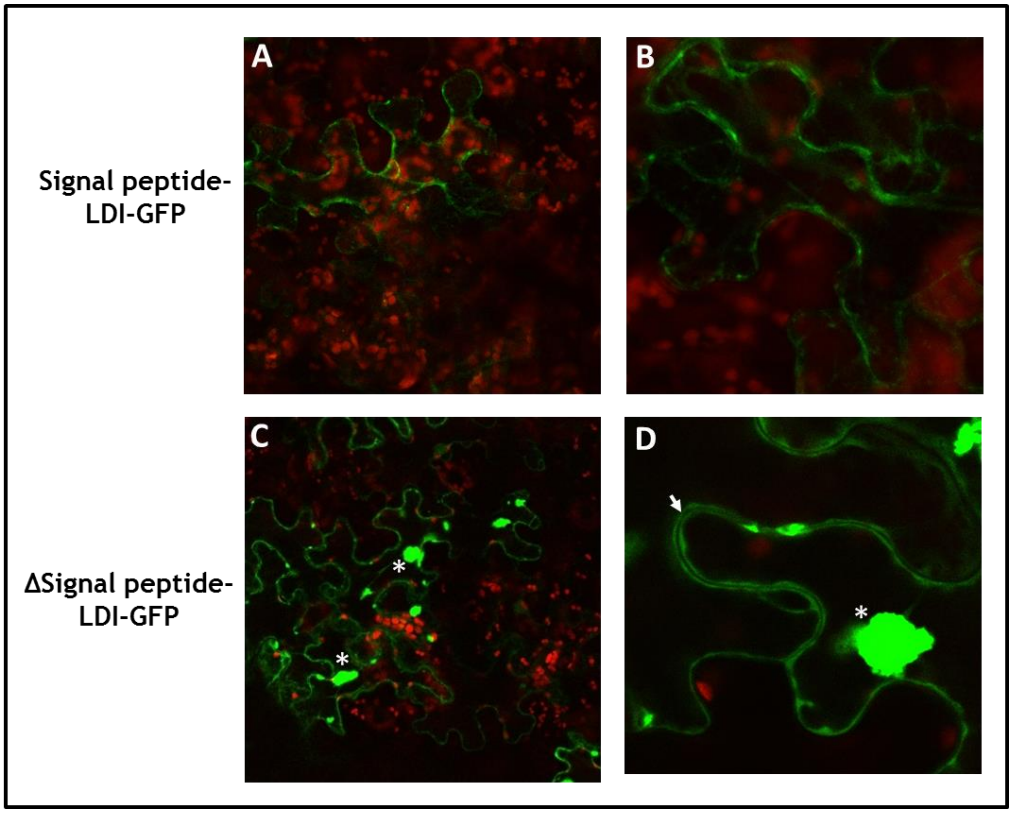

Figure 6.9 The sub-cellular localisation of limit dextrinase inhibitor GFP fusion visualised by confocal microscopy
Epidermal cells of *N. benthamiana*. GFP- green. Chloroplast autofluorescence- red. Arrow indicates a gap between the cytosol of two cells. Star indicates aggregate structures.

Expression of cTP-LD-GFP yields an orange colour within the chloroplasts (Figure 6.10, A, arrow) indicative of GFP and chloroplast merged fluorescence. Under the same conditions Δ-cTP-LD-GFP does not show co-fluorescence, with GFP fluorescence visible at the edges of the cells (Figure 6.10, B, star).

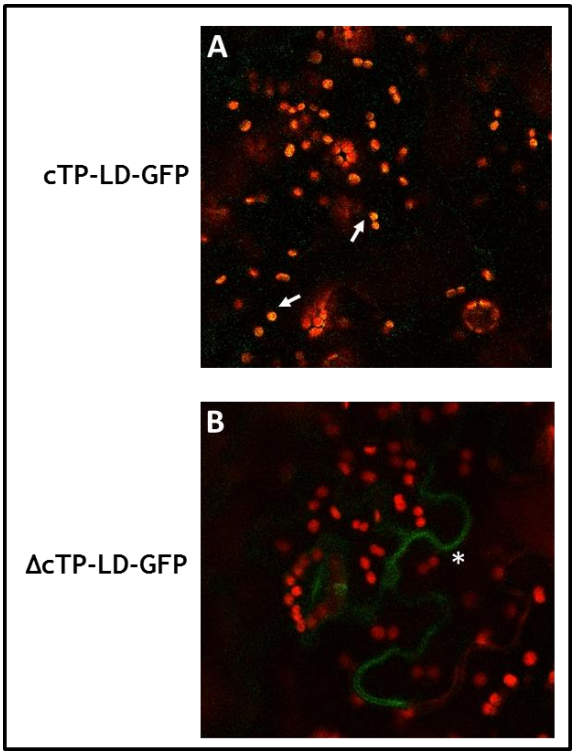

Figure 6.10 The sub-cellular localisation of limit dextrinase GFP fusion visualised by confocal microscopy
Epidermal cells of *N. benthamiana*. GFP- green. Chloroplast autofluorescence- red. Arrow indicates co-localisation of GFP and plastid. Star indicates GFP tagged protein not in the cytosol.

6.3.3 Generation of Transgenic RNAi Knock-down Lines for Limit Dextrinase and Limit Dextrinase Inhibitor

RNAi lines were generated with the support of the BRACT facility at John Innes Centre.

RNAi constructs were generated for LD and LDI using sequences of 301 bp and 243 bp, respectively, which cover the 3' end of the mRNA sequence and the 3'-UTR (Appendix). Fragments were PCR amplified from barley gDNA and cloned into the pCR8-GW-TOPO vector. These were then used in a Gateway LR reaction to transfer the sequences into pBRACT-207 transformation vector, which contains two sets of att recombination sites and therefore generates hairpin RNA (Figure 6.11). The pBRACT-270 vector encodes a constitutive ubiquitin promoter and hygromycin resistance cassette for selection of transformants.

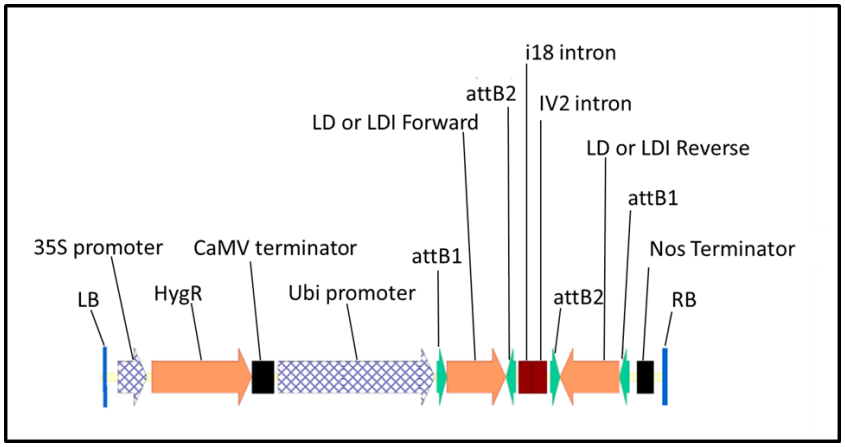

Figure 6.11 Map showing the RNAi cassette transformed into barley.

Immature embryos of barley cultivar golden promise were transformed using *Agrobacterim*, plants were regenerated from callose and selected using hygromycin. 32 lines were generated, 20 LD, 19 LDI and 3 GUS control lines, grown to maturity and allowed to self-fertilise (Figure 6.12).

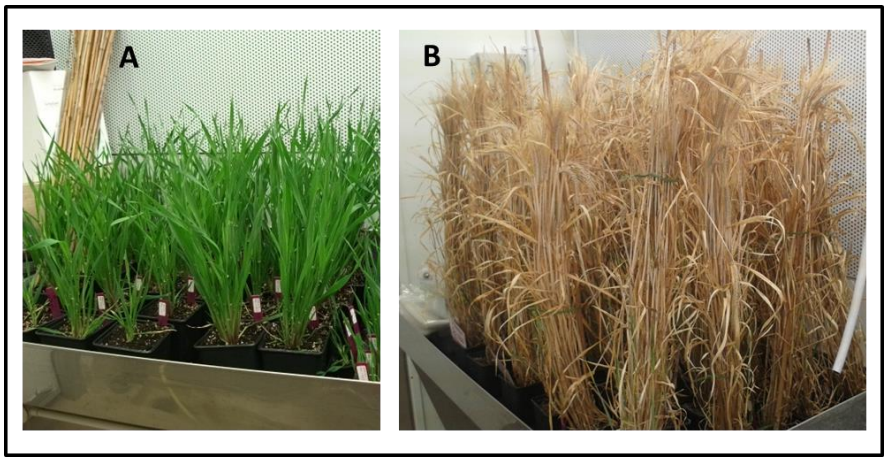

Figure 6.12 T_0 barley lines growing in a controlled environment room.

Leaves from T_0 plants were analysed for copy number using the G-count gene copy number testing (iDNA Genetics) with hygromycin resistance gene specific primers. 10 LD, 9 LDI and 3 GUS single copy lines were identified (Table 6.3). Seeds were collected from all lines.

T_0	**# of Plants**		
Hygromycin Copy Number	**LD**	**LDI**	**GUS**
1	10	9	3
2-8	10	10	0
Total	20	19	3

Table 6.3 Copy number analysis of T_0 transgenic lines

6.3.4 Generation of T_1 Transgenic Plants

10 seeds for each of the 10 LD, 9 LDI and 3 GUS single copy lines were germinated, potted on and allowed to grow for 2 weeks. Leaf samples were taken from these lines and used to prepare gDNA, problems arose with the preparation of DNA. Due to time restrictions it ws decided to grow 4 plants from each single copy line. Plants were grown to maturity and allowed to self-fertilise. Leaves from T_1 plants were analysed for copy number. 12 LD, 8 LDI and 1 GUS homozygous lines were identified (Table 6.4). Seeds were collected from all lines. The lines generated were from 8 (LD) and 5 (LDI) different single copy parental lines. These RNAi lines have not been further analysed.

T_1	**# of Plants**		
Hygromycin Copy Number	**LD**	**LDI**	**GUS**
0	8	15	5
1	16	11	4
2	12	8	1
Other	4	2	2
Total	40	36	12

Table 6.4 Copy number analysis of T_1 transgenic lines

6.4 Discussion

6.4.1 The Release and Activation of Limit Dextrinase During Germination

The analysis of germinated barley grains showed that LD is neither active nor detectable at high levels in whole grain at 0 dpi. By 3 dpi LD is detectable by both anti-LD antibody and using red pullulan zymography, this agrees with the literature precedent for whole grain (Longstaff and Bryce, 1993); when LD was studied in GA treated aleurone layer cultures its release may be earlier (Shahpiri et al., 2015). Incubation of the red pullulan zymogram in the presence of DTT indicates that multiple forms of LD are present, this phenomenon has previously been identified in wheat and spinach LD (Repellin et al., 2008, Schindler et al., 2001). It is not clear how DTT activates LD or what impact the different forms of LD have on glucan metabolism. Within this work multiple forms of LD were identified during the purification of recombinant protein from *E. coli* (Appendix) indicating the redox and pH sensitivity is an inherit property of the enzyme and is not dependent on the source.

6.4.2 Limit Dextrinase and Limit Dextrinase Inhibitor Sub-cellular Localisation

Fusion of LDI to GFP enabled the study of the proteins subcellular localisation. The N-terminal sequence of LDI contains a putative secretory peptide. In the presence of this peptide LDI appears to be localised to the cell wall. Deletion of the secretory peptide leads to the generation of aggregate like structures. LDI is prone to aggregation when expressed in *E. coli*; it is possible that conditions may also generate aggregates *in planta*. LD has been shown to be targeted to the chloroplast in Arabidopsis leaves. Comparison of the barley LD N-terminal sequence with that of Arabidopsis revealed the presence of similar motifs associated with plastid targeting (Chapter 5). Fusion of LD to GFP shows putative targeting to the plastid. It remains unclear what the role the cTP plays in the aleurone of germinating grain. This data hints that LD and LDI may be spatially separated, however, further experiments are required to fully validate the protein subcellular localisation.

6.4.3 Generation of Limit Dextrinase and Limit Dextrinase Inhibitor RNAi Barley Lines

12 LD, 8 LDI and 1 GUS homozygous lines have been generated. Due to the time taken to generate the lines time for analysis was limited. These lines, once analysed, will give a better understanding of the importance of LD and LDI during germination, in contrast to other studies which were focussed on the role of LD during starch synthesis.

6.5 Future Directions

6.5.1 Further Studies on the Localisation of Limit Dextrinase and Limit Dextrinase Inhibitor *in Planta*

A repeat of the subcellular localisation experiment is required with necessary markers of cell localisation as controls. The co-localisation of LD and LDI could also be analysed using two different fluorescent markers or a split YFP system. Barley protoplasts and transformed aleurone layers provide suitable alternatives to *N. benthamiana* leaves.

6.5.2 The Release of Limit Dextrinase During Germination

To determine whether LD release coincides with cell death, inducers or inhibitors of PCD can be utilised in conjunction with the LD specific antibodies that have been developed. Nitric oxide (NO) donors can act as an antioxidants and delay PCD but do not inhibit metabolism. α-amylase has been studied in aleurone cultures treated with SNAP (S-Nitroso-N-acetyl-DL-penicillamine, a NO donor) (Beligni et al., 2002), a similar methodology could be applied to the study of LD release. Aleurone protoplasts could also be studied (Gopalakrishnan et al., 1991).

6.5.3 Analysis of Limit Dextrinase and Limit Dextrinase Inhibitor RNAi Lines

The RNAi lines developed in this chapter require further analysis by qRT-PCR to determine the levels of LD and LDI transcripts, but also require analysis using assays to determine protein activity and western blots to determine protein abundance. The antibodies generated against recombinant LD and LDI are suitable for this purpose.

The protein extracts for assay of LD and LDI must be generated at different time points as LDI levels are at their highest in the early stages of germination whereas LD is not seen at high levels until 3 day in to germination. The amount of DTT used in protein extraction may also effect protein levels, particularly if DTT enables the degradation of LDI. Recombinant LD generated herein can be utilised to assay the levels of LDI present in samples.

Once strong knock-down lines have been identified, these can be father analysed to determine the effect of decreasing LD or LDI levels. Potential techniques for analysis include: micromalting to test effect of protein levels in brewing; microscopy to determine the effect on starch granules; measurements of grain yield and size; germination and measurement of root and shoot length; capillary electrophoresis, gel permeation chromatography of mass spectrometry to study dextrin levels.

6.6 References

Alliegro, M. C. 2000. Effects of dithiothreitol on protein activity unrelated to thiol–disulfide exchange: For consideration in the analysis of protein function with Cleland's reagent. *Analytical Biochemistry,* 282, 102-106.

Bacic, A. & Stone, B. 1981. Chemistry and organization of aleurone cell wall components from wheat and barley. *Functional Plant Biology,* 8, 475-495.

Bamforth, C. W. 2009. Current perspectives on the role of enzymes in brewing. *Journal of Cereal Science,* 50, 353-357.

Baulcombe, D. 1996. RNA as a target and an initiator of post-transcriptional gene silencing in trangenic plants. *Plant Molecular Biology,* 32, 79-88.

Beligni, M. V., Fath, A., Bethke, P. C., Lamattina, L. & Jones, R. L. 2002. Nitric oxide acts as an antioxidant and delays programmed cell death in barley aleurone layers. *Plant Physiology,* 129, 1642-50.

Bethke, P. C. & Jones, R. L. 2001. Cell death of barley aleurone protoplasts is mediated by reactive oxygen species. *The Plant Journal,* 25, 19-29.

Bethke, P. C., Lonsdale, J. E., Fath, A. & Jones, R. L. 1999. Hormonally regulated programmed cell death in barley aleurone cells. *The Plant Cell,* 11, 1033-1046.

Blennow, A. & Svensson, B. 2009. Dynamics of starch granule biogenesis-the role of redox-regulated enzymes and low-affinity carbohydrate-binding modules. *Biocatalysis and Biotransformation,* 28, 3-9.

Bovina, R., Talamè, V., Silvio, S., Sanguineti, M. C., Trost, P., Sparla, F. & Tuberosa, R. 2011. Starch metabolism mutants in barley: A tilling approach. *Plant Genetic Resources,* 9, 170-173.

Burton, R. A., Collins, H. M. & Fincher, G. B. 2010. The role of endosperm cell walls in barley malting quality. *In:* ZHANG, G. & LI, C. (eds.) *Genetics and improvement of barley malt quality.* Springer Berlin Heidelberg.

Burton, R. A., Zhang, X. Q., Hrmova, M. & Fincher, G. B. 1999. A single limit dextrinase gene is expressed both in the developing endosperm and in germinated grains of barley. *Plant Physiology,* 119, 859-71.

Bush, D. S., Cornejo, M. J., Huang, C. N. & Jones, R. L. 1986. Ca-stimulated secretion of alpha-amylase during development in barley aleurone protoplasts. *Plant Physiology,* 82, 566-74.

Buttimer, E. T. & Briggs, D. E. 2000. Mechanisms of the release of bound β-amylase. *Journal of the Institute of Brewing,* 106, 83-94.

Carciofi, M., Blennow, A., Jensen, S., Shaik, S., Henriksen, A., Buléon, A., Holm, P. & Hebelstrup, K. 2012. Concerted suppression of all starch branching enzyme genes in barley produces amylose-only starch granules. *BMC Plant Biology,* 12, 1-16.

Carciofi, M., Shaik, S. S., Jensen, S. L., Blennow, A., Svensson, J. T., Vincze, É. & Hebelstrup, K. H. 2011. Hyperphosphorylation of cereal starch. *Journal of Cereal Science,* 54, 339-346.

Caspers, M. P., Lok, F., Sinjorgo, K. M., Van Zeijl, M. J., Nielsen, K. A. & Cameron-Mills, V. 2001. Synthesis, processing and export of cytoplasmic endo-beta-1,4-xylanase from barley aleurone during germination. *The Plant Journal,* 26, 191-204.

Chen, M. H., Huang, L. F., Li, H. M., Chen, Y. R. & Yu, S. M. 2004. Signal peptide-dependent targeting of a rice alpha-amylase and cargo proteins to plastids and extracellular compartments of plant cells. *Plant Physiology,* 135, 1367-77.

Chiang, C.-M., Yeh, F.-S., Huang, L.-F., Tseng, T.-H., Chung, M.-C., Wang, C.-S., Lur, H.-S., Shaw, J.-F. & Yu, S.-M. 2005. Expression of a bi-functional and thermostable amylopullulanase in transgenic rice seeds leads to autohydrolysis and altered composition of starch. *Molecular Breeding,* 15, 125-143.

Cho, M. J., Wong, J. H., Marx, C., Jiang, W., Lemaux, P. G. & Buchanan, B. B. 1999. Overexpression of thioredoxin h leads to enhanced activity of starch debranching enzyme (pullulanase) in barley grain. *Proceedings of the National Academy of Sciences of the United States of America,* 96, 14641-6.

Chrispeels, M. J. & Varner, J. E. 1967. Gibberellic acid-enhanced synthesis and release of α-amylase and ribonuclease by isolated barley and aleurone layers. *Plant Physiology,* 42, 398-406.

Dinges, J. R. 2003. Mutational analysis of the pullulanase-type debranching enzyme of maize indicates multiple functions in starch metabolism. *The Plant Cell Online,* 15, 666-680.

Domínguez, F. & Cejudo, F. J. 2014. Programmed cell death (PCD): An essential process of cereal seed development and germination. *Frontiers in Plant Science,* 5, 366.

Duke, S. H., Vinje, M. A. & Henson, C. A. 2012. Tracking amylolytic enzyme activities during congress mashing with north american barley cultivars: Comparisons of patterns of activity and beta-amylases with differing bmy1 intron iii alleles and correlations of amylolytic enzyme activities. *Journal of the American Society of Brewing Chemists*, 70, 10-28.

Eastwell, K. C. & Spencer, M. S. 1982. Modes of ethylene action in the release of amylase from barley aleurone layers. *Plant Physiology,* 69, 563-567.

Fincher, G. B. & Shewry, P. 1992. Cell wall metabolism in barley. *Barley: genetics, biochemistry, molecular biology and biotechnology.*, 413-437.

Finnie, C., Andersen, B., Shahpiri, A. & Svensson, B. 2011. Proteomes of the barley aleurone layer: A model system for plant signalling and protein secretion. *Proteomics,* 11, 1595-605.

Fire, A., Xu, S., Montgomery, M. K., Kostas, S. A., Driver, S. E. & Mello, C. C. 1998. Potent and specific genetic interference by double-stranded RNA in caenorhabditis elegans. *Nature,* 391, 806-811.

Frandsen, T. P., Lok, F., Mirgorodskaya, E., Roepstorff, P. & Svensson, B. 2000. Purification, enzymatic characterization, and nucleotide sequence of a high-isoelectric-point alpha-glucosidase from barley malt. *Plant Physiology,* 123, 275-86.

Fujita, N., Toyosawa, Y., Utsumi, Y., Higuchi, T., Hanashiro, I., Ikegami, A., Akuzawa, S., Yoshida, M., Mori, A., Inomata, K., Itoh, R., Miyao, A., Hirochika, H., Satoh, H. & Nakamura, Y. 2009. Characterization of pullulanase (pul)-deficient mutants of rice (*Oryza sativa*) and the function of pul on starch biosynthesis in the developing rice endosperm. *Journal of Experimental Botany,* 60, 1009-23.

Gelhaye, E., Rouhier, N., Navrot, N. & Jacquot, J. P. 2005. The plant thioredoxin system. *Cellular and Molecular Life Sciences CMLS,* 62, 24-35.

Gianinetti, A., Ferrari, B., Frigeri, P. & Stanca, A. M. 2007. In vivo modeling of beta-glucan degradation in contrasting barley (*Hordeum vulgare*) genotypes. *Journal of Agricultural and Food Chemistry,* 55, 3158-66.

Gibbons, G. C. 1980. On the sequential determination of α-amylase transport and cell wall breakdown in germinating seeds of *Hordeum vulgare*. *Carlsberg Research Communications,* 45, 177-184.

Glaring, M. A., Skryhan, K., Kotting, O., Zeeman, S. C. & Blennow, A. 2012. Comprehensive survey of redox sensitive starch metabolising enzymes in *Arabidopsis thaliana*. *Plant Physiology and Biochemistry,* 58, 89-97.

Goedeke. S., Hensel. G., Kapusi. E., Gahrtz, M., Kumlehn, J. 2007. Transgenic barley in fundamental research and biotechnology. *Transgenic Plant Journal,* 1, 104-117.

Goff, S. A. 1999. Rice as a model for cereal genomics. *Current Opinion in Plant Biology,* 2, 86-9.

Gopalakrishnan, B., Sonthayanon, B., Rahmatullah, R. & Muthukrishnan, S. 1991. Barley aleurone layer cell protoplasts as a transient expression system. *Plant Molecular Biology,* 16, 463-7.

Gubler, F., Ashford, A. E. & Jacobsen, J. V. 1987. The release of alpha-amylase through gibberellin-treated barley aleurone cell walls : An immunocytochemical study with lowicryl k4m. *Planta,* 172, 155-61.

Gubler, F. & Jacobsen, J. V. 1992. Gibberellin-responsive elements in the promoter of a barley high-pi alpha-amylase gene. *The Plant Cell,* 4, 1435-1441.

Guerin, J. R., Lance, R. C. M. & Wallace, W. 1992. Release and activation of barley beta-amylase by malt endopeptidases. *Journal of Cereal Science,* 15, 5-14.

Guillon, F., Larre, C., Petipas, F., Berger, A., Moussawi, J., Rogniaux, H., Santoni, A., Saulnier, L., Jamme, F., Miquel, M., Lepiniec, L. & Dubreucq, B. 2012. A comprehensive overview of grain development in *Brachypodium distachyon* variety bd21. *Journal of Experimental*, Botany*,* 63, 739-55.

Hardie, D. G. 1975. Control of carbohydrase formation by gibberellic acid in barley endosperm. *Phytochemistry,* 14, 1719-1722.

He, X. & Kermode, A. R. 2003. Proteases associated with programmed cell death of megagametophyte cells after germination of white spruce (Picea glauca) seeds. *Plant Molecular Biology,* 52, 729-44.

Heisner, C. B. & Bamforth, C. W. 2008. Thioredoxin in barley: Could it have a role in releasing limit dextrinase in brewery mashes? *Journal of the Institute of Brewing,* 114, 122-126.

Horvath, H., Huang, J., Wong, O., Kohl, E., Okita, T., Kannangara, C. G. & Von Wettstein, D. 2000. The production of recombinant proteins in transgenic barley grains. *Proceedings of the National Academy of Sciences of the United States of America,* 97, 1914-9.

Jamar, C., Du-Jardin, P. & Fauconnier, M.-L. 2011. Cell wall polysaccharides hydrolysis of malting barley (*Hordeum vulgare*): A review. *Biotechnology, Agronomy, Society and Environment* 15, 301-313.

Jensen, J. M., Hagglund, P., Christensen, H. E. & Svensson, B. 2012. Inactivation of barley limit dextrinase inhibitor by thioredoxin-catalysed disulfide reduction. *FEBS Letters,* 586, 2479-82.

Jensen, J. M., Vester-Christensen, M. B., Møller, M. S., Bonsager, B. C., Christensen, H. E., Hachem, M. A. & Svensson, B. 2011. Efficient secretory expression of functional barley limit dextrinase inhibitor by high cell-density fermentation of *Pichia pastoris*. *Protein Expression and Purification,* 79, 217-22.

Jensen, L. G., Olsen, O., Kops, O., Wolf, N., Thomsen, K. K. & Von Wettstein, D. 1996. Transgenic barley expressing a protein-engineered, thermostable (1,3-1,4)-beta-glucanase during germination. *Proceedings of the National Academy of Sciences of the United States of America,* 93, 3487-3491.

Jones, B. L. & Budde, A. D. 2005. How various malt endoproteinase classes affect wort soluble protein levels. *Journal of Cereal Science,* 41, 95-106.

Kanauchi, M. & Bamforth, C. W. 2002. Enzymic digestion of walls purified from the starchy endosperm of barley. *Journal of the Institute of Brewing,* 108, 73-77.

Kitajima, A., Asatsuma, S., Okada, H., Hamada, Y., Kaneko, K., Nanjo, Y., Kawagoe, Y., Toyooka, K., Matsuoka, K., Takeuchi, M., Nakano, A. & Mitsui, T. 2009. The rice α-amylase glycoprotein is targeted from the golgi apparatus through the secretory pathway to the plastids. *The Plant Cell,* 21, 2844-2858.

Koehler, S. M. & Ho, T. H. 1990. Hormonal regulation, processing, and secretion of cysteine proteinases in barley aleurone layers. *The Plant Cell,* 2, 769-783.

Kotting, O., Kossmann, J., Zeeman, S. C. & Lloyd, J. R. 2010. Regulation of starch metabolism: The age of enlightenment? *Current Opinion in Plant Biology,* 13, 321-9.

Kurowska, M., Daszkowska-Golec, A., Gruszka, D., Marzec, M., Szurman, M., Szarejko, I. & Maluszynski, M. 2011. Tilling - a shortcut in functional genomics. *Journal of Applied Genetics,* 52, 371-390.

Locy, R., Kende, H. 1978. The mode of secretion of α-amylase in barley aleurone layers. *Planta*, 143, 89-99.

Longstaff, M. A. & Bryce, J. H. 1993. Development of limit dextrinase in germinated barley (*Hordeum vulgare*) (evidence of proteolytic activation). *Plant Physiology,* 101, 881-889.

Macgregor, A. W., Macri, L. J., Schroeder, S. W. & Bazin, S. L. 1994a. Limit dextrinase from malted barley: Extraction, purification, and characterization. *Cereal Chemistry*, 71, 610-617.

Mangan, D., Mccleary, B. V., Cornaggia, C., Ivory, R., Rooney, E. & Mckie, V. 2015. Colourimetric and fluorimetric substrates for the assay of limit dextrinase. *Journal of Cereal Science,* 62, 50-57.

Matthews, P. & Jacobsen, J. 2001. Transformation breeding of barley: Towards malting quality improvement. *Transformation*, M4.

Mccafferty, C. A., Jenkinson, H. R., Brosnan, J. M. & Bryce, J. H. 2004. Limit dextrinase — does its malt activity relate to its activity during brewing? *Journal of the Institute of Brewing,* 110, 284-296.

Mccallum, C. M., Comai, L., Greene, E. A. & Henikoff, S. 2000. Targeting induced locallesions in genomes (TILLING) for plant functional genomics. *Plant Physiology,* 123, 439-442.

Mcginnis, K. M. 2010. RNAi for functional genomics in plants. *Briefings in Functional Genomics,* 9, 111-117.

Meyer, Y., Siala, W., Bashandy, T., Riondet, C., Vignols, F. & Reichheld, J. P. 2008. Glutaredoxins and thioredoxins in plants. *Biochimica et Biophysica Acta (BBA) - Molecular Cell Research,* 1783, 589-600.

Mikkelsen, R., Mutenda, K. E., Mant, A., Schürmann, P. & Blennow, A. 2005. α-glucan, water dikinase (gwd): A plastidic enzyme with redox-regulated and coordinated catalytic activity and binding affinity. *Proceedings of the National Academy of Sciences of the United States of America,* 102, 1785-1790.

Møller, M. S., Vester-Christensen, M. B., Jensen, J. M., Abou Hachem, M., Henriksen, A. & Svensson, B. 2015. Crystal structure of barley limit dextrinase:Limit dextrinase inhibitor (LD:LDI) complex reveals insights into mechanism and diversity of cereal-type inhibitors. *Journal of Biological Chemistry*.

Morell, M. K., Kosar-Hashemi, B., Cmiel, M., Samuel, M. S., Chandler, P., Rahman, S., Buleon, A., Batey, I. L. & Li, Z. 2003. Barley sex6 mutants lack starch synthase iia activity and contain a starch with novel properties. *The Plant Journal,* 34, 173-185.

Morrell, P. L., Buckler, E. S. & Ross-Ibarra, J. 2012. Crop genomics: Advances and applications. *Nature Reviews Genetics,* 13, 85-96.

Morris, P. C. & Stahl, Y. 2004. Plant limit dextrinase inhibitor. Patent WO 2004112468 A1.

Mrizova, K., Holaskova, E., Oz, M. T., Jiskrova, E., Frebort, I. & Galuszka, P. 2014. Transgenic barley: A prospective tool for biotechnology and agriculture. *Biotechnology Advances,* 32, 137-57.

Opanowicz, M., Hands, P., Betts, D., Parker, M. L., Toole, G. A., Mills, E. N., Doonan, J. H. & Drea, S. 2011. Endosperm development in brachypodium distachyon. *Journal of Experimental Botany,* 62, 735-48.

Penson, S. P., Schuurink, R. C., Fath, A., Gubler, F., Jacobsen, J. V. & Jones, R. L. 1996. cGMP is required for gibberellic acid-induced gene expression in barley aleurone, *The Plant Cell*, 8, 2325-2333.

Pettolino, F. A., Walsh, W., Fincher, G. B., Bacic, A. 2012. Determining the polysaccharide composition of plant cell walls, *Nature Protocols*, 7, 1590–1607.

Radchuk, V. V., Borisjuk, L., Sreenivasulu, N., Merx, K., Mock, H.-P., Rolletschek, H., Wobus, U. & Weschke, W. 2009. Spatiotemporal profiling of starch biosynthesis and degradation in the developing barley grain. *Plant Physiology,* 150, 190-204.

Ral, J. P., Bowerman, A. F., Li, Z., Sirault, X., Furbank, R., Pritchard, J. R., Bloemsma, M., Cavanagh, C. R., Howitt, C. A. & Morell, M. K. 2012. Down-regulation of glucan, water-dikinase activity in wheat endosperm increases vegetative biomass and yield. *Plant Biotechnology Journal*, 10, 871-82.

Ranki, H., Sopanen, T. 1984. Secretion of α-amylase by the aleurone layer and the scutellum of germinating barley grain. *Plant Physiology*, 75, 710–715.

Raven, P. H., Evert, R. F. & Eichhorn, S. E. 2005. *Biology of plants*, Macmillan.

Regina, A., Kosar-Hashemi, B., Ling, S., Li, Z., Rahman, S. & Morell, M. 2010. Control of starch branching in barley defined through differential RNAi suppression of starch branching enzyme iia and iib. *Journal of Experimental Botany*, 61, 1469-82.

Ren, J. P., Li, Y., Wong, J. H., Meng, L., Cho, M. J., Buchanan, B. B., Yin, J. & Lemaux, P. G. 2012. Modifying thioredoxin expression in cereals leads to improved pre-harvest sprouting resistance and changes in other grain properties. *Seed Science Research,* 22, S30-S35.

Renz, A., Schikora, S., Schmid, R., Kossmann, J. & Beck, E. 1998. cDNA sequence and heterologous expression of monomeric spinach pullulanase: Multiple isomeric forms arise from the same polypeptide. *Biochemical Journal,* 331, 937-945.

Repellin, A., Båga, M. & Chibbar, R. N. 2008. In vitro pullulanase activity of wheat (*Triticum aestivum*) limit-dextrinase type starch debranching enzyme is modulated by redox conditions. *Journal of Cereal Science,* 47, 302-309.

Ross, H. A., Sungurtas, J., Ducreux, L., Swanston, J. S., Davies, H. V. & Mcdougall, G. J. 2003. Limit dextrinase in barley cultivars of differing malting quality: Activity, inhibitors and limit dextrin profiles. *Journal of Cereal Science,* 38, 325-334.

Schindler, I., Renz, A., Schmid, F. X. & Beck, E. 2001. Activation of spinach pullulanase by reduction results in a decrease in the number of isomeric forms. *Biochimica et Biophysica Acta,* 1548, 175-86.

Schmitt, M. R. & Marinac, L. 2008. Beta-amylase degradation by serine endoproteinases from green barley malt. *Journal of Cereal Science,* 47, 480-488.

Schroeder, S. & Macgregor, A. 1998. Synthesis of limit dextrinase in germinated barley kernels and aleurone tissues. *Journal of the American Society of Brewing Chemists,* 56, 32-37.

Shahpiri, A., Talaei, N. & Finnie, C. 2015. Spatio-temporal appearance of alpha-amylase and limit dextrinase in barley aleurone layer in response to gibberellic acid, abscisic acid and salicylic acid. *Journal of the Science of Food and Agriculture,* 95, 141-7.

Shaik, S. S., Carciofi, M., Martens, H. J., Hebelstrup, K. H. & Blennow, A. 2014. Starch bioengineering affects cereal grain germination and seedling establishment. *Journal of Experimental Botany,* 65, 2257-70.

Silver, D. M., Silva, L. P., Issakidis-Bourguet, E., Glaring, M. A., Schriemer, D. C. & Moorhead, G. B. 2013. Insight into the redox regulation of the phosphoglucan phosphatase sex4 involved in starch degradation. *FEBS Journal,* 280, 538-48.

Sparla, F., Costa, A., Lo Schiavo, F., Pupillo, P. & Trost, P. 2006. Redox regulation of a novel plastid-targeted beta-amylase of *Arabidopsis*. *Plant Physiology,* 141, 840-50.

Sparla, F., Falini, G., Botticella, E., Pirone, C., Talamè, V., Bovina, R., Salvi, S., Tuberosa, R., Sestili, F. & Trost, P. 2014. New starch phenotypes produced by TILLING in barley. *PLoS ONE,* 9, e107779.

Stahl, Y., Alexander, R. D., Coates, S., Bryce, J. H., Jenkinson, H. R. & Morris, P. C. 2007. The barley limit dextrinase inhibitor: Gene expression, protein location and interaction with 14-3-3 protein. *Plant Science,* 172, 452-461.

Stanley, D., Rejzek, M., Naested, H., Smedley, M., Otero, S., Fahy, B., Thorpe, F., Nash, R. J., Harwood, W., Svensson, B., Denyer, K., Field, R. A. & Smith, A. M. 2011. The role of alpha-glucosidase in germinating barley grains. *Plant Physiology,* 155, 932-43.

Subbarao, K. V., Datta, R. & Sharma, R. 1998. Amylases synthesis in scutellum and aleurone layer of maize seeds. *Phytochemistry,* 49, 657-66.

Taiz, L. & Honigman, W. A. 1976. Production of cell wall hydrolyzing enzymes by barley aleurone layers in response to gibberellic acid. *Plant Physiology,* 58, 380-386.

Talame, V., Bovina, R., Sanguineti, M. C., Tuberosa, R., Lundqvist, U. & Salvi, S. 2008. Tillmore, a resource for the discovery of chemically induced mutants in barley. *Plant Biotechnology Journal,* 6, 477-85.

Tanackovic, V., Svensson, J. T., Jensen, S. L., Buleon, A. & Blennow, A. 2014. The deposition and characterization of starch in *Brachypodium distachyon*. *Journal of Experimental Botany,* 65, 5179-92.

Tibbot, B. K. & Skadsen, R. W. 1996. Molecular cloning and characterization of a gibberellin-inducible, putative alpha-glucosidase gene from barley. *Plant Molecular Biology,* 30, 229-41.

Varshney, R. K., Terauchi, R. & Mccouch, S. R. 2014. Harvesting the promising fruits of genomics: Applying genome sequencing technologies to crop breeding. *PLoS Biology,* 12, e1001883.

Villarejo, A., Buren, S., Larsson, S., Dejardin, A., Monne, M., Rudhe, C., Karlsson, J., Jansson, S., Lerouge, P., Rolland, N., Von Heijne, G., Grebe, M., Bako, L. & Samuelsson, G. 2005. Evidence for a protein transported through the secretory pathway en route to the higher plant chloroplast. *Nature Cell Biology,* 7, 1224-1231.

Vlodawsky, L. E. A., Harel, E. & Mayer, A. M. 1971. The effect of growth regulators and Cu2+ on the activation of amylopectin-1,6-glucosidase activity in pea seedlings. *Physiologia Plantarum,* 25, 363-368.

Von Wettstein, D., Mikhaylenko, G., Froseth, J. A. & Kannangara, C. G. 2000. Improved barley broiler feed with transgenic malt containing heat-stable (1,3-1,4)-beta-glucanase. *Proceedings of the National Academy of Sciences of the United States of America,* 97, 13512-7.

Wang, S. M., Lue, W. L., Wu, S. Y., Huang, H. W. & Chen, J. 1997. Characterization of a maize beta-amylase cDNA clone and its expression during seed germination. *Plant Physiology,* 113, 403-409.

Wang, S. M., Yang, F. M. & Chou, A. H. 2004. Beta-amylase is not involved in degradation of endosperm starch during seed germination of maize. *Taiwania,* 49, 263-272.

Wasi, S. 2003. Rna interference: The next genetics revolution? from Horizon Symposia; Understanding the RNAissance. Nature Publishing Group, 1-4.

Whan, A., Dielen, A. S., Mieog, J., Bowerman, A. F., Robinson, H. M., Byrne, K., Colgrave, M., Larkin, P. J., Howitt, C. A., Morell, M. K. & Ral, J. P. 2014. Engineering alpha-amylase levels in wheat grain suggests a highly sophisticated level of carbohydrate regulation during development. *Journal of Experimental Botany,* 65, 5443-57.

Wilson, S. M., Burton, R. A., Collins, H. M., Doblin, M. S., Pettolino, F. A., Shirley, N., Fincher, G. B. & Bacic, A. 2012. Pattern of deposition of cell wall polysaccharides and transcript abundance of related cell wall synthesis genes during differentiation in barley endosperm. *Plant Physiology,* 159, 655-70.

Wise, R. 2006. The diversity of plastid form and function. *In:* WISE, R. & HOOBER, J. K. (eds.) *The structure and function of plastids.* Springer Netherlands.

Wong, J. H., Kim, Y. B., Ren, P. H., Cai, N., Cho, M. J., Hedden, P., Lemaux, P. G. & Buchanan, B. B. 2002. Transgenic barley grain overexpressing thioredoxin shows evidence that the starchy endosperm communicates with the embryo and the aleurone. *Proceedings of the National Academy of Sciences of the United States of America,* 99, 16325-30.

Wrobel, R. & Jones, B. L. 1992. Appearance of endoproteolytic enzymes during the germination of barley. *Plant Physiology,* 100, 1508-16.

Wu, C., Colleoni, C., Myers, A. M. & James, M. G. 2002. Enzymatic properties and regulation of zpu1, the maize pullulanase-type starch debranching enzyme. *Archives of Biochemistry and Biophysics,* 406, 21-32.

Yamada, J. 1981. Inactive debranching-enzyme in rice seeds, and its activation. *Carbohydrate Research,* 90, 153-157.

Zhu, F., Bertoft, E., Szydlowski, N., D'hulst, C. & Seetharaman, K. 2015. Branching patterns in leaf starches from *Arabidopsis* mutants deficient in diverse starch synthases. *Carbohydrate Research,* 401, 96-108.

Chapter 7- General Discussion

7.1 Inhibition of Plant Growth by Iminosugars

DNJ was shown to affect *N*-linked glycoprotein metabolism, this phenomenon has been previously identified (Mega, 2005), however, advances in analytical techniques have enabled the identification of a root specific increase in $Man_{8/9}$. The root specific growth inhibition caused by DNJ is likely linked to the changes seen in *N*-linked glycan structure. The precise mode by which DNJ perturbs root growth remains to be identified. Other, unidentified, targets of DNJ probably exist in plants, mammalian proteins capable of binding DNJ (Cruz et al., 2013) have orthologues in Arabidopsis.

GCS was also shown to be a likely target for the inhibition of root growth, two types of known GCS inhibitors both showed root inhibition, this hypothesis is further supported by a recent publication identifying GCS as an important protein for plant development (Msanne et al., 2015). It remains to be tested whether there is cross talk between interference with glycoprotein processing and GCS within plants. Ceramide metabolism has been linked to glycoproteins within mammalian systems, with correct *N*-linked glycans being required for the formation of protein complexes involved in glycosphingolipid metabolism (Bieberich, 2014).

Ido-AEP-DNJ will prove a useful tool to help dissect the roles of GC and ceramide in plants, as mutants in GCS are lethal the ability to add a compound to knock out protein activity enables study at particular time points that could not be achieved using genetics. Ceramide has been implicated in important developmental processes, including PCD, in plants. This has potential application in regulation of plant pathogen resistance, yield and stress tolerance (Berkey et al., 2012).

Both Arabidopsis and tef have proven to be suitable models for chemical genetic screens to identify novel inhibitors of root growth. There are numerous potential libraries that can be screened using these systems.

7.2 *In Vitro* Inhibition of Glycosyl Hydrolases

It has been demonstrated that compounds with partial inhibitory activity towards recombinant LD (expressed in *P. pastoris*, by collaborators) can be developed. Current iminosugars show only partial inhibition of LD due to small size and weak binding, there is potential for the generation of novel iminosugars which may show strong (µM/nM) LD inhibition. A potent,

specific, inhibitor could complement genetic knock-down studies. There is also further potential that an inhibitor could modulate LD activity during the malting and mashing steps of brewing, to control the glycan profile of beer (Petersen et al., 2014). Chemical leads also have implications in medicine, the pullulanase of *Streptococcal* species is a key virulence factor (Van Bueren et al., 2007).

The peptide based inhibitors identified represent a starting point that could be further rationally designed, particularly in the light of the publication of the LD:LDI crystal structure. Peptides modelled on LDI are inhibitors of LD at high concentration, good structural mimics can be modelled based on the LDI structure and sequence. There is the potential to modify the specificity of proteinaceous inhibitors, such as LDI, for biotechnological applications. For example transgenic expression of an insect antimicrobial peptide in potato enhanced pathogen resistance (Osusky et al., 2000).

The biosynthetic pathway of DNJ is different between plants and bacteria, identification of the enzymes involved in these pathways may enable the manipulation of DNJ metabolism to generate novel iminosugars (Shibano et al., 2004, Kang et al., 2011). Mining the genomes of iminosugar producing plants, such as mulberry (He et al., 2013), may offer opportunities to engineer biosynthesis into a heterologous host for the production of modified iminosugars.

7.3 Cloning and Expression

LD and LDI were cloned, expressed in *E. coli* and purified to meet the need for recombinant LD for further chemical screening. Utilising recombinant LD protein in further compound screens opens up the potential of identifying a chemical inhibitor that may have use in dissecting the roles of LD and LDI *in planta*. Soluble LD was produced however there remains room for further optimisation of the expression and purification methods. LD and LDI were used for antibody production which will enable better analysis of these proteins in barley grains.

The role of transglycosylation catalysed by LD remains an unanswered question. It is unknown whether transglycosylation is important for either starch synthesis or degradation. Recombinant LD can be utilised to better understand this process as well as having the potential in the synthesis of novel compounds (Wang and Huang, 2009).

There is commercial interest in LD as a standard for use in analysis of brewing or as an exogenous enzyme to add during mashing to reduce branching levels. Currently pullulanase is

used for this purpose. The complete conversion of starch to glucose is important in the creation of distilled spirits, in which the concentration of ethanol generated is proportional to the amount of available glucose for metabolism by yeast. Yeast is unable to efficiently hydrolyse starch and limit dextrins meaning incomplete conversion to glucose during mashing represents a loss of fermentable material (Sapińska et al., 2014). Efficient use of starch feedstocks is also important in bioethanol production (Nahampun et al., 2013, Favaro et al., 2013).

7.4 The Roles of Limit Dextrinase and Limit Dextrinase Inhibitor

It remains unknown whether LD and LDI interact within plants, it is possible that temporal and spatial separation mean the two proteins never come into contact in the context of the germinating endosperm. The question that arises is why do the two proteins interact *in vitro*. To enable the study of LD and LDI sub-cellular and tissue specific localisation GFP-fusion constructs and protein specific antibodies have been generated.

Cereals have been bred to contain more starch than is required for seedling establishment. It is imaginable that LD played an important role in the hydrolysis of dextrins in the progenitor of barley, allowing for a gradual breakdown of starch at a steady rate. Rapid starch hydrolysis could lead to the production of glucose at a rate faster than it can be used by a growing embryo. Excess glucose may leave a grain more susceptible to pathogen attack. LDI may also act as a failsafe to stop rapid exhaustion of carbohydrate reserves or may confer resistance to a hitherto unidentified pathogen *via* inhibition of glycosyl hydrolases. Brachypodium may be suitable as a tool to look into starch metabolism before domestication (Tanackovic et al., 2014), this is particularly useful as LDI has been identified in Barchypodium (Møller et al., 2015).

To better understand the roles of LD and LDI during germination homozygous RNAi lines have been generated. All grains used in this study germinated normally and transgenic plant growth was identical to controls suggesting that LD or LDI are likely not essential. Further testing is required to determine the level of knock-down within these lines and understand how LD and LDI contribute to starch metabolism. If the LD and LDI RNAi lines show promising results there is the possibility to look into TILLING populations that can potentially be crossed into the barley lines used for brewing.

Sphingolipids, including ceramide and derivatives act as intracellular signalling molecules, linked to redox regulation and cell death in mammals (Won and Singh, 2006). If this is also the case for plants there may be a link between GCS inhibition and other endosperm processes during germination. Thioredoxin, hormone control and PCD have all been shown to be important for seed germination (Hagglund et al., 2013, Domínguez and Cejudo, 2014). Transcriptomics, proteomics and metabolite profiling have all been carried out on germinating barley (Sreenivasulu et al., 2008, Frank et al., 2011, Barba-Espin et al., 2014). Complete integration of this data will generate a thorough analysis of the germination process and may help elucidate the roles and importance of LD, LDI and other hydrolytic enzymes.

7.5 The Future of Starch Metabolism

Starch is important, not only as a foodstuff, but also as a higher value commodity generated bymodification through physical, chemical or enzymatic treatments. Their remains large gaps in our understanding of this abundant biopolymer. Recently a number of advances have been made in the understanding of regulation of starch biosynthesis and degradation (Stitt and Zeeman, 2012, Smith, 2012). The regulation of starch metabolism by phosphorylation, redox, T6P and circadian clock have been shown in Arabidopsis (Lloyd and Kossmann, 2015)

One of the most pressing questions is: how do plants to make starch? The synthesis of glycogen is well understood, however the process by which amylopectin, a similar polymer, forms insoluble, crystalline, starch granules remains unclear (D'hulst and Merida, 2010). Protein-protein and protein-substrate interactions are implicated as important for correct starch synthesis and degradation (Cockburn et al., 2015, Seung et al., 2015). Furthermore branch point distributions and glucose chain length are important for correct starch structure *in planta* (Zhu et al., 2015, Pfister et al., 2014). An understanding of these enzymes requires analysis of their function, these type of studies are often performed using solubilised substrates. Analysis of enzymes on a surface more similar to a starch granule surface may enable a more realistic analysis of their activities (O'Neill et al., 2014).

GM crops offer advantages over existing crops for farmers, giving increased yield and lower reliance on chemicals such as pesticides (Klumper and Qaim, 2014). The advent of CRISPR/Cas9 within wheat, rice and maize offers an exciting avenue for the production of plants lacking genes of interest (Shan et al., 2014, Bortesi and Fischer, 2015, Liang et al., 2014, Cong et al., 2013, Belhaj et al., 2013). CRISPR/Cas9 has recently been developed in barley at the John Innes Centre (Lawrenson et al., 2015).

The use of complementary *in vitro* and *in vivo* techniques using both plant and microbial enzymes and expression systems offers the widest scope for the manipulation of starch metabolism (Hebelstrup et al., 2015, O'neill and Field, 2015).

7.6 Conclusions and Perspective

A vast proportion of the human diet comes from carbohydrates. With the growing global population and the increasing prevalence of carbohydrate linked diseases, such as diabetes and obesity (Boling et al., 2009), improvements in the way we utilise cereals are required (Lafiandra et al., 2014, Blennow et al., 2013). A fundamental understanding of the roles that carbohydrates play in metabolism is essential if we are to manipulate processes such as starch and cell wall biosynthesis, modification and degradation.

Chemical genetics and genetics provide complementary approaches that can be utilised in conjunction to dissect complex biological processes and pathways. Both techniques have advantages and disadvantages. Chemical inhibitors can often target multiple proteins, this can be a blessing or a curse. The rigorous identification of biological targets represents the key step in chemical genetics (Kaschani and Van Der Hoorn, 2007, Kasper et al., 2009, Hicks and Raikhel, 2014). Perhaps the largest benefit in the use of chemical genetics is the ability to study essential developmental processes, such as embryo growth, as seen in germinating seeds.

Chemical genomics (genome scale chemical genetics) coupled with genomics, transcriptomics and proteomics offers the potential to obtain and analyse a large amount of data to better elucidate a chemicals effect on a system (Norambuena et al., 2009). The sheer diversity and complexity of carbohydrates within biological systems implies many undiscovered avenues remain for future scientific discovery and study, using both chemical genetics and transgenics.

7.7 References

Barba-Espin, G., Dedvisitsakul, P., Hagglund, P., Svensson, B. & Finnie, C. 2014. Gibberellic acid-induced aleurone layers responding to heat shock or tunicamycin provide insight into the N-glycoproteome, protein secretion, and endoplasmic reticulum stress. *Plant Physiology,* 164, 951-65.

Belhaj, K., Chaparro-Garcia, A., Kamoun, S. & Nekrasov, V. 2013. Plant genome editing made easy: Targeted mutagenesis in model and crop plants using the CRISPR/Cas system. *Plant Methods,* 9, 39.

Berkey, R., Bendigeri, D. & Xiao, S. 2012. Sphingolipids and plant defense/disease: The "death" connection and beyond. *Frontiers in Plant Science,* 3, 68.

Bieberich, E. 2014. Synthesis, processing, and function of N-glycans in N-glycoproteins. *Advances in Neurobiology,* 9, 47-70.

Blennow, A., Jensen, S. L., Shaik, S. S., Skryhan, K., Carciofi, M., Holm, P. B., Hebelstrup, K. H. & Tanackovic, V. 2013. Future cereal starch bioengineering: Cereal ancestors encounter gene technology and designer enzymes. *Cereal Chemistry Journal,* 90, 274-287.

Boling, C. L., Westman, E. C. & Yancy, W. S., Jr. 2009. Carbohydrate-restricted diets for obesity and related diseases: An update. *Current Atherosclerosis Reports,* 11, 462-9.

Bortesi, L. & Fischer, R. 2015. The CRISPR/Cas system for plant genome editing and beyond. *Biotechnology Advances,* 33, 41-52.

Cockburn, D., Nielsen, M. M., Christiansen, C., Andersen, J. M., Rannes, J. B., Blennow, A. & Svensson, B. 2015. Surface binding sites in amylase have distinct roles in recognition of starch structure motifs and degradation. *International Journal of Biological Macromolecules,* 75, 338-45.

Cong, L., Ran, F. A., Cox, D., Lin, S., Barretto, R., Habib, N., Hsu, P. D., Wu, X., Jiang, W., Marraffini, L. A. & Zhang, F. 2013. Multiplex genome engineering using CRISPR/Cas systems. *Science,* 339, 819-23.

Cruz, I. N., Barry, C. S., Kramer, H. B., Chuang, C. C., Lloyd, S., Van Der Spoel, A. C., Platt, F. M., Yang, M. & Davis, B. G. 2013. Glycomimetic affinity-enrichment proteomics identifies partners for a clinically-utilized iminosugar. *Chemical Science,* 4, 3442.

D'hulst, C. & Merida, A. 2010. The priming of storage glucan synthesis from bacteria to plants: Current knowledge and new developments. *New Phytologist,* 188, 13-21.

Domínguez, F. & Cejudo, F. J. 2014. Programmed cell death (PCD): An essential process of cereal seed development and germination. *Frontiers in Plant Science,* 5, 366.

Favaro, L., Jooste, T., Basaglia, M., Rose, S. H., Saayman, M., Görgens, J. F., Casella, S. & Van Zyl, W. H. 2013. Designing industrial yeasts for the consolidated bioprocessing of starchy biomass to ethanol. *Bioengineered,* 4, 97-102.

Frank, T., Scholz, B., Peter, S. & Engel, K.-H. 2011. Metabolite profiling of barley: Influence of the malting process. *Food Chemistry,* 124, 948-957.

Hagglund, P., Bjornberg, O., Navrot, N., Morch Jensen, J., Maeda, K., Kirkensgaard, K., Shahpiri, A., Sultan, A., Bunkenborg, J., Gubler, F., Barrero, J. M., Henriksen, A., Finnie, C. & Svensson, B. 2013. The barley grain thioredoxin system - an update. *Front Plant Sci,* 4, 151.

He, N., Zhang, C., Qi, X., Zhao, S., Tao, Y., Yang, G., Lee, T. H., Wang, X., Cai, Q., Li, D., Lu, M., Liao, S., Luo, G., He, R., Tan, X., Xu, Y., Li, T., Zhao, A., Jia, L., Fu, Q., Zeng, Q., Gao, C., Ma, B., Liang, J., Wang, X., Shang, J., Song, P., Wu, H., Fan, L., Wang, Q., Shuai, Q., Zhu, J., Wei, C., Zhu-Salzman, K., Jin, D., Wang, J., Liu, T., Yu, M., Tang, C., Wang, Z., Dai, F., Chen, J., Liu, Y., Zhao, S., Lin, T., Zhang, S., Wang, J., Wang, J.,

Yang, H., Yang, G., Wang, J., Paterson, A. H., Xia, Q., Ji, D. & Xiang, Z. 2013. Draft genome sequence of the mulberry tree *Morus notabilis*. *Nature Communications,* 4, 2445.

Hebelstrup, K. H., Sagnelli, D. & Blennow, A. 2015. The future of starch bioengineering: GM microorganisms or GM plants? *Frontiers in Plant Science,* 6, 247.

Hicks, G. R. & Raikhel, N. V. 2014. Plant chemical biology: Are we meeting the promise? *Frontiers in Plant Science,* 5, 455.

Kang, K. D., Cho, Y. S., Song, J. H., Park, Y. S., Lee, J. Y., Hwang, K. Y., Rhee, S. K., Chung, J. H., Kwon, O. & Seong, S. I. 2011. Identification of the genes involved in 1-deoxynojirimycin synthesis in *Bacillus subtilis* mori 3k-85. *Journal of Microbiology,* 49, 431-40.

Kaschani, F. & Van Der Hoorn, R. 2007. Small molecule approaches in plants. *Current Opinion in Chemical Biology,* 11, 88-98.

Kasper, A. C., Baker, J. B., Kim, H. & Hong, J. 2009. The end game of chemical genetics: Target identification. *Future Medicinal Chemistry,* 1, 727-736.

Klumper, W. & Qaim, M. 2014. A meta-analysis of the impacts of genetically modified crops. *PLoS One,* 9, e111629.

Lafiandra, D., Riccardi, G. & Shewry, P. R. 2014. Improving cereal grain carbohydrates for diet and health. *Journal of Cereal Science,* 59, 312-326.

Lawrenson, T., Shorinola, O., Stacey, N., Li, C., Patron, N., Uauy, C., Harwood, W. 2015. Induction of targeted, heritable mutations in barley and Brassica oleracea using RNA-guided Cas9 nuclease. *Genome Biology*, 16:258

Liang, Z., Zhang, K., Chen, K. & Gao, C. 2014. Targeted mutagenesis in zea mays using TALENs and the CRISPR/Cas system. *Journal of Genetics and Genomics,* 41, 63-68.

Lloyd, J. R. & Kossmann, J. 2015. Transitory and storage starch metabolism: Two sides of the same coin? *Current Opinion in Biotechnology,* 32, 143-148.

Mega, T. 2005. Glucose trimming of n-glycan in endoplasmic reticulum is indispensable for the growth of Raphanus sativus seedling (kaiware radish). *Bioscience, Biotechnology, and Biochemistry,* 69, 1353-64.

Møller, M. S., Vester-Christensen, M. B., Jensen, J. M., Abou Hachem, M., Henriksen, A. & Svensson, B. 2015. Crystal structure of barley limit dextrinase:Limit dextrinase inhibitor (LD:LDI) complex reveals insights into mechanism and diversity of cereal-type inhibitors. *The Journal of Biological Chemistry*.

Msanne, J., Chen, M., Luttgeharm, K. D., Bradley, A. M., Mays, E. S., Paper, J. M., Boyle, D. L., Cahoon, R. E., Schrick, K. & Cahoon, E. B. 2015. Glucosylceramide is critical for cell-type differentiation and organogenesis, but not for cell viability in arabidopsis. *The Plant Journal*, 84, 188-201.

Nahampun, H. N., Lee, C. J., Jane, J. L. & Wang, K. 2013. Ectopic expression of bacterial amylopullulanase enhances bioethanol production from maize grain. *Plant Cell Reports,* 32, 1393-405.

Norambuena, L., Raikhel, N. V. & Hicks, G. R. 2009. Chemical genomics approaches in plant biology. *Methods in Molecular Biology,* 553, 345-54.

O'Neill, E. C. & Field, R. A. 2015. Underpinning starch biology with in vitro studies on carbohydrate-active enzymes and biosynthetic glycomaterials. *Frontiers in Bioengineering and Biotechnology,* 3.

O'Neill, E. C., Rashid, A. M., Stevenson, C. E. M., Hetru, A.-C., Gunning, A. P., Rejzek, M., Nepogodiev, S. A., Bornemann, S., Lawson, D. M. & Field, R. A. 2014. Sugar-coated sensor chip and nanoparticle surfaces for the in vitro enzymatic synthesis of starch-like materials. *Chemical Science,* 5, 341-350.

Osusky, M., Zhou, G., Osuska, L., Hancock, R. E., Kay, W. W. & Misra, S. 2000. Transgenic plants expressing cationic peptide chimeras exhibit broad-spectrum resistance to phytopathogens. *Nature Biotechnology,* 18, 1162-6.

Petersen, B. O., Nilsson, M., Bojstrup, M., Hindsgaul, O. & Meier, S. 2014. (1)h NMR spectroscopy for profiling complex carbohydrate mixtures in non-fractionated beer. *Food Chemistry,* 150, 65-72.

Pfister, B., Lu, K. J., Eicke, S., Feil, R., Lunn, J. E., Streb, S. & Zeeman, S. C. 2014. Genetic evidence that chain length and branch point distributions are linked determinants of starch granule formation in *Arabidopsis*. *Plant Physiology,* 165, 1457-1474.

Sapińska, E., Balcerek, M., Pielech-Przybylska, K. & Stanisz, M. 2014. The impact of treatment of cereal mashes with hydrolases of non-starch polysaccharides and pullulanase on the chemical composition of the obtained distillates. *Journal of the Institute of Brewing,* 120, 105-110.

Seung, D., Soyk, S., Coiro, M., Maier, B. A., Eicke, S. & Zeeman, S. C. 2015. Protein targeting to starch is required for localising granule-bound starch synthase to starch granules and for normal amylose synthesis in arabidopsis. *PLoS Biology,* 13, e1002080.

Shan, Q., Wang, Y., Li, J. & Gao, C. 2014. Genome editing in rice and wheat using the CRISPR/Cas system. *Nature Protocols,* 9, 2395-2410.

Shangguan, L., Song, C., Leng, X., Kayesh, E., Sun, X. & Fang, J. 2014. Mining and comparison of the genes encoding the key enzymes involved in sugar biosynthesis in apple, grape, and sweet orange. *Scientia Horticulturae,* 165, 311-318.

Shibano, M., Fujimoto, Y., Kushino, K., Kusano, G. & Baba, K. 2004. Biosynthesis of 1-deoxynojirimycin in Commelina communis: A difference between the microorganisms and plants. *Phytochemistry,* 65, 2661-2665.

Smith, A. M. 2012. Starch in the arabidopsis plant. *Starch - Stärke,* 64, 421-434.

Sreenivasulu, N., Usadel, B., Winter, A., Radchuk, V., Scholz, U., Stein, N., Weschke, W., Strickert, M., Close, T. J., Stitt, M., Graner, A. & Wobus, U. 2008. Barley grain maturation and germination: Metabolic pathway and regulatory network commonalities and differences highlighted by new mapman/pageman profiling tools. *Plant Physiology,* 146, 1738-58.

Stitt, M. & Zeeman, S. C. 2012. Starch turnover: Pathways, regulation and role in growth. *Current Opinion in Plant Biology,* 15, 282-92.

Tanackovic, V., Svensson, J. T., Jensen, S. L., Buleon, A. & Blennow, A. 2014. The deposition and characterization of starch in *Brachypodium distachyon*. *Journal of Experimental Botany,* 65, 5179-92.

Van Bueren, A. L., Higgins, M., Wang, D., Burke, R. D. & Boraston, A. B. 2007. Identification and structural basis of binding to host lung glycogen by streptococcal virulence factors. *Nature Structural & Molecular Biology,* 14, 76-84.

Wang, L.-X. & Huang, W. 2009. Enzymatic transglycosylation for glycoconjugate synthesis. *Current Opinion in Chemical Biology,* 13, 592-600.

Won, J.-S. & Singh, I. 2006. Sphingolipid signaling and redox regulation. *Free Radical Biology and Medicine,* 40, 1875-1888.

Zhu, F., Bertoft, E., Szydlowski, N., D'hulst, C. & Seetharaman, K. 2015. Branching patterns in leaf starches from *Arabidopsis* mutants deficient in diverse starch synthases. *Carbohydrate Research,* 401, 96-108.

Chapter 8- Appendix

8.1 Supplementary Data Chapter 3

8.1.1 Glycoprotein Analysis

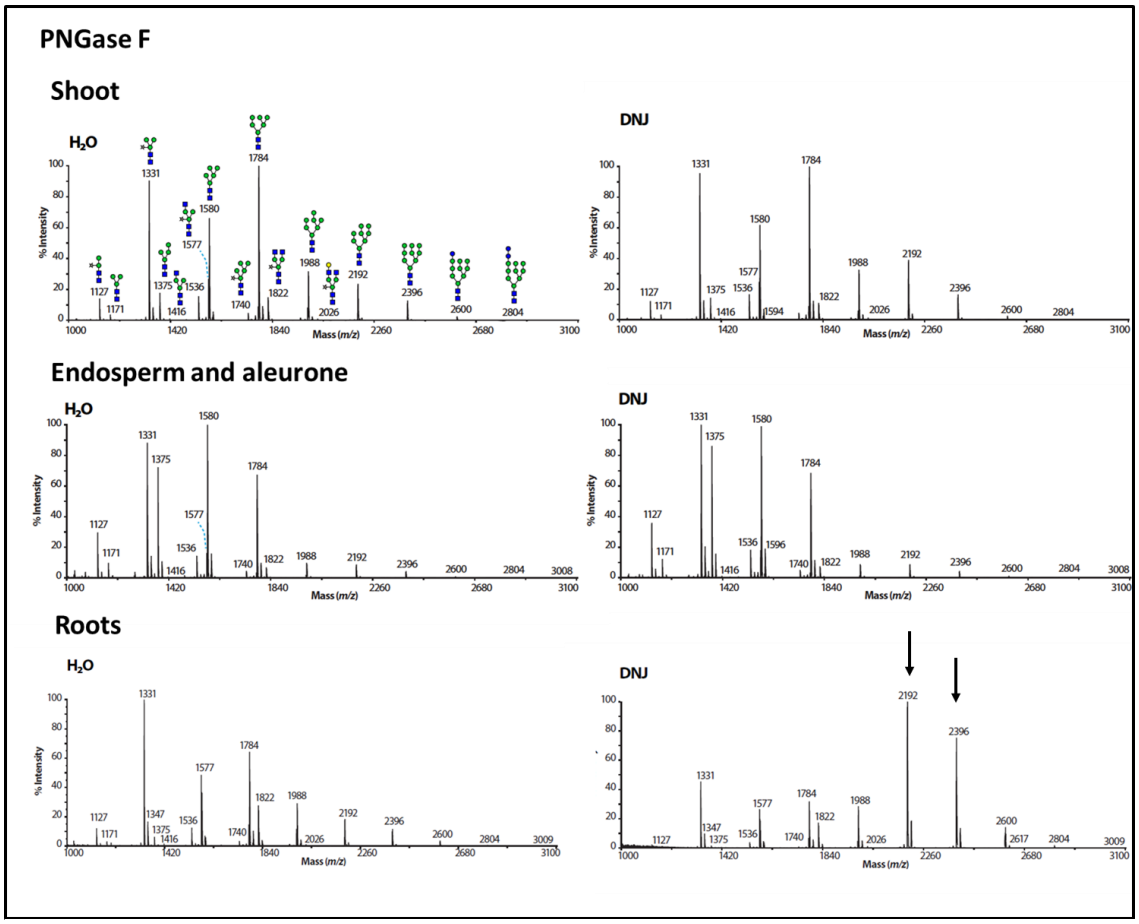

Figure 8.1 Analysis of glycoprotein from barley by MS, PNGase F treated, first analysis.
7 d germinated barley protein samples grown in the presence of 200 µM DNJ or H_2O. Arrows indicate a root specific increase in relative levels of $Man_9(GlcNAc)_2$ and $Man_8(GlcNAc)_2$.

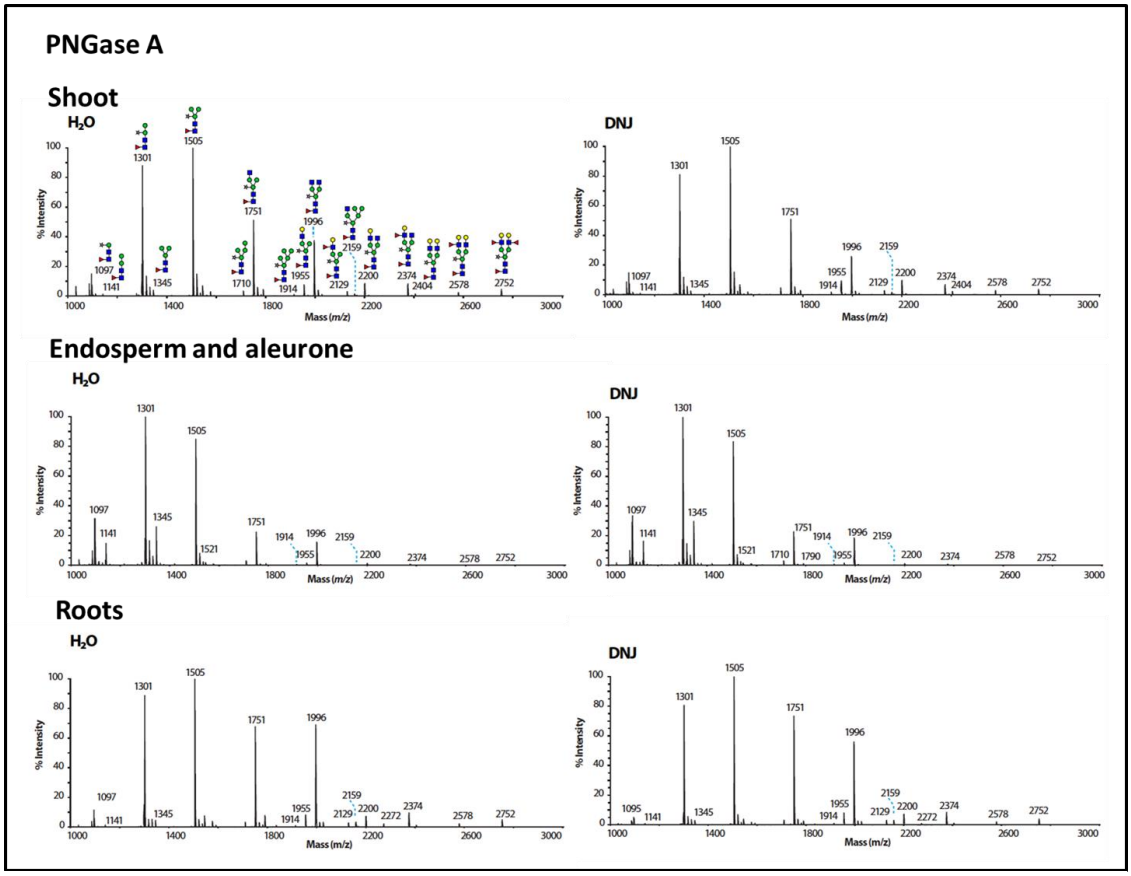

Figure 8.2 Analysis of glycoprotein from barley by MS, PNGase A treated, first analysis.
7 d germinated barley protein samples grown in the presence of 200 µM DNJ or H_2O. No distinct difference in glycan structures can be seen between H_2O and DNJ treated samples.

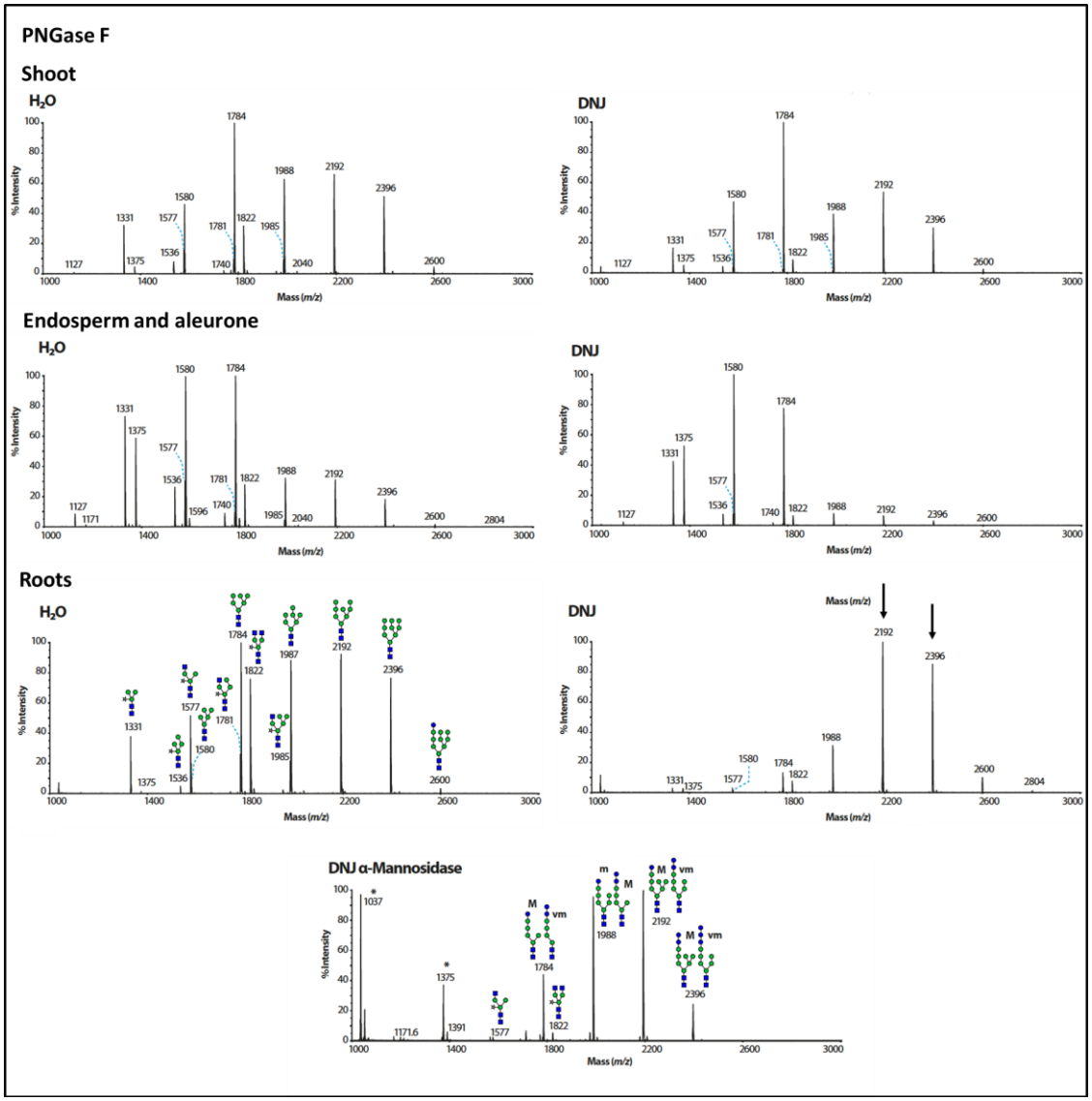

Figure 8.3 Analysis of glycoprotein from barley by MS, PNGase F treated, second analysis.
7 d germinated barley protein samples grown in the presence of 200 µM DNJ or H_2O. Arrows indicate a root specific increase in relative levels of $Man_9(GlcNAc)_2$ and $Man_8(GlcNAc)_2$. A mannosidase treatment was used alongside MS/MS (data not shown) on the DNJ treated root sample to confirm the structures of the glycans.

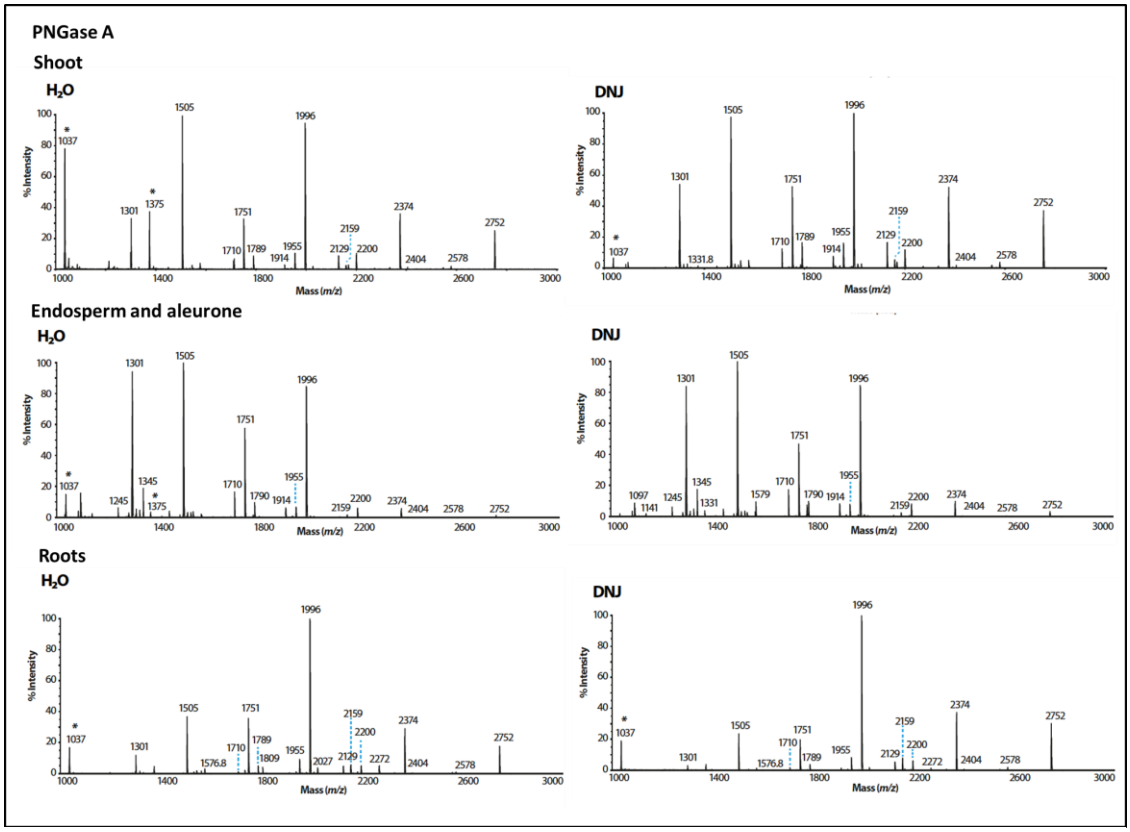

Figure 8.4 Analysis of glycoprotein from barley by MS, PNGase A treated, second analysis.
7 d germinated barley protein samples grown in the presence of 200 µM DNJ or H_2O. No distinct difference in glycan structures can be seen between H_2O and DNJ treated samples.

8.1.2 Overkleeft Library Compounds on Arabidopsis

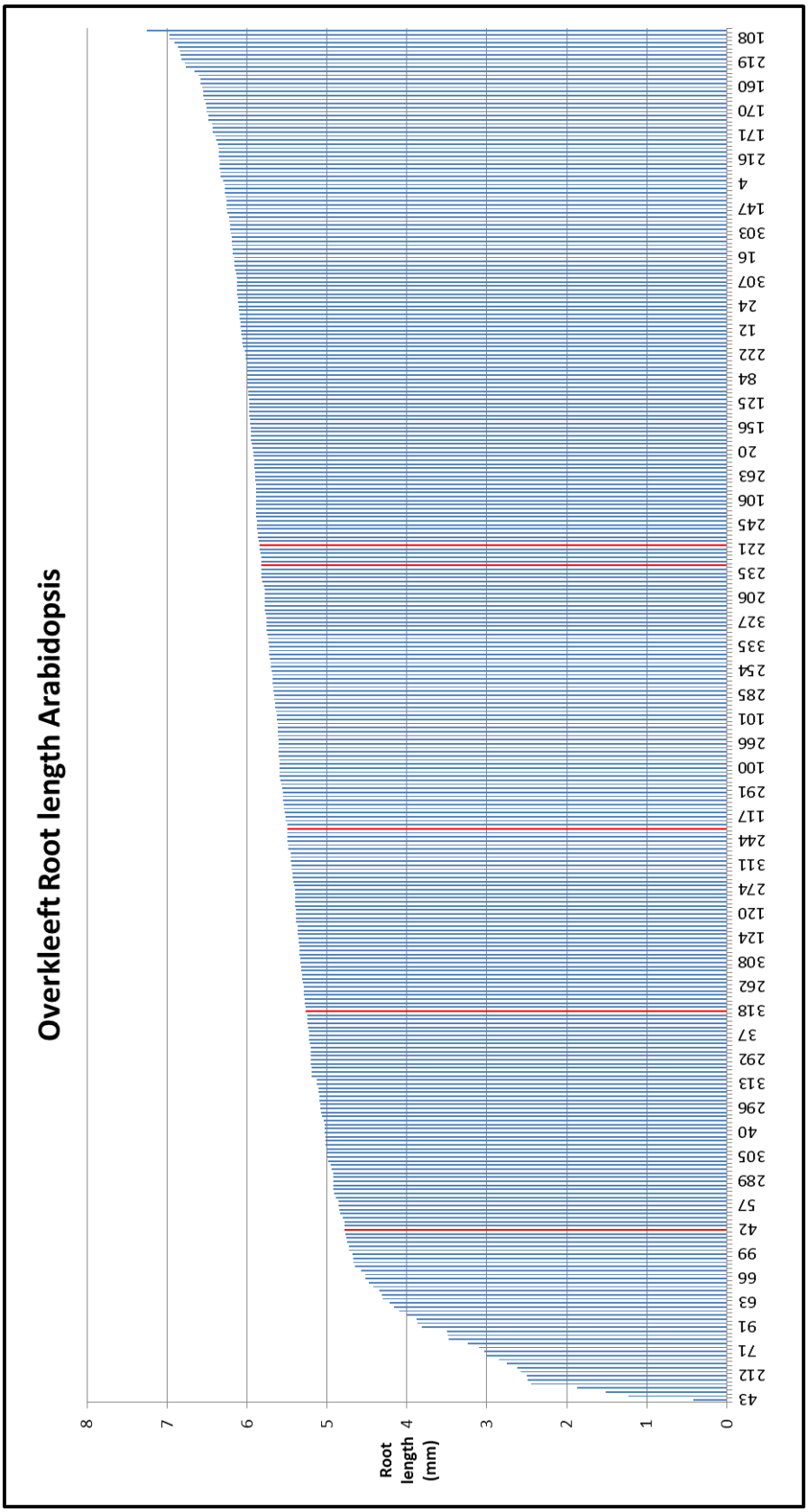

Figure 8.5 Average root lengths for all Overkleeft library compounds analysed on Arabidopsis.
Mean of 10 root length measurements.

8.1.3 Other Compounds from Overkleeft Library Showing Partial Root Growth Inhibition in Arabidopsis

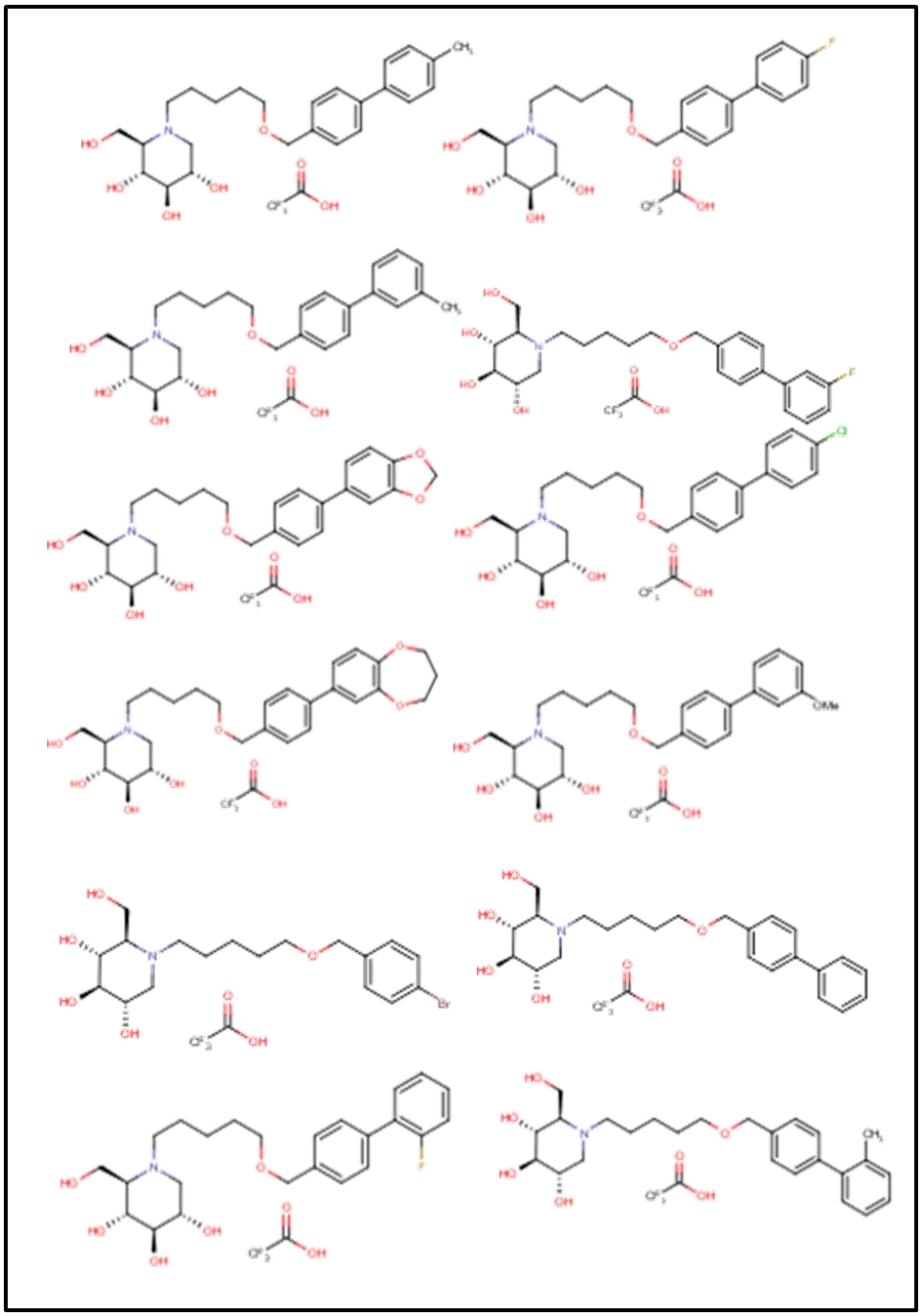

Figure 8.6 Compounds which gave partial inhibition of root growth but were not considered hits in the first round of analysis.
All are *gluco*-configured iminosugars.

8.1.4 Overkleeft Library Compounds on Tef

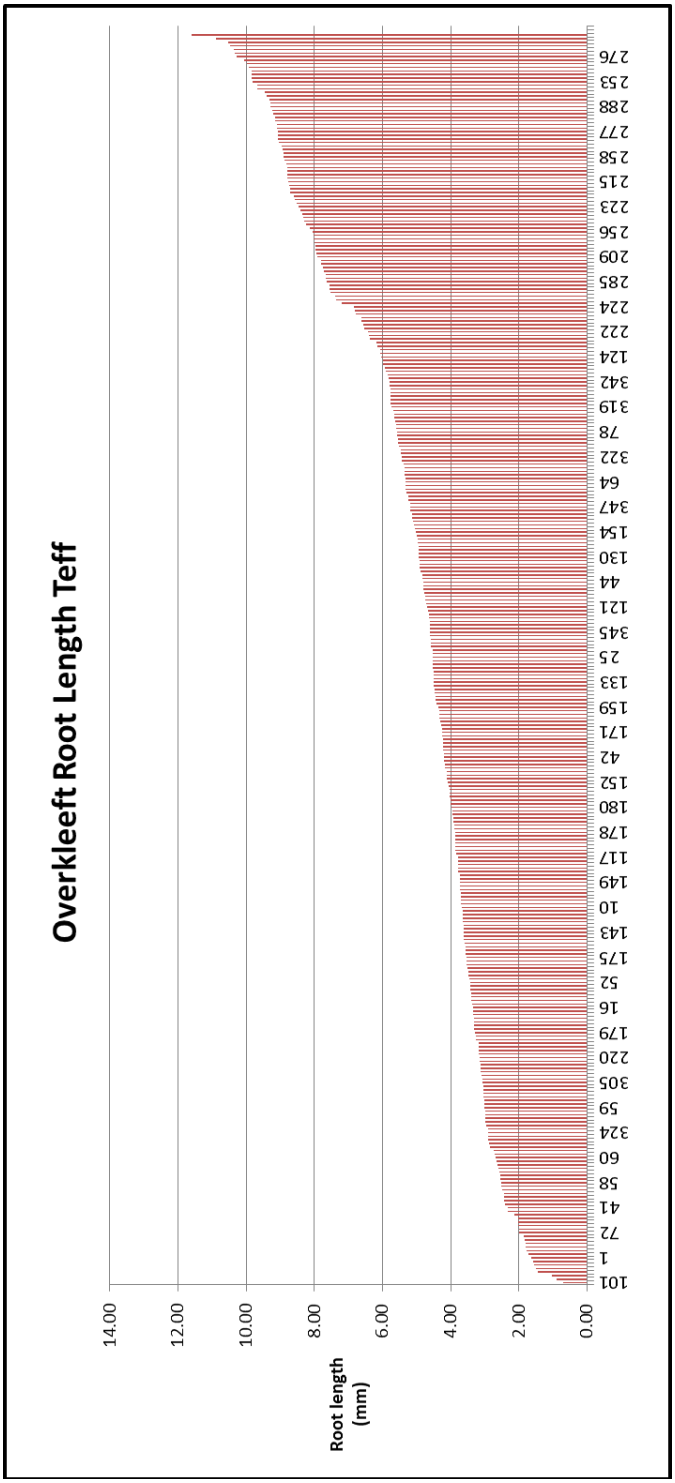

Figure 8.7 Average root lengths for all Overkleeft library compounds analysed on Arabidopsis.
Mean of 8 root length measurements.

8.1.5 Comparison of Tef and Arabidopsis Overkleeft Library Hits

		Teff		Arabidopsis	
	code	**% of control**	**Root length (mm)**	**% of control**	**Root length (mm)**
Teff hits	60	8	0.39	111	5.9
	361	15	0.71	100	5.3
	540	18	0.89	132	7
	61	21	1.03	102	5.4
	433	25	2.01	108	5.7
	514	27	1.73	108	5.7
	437	29	2.32	96	5.1
both	41	11	0.41	8	0.4
Arabidopsis hits	360	37	1.85	23	1.2
	701	63	3.4	28	1.5
	441	53	4.23	36	1.9
	64	40	3.16	47	2.5
	523	77	3.8	49	2.6

Table 8.1 Root length and percent of control measurements for comparison of inhibitors identified using Tef and Arabidopsis.

8.1.6 Assay for Glucosylceramide Synthase Activity

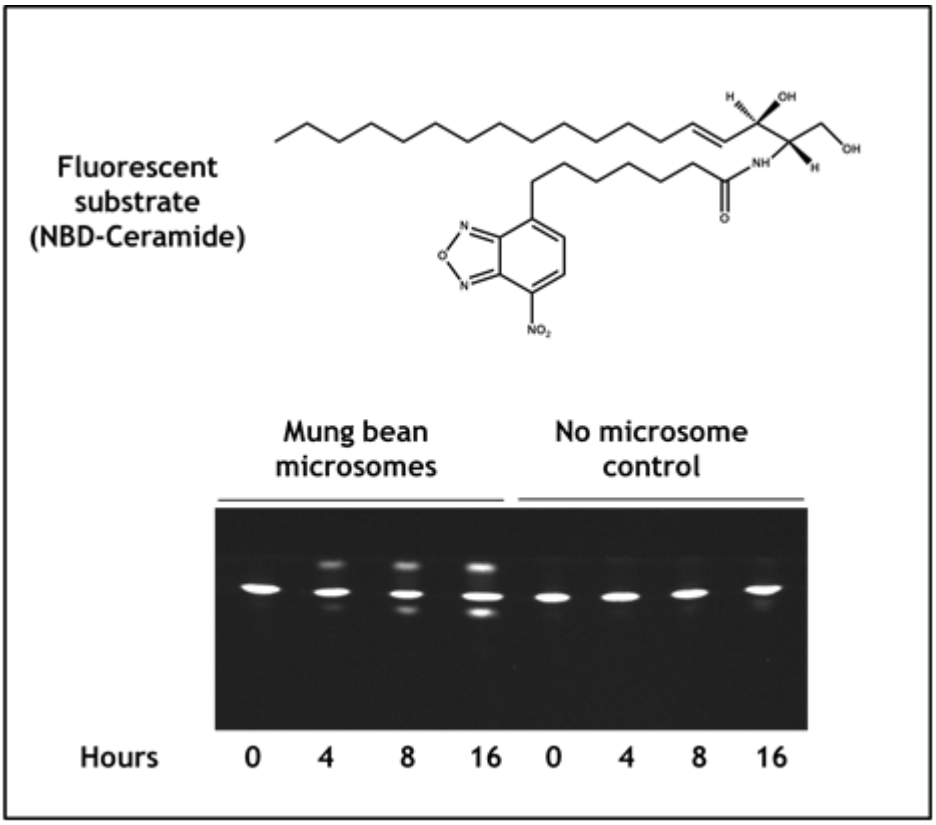

Figure 8.8 Fluorecsent based assay for glucosylceramide synthase
The assay involves the incubation of liposomes containing the fluorescent ceramide mimic with plant microsomes. Products are separated by TLC and visualised by fluorescence.

The TLC shows a product in the presence of mung bean micrsomes, attempts to identify glycosylated NBD-ceramide using LC-MS did not yield positive results. It is possible that the new product generated in the presence of mung bean microsomes is a deacetylated or oxidised NBD-ceramide variant.

The GCS gene from Arabidopsis and barley were cloned from RNA in order to overexpress these proteins for use in enzyme inhibition assays.

8.2 Supplementary Data Chapter 4

8.2.1 Limit Dextrinase Assay with Compounds from Starch Library

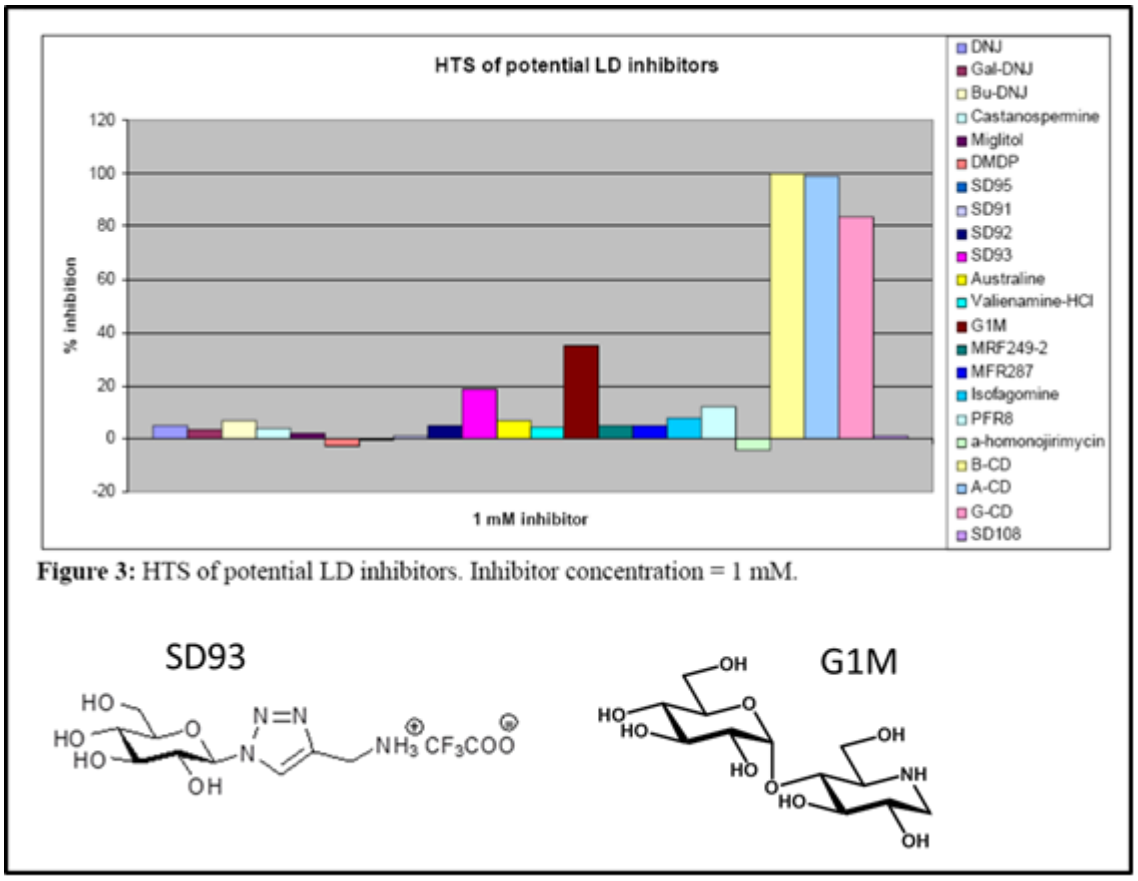

Figure 3: HTS of potential LD inhibitors. Inhibitor concentration = 1 mM.

Figure 8.9 Selected compounds from starch library of iminosugars other compounds with potential activity against starch active enzymes.
Experiment performed by Malene Vester-Christensen (DTU).
Very few compounds are capable of inhibiting LD by over 10 %. Only SD93 and G1M give inhibition over 20 %. 100 % inhibition is caused by β-CD. Screen performed using BCA assay.

8.3 Supplementary Data Chapter 5

8.3.1 Expression and Solubility Screening of Limit Dextrinase

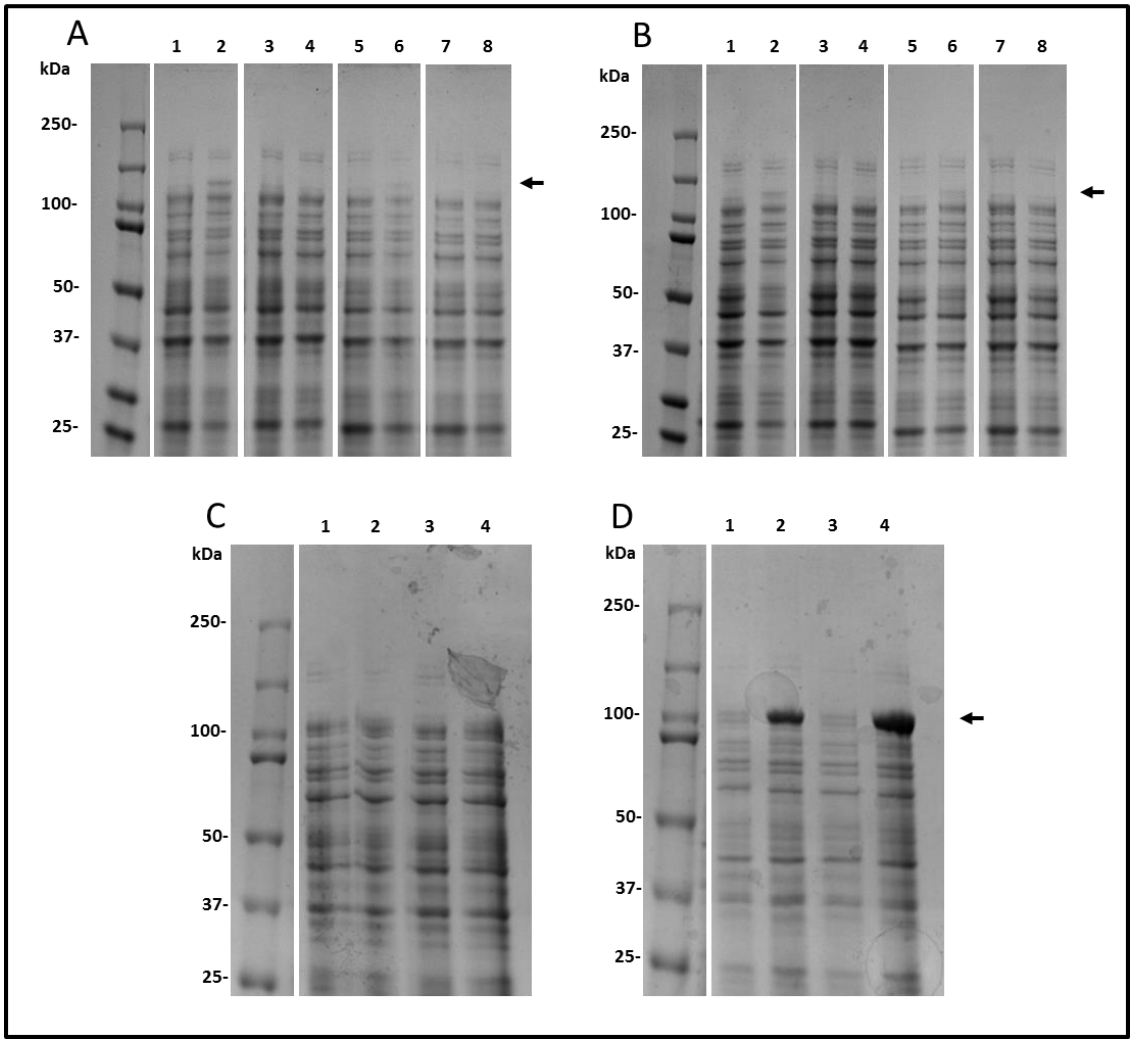

Figure 8.10 Screening for optimal limit dextrinase expression in *E. coli.*
SDS-PAGE analysis. **A.** pETG-10A constructs in Rosetta **B.** pDEST17 constructs in Rosetta **C.** pETG-10A constructs in SoluBL21 **D.** pDEST17 constructs in SoluBL21. In all gels lanes 1&2 correspond to LD-FL, lanes 3&4 correspond to LD-NT all expressed at 28 °C overnight. Lanes 5&6 and 7&8 are in the same order but expressed at 37 °C for 3 h. Odd numbers are uninduced, even numbers are induced with 1 mM IPTG. All lanes loaded with the same volume of whole cells.

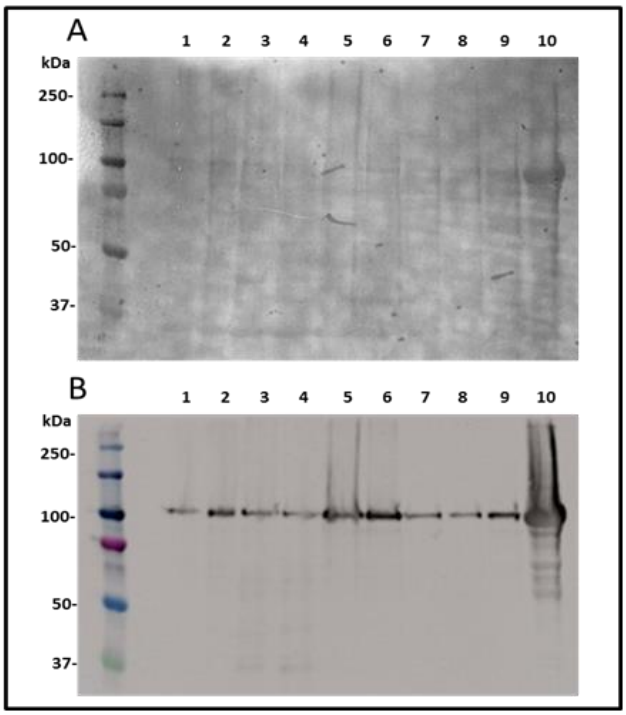

Figure 8.11 Limit dextrinase expression level screening in various *E. coli* strains 1
pDEST17- LD-NT construct expressed at 28 °C overnight. **A.** Ponceau stain for protein **B.** Western blot with anti-His_6 antibody. Lanes correspond to the following: 1&2 BL21 Codon +, 3&4 Rosetta PlysS, 5&6 Rosetta, 7&8 Rosetta Gami 2, 9&10 SoluBL21. Odd numbers are uninduced, even numbers are induced with 0.2 mM IPTG. All lanes loaded with the same volume of whole cells.

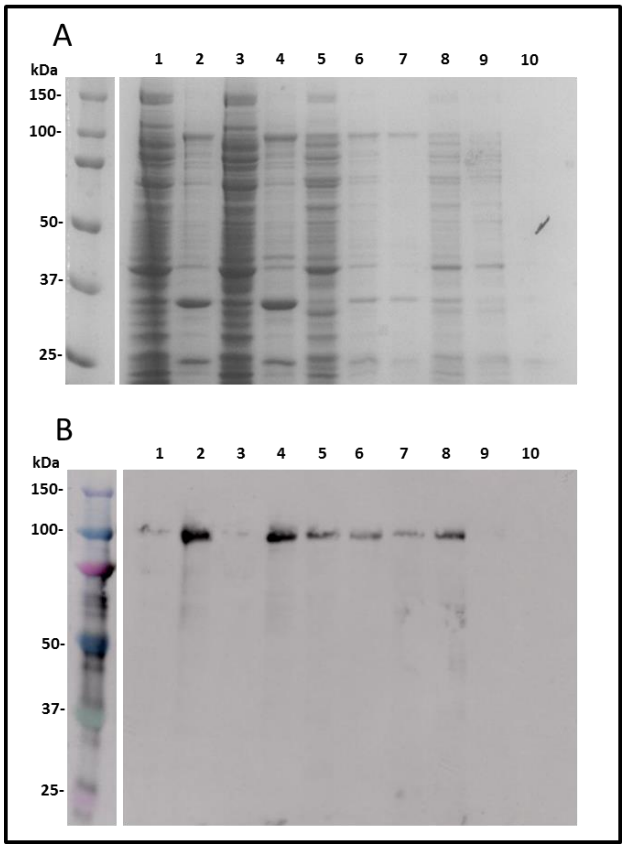

Figure 8.12 Limit dextrinase expression level screening in various *E. coli* strains 2
pDEST17- LD-NT construct expressed at 28 °C overnight. **A.** SDS-PAGE **B.** Western blot with anti-His_6 antibody. Lanes correspond to the following: 1&2 BL21 Codon +, 3&4 Rosetta, 5&6 SoluBL21, 7&8 Rosetta PlysS, 9&10 Rosetta Gami 2. Odd numbers are soluble fraction, even numbers are insoluble fraction. All lanes loaded with the same volume of cell lysate.

Supplier and Strain	Expression	Solubility	Comments
Agilent BL21 Codon Plus	++	soluble protein	--
Novagen Rosetta 2 (DE3)	++	soluble protein	--
Novagen Rosetta 2 (DE3) pLysS	+++	soluble protein	--
Novagen Rosetta-gami (DE3) pLysS	+	soluble protein	Slow growing
Genlantis SoluBL21(DE3)	+++	soluble protein	Highest levels of soluble LD
NEB SHuffle	Not tested	--	--

Table 8.2 Summary table of *E. coli* stains screened for expression of soluble limit dextrinase.

8.3.2 MonoQ Anion Exchange on Limit Dextrinase

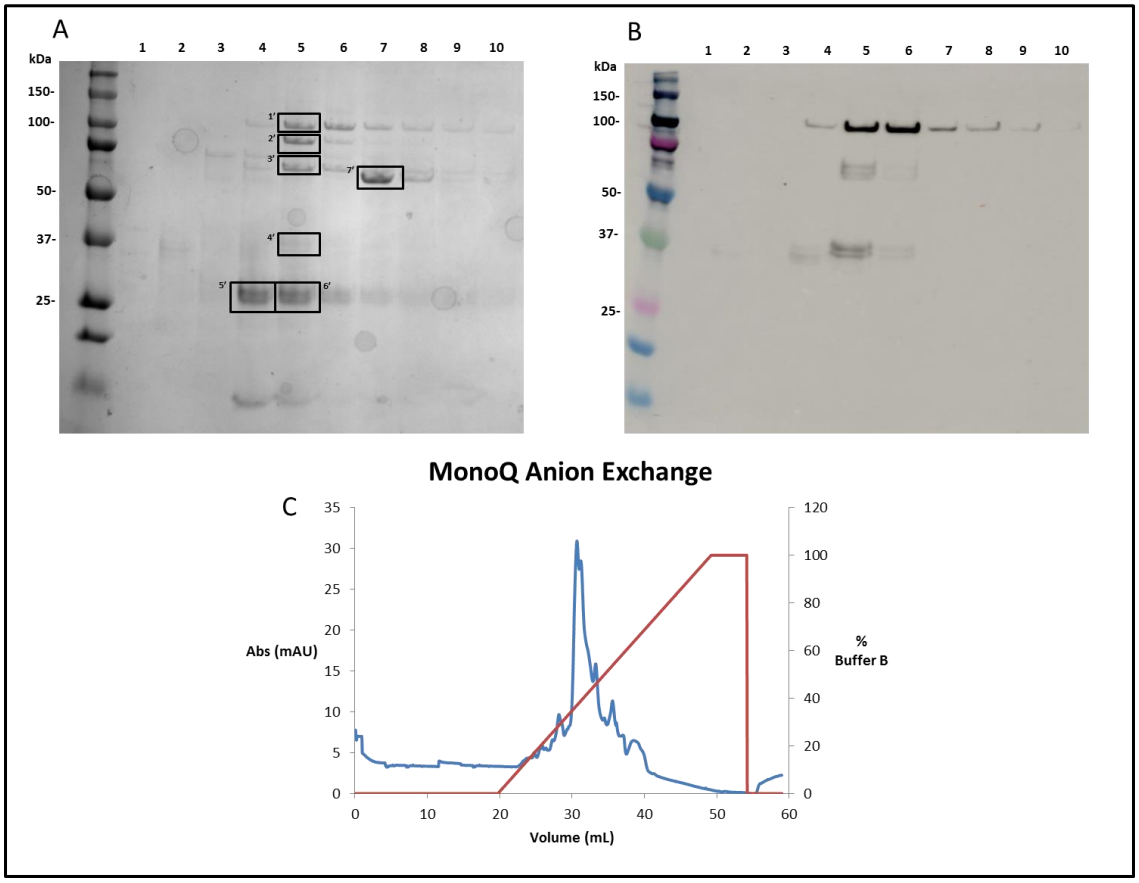

Figure 8.13 Anion Exchange Chromatography on LD form Nickel Affinity Chromatography Purification **A.** SDS-PAGE 12 % gel showing fractions. **B** Western blot with anti-His_6 antibody. **C.** Chromatogram showing UV trace and corresponding elution from the column. Purification performed using MonoQ elution was with 0-100 % 1 M NaCl. Boxes show gel bands analysed mass spectrometry.

The elution from a LD nickel purification was used in MonoQ anion exchange. A number of distinct protein bands were observed in the elutions. The protein corresponding to the highest elution peak contained a His-tagged LD protein of ~100 kDa, other protein bands were also present in this fraction (masses ~85 kDa and ~67 kDa). Selected protein bands were excised from the gel, digested with trypsin and analysed by MALDI-ToF. Peptides fragments were compared to the MASCOT database to identify the parent protein. Band 1' was identified as *H. vulgare* LD. Bands 2' and 3' were *E. coli* catalase HPII (84224 Da, pI 5.54) and glutamine-fructose-6-phosphate aminotransferase (66965 Da, pI 5.6) respectively. These proteins both have a pI value that will give them a net negative charge at pH 7.5 which explains why they bind to the MonoQ column, their charge may also explain why they bound to the nickel resin. The other bands, 4'-7', could not be identified by MS.

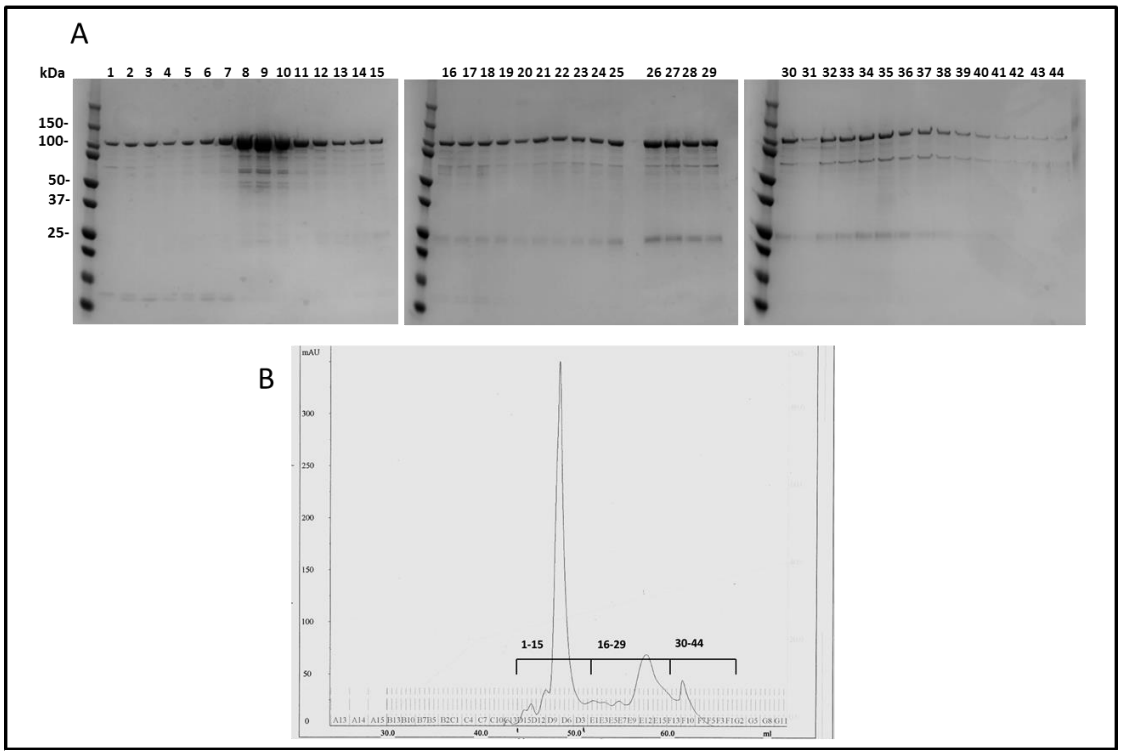

Figure 8.14 Anion Exchange Chromatography on His-LD from β-Cyclodextrin Affinity Chromatography
A. SDS-PAGE 12 % gel showing fractions from purification. **B.** Chromatogram showing UV trace and elutions. Elution was by stepwise gradient of 0-20 % for 6 mL 20-50 % for 30mL and 50-100 % for 10mL using 0-100 % 1 M NaCl

LD protein from a β-CD affinity purification was further purified by anion exchange. The protein eluted as multiple peaks between 20-40 % 1 M NaCl. The discrete peaks were analysed by SDS-PAGE and all contained LD. Different elution peaks are proposed to arise because of different species or conformations of LD that exist on the column. The strongest band in the SDS-PAGE for each elution fraction corresponds to the correct size for LD. As the protein used in this purification is the product of β-CD purification it is almost pure LD. This phenomenon has been seen with spinach pullulanase and has been termed microheterogeneity. Degradation products, likely from thermal degradation caused by heating during SDS-PAGE sample preparation, are visible on the SDS-PAGE gel. Different degradation products are seen for the different LD species and are proportional to the concentration of LD in each fraction. Because of these phenomena it was concluded that LD from β-CD purification could not be further purified using anion exchange chromatography.

8.3.3 Generation of β-CD-Sepharose Resin

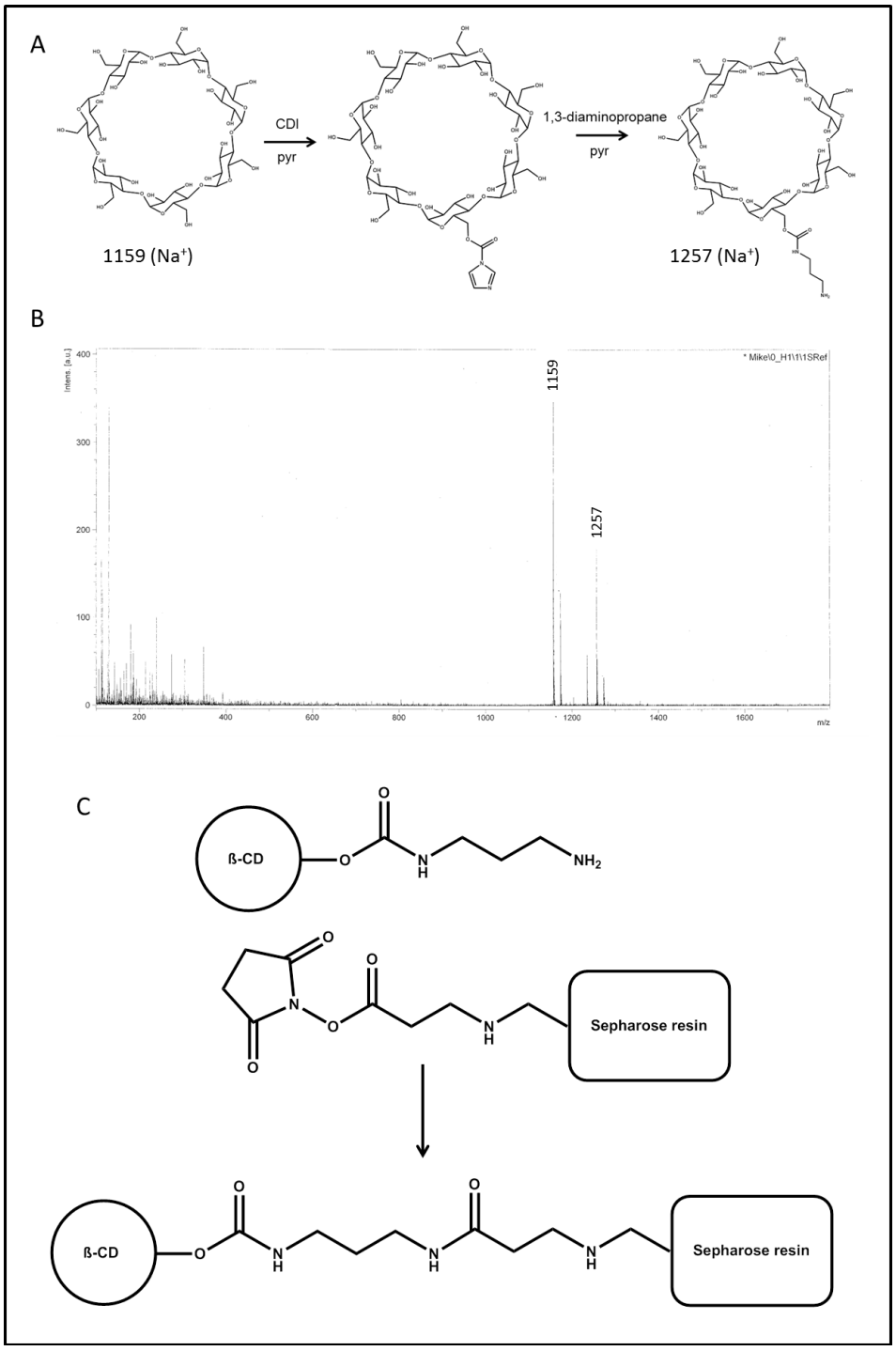

Figure 8.15 Generation of β-cyclodextrin Sepharose column
A. Scheme showing chemical derivatisation of β-CD. **B.** MALDI-ToF performed on derivatised amino-β-CD, a peak corresponding to the correct mass for a sodium adduct is present (1257), unreacted starting material is also present as a sodium adduct (1159). **C.** Scheme showing the process for conjugation of amino-β-CD to NHS-Sepharose resin.

8.3.4 Expression and Solubility Screening of Limit Dextrinase Inhibitor

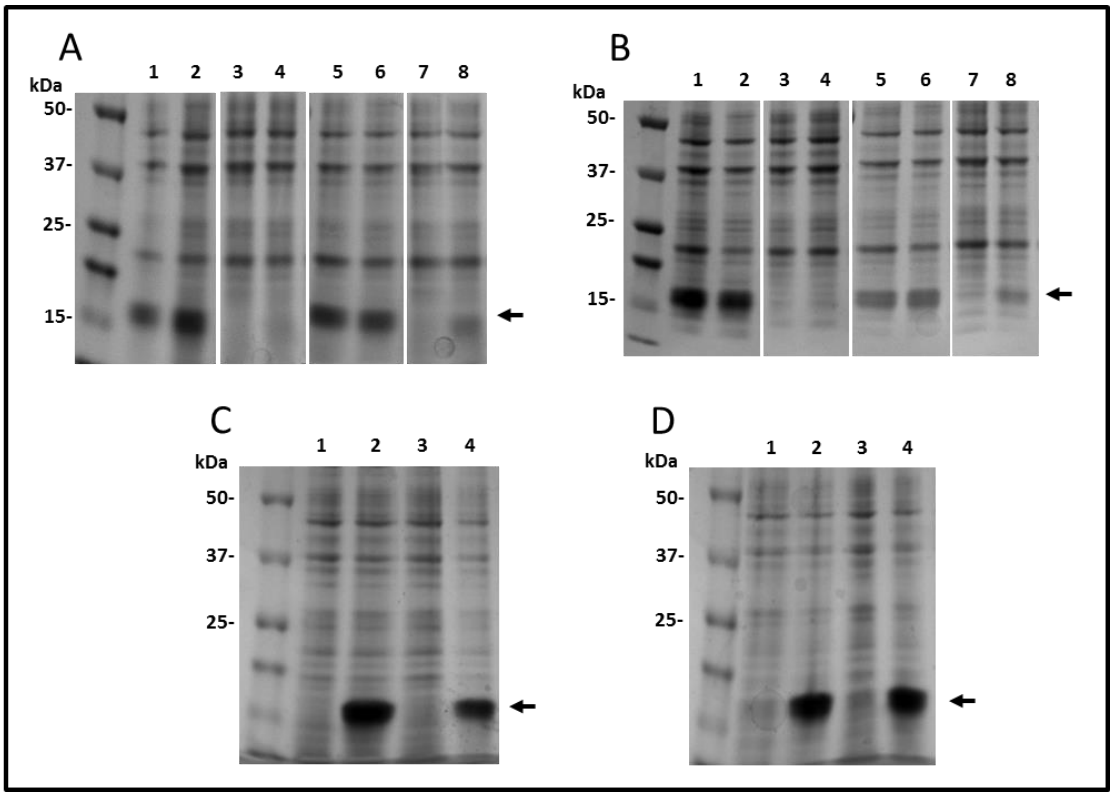

Figure 8.16 Screening for optimal limit dextrinase inhibitor expression in *E. coli.*
A. pETG-10A constructs in Rosetta **B.** pDEST17 constructs in Rosetta **C.** pETG-10A constructs in SoluBL21 **D.** pDEST17 constructs in SoluBL21. In all gels lanes 1&2 correspond to LDI-FL, lanes 3&4 correspond to LDI-NS all expressed at 28 °C overnight. Lanes 5&6 and 7&8 are in the same order but expressed at 37 °C for 3 h. Odd numbers are uninduced, even numbers are induced with 1 mM IPTG. All lanes loaded with the same volume of whole cells.

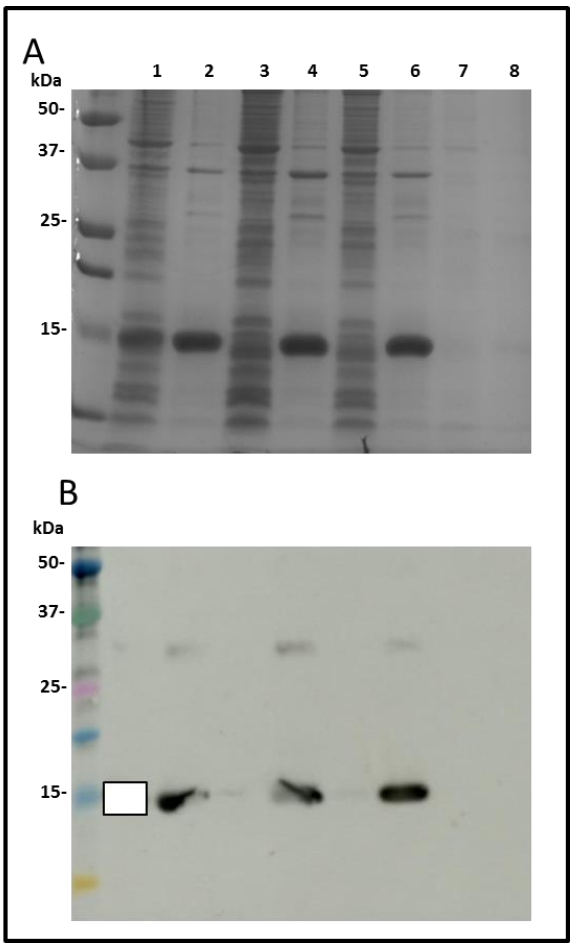

Figure 8.17 Limit dextrinase inhibitor expression level screening in various *E. coli* strains 1
pDEST17-LDI-NS construct expressed at 28 °C overnight. **A.** SDS-PAGE **B.** Western blot with anti-His_6 antibody. Lanes correspond to the following: 1&2 BL21 Codon +, 3&4 Rosetta, 5&6 SoluBL21, 7&8 Rosetta PlysS. Odd numbers are soluble fraction, even numbers are insoluble fraction. All lanes loaded with the same volume of cell lysate. Lane 1 was incorrectly loaded due to protein aggregation.

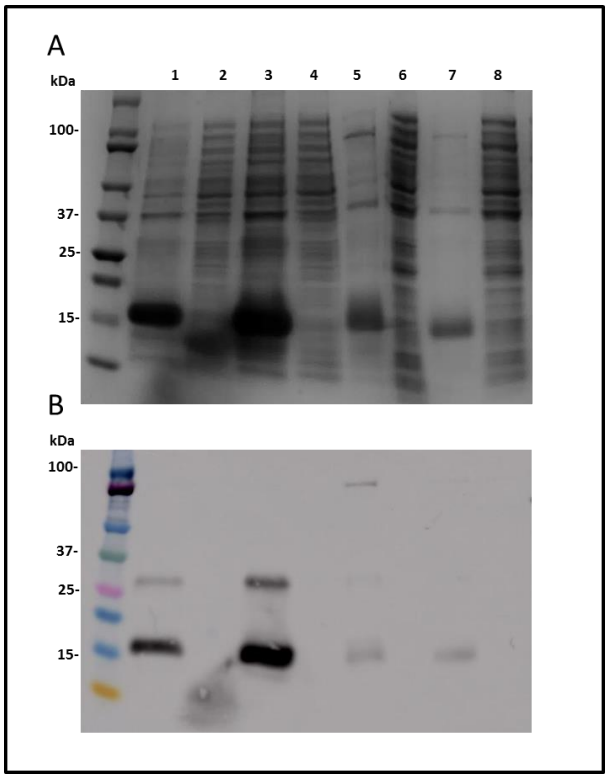

Figure 8.18 Limit dextrinase inhibitor expression level screening in various *E. coli* strains 2
pDEST17-LDI-NS construct expressed at 28 °C overnight. **A.** SDS-PAGE **B.** Western blot with anti-His_6 antibody. Lanes correspond to the following: 1-4 SoluBL21 5-8 Rosetta Gami 2. Even numbers are soluble fraction, odd numbers are insoluble fraction. All lanes loaded with the same volume of cell lysate.

Supplier and Strain	Expression	Solubility	Comments
Agilent BL21 Codon Plus	++	no soluble protein	--
Novagen Rosetta 2 (DE3)	++	no soluble protein	--
Novagen Rosetta 2 (DE3) pLysS	++	no soluble protein	--
Novagen Rosetta-gami (DE3) pLysS	+	no soluble protein	Slow growing
Genlantis SoluBL21(DE3)	+++	no soluble protein	High levels of insoluble LDI
NEB SHuffle	+	no soluble protein	Low amounts of LDI produced

Table 8.3 Summary table of *E. coli* stains screened for expression of soluble limit dextrinase inhibitor.

8.3.5 MonoQ on Limit Dextrinase Inhibitor

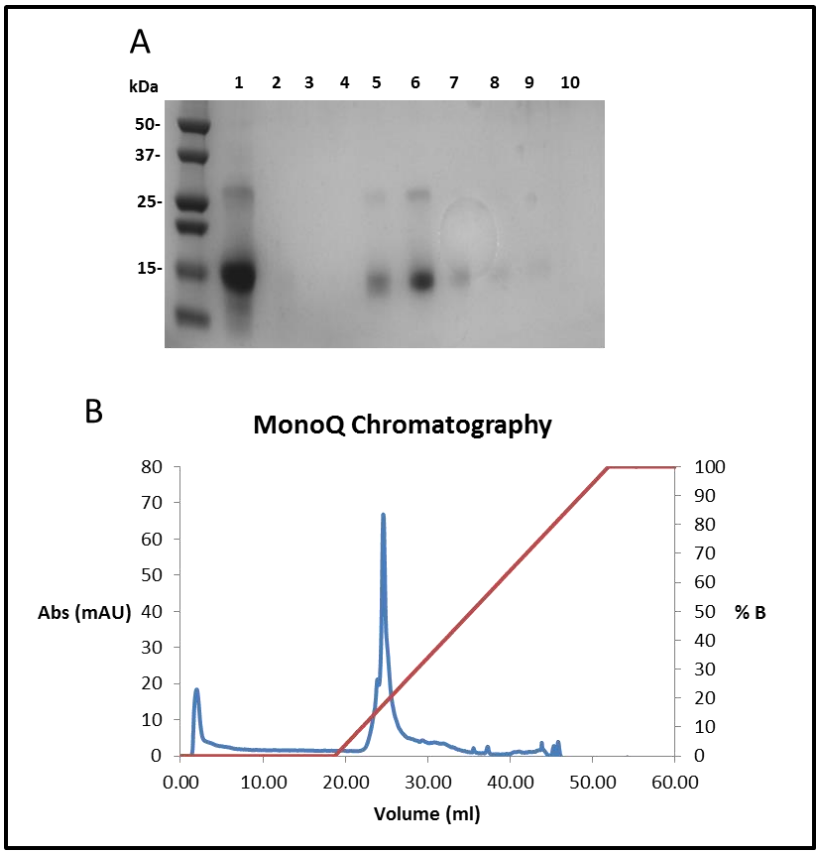

Figure 8.19 Anion exchange chromatography of solubilised and refolded LDI
A. SDS-PAGE of samples from anion exchange. Lane 1 sample prior to anion exchange. Lanes 2-10 elution fractions. **B.** Chromatogram showing UV trace and elutions.

MonoQ anion exchange was attempted on LDI from HisTrap refolding in an attempt to further purify the protein. The pI of LDI is 6.81, at pH7.5 thus the protein will possess a negative charge and will therefore bind to the MonoQ column. Some protein did not bind to the resin as indicated by a peak in the low through (Figure 8.19, B). The protein eluted as one peak between 10-20 % 1 M NaCl. Both monomeric (16 kDa) and dimeric (32 kDa) forms LDI eluted together. The eluted protein is of a similar purity as that which was loaded (Figure 8.19, A, lane 1). It was concluded that LDI from the solubilisation, refolding and HisTrap purification was sufficiently pure.

8.3.6 Limit Dextrinase Inhibitor Refolding Using Quickfold

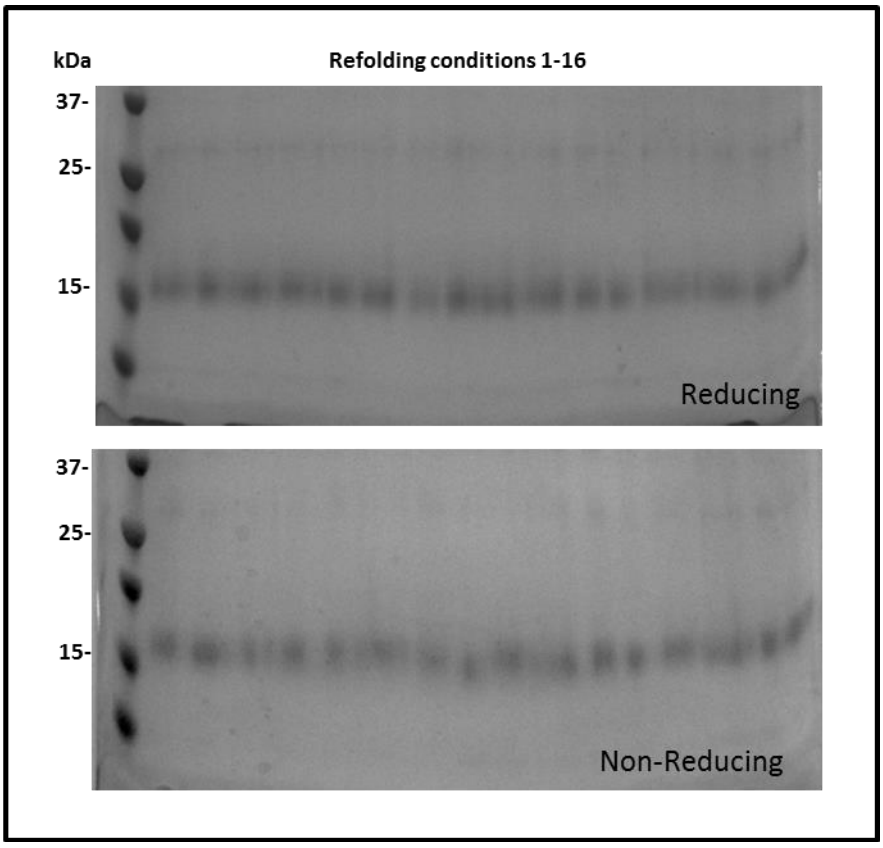

Figure 8.20 Refolding of LDI using Quickfold
Reducing SDS-PAGE and Non-reducing SDS-PAGE. Lanes 1-16. Different refolding conditions tested.

Solubilised LDI was used in a protein refolding experiment using the Quickfold protein refolding system. Quickfold is a protein refolding screening kit which contains 15 buffers, each with a different composition. LDI in urea buffer was combined with each buffer and incubated to allow refolding. Protein was then centrifuged to remove insoluble aggregates and the soluble product analysed by reducing and non-reducing SDS-PAGE. Diffuse bands at a correct size for LDI were present in both gels for all buffer conditions. It was concluded that the starting material was already folded to some extent and incubation in refolding buffer made little difference.

8.4 Sequences

8.4.1 Vector Map of Limit Dextrinase from Gene Synthesis

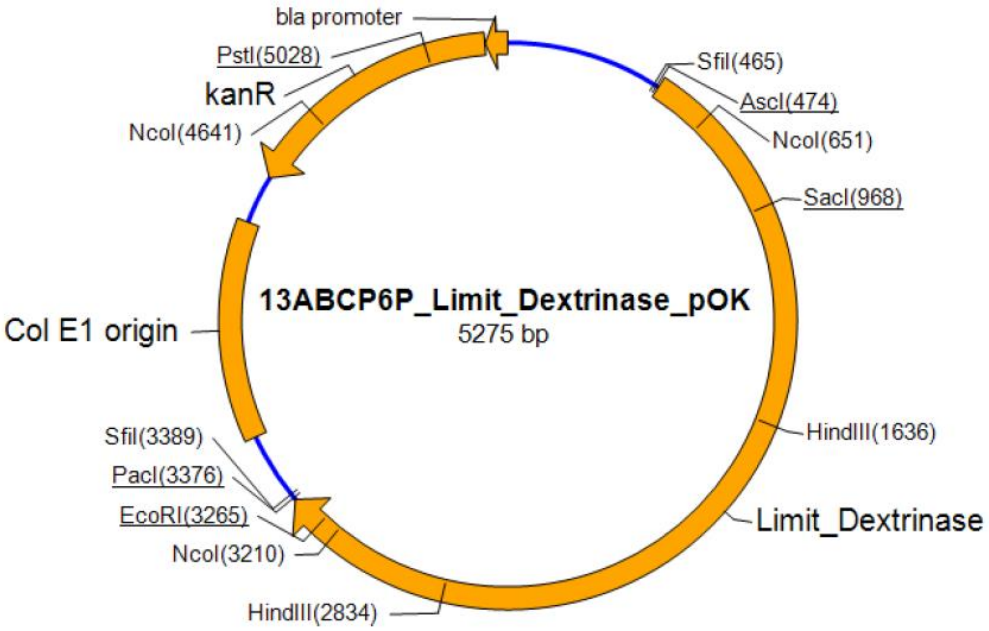

8.4.2 Limit Dextrinase Sequences

Hordeum vulgare tissue-type aleurone limit dextrinase mRNA complete cds

atacaaaatgccaatgccgatgcgaacgatgctgctccgccaccttagtccccctccgc
cgtgcccaatccccggcgctcctccgtctcctcgccgcagcggataccggtgagggcccg
gccaccgccgctgcattccgcccgcgccaccgcgctccgggcccggcggaggacgcccat
ggcggtcggggagaccggcgcctccgtctccgccgccgaggccgaggccgaggccaccca
ggcgttcatgccggacgccagggcgtactgggtgacgagcgacctcatcgcctggaacgt
cggcgagctggaagcgcagtccgtctgcctgtacgccagcagagccgccgcgatgagcct
ctcgccgtcgaatggcggcatccaaggctacgactccaaggttgagctgcaaccggagag
cgccgggctcccggaaaccgtgacccagaagttccctttcatcagcagttacagagcatt
cagggtcccgagctctgtcgacgtcgccagccttgtgaaatgccaactggtcgtcgcttc
tttcggcgctgacgggaaacacgtagatgttactggactgcaattacccggcgtgctgga
tgatatgttcgcatacacgggaccgctcggtgcggttttcagcgaggactctgtgagcct
gcacctttgggctcctacagcacagggcgtgagcgtgtgcttctttgatggtccagcagg
ccctgcgctagagacggtgcagctcaaggagtcaaatggtgtttggagtgtcactggacc
aagagagtgggaaaaccggtactatttgtatgaagtcgacgtgtatcatccaactaaggc
gcaggttctgaaatgtttagctggtgacccttatgctagaggcctttctgcaaatggagc
gcgtacctggttggttgacattaacaatgagacattgaagccggcttcctgggatgaatt
ggctgatgagaagccaaaacttgattccttctctgacataaccatctatgaattgcacat
tcgtgattttagcgcccacgatggcacagtggacagtgactctcgtggagcatttcgtgc
atttgcatatcaggcctcggcaggaatggagcacctacggaaattatctgatgctggttt
gactcatgtgcatttgttgccaagctttcattttgctggcgttgacgacattaagagcaa
ctggaaatttgtcgatgagtgtgaactagcaacattccctccagggtcagatatgcaaca
agcagcagtagtagctattcaggaagaggacccttataattgggggtataaccctgtgct
ctgggggggttccaaaaggaagctatgcaagtgaccctgatggcccgagtcgaattattga
atatcgtcagatggtccaggccctcaatcgcataggtcttcgtgttgtcatggatgttgt
atacaatcatctagactcaagtggcccctgcggtatcagctcagtgcttgacaagattgt
tcctgggtactatgttagaagggatactaatggccagattgagaacagtgcagctatgaa
caatacagcaagtgagcatttcatggttgataggttaatcgtggatgacctttgaactg
ggcagtaaactacaaagttgacgggttcagatttgatcttatgggccatatcatgaaacg
cacaatgatgagagcaaaatctgctcttcaaagccttacaacagatgcacatggagttga
tggttcaaaaatatacttgtatggtgaaggatgggacttcgctgaagttgcacgcaatca
acgtggaataaatgggtcccagcttaatatgagtggaacggggattggtagcttcaatga
tagaatccgggatgctattaatgggggtaatccctttggtaatccgctccagcaaggctt
caatactggtctgttcttagagccgaatgggttttatcagggcaatgaagcagataccag
gcgctcgctcgctacttatgctgaccaaatacagattggactagctggtaatctcaggga
ttatgtactaatatctcatactggagaagctaagaagggatcagaaattcacacttttga
tggattaccagtaggctatactgcgtccccaatagaaacgataaactatgtttctgctca
tgacaatgagactctatttgatgttatcagtgtgaagaccccaatgatcctttcagttga
tgagagatgcaggataaatcatttggcctccagcatgatggcattatcccagggaatacc
cttcttccacgctggtgacgagatactaagatctaagtccatcgaccgagattcatataa
ctctggtgattggtttaacaagcttgattttacctatgaaacaaacaattggggtgttgg
gcttcctccaagtgaaaagaacgaagataattggcccctgatgaaaccaagattggaaaa
tccgtcttttaaacctgcaaaaggacacattcttgctgccctagacagttttgttgacat
cttgaagatcagatactcatctccacttttcgtctcagtacagcaaatgacattaagca
aagggtacgctttcacaacacagggccctccttagtcccaggtgttattgtcatgggcat
tgaagatgcacgaggtgagagccccgagatggctcaattagacacgaacttctcttatgt
cgtaaccgtcttcaatgtgtgtccgcacgaagtgtccatggatatccccgctctcgcttc
gatggggtttgaactgcatcctgtgcaggtgaattcatcagatactttggtgaggaaatc
tgcgtacgagtccgcgacgtgcaggttcaccgtgcccggaagaaccgtgtcagtctttgt
cgaacctcggtgttgatgcctcctcggtttcaacacgaggatctgttctacaagttgtcg
aagcaaccgaagatctttctgtttttgtgttgaagtaaataataaatgaagaataagaga
ggagaggcgctgctgcctgccagattacactgctgaaggaacaaacccaagaataagaag
gttggcttatgtatatgtatagtgcccaagctgcctagtcctgtttttctttcctaatcc
attttgattttatatatcaaaaggaaaacacatatatcgtgttataagtattgtataaca
tgtactccctccaactgaaaatacttgtcataggaatgtatgtatctagatgtattataa
ttctagatacatccatttttatacatttatgtgacaagtaattccggacggagggagtat
gtgttaaacaaatttcacaaaaatgtatgtgttaaacaaggatgcataatgattttgtac
tgtactctctttttactatgtatattacatattatttttaccgaagaaaagaaagtaca
atttctcta

Hordeum vulgare limit dextrinase protein

mpmpmrtmllrhlsppsavpnprrssvsspqripvrarppplhsaratalrarrrtpmav
getgasvsaaeaeaeatqafmpdaraywvtsdliawnvgeleaqsvclyasraaamslsp
snggiqgydskvelqpesaglpetvtqkfpfissyrafrvpssvdvaslvkcqlvvasfg
adgkhvdvtglqlpgvlddmfaytgplgavfsedsvslhlwaptaqgvsvcffdgpagpa
letvqlkesngvwsvtgprewenryylyevdvyhptkaqvlkclagdpyarglsangart
wlvdinnetlkpaswdeladekpkldsfsditiyelhirdfsahdgtvdsdsrgafrafa
yqasagmehlrklsdaglthvhllpsfhfagvddiksnwkfvdecelatfppgsdmqqaa
vvaiqeedpynwgynpvlwgvpkgsyasdpdgpsriieyrqmvqalnriglrvvmdvvyn
hldssgpcgissvldkivpgyyvrrdtngqiensaamnntasehfmvdrlivddllnwav
nykvdgfrfdlmghimkrtmmraksalqslttdahgvdgskiylygegwdfaevarnqrg
ingsqlnmsgtgigsfndrirdainggnpfgnplqqgfntglflepngfyqgneadtrrs
latyadqiqiglagnlrdyvlishtgeakkgseihtfdglpvgytaspietinyvsahdn
etlfdvisvktpmilsvdercrinhlassmmalsqgipffhagdeilrsksidrdsynsg
dwfnkldftyetnnwgvglppseknednwplmkprlenpsfkpakghilaaldsfvdilk
iryssplfrlstandikqrvrfhntgpslvpgvivmgiedargespemaqldtnfsyvvt
vfnvcphevsmdipalasmgfelhpvqvnssdtlvrksayesatcrftvpgrtvsvfvep
rc

8.4.3 Limit Dextrinase Inhibitor Sequences

Hordeum vulgare limit dextrinase inhibitor mRNA complete cds

actagtatcaacaatggcatccgaccatcgtcgcttcgtcctctccggcgccgtcttgct
ctcggtcctcgccgtcgccgccgccaccctggagagcgtcaaggacgagtgccaaccagg
ggtggacttcccgcataacccgttagccacctgccacacctacgtgataaaacgggtctg
cggccgcggtcccagccggcccatgctggtgaaggagcggtgctgccgggagctggcggc
cgtcccggatcactgccggtgcgaggcgctgcgcatcctcatggacggggtgcgcacgcc
ggagggccgcgtggttgagggacggctcggtgacaggcgtgactgcccgagggaggagca
gagggcgttcgccgccacgcttgtcacggcggcggagtgcaacctatcgtccgtccagga
gccgggagtacgcttggtgctactggcagatggatgacgatcgaaatgcgccaaggtaat
gaagcggagtactgtatacagaataaaagta

Hordeum vulgare limit dextrinase inhibitor protein

masdhrrfvlsgavllsvlavaaatlesvkdecqpgvdfphnplatchtyvikrvcgrgp
srpmlvkerccrelaavpdhcrcealrilmdgvrtpegrvvegrlgdrrdcpreeqrafa
atlvtaaecnlssvqepgvrlvlladg

8.4.4 Glucosylceramide synthase sequences

Barley GCS Gene

atgaggcgcaaaatggcatctggacatagttttgcctttctttgtgatgacgtagatgagcttgagcactccgtgcag
cagaaattacctatggtctctgtagtcatgcctttgaagggctttggggagcacaatttgcaaaattggagaactcag
attacttctctttatgggggaccattggaattcttgtttgtagtagaaagcaaagatgatccagcttatcgtgccgtc
tcccgattgattgtagagtacaaggacaaattggacgcaaaggtggttgtagctgggttttcaacaacttgtagccag
aaaattcataatcagttaattggtgttgaaaagatgcacaaggacagcaaatatgttctatttctggacgatgatgtc
agactgcatcctgggacagtcggagctctcacaaaagaaatggagaagaaccctgagatatttatccaaacgggatac
cctcttgacttgccttctggcagcttgggaagctattgcatatatgaatatcacatgccctgttcgattggatttgca
actggcgggaggactttctttttgtggggtggctgtatgatgatgcatgctgatgatttccggcaagacctgtatggt
ttagtcacagcactaaaaaatggtggttactcagatgatatgacccttgctgcaatcgctgggcaacataagaggctg
ataacttcaccacctgttgctgtgtttccacaccctcttgcaagtgatctcagcttctccagatactggaattatcta
aggaaacaaacttttgttcttgaatcgtatgtttcaaaggtcaactggataatgaaccgtgcactgtttggtgtacat
ttctatttgtcatggggatttgtttgtccctatgttatggctttggtacatattgcgactactcttagagcaccatat
agcgcaattgtaaaggaagcagctgagtcgtcttgtggtctgaaactagtgagcttcttgttaatatgcactctcact
gaactcgtttcgatgtggaatttgacgagagttgagatccaactctgcaacatgttatctccagaaggaccacaagac
tcccttcgttcatataactgggggcttgtgttcgttgccgtgttagtagacaatttcctctacccgatatctgccatc
cggtccaatttctcccaatcaatcaattggtctggtatcaggtactacctgagagatgggaaaataagcaagattgaa
agggagaacagttcgaagtacaccgatctcggtgggaagcatctctatggcaagaggacataccctgctggaaagtcg
ttgctcggctacctgtccataagcctagcccaatggcaccagccgaagaagtatgatgtctga

Arabidopsis GCS gene

atgtctacattggactccattgatgcgattctcttctctcttagcagagcttttacaagccctttcgctgtcttcgtt
cagatccaggggtgtacaatatgcttactacttgctctcggctggttattggctgaatatgtcaggaatcgtgaggtt
aagagaattaaaaacagcataaaagcgggcaatagcttggcgtttctttatcaagatatcaatgaacttgagcactct
aggcaggttaaacttcctagagtttcagttgtcatgcctctaaaaggttttggagaacacaatttacacaactggaga
agtcagattacttctctctatggtgggccattggaattccttttgttgtagaaagtacggaagaccctgcatatcac
gctgtttcccgtctattatctatgtatcaggatcatgttgaagctaaggtcgtggttgctggtttatcaacaacatgt
agccagaaaattcataatcagttgattggagttgaaaaaatgcacaaagataccaaatatgtgttatttttggatgat
gatgttagactgcatcctggaacaatcggagctctcacgactgagatggagaaaaatccagagatatttattcaaact
gggtatcctctagacttgccgtctgggactcttgggagttattgcatctatgagtaccacatgccttgctcaatggga
tttgcgactggtggaagaacattctttttgtggggaggatgtatgatgatgcatgctgatgatttcagacaagatcgg
tacggtgttgtctctggcttacgtgatggtggatattcagatgatatgacacttgcctctctagcaggtgctcataag
aggctcattacatctcctcctgttgctgttttccctcaccctctcgcgagtgatctaagttttggacgatactggaac
tacttgagaaaacaaaccctttgtgctagaatcatacatatcgaaagttaactggataatgaacaaggctttgtttgct
gtccattgttatctttcatggggttttgttgcaccatatgttatggctatcattcacatcacatcagctttaagaatc
tacatcaagggctatcatcaacttgaagacacgacctctgcttctggtggtatgatgcttgttataacgttggcgatc
tgcaccttcatcgagcttctgtcaatgtggaatttgacgagacgagaagttcagctatgcaatatgttatcccctgag
gctccccgtctctctcttgcaacttacaactggggacttgtttttgtagcaatgcttgtagacaacttcctatatccg
atatcagctttccggtctcatttttctcaatccataaactggtctggaatcagataccacttgaaagatggaaagata
ttcaagattgagagacgaaaggatatgggaccaacaaagactgatttaggaggcaaacatttgtatggtaagaaagga
gctcctcagaaagcttcattcttaagctcattgggaagaaatttggctcactggcgacaaccgaaaaaattcgatgta
a

8.4.5 RNAi Sequences

Limit Dextrinase Inhibitor

LDi F ctgcgcatcctcatggac

LDi R actccgcttcattaccttgg

ctgcgcatcctcatggacggggtgcgcacgccggagg
gccgcgtggttgagggacggctcggtgacaggcgtgactgcccgagggaggagcagaggg
cgttcgccgccacgcttgtcacggcggcggagtgcaacctatcgtccgtccaggagccgg
gagtacgcttggtgctactggcagatggatgacgatcgaaatgcgccaaggtaatgaagc
ggagtactgtatacagaataaaagta

243 bp

Limit Dextrinase

LD F aaagcgaaacattgcaaacc

LD R aaagatcttcggttgcttcg

aaagcgaaacattgcaaaccctaacagctgaccactgtcc
aatcctaaaacccaatgaatcatcaacccaaaaggttgtgaaactgggagagcaattctg
aatacgcaacggctattccggactgtttcaggtgaattcatcagatactttggtgaggaa
atcggcgtacgagtccgcgacatgcaggttcaccgtgcccggaagaaccgtgtcagtctt
tgtcgaacctcggtgttgacgcctcctcggtttcaacacgaggatctgttctacaagttg
tcgaagcaaccgaagatcttt

301 bp